

**DEVELOPMENT OF RAPID PHAGE BASED DETECTION METHODS FOR
MYCOBACTERIA**

By

Benjamin Swift, BSc (Hons), MRes.

**Thesis submitted to the University of Nottingham
for the degree of Doctor of Philosophy**

2014

Supervisors

Dr Cath Rees

Prof Jon Huxley

For my brothers.

ABSTRACT

MAP is the causative agent of a wasting disease in ruminants and other animals called Johne's disease. Culture of the organism can take months and in the case of some sheep strains of MAP, culture can take up to a year. It can take several years for an animal infected with MAP to show clinical symptoms of disease. During this subclinical stage of infection, MAP can be shed into the environment contaminating their surroundings and infecting other animals. As well as this Johne's disease is particularly difficult to diagnose during the subclinical stage of infection.

Culture is very difficult and takes too long to be a viable method to diagnose Johne's disease. Microscopic methods can be used on histological samples to detect MAP, however common acid-fast stains used are not specific for MAP and other mycobacteria and acid-fast organisms can be detected. Molecular methods, such as PCR, exist to rapidly detect the signature DNA sequences of these organisms, however they have the disadvantage of not being able to distinguish between live and dead organisms. Other methods immunological methods, such as ELISA tests, exist and are routinely used to diagnose Johne's disease, however their sensitivity is very poor especially during the subclinical stage of disease.

The aim of these studies was to develop novel rapid methods of detecting MAP to act as an alternative to methods already available. Sample processing using magnetic separation was carried out to allow good capture of MAP cells and to allow efficient phage infection. Using the phage assay, a specific, sensitive phage based method was developed that could detect approximately 10 cells per ml of blood within 24 h in the laboratory with a sensitive, specific plaque-PCR.

This optimised detection method was then used to determine whether MAP cells could be detected in clinical blood samples of cattle suffering from Johne's disease. The results suggest that animals experimentally and naturally infected with MAP harboured cells in their blood during subclinical and clinical stages of infection.

A novel high-throughput method of detecting mycobacteria was also developed. Using phage D29 as a novel mycobacterial DNA extraction tool, viable MAP cells

were detected within 8 h and the format of the assay means that it can be adapted to be used in a high-throughput capacity.

Factors affecting phage infection and phage-host interactions were investigated to make sure the phage based methods of detection were as efficient as possible. It was found that periods of recovery were often necessary to not only make sure the phage were not inhibited but to also allow the host cells to be metabolically active as it was found that phage D29 can only infect mycobacteria cells that are metabolically active.

A fluorescent fusion-peptide capable of specifically labelling MAP cells was also developed to be used as an alternative to acid-fast staining. Peptides that were found to specifically bind to MAP cells were fused with green fluorescent protein and cells mounted on slides were specifically labelled with the fluorescent fusion protein. This resulted in a good alternative to the generic acid-fast staining methods.

The blood phage assay has shown that viable MAP cells can be found in the blood of animals suffering from Johne's disease within 24 h and this can be confirmed using a MAP specific plaque-PCR protocol. A novel faster method to detect MAP was also developed, to cut down the time to detection of viable MAP cells to 8 h, which can be formatted to be used in a high-throughput capacity. The phage assay was used as a tool to determine different metabolic states of mycobacteria, and helped investigate optimal detection conditions when using the phage assay. Finally a novel fluorescent label was developed to detect MAP as an alternative to insensitive acid-fast staining. The development of these novel methods to rapidly, specifically and sensitively detect MAP will push further the understanding of Johne's disease and help control it.

ACKNOWLEDGEMENTS

I would like to thank all the people who helped me and gave me advice during my PhD. I would like to firstly say a massive thank you to my PhD supervisor Cath Rees, who gave me the opportunity to carry out my PhD and for her support, enthusiasm and her constant open door policy which meant we could bother her most of the time.

I would like to thank Jon Huxley, my second supervisor, who without his knowledge of all things cow, I would not have been able to get any samples, understand Johne's disease from a farmer's point of view or write up much of my work that involved clinical samples.

I would like to thank Phil Hill for his help with his help with molecular my cloning especially with developing my GFP fusion peptides.

I would like to thank Chris Dodd, who with Cath gave me the opportunity to do a Master's that led to my PhD... I hope their faith was justified!

Finally I want to say thanks to the technical staff who have made my experiments run as smoothly as possible and always helped me out, so Lorraine, Dave and Wendy, thank you very much!

TABLE OF CONTENTS

Title Page	I
Abstract	III
Acknowledgements	V
Table of Contents	VI
List of Figures	XIII
List of Tables	XVI
List of Abbreviations	XVII

1. INTRODUCTION AND LITERATURE REVIEW	1
1.1. PROLOGUE	2
1.2. MYCOBACTERIA	2
1.2.1. The <i>Mycobacterium</i> Cell Wall	3
1.2.2. An overview of pathogenic mycobacteria	7
1.2.2.1 <i>Mycobacterium tuberculosis</i>	7
1.2.2.2 <i>Mycobacterium bovis</i>	8
1.2.2.3 <i>Mycobacterium leprae</i>	9
1.2.2.4 <i>Mycobacterium avium</i>	10
1.2.2.5. <i>Mycobacterium avium</i> subspecies <i>paratuberculosis</i> affecting animals	10
1.2.2.6. <i>Mycobacterium avium</i> subspecies <i>paratuberculosis</i> affecting humans	11
1.3. MAP AND JOHNE'S DISEASE	15
1.3.1. Establishment of Infection Transmission of MAP	15
1.3.2. Impact of Johne's disease	18
1.3.3. Detection of <i>Mycobacterium avium</i> subsp. <i>paratuberculosis</i>	19
1.3.3.1. Ziehl-Neelsen staining	20
1.3.3.2. Improved culture methods	21
1.3.3.3. Use of ELISAs to detect host responses to MAP	22
1.3.3.4. PCR-based methods	25
1.3.4. Bacteriophage	29
1.3.4.1 Phage life cycles	31
1.3.4.2. Bacteriophage-based detection	34
1.3.4.3. Reporter phage technology	34
1.3.4.4. Phage amplification detection	36
1.3.4.5. The FASTPlaqueTB™ Assay and MAP	40
1.4. AIM	41

2. MATERIALS, METHODS AND STANDARD PROCEDURES	43
2.1. GENERAL MEDIA AND REAGENTS	44
2.1.1. Culture and growth conditions	44
2.1.1.1. <i>In house Herrold's Egg Yolk Media (HEYM)</i>	44
2.1.1.2. <i>Commercial HEYM</i> <i>(Becton Dickinson, France)</i>	45
2.1.1.3. <i>HEYM inoculation</i>	45
2.1.1.4. <i>Middlebrook 7H10 and 7H9 mycobacteria</i> <i>culture</i>	45
2.1.1.5. <i>Slope wash</i>	46
2.1.2. FASTPlaqueTB™ assay media and reagents	46
2.1.2.1. <i>Media Plus</i>	46
2.1.2.2. <i>Virusol</i>	46
2.1.2.3. <i>Actiphage</i>	46
2.1.2.4. <i>Sensor cells</i>	46
2.1.2.5. <i>FASTPlaqueTB™ Agar</i>	47
2.1.3. The FASTPlaqueTB™ assay	47
2.1.3.1. <i>Controls</i>	47
2.1.3.2. <i>FASTPlaqueTB™ assay</i>	47
2.1.3.3. <i>Mycobacteria enumeration using the</i> <i>FASTPlaqueTB™ assay</i>	52
2.1.4. Bacteria strains	53
2.2. MAGNETIC SEPERATION OF MAP	54
2.2.1. Preparing magnetic beads	54
2.2.2. Peptide mediated magnetic separation (PMMS)	54
2.2.2.1. <i>Magnetic separation from blood</i>	55
2.3. PHAGE BASED DETECTION OF MAP	55
2.3.1. Detecting MAP in milk	55
2.3.2. Detecting MAP in blood	56
2.3.2.1. <i>Buffy coat isolation</i>	56
2.4. MAP SPECIFIC POLYMERASE CHAIN REACTION'S (PCR)	57
2.4.1. Genomic DNA preparation and purification	57
2.4.1.1. <i>Heat extraction</i>	57
2.4.1.2. <i>DNEasy™ DNA extraction kit (Qiagen, UK)</i>	57
2.4.2. Plaque DNA preparation	58
2.4.2.1. <i>Plaque extraction</i>	58
2.4.2.2. <i>ZymoResearch™ Gel DNA extraction</i>	58
2.4.2.3. <i>ZymoResearch™ DNA concentration</i>	59

2.4.3. DNA molecular weight marker	60
2.4.4. Primers used in PCR reactions	62
2.4.5. PCR reactions	63
2.4.5.1. <i>IS900-PCR</i>	63
2.4.5.2. <i>Nested IS900-PCR</i>	63
2.4.5.3. <i>MAP-specific F57 PCR</i>	64
2.4.5.4. <i>Quantitative real-time PCR</i>	65
2.5. GENERAL CLONING, TRANSFORMATION AND EXPRESSION OF PROTEINS IN <i>E. COLI</i>	67
2.5.1. PCR amplification of GFP-fusion peptides	69
2.5.1.1. <i>Amplifying gfp-peptide fusion</i>	69
2.5.1.2. <i>Gel-DNA extraction and Restriction Digests</i>	69
2.5.1.3. <i>Ligation Reaction</i>	70
2.5.1.4. <i>Preparing chemically competent <i>E. coli</i></i>	70
2.5.1.5. <i>Transformation of chemically competent cells</i>	71
2.5.1.6. <i>Protein extraction</i>	72
2.5.1.7. <i>Protein purification</i>	72
2.5.1.8. <i>SDS-page analysis</i>	73
2.5.1.9. <i>Bradford Assay</i>	75
2.5.2. TOPO-Cloning (Invitrogen)	75
2.5.3. Plasmid DNA extraction	76
2.5.4. DNase I (NEB) treatment	77
2.6. PREPARATION OF CELLS FOR SCANNING ELECTRON MICROSCOPE (SEM)	77
2.7.1. GFP-fusion peptide binding protocol	77
2.7.2. Cell capture assay	78
2.8. ZIEHL-NEELSEN (ZN) STAINING	79
2.9. DETECTION AND ENUMERATION OF MAP USING PHAGE TM4 INSTEAD OF D29	79
2.10. INDUCING STATIONARY PHASE IN MYCOBACTERIA	79
2.10.1. Phage attachment assay	80
2.10.2. Effect of inhibition of RNA synthesis on phage infection	80
2.11. STATISTICAL ANALYSIS	80
3. DEVELOPMENT AND EVALUATION OF A RAPID PHAGE-BASED METHOD FOR DETECTION OF VIABLE <i>MYCOBACTERIUM AVIUM</i> SUBSP. <i>PARATUBERCULOSIS</i> IN BOVINE BLOOD	82

3.1. INTRODUCTION	83
3.2. RESULTS	85
3.2.1. Initial detection of MAP in blood	85
3.2.2. Optimising bead capture efficiency in Media Plus	85
3.2.3. Optimising PMMS-MAP detection in blood	92
3.2.4. Determining limit of detection of PMMS-phage method	94
3.2.5. Molecular identification of MAP	96
<i>3.2.5.1. Detection of MAP specific DNA from plaques</i>	96
<i>3.2.5.2. Nested-PCR amplification of signature MAP DNA</i>	102
<i>3.2.5.3. Quantitative Real-Time PCR</i>	109
3.3. DISCUSSION	112
4. APPLICATION OF THE PHAGE ASSAY ON FIELD SAMPLES	115
4.1. INTRODUCTION	116
4.2. ETHICAL APPROVAL FOR THE COLLECTION OF BLOOD SAMPLES	117
4.2.1. Initial trial of the phage assay using field samples	117
4.2.2. Use of the phage assay on Johne's milk ELISA positive, negative and inconclusive animals	122
4.2.3. Comparison of MAP detection from whole blood and the buffy coat	124
4.2.4. Culture of MAP following PMMS of blood	125
4.2.5. Statistical analysis of results	126
4.2.6. Use of the phage assay on blood samples from experimentally infected animals	127
4.2.7. Detection of early infection in experimentally infected calves	128
4.2.8. Use of the blood assay on experimentally infected subclinical cattle	130
4.2.9. Using the phage assay on experimentally infected sheep	134
4.3. COMPARISON OF OVERALL TEST RESULTS	138
4.4. DISCUSSION	144
5. DEVELOPMENT OF A NEW HIGH-THROUGHPUT ASSAY FORMAT FOR THE DETECTION OF VIABLE MAP	151

5.1. INTRODUCTION	152
5.2. RESULTS	153
5.2.1. Determining the time taken for bacteriophage D29 to release DNA from MAP	153
5.2.2. Isolating MAP and extracting DNA using bacteriophage	156
5.2.3. Optimising bacteriophage mediated cell lysis PCR-detection	159
<i>5.2.3.1. Removing potential free MAP DNA</i>	159
<i>5.2.3.2. Improving peptide-mediated magnetic capture efficiency</i>	162
<i>5.2.3.3. Preventing detection of unlysed MAP cells by limiting thermal lysis</i>	167
<i>5.2.3.4. Preventing detection of unlysed MAP cells by separation</i>	169
5.2.4. Discussion of development of the one tube assay format	178
5.2.5. Testing the non-fully optimised one day assay on experimentally infected calves	180
5.3. DISCUSSION	188
6. AN INVESTIGATION OF FACTORS AFFECTING BACTERIOPHAGE D29 INFECTION	193
6.1. INTRODUCTION	194
6.2. RESULTS	195
6.2.1. Ability of phage D29 to infect mycobacteria in different growth phases	195
6.2.2. Determining whether the phage-resistant state is reversible	198
6.2.3. Infection with a phage TM4	202
6.2.4. Phage attachment to non-infectable MAP cells	207
6.2.5. Role of RNA synthesis inhibition on phage infection	209
6.2.6. Effect of freezing on phage infection	212
6.3. DISCUSSION	217
7. DEVELOPMENT OF A NOVEL FLUORESCENT PROTEIN FOR LABELLING <i>MYCOBACTERIUM AVIUM</i> SUBSP. <i>PARATUBERCULOSIS</i>	222

7.1. INTRODUCTION	223
7.2. CONSTRUCTING FLUORESCENT PEPTIDES	225
7.2.1. Primer Design	225
7.2.2. PCR of GFP-fusion peptide	228
7.2.3. Cloning and Analysis of GFP-fusion PCR products	232
7.2.4. Transformation and expression of GFP-fusion peptides	235
7.2.5. Evaluating the ability of the GFP-fusion peptides to bind to MAP cells	237
7.2.6. Optimising GFP-fusion peptide binding assay	239
7.2.7. Using GFP-fusion peptides to visualise MAP cells	239
7.2.8. Ziehl-Neelsen staining on fixed MAP samples	245
7.2.9. Development of fluorescent cell capture MAP detection assay	247
<i>7.2.9.1. Optimising the cell capture assay</i>	251
7.3. DISCUSSION	257
7.3.1. GFP-fusion tag expression and purification	257
7.3.2. Cell capture assay development	257
7.3.3. Conclusion	258
8. GENERAL DISCUSSION AND FUTURE WORK	260
8.1. THE BLOOD PHAGE ASSAY	262
8.1.1. Developing phage assay protocols	263
8.1.2. Using the phage assay on clinical samples	266
<i>8.1.2.1. Future applications for the detection of MAP and other mycobacteria</i>	268
8.2. DEVELOPMENT OF A HIGH-THROUGHPUT MAP DETECTION PLATFORM	269
8.2.1. Future developments of the high-throughput MAP detection assay	270
8.3. NOVEL MAP-SPECIFIC FLUORESCENT FUSION PEPTIDES	271
8.4. CONCLUSION	271
9. BIBLIOGRAPHY	272

10. APPENDICES	291
1. Paper in production: Induction of pigment production in cattle strains of <i>Mycobacterium avium</i> subsp. <i>paratuberculosis</i>	291
2. Paper in production: Cloning and expression of bacteriophage D29 lysins and their application in lysing mycobacteria	298
4.1. Mead's resource equations	302
7.1. CODON optimisation table for <i>E. coli</i>	303
7.2. Plasmid maps	304
11. Publications	310

LIST OF FIGURES

1.1. Comparison of different bacterial cell wall structures	5
1.2. Typical Ziehl-Neelsen stain of the acid-fast bacteria <i>M. tuberculosis</i>	6
1.3. Pathology of Crohn's disease and Johne's disease	14
1.4. Relative sensitivities of ELISA tests during different phases of Johne's infection	24
1.4. Probability of Johne's infected cows testing positive using milk ELISA	24
1.5. Structure of Bacteriophage	30
1.6. The lytic and lysogenic life cycle of bacteriophage	33
1.7. Overview of the <i>FASTPlaqueTB</i>TM assay	39
2.1. Schematic diagram of the preparation of controls used in the <i>FASTPlaqueTB</i>TM assay	49
2.2. An example of positive and negative control plates	49
2.3. Schematic diagram of the <i>FASTPlaqueTB</i>TM assay	50
2.4. Interpretation of the results from the <i>FASTPlaqueTB</i>TM assay	51
2.5. Molecular DNA markers	61
2.6. Protein markers	74
3.1. SEM of MAP cells bound to paramagnetic beads	90
3.2. Effect of capture time on capture efficiency of MAP cells	91
3.3. Effect of blood on detection of MAP by PMMS-phage assay	93
3.4. Development of the IS900 PCR amplification assay	98
3.5. Establishing the P90-P91 plaque-PCR assay	101
3.6. Developing DNA extracted method using Zymo-spin columns	101
3.7. Determining the sensitivity of the IS900 PCR assay	103
3.8. Determining the sensitivity of the nested IS900-PCR assay	103
3.9. Optimised nested-PCR sensitivity (A) and its ability to detect MAP plaque DNA (B)	106
3.10. Sensitivity of the optimised nested-PCR using mixed MAP and <i>M. smegmatis</i> plaques	108
3.11. Sensitivity of the Tetracore qRT-PCR MAP detection assay	111
4.1. Detection of IS900 by nested PCR from plaque DNA	121
4.2. Detection of MAP by direct blood-PCR and the phage assay in blood samples from experimentally infected calves	129
4.3. Comparison of the distribution of positive results using phage-PCR assay and the blood ELISA tests	140

4.4. Relationship between positive phage assay, faecal PCR and blood ELISA results	143
5.1. Use of FAS to determine the eclipse phase of bacteriophage D29 infecting <i>M. smegmatis</i> and MAP	155
5.2. Detection of MAP DNA following lysis by bacteriophage	158
5.4. The effect of DNase I treatment to remove potential DNA contamination	161
5.5. Experiment to rule out bacteriophage contamination of uninfected MAP cells	161
5.6. Number of dissociated MAP cells detected in the supernatant during 3 h incubation on magnetic beads	163
5.7. Number of MAP cells dissociated from the magnetic beads during incubation	163
5.8. MAP cell dissociation in PBS compared to Media Plus	165
5.9. MAP cell dissociation in MP with pH 7.4 compared to 6.6	165
5.10. Effect of reducing the denaturation temperature on PCR amplification and cell lysis	168
5.11. Use of spin column to separate out intact MAP cells	170
5.12. Effect of using spin column to remove intact MAP cells	172
5.13. Effect of using spin columns and PMMS to remove intact MAP cells	172
5.14. Determining if spin column buffer can cause the release of MAP DNA from intact cells	175
5.15. Effect of removing intact MAP cells from the phage lysis supernatant by PMMS without DNA concentration	175
5.16. Detection of MAP cells after one or two rounds of PMMS	177
5.17. Detection of MAP ATCC 19851 after two rounds of PMMS	177
5.18. Schematic diagram of the one day – one tube format assay	182
6.1. Comparison between the number of <i>M. smegmatis</i> cells detected by phage and viable count following growth under self-inducing hypoxia conditions	197
6.2. Recovery of phage D29 infectivity by <i>M. smegmatis</i> cells	200
6.3. Recovery of phage D29 infectivity by three strains of MAP	201
6.4. Difference in infectivity of <i>M. smegmatis</i> by D29 and TM4	204
6.5. Difference in infectivity of MAP cells by D29 and TM4	206
6.6. Effect of stationary phase bacteria on the attachment of phage D29 to MAP cells	208

6.7. Investigation of role of gene expression on recovery of sensitivity of MAP to phage D29	211
6.8. Effect of freezing on MAP cell detection	214
6.9. Effect of longer recovery periods on number of MAP cells detected after freezing at -20 °C	216
7.1. Schematic of fusion protein construct orientation	227
7.2. Comparison of PCR of GFP amplification using a proof-reading and non-proof reading DNA polymerase	230
7.3. Effect of DMSO and annealing temperature on PCR amplification of the GFP-peptide fusion sequence	231
7.4. Predicted restriction enzyme sites in GFP gene	234
7.5. Fluorescence of purified GFP fusion-peptides	236
7.6. SDS-Page analysis of GFP-fusion samples	236
7.7. Binding of mixed GFP-fusion peptides to Mycobacteria	238
7.8. Specificity of GFP-fusion peptide binding	240
7.9. Comparison of fluorescent confocal and brightfield images of MAP cells labelled with N-terminal Gfp peptide fusions	241
7.10. Comparison of fluorescent confocal and brightfield images of MAP cells labelled with N-terminal Gfp peptide fusions and DAPI	243
7.11. Comparison of fluorescent confocal and brightfield Images of <i>M. smegmatis</i> cells labelled with N-terminal Gfp peptide fusions and DAPI	244
7.12. Comparison of fluorescent, brightfield and ZN stained images of <i>M. smegmatis</i> and MAP cells	246
7.13. Schematic of the ELISA-like cell capture assay	248
7.14. Microtitre plate cell capture and fluorescent identification with GFP-fusion peptides	250
7.15. Effect of BSA concentration on blocking non-specific GFP-fusion peptide binding to MAP and <i>M. smegmatis</i>	252
7.16. Specificity of GFP-fusion peptide binding to MAP and other closely related mycobacteria	255
7.17. Effect of temperature on GFP-fusion binding to MAP cells	256
7.18. Effect of increasing NaCl concentrations on GFP-fusion binding	256

LIST OF TABLES

1.1. Summary of the different costs and sensitivities of Johne's disease diagnostic tests	28
2.1. Table of bacteria strains used during this project	53
2.2. Primer sequences	62
2.3. Plasmids	68
3.1. Capture efficiency of Pathatrix and Dynabeads after the FPTB assay	88
3.2. Effect of increasing beads concentration on the capture efficiency of Pathatrix and Dynabeads	88
3.3. Limit of detection of phage assay in spiked sheep blood	95
4.1. Results of phage, milk & blood ELISA and real-time PCR assays from Set A and B	120
4.2. Results of analysis of blood samples from animals with different milk ELISA status	123
4.3. Comparison of test results by the phage assay and direct PCR	129
4.4. Results for sub-clinical, experimentally infected cattle	133
4.5. Results of MAP detection for experimentally infected sheep	137
4.6. Contingency table of phage assay and the blood ELISA test results for comparable cattle samples	141
5.1. Comparison of the one tube assay results with conventional phage-PCR results.	184
5.2. Comparison of the one tube assay results with direct-PCR Results	186
5.3. Comparison of the phage assay results with direct-PCR results	187
5.4. Agreement between test results over time	191
7.1. Codon optimisation of MAP specific peptides	226
7.2. Sequences of primers use to create Gfp fusions	226
7.3. Concentration of the purified GFP-fusion PCR amplicons	234

LIST OF ABBREVIATIONS

ABC	Avidin-binding complex
BCG	Bacillus Calmette-Guérin
BSA	Bovine serum albumin
Btb	<i>Mycobacterium bovis</i>
bTB	Bovine tuberculosis
CBD	Cell-wall binding domain
cfu	Colony forming units
CT	Cycle Threshold
DIVA	Differentiate Infected and Vaccinated Animals
DMSO	Dimethyl sulphoxide
DNA	Deoxyribonucleic acid
ELISA	Enzyme linked immunosorbent assay
FAS	Ferrous ammonium sulphate
FPTB	FASTplaqueTBTM
GFP	Green fluorescent protein
HEYM	Herrold's egg yolk medium
HPA	Health Protection Agency
IBD	Inflammatory bowel disease
IMS	Immuno-magnetic separation
INH	Isoniazid
LPS	Lipopolysaccharides
LRP	Luciferase reporter phage
MAC	Mycobacterium avium Complex
MAP	<i>Mycobacterium avium</i> subsp. <i>paratuberculosis</i>
MGIT	Mycobacterial growth indicator tube
MP	Media Plus
Mtb	<i>Mycobacterium tuberculosis</i>
MTC	Mycobacterium tuberculosis Complex
OD	Optical Density
PCR	Polymerase chain reaction
pfu	Plaque forming units
PMMS	Peptide mediated magnetic separation
RFU	Relative fluorescent units
RIF	Rifampicin
RO	Reverse osmosis
RT	Room temperature

SDW Sterile distilled water
SEM Scanning electron microscope
TB Tuberculosis
TNTC Too numerous to count
WBC White blood cell
WHO World Health Organisation
XDR Extensively drug-resistant
ZN Ziehl-Neelsen

CHAPTER 1
INTRODUCTION AND LITERATURE REVIEW

1.1. PROLOGUE

Some pathogenic members of the *Mycobacterium* genus are part of a group of organisms that are very difficult to culture and detect rapidly with any reliability. The tendency for these organisms to lie dormant for years within their host adds to the difficulties in detection. Novel tools are needed to be able to detect and understand mycobacterial infection fully so that diseases caused by these organisms can be controlled.

1.2. MYCOBACTERIA

The *Mycobacterium* genus consists of many G+C rich, aerobic, non-motile species (Gutierrez et al., 2009). They are classified as Gram positive, but have a distinctive acid-fast cell wall made up of mycolic acid that resists the Gram stain. Mycobacteria can be divided into two groups; fast and slow growing (Wayne and Kubica, 1986). The fast growing mycobacteria can produce visible colonies in less than 7 d and the slow growing ones grow after 7 d of incubation. The pathogenic mycobacteria are generally found in the slow growing group. Members of the mycobacterium tuberculosis complex (MTC) group cause major disease in humans and animals, such as; *Mycobacterium tuberculosis* (the causative agent of tuberculosis) and *Mycobacterium bovis* (the causative agent of bovine tuberculosis). Other mycobacteria part of the mycobacterium avium complex (MAC) group of organism can also cause significant disease such as; *M. avium*, *M. intracellulare*, *M. marinum*, *M. kansasii*, *M. chelonae* and *Mycobacterium avium* subspecies *paratuberculosis* (Rezwan et al., 2007).

MAC organisms can be grouped based on Runyon's Classification of mycobacteria which places members of non-tuberculosis causing bacteria into classifications based on their ability to produce pigments under different light conditions (Runyon, 1959). This was an important way of diagnosing diseases caused by different mycobacterial pathogens.

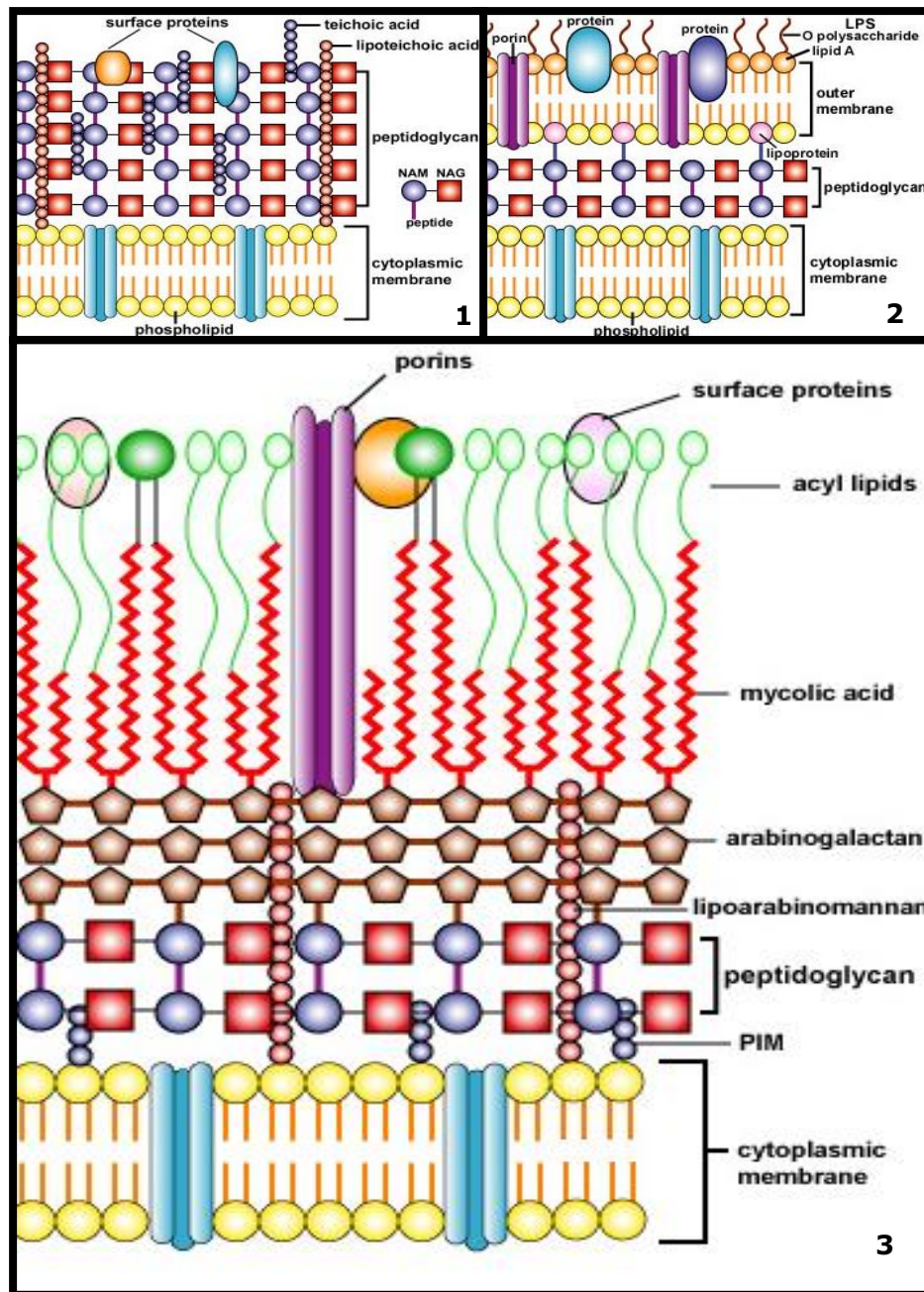
1.2.1. The *Mycobacterium* cell wall

Mycobacteria are a peculiar group of organisms because, although genetically they fall into the Gram-positive group, they have a lipid-rich cell wall that is different to that of other Gram-positive organisms (Figure 1.1). The thick waxy cell wall ('Myco' is from the Latin meaning waxy) is resistant to conventional Gram staining techniques and gives rise to their typical acid-fast characteristic which is used to identify the organism. Hence the Ziehl-Neelsen (ZN) method (amongst others) is used to stain acid-fast organisms and forms bright red cells on a blue background (Barksdale and Kim, 1977; Figure 1.2).

The cell wall is made up of a covalently-linked complex of mycolic acids, heteropolysaccharide arabinogalactans and peptidoglycans (Lederer, 1977; Figure 1.1). The peptidoglycan is covalently attached to arabinogalactan, which in turn is attached to the mycolic acids (Brennan, 2003). The low permeability and a thick cell wall means that the cells can survive the antimicrobial challenge of the macrophage during host infection (Gao et al., 2003) as well as helping the bacterium to persist in the environment by resisting desiccation (Whittington et al., 2004). The low permeability of the mycobacterial cell wall, and its unusual structure, is also known to be a major factor contributing to antibiotic resistance in the organisms. Indeed mycobacteria show a high degree of intrinsic resistance to many common antibiotics and chemotherapeutic agents (Jarlier and Nikaido, 1994). This is partly due to limitations of drug penetration but also due to the presence of enzymes that actively degrade antibiotics such as the β lactams (see Da Silva and Palomino, 2011). However, research into the unique pathways used to synthesise the cell wall of mycobacteria has also allowed the development of novel drugs that target the components of the cell wall biosynthetic machinery, although there are now reports of drug resistance to these new drugs (Da Silva and Palomino, 2011).

Chatterjee (1997) produced a comprehensive review of what was, at the time, the latest knowledge of drug targets found in the mycobacterial cell wall. These include some of the most effective anti-tuberculosis drugs, isoniazid (INH) and ethambutol that affect mycolic acid and arabinan biosynthesis, respectively (Winder, 1982). Rifampicin is a lipophilic antibiotic that targets the RNA polymerase of mycobacteria and inhibits the synthesis of mRNA. However varying degrees of drug resistance, including extensively drug-resistant (XDR) TB, have been described. Today multidrug therapy is fundamental for control of the disease (Da Silva and Palomino, 2011) and a deeper understanding of the physiology these bacteria is needed to develop novel drugs to combat problems of drug resistance. The sequencing of several mycobacterial genomes has allowed significant advances in the understanding of the unique cell wall features, which are often thought as the best candidate targets for anti-mycobacterial treatment. These advances in knowledge can now be used to gain a better understanding of the molecular basis of drug action in mycobacteria (Brown-Elliott et al., 2012).

Figure 1.1. Comparison of different bacterial cell wall structures

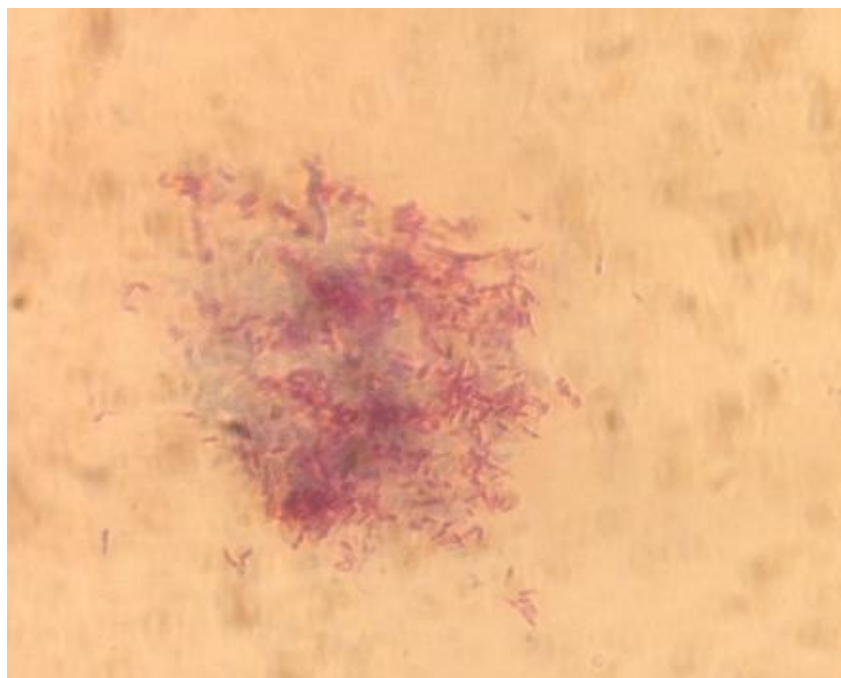


Box 1: typical Gram-positive cell wall structure with the thick peptidoglycan layer attached to the cytoplasmic membrane by lipoteichoic acids.

Box 2: typical Gram-negative cell wall structure with the cytoplasmic membrane surrounded by a thin peptidoglycan layer. The outer leaflet of the outer membrane includes lipopolysaccharides (LPS).

Box 3: typical acid-fast cell wall structure with the cytoplasmic membrane surrounded by a thin peptidoglycan layer and then the unique waxy layer containing a high proportion of mycolic acid (~60%). Porin proteins are essential for transport of small molecules across this barrier (Images sourced with permission from Kaiser, 2010).

Figure 1.2. Typical Ziehl-Neelsen stain of the acid-fast bacteria *M. tuberculosis*



The ZN stains the mycolic acid rich cell wall of the mycobacteria purple. If histopathological samples were taken, the background tissue would stain blue, which adds better contrast the acid fast cells (Swift, 2013).

1.2.2. An overview of pathogenic mycobacteria

The genus *Mycobacterium* is typically split into two distinct groups; fast-growing and slow-growing. Those in the fast growing group are defined as those that will form colonies within seven days, whereas the slow growers take more than seven days to form visible colonies (Wayne, 1986). This slow growing attribute is normally associated with pathogenic mycobacteria (Chacon et al., 2004) and this characteristic poses the greatest threat to treating and controlling diseases due to the difficulties it creates for rapidly diagnosing infections by these bacteria using conventional culture techniques.

1.2.2.1. Mycobacterium tuberculosis

Mycobacteria are responsible for a wide range of human and animal diseases. The most notable human pathogen in this genus is *Mycobacterium tuberculosis* (Mtb), which is the causative agent of tuberculosis (TB) in humans. It claims over two million lives a year, especially in patients with HIV in the African continent. One in 10 people are thought to be asymptomatic carriers of the disease, especially in urbanised areas (Gomez and McKinney, 2004). In the UK there are reported to be 9000 new cases each year (HPA, 2013). The disease causes the classic symptoms of a chronic cough with blood-tinged sputum, fever, night sweats, and weight loss. It is normally spread by coughing and diagnosed by culture of the organism in the sputum of patients although X-rays can identify the extensive scarring of lungs characteristic of TB infection. A feature of many mycobacterial infections is the ability to lie dormant for years. Mtb is capable of remaining dormant for prolonged periods in their host tissues, and it is these dormant bacilli that are responsible for latency of the disease (Wayne, 1994). This transition into dormancy renders the bacteria resistant to host defences and also to drug treatments where the targets are associated with cell wall synthesis (Gengenbacher and Kaufmann, 2012). The bacteria can then reawaken from this

dormant state into an active growth phase when the host's immune system is compromised, resulting in reactivated TB infection.

1.2.2.2. *Mycobacterium bovis*

Mycobacterium bovis (Btb) is the cause of a zoonotic disease; Bovine tuberculosis (bTB). It infects a variety of animals and humans, although this occurs relatively rarely in the UK, it is by far a bigger problem in the developing world. Milk pasteurisation was developed and introduced to prevent the infection of humans with bTB. In the United Kingdom where pasteurisation of milk is routine, only about 1% of clinically diagnosed cases of TB are subsequently proven bacteriologically to be attributed to *M. bovis* (Drobniewski et al., 2003). However, in the developing world *M. bovis* is still a cause for concern. For example, in most countries in Africa where effective disease control by methods such as regular milk pasteurisation are absent, bTB is still prevalent compared to developed nations. This situation is exacerbated by the presence of multiple additional risk factors in the population such as the high prevalence of HIV infection and consequently high numbers of adults with a compromised immune system (Muller et al., 2013).

The annual losses worldwide for agriculture attributed to *M. bovis* was estimated to be to \$3 billion in 2004 (Stermann et al., 2004). In 2009 the UK government spent £63 million trying to reduce losses to the industry and contain the spread of disease in the national herd. In the next decade, the UK Government predict that £1 billion will be spent on this problem (DEFRA, 2013). Most recently pilot badger culls have been introduced in the UK to try and control the spread of Btb among cattle populations. This highly contentious practice has been introduced primarily due to the difficulties in detecting Btb infection by conventional tests, which leads to the use of immunological tests which cannot differentiate between vaccinated and naturally infected animals.

It is believed that the best long-term prospect for Btb control in British herds is the development of a cattle vaccine against *M. bovis* (Vordermeier et al., 1999). A vaccine to prevent TB infection of humans was developed based on a live attenuated strain of *M. bovis* (Bacillus Calmette-Guérin; BCG) and this has subsequently been used to vaccinate cattle with variable results (Buddle et al., 2011). However the use of this vaccine can interfere with the current widely used tuberculin skin test, which measures a host's immune response to purified tuberculin protein. As bTB in the UK is a notifiable disease, animals with positive skin test reactions are culled and so if animals are vaccinated with the BCG vaccine, false-positive skin test results are given and this renders the vaccine unusable as the skin test cannot differentiate between vaccinated and naturally infected animals and currently no alternative to this test is available.

1.2.2.3. *Mycobacterium leprae*

Leprosy (also known as Hansen disease) is a serious disease caused by *Mycobacterium leprae* that results in irreversible nerve and skin damage. The organism is extremely fastidious and incapable of growth *in vitro* using conventional laboratory culture techniques. The main sources of *M. leprae* available for research have been isolated directly from infected human tissue or grown in two specific animal models (mouse foot pad tissue and the nine-banded armadillo; Hunter and Brennan, 1981). Due to the inability to readily culture the organism, identification of the disease in patients relies on clinical symptoms alone, which can make diagnosis difficult. The World Health Organisation (WHO) classifies leprosy according to the number of lesions and the microscopic detection of the presence of bacilli in a skin smear. Paucibacillary leprosy is characterized by five or fewer lesions with absence of organisms on smear and multibacillary leprosy is marked by six or more lesions with possible visualization of bacilli on smear (World Health Organisation, 2011). It is very difficult to treat

leprosy, with outbreaks occurring in remote areas of the developing world where access and medical supplies are limited. This also hinders information about the epidemiology of the disease since reporting of cases is sporadic.

1.2.2.4. *Mycobacterium avium*

Mycobacterium avium and *Mycobacterium intracellulare* are part of the MAC group of organisms. These slow growing organisms are known to infect humans and animals. The prominence has mainly risen with HIV and AIDS epidemic, where immuno-compromised individuals have significantly higher mortality rates when co-infected with HIV and MAC (Inderlied et al., 1993). Disseminated infection normally occurs late on in the progression of AIDS in individuals, where MAC co-infection is diagnosed but detecting the organism in the blood is very difficult. Similar treatments can be used to treat MAC infection in humans, to those used with TB infected individuals (Bermudez et al., 1999). Although, like the treatment for people with active TB infection, the course of treatment can take several months.

1.2.2.5. *Mycobacterium avium* subspecies *paratuberculosis* affecting animals

Mycobacterium avium subspecies *paratuberculosis* (MAP) is a pathogen that affects ruminants and has been proposed to cause disease in humans. It is the slowest growing member of the *Mycobacterium* genus that can be cultured in the laboratory and this feature makes it difficult to both detect and study. It causes an inflammatory bowel disease and gastroenteritis in ruminants known as Johne's disease. The disorder (also known as paratuberculosis) was first described in 1895 by Johne and Frothingham (1895) and results in reduced meat and milk yields. MAP is found throughout the world and is considered endemic in some countries where infected animals have been imported and the disease has spread (Greig et al., 1997, Fridriksdottir et al., 1999). Despite the disease being

notifiable in countries such as currently in Australia and formally (before 2009) in the Republic of Ireland, the subclinical nature of the disease can result in underreporting and inconsistent data about the incidence of Johne's disease. Indeed it has been reported that within Europe herd prevalence of the disease ranges from 7% to 55%, in Australia herd infection rates range between 9% and 22% and in the UK prevalence rates were reported to be 35 % (Manning and Collins, 2001, Beasley et al., 2011). MAP cells have the ability to survive in the environment for up to 55 weeks (Whittington et al., 2004). Coupled with underreporting, this then allows MAP to spread throughout a herd easily and undetected.

1.2.2.6. *Mycobacterium avium* subspecies *paratuberculosis* affecting humans

There is an on-going debate among the research community as to whether MAP can also cause Crohn's disease in humans, the symptoms of which are similar to those of Johne's disease. Crohn's disease is one cause of inflammatory bowel disease (IBD). It was first discovered and described as a chronic low-grade inflammation of the terminal ileum (Crohn et al., 1932). It is now known that Crohn's disease can occur anywhere along the gastrointestinal tract. Patients afflicted with this disorder generally suffer from chronic weight loss, abdominal pain, diarrhoea or constipation, vomiting, and general malaise (Chiodini, 1989). These symptoms can arise throughout the sufferer's lifetime and may be severe or mild. There are many factors involved in contracting Crohn's disease. Environmental factors (geography, cigarette smoking, sanitation and hygiene), infectious microbes, ethnic origin, genetic susceptibility, and a poor immune system can result in mucosal inflammation (Baumgart and Carding, 2007). It is generally thought that several of these factors are involved in causing Crohn's disease.

MAP is considered as the leading infectious cause for Crohn's due to the similarity of the symptoms and aetiology of the disease in animals (see Figure 1.3). An individual with an autoimmune disorder would be more likely to develop Crohn's disease than a separate individual if they are both exposed to MAP (Chamberlin et al., 2001).

The role of MAP in causing Crohn's is debated. Initially Koch's postulates (Table 1.1) needed to be fulfilled before MAP can be confirmed as a cause for Crohn's disease. However it is difficult to identify MAP from patients with Crohn's disease every time due to many reasons, indeed Koch himself had to dismiss some of his postulates with regards to Mtb latent infection. Mycobacteria are not visualised using standard mycobacterial cell wall staining techniques which may be due to changes in the organism's cell wall during infection. Cell wall deficient forms (CWD, spheroplasts) genetically indistinguishable from MAP have been isolated from patients with Crohn's disease (Hines and Styer, 2003). As well as this in most antibiotic clinical trials, Crohn's disease has not been cured using routine antibiotics known to kill MAP in Johne's disease infected animals (Greenstein, 2003).

Koch's postulates:

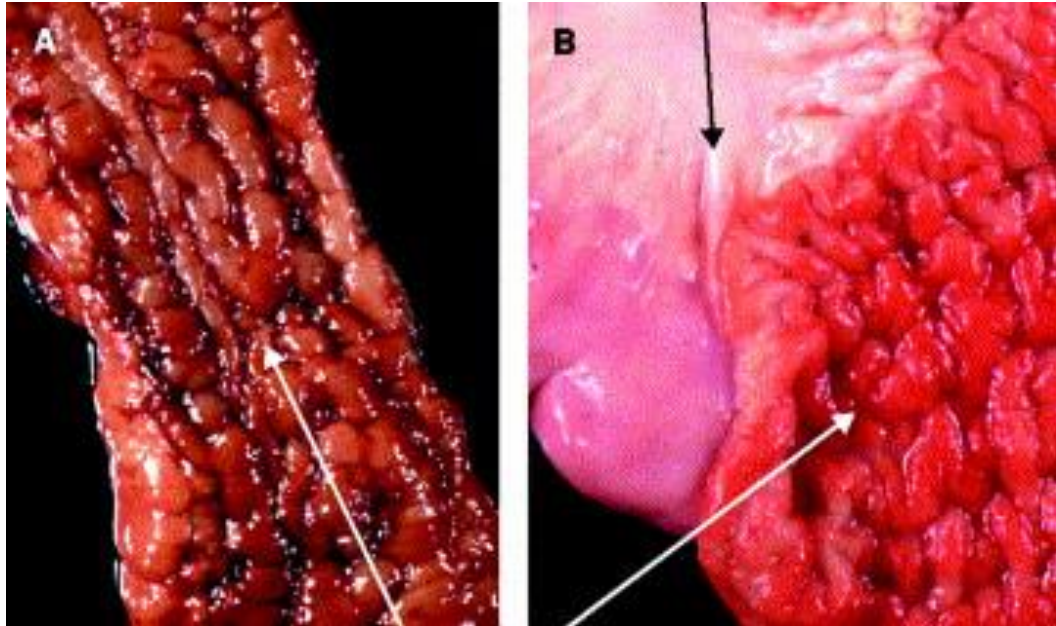
- 1** The microorganism must be found in abundance in all organisms suffering from the disease, but should not be found in healthy organisms.
- 2** The microorganism must be isolated from a diseased organism and grown in pure culture.
- 3** The cultured microorganism should cause disease when introduced into a healthy organism.
- 4** The microorganism must be re-isolated from the inoculated, diseased experimental host and identified as being identical to the original specific causative agent.

There is however more and more evidence suggesting that MAP has a significant role in Crohn's disease (Feller et al., 2007). Naser et al. (2004) cultured MAP from patients with Crohn's disease, and they have also been isolated from breast milk of mothers suffering from Crohn's disease (Naser et al., 2000). MAP has also been shown to survive in synthetic gastric juice and bile (Dalton and Hill, 2013), so it has the ability to reach the human gut intact. Whether MAP plays a causal role or whether it is as an opportunistic pathogen that infects the host's gastrointestinal tract when weakened is still undetermined.

However, as there is no appropriate animal model to facilitate studies and due to a failure in routinely isolating this organism from infective human tissues, Koch's postulates have not been satisfied. Thus there is great difficulty in confirming or disproving the role of MAP in causing Crohn's disease. There is however an association between this disease and MAP that has been revealed by a number of reviews and meta analyses (Chiodini, 1989, Feller et al., 2007, Abubakar et al., 2008) and therefore the debate continues.

Clearly what is needed are more tools to facilitate the detection of the organism so that this, and other questions about Johne's disease, can be answered. The remainder of this thesis will focus on developing such technology and MAP will constitute the main organism of research described in this thesis.

Figure 1.3. Pathology of Crohn's disease and Johne's disease



Images showing the pathophysiology of Crohn's disease (A) and of Johne's disease (B) on human and bovine intestinal samples, respectively. Note the very similar 'cobbling' effect on the surface of the gut lining (white arrows) and fat deposits (black arrow). Image sourced from Greenstein (2003).

1.3. MAP AND JOHNE'S DISEASE

1.3.1. Establishment of infection transmission of MAP

MAP is the causative agent of Johne's disease. It has been isolated from the ileum, milk, blood and faeces of animals suffering from Johne's disease. In the clinical stages of infection it causes wasting in ruminants such as cattle, sheep, goats, deer, and bison. During the clinical stage of the disease, animals exhibit extreme weight-loss around the time of calving and profuse diarrhoea containing bubbles (Eddy, 2004). On the lead up to clinical infection in milking animals, milk yield begins to drop significantly (Giese and Ahrens, 2000).

The main pathological features of the disease are gross lesions of MAP cells (internalised by macrophages) and mucosal thickening of the distal ileum giving rise to a corrugated appearance (Buergelt et al., 1978, Eddy, 2004) (Figure 1.3). During early infection MAP, like other mycobacteria, preferentially infect macrophages, found in the Peyer's patches in the ileum. Unlike Mtb and Btb, MAP is ingested rather than inhaled and causes infection of the gut and hence the organism can be shed in the faeces of infected animals. Although the sites of infection are different, there are parallels that can be made between the pathophysiology of MAP and Btb. For example both MAP and Btb can persist within macrophages, although MAP is phagocytised by the macrophages via the M cells in the gut and Btb typically enters alveolar macrophages (Knechel, 2009). The natural response of the immune system is to recruit more macrophages and lymphocytes which in turn signal for cytokines to increase the killing power of the macrophages. It is generally agreed that either the mycobacteria will be killed by the initial host response preventing clinical infection (Gonzalez et al., 2005) or the mycobacteria will survive persisting within the macrophages (Zurbrick et al., 1988).

The MAP cells that are able to survive and proliferate within these macrophages manage to do so, by evading and even redirecting the host's

immune response (Coussens, 2001). The MAP cells can then lie in a dormant state or they slowly proliferate attracting more macrophages and lymphocytes to the site of infection. Over time this increase in macrophages causes thickening in the intestine wall, which in turn reduces the ability to absorb nutrients which can then lead to clinical symptoms of Johne's disease (Sweeney, 2011). Although it is not known how the MAP cells become systemic and move around the bloodstream, research has been carried out with Mtb. It is postulated that the Mtb cells that are able to survive, proliferate, and kill their macrophage. In patients with normal immune systems, more macrophages are recruited and granuloma is formed, where there is low oxygen availability and a low pH to limit the growth of the mycobacteria leading to latent infection (Dheda et al., 2005). In immunocompromised patients, the granuloma formation is less robust. The tissues surrounding the mycobacteria undergo liquefaction, resulting in drainage into a bronchus or nearby blood vessel (Knechel, 2009). A similar process may be involved within animals that are unable to control MAP infection, resulting in systemic infection.

How the MAP cells are able to survive the harsh environment of the macrophage is not completely known (Sweeney, 2011). However, recent research has shown that MAP cells can up-regulate sigma factors involved in resisting oxidative stress as well as preventing the macrophage's phagosome maturation, to reduce their acidification (Ghosh et al., 2013). Mtb has been found to avoid macrophage destruction by blocking the delivery of the bacteriocidal lysosomes to the mycobacterial phagosome, and to dampen the acidity of the macrophage vacuole (Jayachandran et al., 2007). Thus MAP may have the ability to avoid macrophage destruction using some of these strategies. The infected macrophages, unable to kill them, then harbour the MAP cells and the cells are able to persist within the host during a latent, sub-clinical phase of infection. During this incubation period MAP cells may be shed in low numbers

into the environment intermittently before clinical signs of infection are seen (Raizman et al., 2004)

Similar to the observations made with TB patients, where only 1 in 10 people infected, as defined by the tuberculin skin test, are likely to produce clinical manifestations of the disease, not every animal may go on to exhibit clinical symptoms. There are many factors that have been proposed to determine whether or not an animal will become infected with MAP and develop Johne's disease. Specifically, age of infection and genetic susceptibility seem to be key elements to determine whether MAP will establish clinical infection in a particular host animal (Mcleod et al., 1995, Larsen, 1975). Stresses during lactation in dairy herds have been linked to increases in clinical presentation in cattle (Kimura et al., 2006).

In cattle it is known that MAP can be transmitted vertically by contaminated colostrum and milk or horizontally by contaminated food sources, such as pasture. As MAP cells are very hardy organisms, they have been known to persist in pasture, slurry and water sources for up to a year (Whittington et al., 2004, DARDNI, 2006). Over time, low levels of shedding during the subclinical phase of infection can lead to significant contamination of the environment and an insidious spread of infection throughout the herd (Whittington and Sergeant, 2001, Stabel, 1998). Hence the ability of the MAP cells to remain undetected for such long periods as a sub-clinical infection is a very significant factor contributing to the current lack of success in achieving good control of the disease. However in red deer, there is a high risk of transmission of MAP from clinically affected hinds to their foetuses during pregnancy. The mechanism for intra-uterine transmission has not been identified; but there is a theory that macrophages carrying MAP cells may be able to migrate through small gaps between cells lining the placenta. However, this migration would require the macrophages to travel across a six-layer thick barrier between the dam and the

foetus. (van Kooten et al., 2006). If this is also possible in cattle, it would also be a factor that makes disease control difficult to achieve.

1.3.2. Impact of Johne's disease

Given the absence of a fail-safe method of prevention or cure, Johne's disease can inflict significant economic losses on the agricultural sector. In the US dairy industry estimated losses of over \$200 million a year are associated with Johne's disease (Cho et al., 2012). Johne's disease is endemic and poses a worldwide threat. In the UK, Johne's disease was only notifiable in Northern Ireland, however this is now not the case. Due to potential underreporting it is difficult to determine how widespread the organism is throughout the country. This coupled with the dormant nature of the MAP and the lack of symptoms in the sub-clinical phase of infection and the lack of reliable diagnostics, the control of the disease has proved to be almost impossible. With improved diagnostics and good herd management, the disease could be controlled. However there has been limited improvements in diagnostic methods (Collins et al., 2006), and also a recognised reluctance among farmers to introduced the necessary good management and hygiene schemes, so that control of the disease has remained limited (Cho et al., 2012).

Ideally a vaccine would be the best way to prevent or control this animal pathogen. Attenuated strains of MAP have been developed as possible vaccine candidates. However their efficacy as vaccine proved to be poor in reducing Johne's disease and resulted in severe side effects for the animals (Patterson et al., 1988, Heinzmann et al., 2008, Kohler et al., 2001). Another issue that has influenced the development and use of a MAP vaccine are reports that its use can affect the results of the tuberculin skin test used to detect Btb in cattle. Any cross reactivity of a MAP vaccine with the Btb test is not acceptable due to the greater importance and economic implications resulting from a failure to control

Btb (Waters et al., 2004). Thus to date the main methods of control are to cull any animal that has tested positive to Johne's disease and is showing clinical signs (see Section 1.3.2).

The Cattle Health Certification Standards body (CHeCS) has defined the industry standard screening and control programme for the control of Johne's disease. Calves that are born to animals suspected to have Johne's disease are immediately separated from their dams and are reared separately from the adult herd (Eddy, 2004). Hence it is vital to identify any clinical signs as early as possible to prevent the disease from being transmitted. As part of this scheme, vaccination can be used in herds where there is a high prevalence of Johne's disease and is administered to calves under one month in an attempt to break the cycle of infection (Eddy, 2004). As MAP can persist in the environment strategies such as removing animals from pasture that had Johne's infected animals on would be recommended. However limitations with space on farms may reduce the efficacy of this strategy to break the Johne's disease cycle.

1.3.3. Detection of *Mycobacterium avium* subsp. *paratuberculosis*

Due to the long incubation period and fastidious nature of the organism, MAP is extremely difficult to culture. However currently, the cultivation of MAP from faecal samples or tissue specimens is considered to be the most definitive method for determining whether an animal has Johne's disease and is still considered the Gold-standard in the diagnosis of Johne's disease (Nagata et al., 2013). The procedure requires 8–16 weeks of incubation of samples on Herrold's Egg Yolk Medium (HEYM) (Stabel, 1997), although faster liquid culture methods have been developed (see Section 1.3.3.2). When culturing slow growing mycobacteria, decontamination is often required to prevent overgrowth of competing microflora, however this can further reduce the number of viable cells in a sample and thus the sensitivity of the culture method (Grant et al., 2003,

Gumber and Whittington, 2007). Although Bower et al. (2010) has indicated that some decontamination methods may affect certain MAP strains more than others.

As well as the practical difficulties of culture, the long length of time required before results are gained makes control of the disease difficult. In the months it takes for MAP colonies to form, animals that may be infected could be shedding the organism into the environment. This results in more animals coming into contact with contaminated feed and potentially becoming infected with MAP.

1.3.3.1. Ziehl-Neelsen staining

The fact that mycobacteria have a relatively high proportion of mycolic acid in their cell wall means that they are resistant to conventional staining techniques (Glickman et al., 2000) and this means acid-fast stains are needed to identify them microscopically. The Ziehl-Neelsen stain (ZN; Fig. 1.2) is used routinely to confirm the presence of MAP in faecal samples or in tissue samples during the post-mortem examination of suspected cases of Johne's disease. The ability to retain dye after washing with acid (acid-fastness) is a relatively rare attribute for bacterial cells, thus the ZN stain can act as a good marker of Johne's disease infection if an animal is displaying characteristic symptoms of the disease. However there are limitations to the use of this stain, since all other species of mycobacteria are acid-fast the detection of acid-bacteria is not a definitive confirmation of the presence of MAP. For instance, members of the *Nocardia* genus, which can cause problems in lungs of cattle and invade macrophages in much the same way as MAP and other pathogenic mycobacteria (Lerner, 1996), are also acid-fast. Thus the acid-fast characteristic is not even completely specific for the genus *Mycobacterium* and therefore the ZN stain should not be relied upon on its own as a diagnostic tool and it also is limited by the same sensitivity issues that exist for all methods that require microscopic visualisation

of bacterial cells. Zimmer et al. (1999) reported this problem when they found that only the ZN stain had a sensitivity of 37 %, when compared to faecal culture when detecting MAP in clinically and subclinically infected cattle.

1.3.3.2. Improved culture methods

Faster methods for detecting MAP have been developed and sold commercially by companies such as Becton Dickinson who developed a radiometric method for detecting growth of MAP called BACTEC™ (which is now discontinued). This measured the release of ¹⁴C-labelled CO₂ as an indicator of the growth of mycobacteria in selective liquid media. Using the BACTEC™ system according to the manufacturer's literature, MAP growth and identification could be obtained from one to ten cells within seven weeks. Becton Dickinson also developed the Mycobacteria Growth Indicator Tube (MGIT) which is seen as a follow on to the radiometric BACTEC™. Due to the added complications of using radioactive materials a fluorescent system was developed. The MGIT culture system uses a proprietary medium (MGIT Para TB medium), that contains a fluorescent compound that is quenched in the presence of oxygen. Actively respiring microorganisms consume the oxygen leading to fluorescence and when MGIT tubes are placed on an UV transilluminator (365 nm wavelength) growth-positive tubes emit a vivid orange fluorescent at the tube base and at the meniscus, whereas growth-negative tubes show negligible or no fluorescence (Grant et al., 2003). Time to results according to the manufacturers is up to 21 days. Both of these rapid methods can detect pure cultures of mycobacteria quickly and sensitively. However the use of radioactive material in the BACTEC™ system meant that special disposal of materials was required. The BACTEC™ system also required expensive machinery to read and analyse the results, whereas the MGIT system that replaced it does not require expensive machinery and does not use radioactive materials. In addition (Fyock et al., 2005) found that MGIT proved to

be a robust culture system for bovine faecal samples. However it has also been noted that the radiometric BACTEC™ culture system remains the best alternative for the culture MAP from sheep compared to strains cultured from cows (Gumber and Whittington, 2007). Although the liquid culture systems have been shown to decrease the time it takes for MAP to grow (Grant et al., 2003), using them with faecal samples still requires the use of decontamination which can reduce the number of viable cells present and reduces the sensitivity of the method.

One problem of both the liquid culture-based system compared to growth of colonies on solid media, is that the identification of all strains of the organism in liquid media can be more difficult. The appearance of colonies and mycobactin-J dependence are not observable, and the growth of other organisms needs to be distinguished which again needs an end-point PCR (Whittington, 2009).

The use of these liquid culture assays allows vital time to be saved when using culture as the 'gold standard' method to identify the presence of viable MAP in a sample. An improved method has been developed that allows the more rapid confirmation of the presence of MAP in faeces (two weeks) and tissue samples from clinically affected animals (one week) using MGIT liquid culture. This represents a substantial improvement on traditional culture and identification methods (Cousins et al., 1995). However this was achieved by coupling a MAP-specific polymerase chain reaction (PCR) at the end of the culture period.

1.3.3.3. Use of ELISAs to detect host responses to MAP

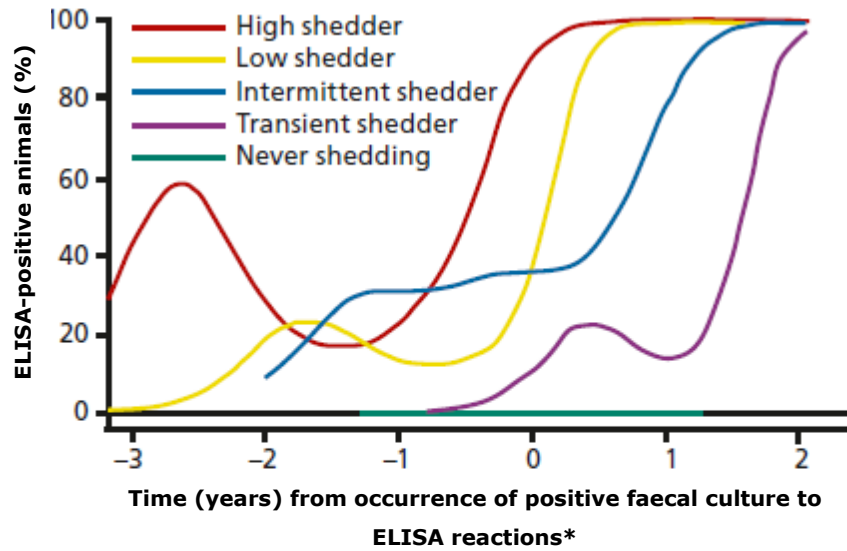
Enzyme Linked Immunosorbent Assays (ELISA) have also been developed commercially as a diagnostic tool for detecting MAP in animal samples. The MAP ELISA can be used to indirectly detect MAP infection based on analysis of blood, and milk samples by detecting the presence of antibodies raised against MAP by the animal. The ELISA test provides a high-throughput rapid turnaround time

when compared to the 'gold standard' method of culture. Its ability to detect MAP in different matrixes allows testing to be tailored to the farms and their practices and ELISA tests are inexpensive and can be easily automated for processing large numbers of samples (Juste et al., 2005).

The levels of sensitivity achieved by the commercial ELISA assays are variable and it is generally accepted that their sensitivity for the detection of infection in animals is only about 50% (Fig.1.5; Meylan et al., 1994). Sensitivities of both the milk and blood ELISA tests are highest for those animals in the later stages of the disease, usually when the animals develop clinical signs, however blood ELISA sensitivity for animals in the early stages of infection will be very low (<10%; where milk is generally not available for testing early in the dairy cattle's life). In fact, because of its low sensitivity, the blood ELISA test is rarely positive in animals under 2 years of age and frequently fails to detect individuals in the early phases of infection (Juste et al., 2005, Whitlock et al., 2000).

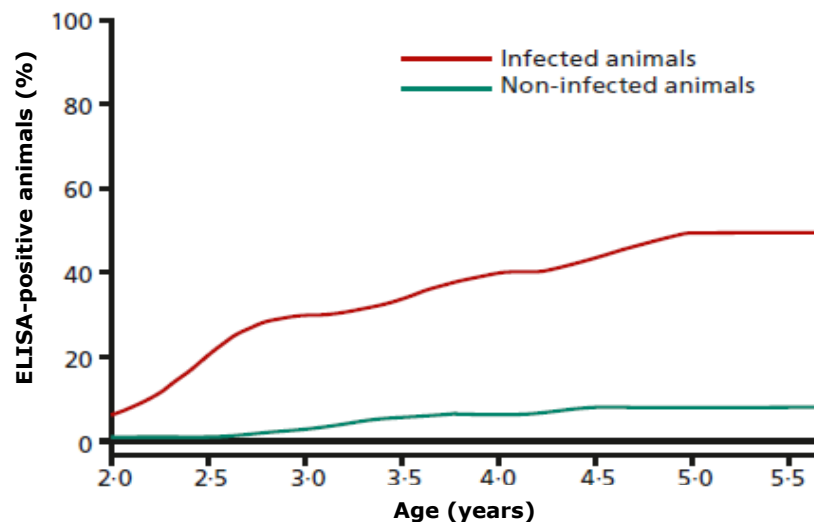
The performance of these tests are compromised by the variability of the immune response depending on the immunopathological form of the paratuberculosis infection, which is believed to occur due to the dormant nature of the organism (Juste et al., 2005; Table 1.1 and Figure 1.4). Although a study carried out by Pinedo et al. (2008) determined that the ELISA test was consistently better at detecting Johne's disease compared to faecal culture and faecal-PCR individually, only when the ELISA test was combined with the faecal-PCR was the overall sensitivity was improved.

Figure 1.4. Relative sensitivities of ELISA tests during different phases of Johne's infection



Graph showing percentage of cows testing positive using the Pourquier ELISA relative to the time they started shedding either high (red), low (yellow), intermittent (turquoise) or transient (purple) levels of MAP cells. Results for animals that never shed MAP are shown in green (Nielsen, 2009).

Figure 1.4. Probability of Johne's infected cows testing positive using milk ELISA



Graph showing the performance of a commercial ELISA kits demonstrating how the sensitivity of the assay increases as the age of cows increases. However even in older cows overall sensitivity is still very low and only around 50% are screened as positive (Nielsen, 2009).

1.3.3.4. PCR-based methods

The identification of the MAP-specific insertion element IS900 by Green et al. (1989) that occurs in multiple copies in the genome has enabled this organism that is notoriously difficult to culture to be detected rapidly using molecular PCR methods. Many primer sets have been described in the literature that target this MAP-specific insertion element and, compared to 'gold standard' culture-based testing, has allowed extremely rapid and specific detection of MAP in a variety of samples. However, like all PCR-based identification methods for bacteria, some cross-reactivity can be recorded and several studies have reported that PCR assays that target this IS900 element have given positive results with non-MAP cells. For instance Englund et al. (2002) isolated a *Mycobacterium* isolate that was IS900 PCR-positive but further investigation proved that it was not MAP. Similarly Cousins et al. (1999) also found that a *Mycobacterium* spp. isolated from the faeces of three clinically normal animals in two Australian states were also suspected to be MAP on the basis of IS900 PCR but classical identification methods indicated that they were not MAP.

To overcome this problem, other MAP-specific genes have been identified. A single-copy gene sequence named F57 has been shown to have no resemblance to other known genes and was specifically found in the genome sequence of MAP (Poupart et al., 1993). In addition the sequence of a gene named *hspX* was found to be *M. paratuberculosis*-specific and distinguished from related mycobacteria, including all closely related members of the MAC (Ellingson et al., 1998). Most recently ISMav2 was identified as another MAP-specific insertion sequence that shows no similarity to other known mycobacterial insertion elements (Strommenger et al., 2001).

All of these unique sequences have been used as a basis of a variety of methods to rapidly detect and identify MAP. However a review by Mobius et al. (2008) determined that, despite possibly being not as specific as other MAP

specific loci, nested-PCR assays based on *IS900* insertion sequences were the better target for MAP-specific amplification detection. Indeed many studies have optimised the primers sequence used for *IS900* PCR so that the region targeted is unique to MAP. This, combined with the increased sensitivity achieved when targeting a multi-copy gene, means that the *IS900* PCR is more widely used for MAP detection than any other gene target. Researchers have also extended the use of this region for use in quantitative real time-PCR (qRT-PCR) assays to allow quantification of the multi-copy element as well as detection (Moravkova et al., 2012).

Like the ELISA tests, specific-MAP PCR assays have been developed to be applied to testing many different matrixes including milk, blood and faecal specimens (Millar et al., 1996, Buergelt and Williams, 2004, Collins et al., 1993). However there are limitations associated with the use of PCR. First the viability of the cells detected is always questionable when using PCR to detect the cells, since DNA can be extracted from a cell whether or not it is viable and therefore PCR alone cannot differentiate between DNA extracted from live or dead cells. Although the issue of PCR and detecting viable cells is currently being addressed, for example Kralik et al. (2010) used propidium monoazide (PMA) treatment on cells to help differentiate between live and dead cells when using PCR. PMA will enter the cells with damaged membranes (I.e. dead cells) and bind to DNA. On exposure to light, the dye is photoactivated, which leads to irreversible modification of the DNA, which strongly interferes with subsequent PCR amplification. However limitations with MAP cells clumping, limit the ability to definitively distinguish between all the live and dead cells.

The amount of material used to extract DNA is a significant problem with PCR. In blood often low numbers of cells are present and without a large volume to test, the PCR sensitivity can be very limited. PCR inhibitors are also a major problem with using this molecular method, inhibitors present in faeces include

phytic acid and polysaccharides that can lead to false-negative results by inhibiting the amplification of DNA (Monteiro et al., 1997, Thornton and Passen, 2004), causing significant drops in the sensitivity of the test (Table 1.1). Often rigorous sample preparation is needed, especially with faecal samples, to remove inhibitors. A critical step in any direct PCR is the extraction method, but with a matrix such as faeces and an organism such as MAP (due to complicated cell wall), efficient extraction is particularly challenging (Leite et al., 2013).

Table 1.1. Summary of the different costs and sensitivities of Johne's disease diagnostic tests

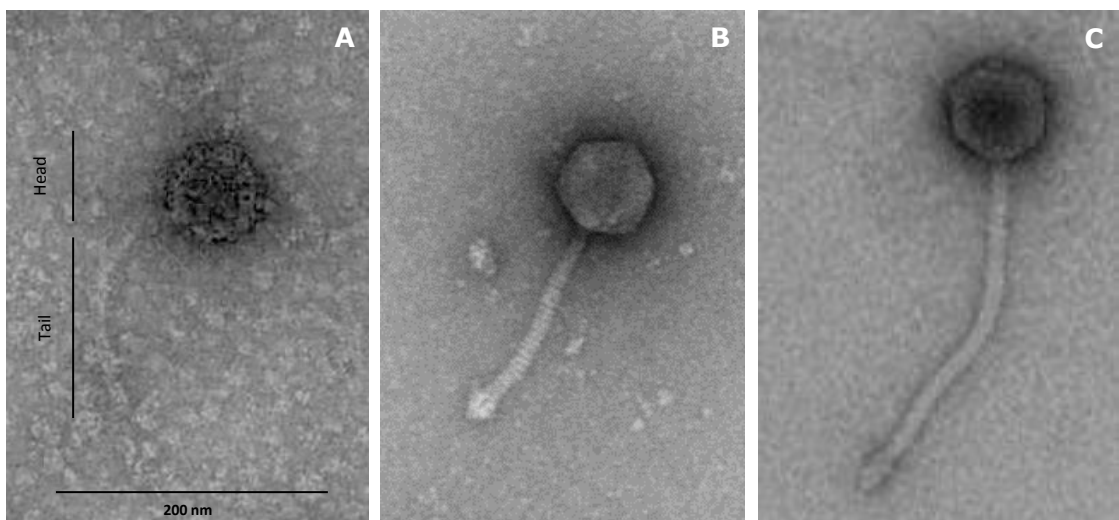
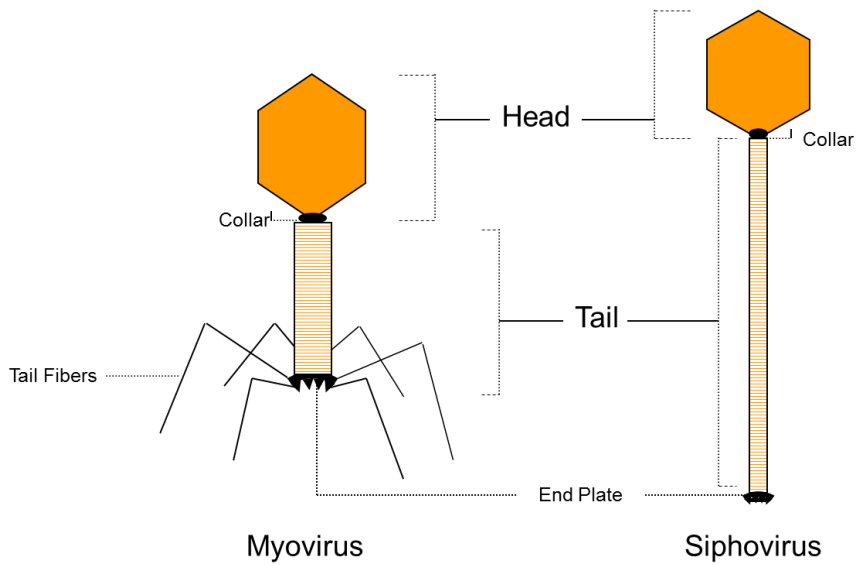
Test	Sensitivity	Cost	Comments
Faecal smear	10-30%	£12.00	Rarely useful due to prohibitively low sensitivity, although short turnaround time may occasionally be useful.
Serology (ELISA)	20-90%	£6.90	Cheaper and more sensitive than faecal smear.
Faecal culture	30-65%	£40.00	Considered the 'gold standard' pre-mortem.
Faecal PCR	35-65%	£24.65	8-12 day turnaround time, cheaper than culture.

Table gives figures for available diagnostic tests for Johne's. Costs are based on the Animal Health Veterinary Laboratories Agency (AHVLA) estimates (Hudson, 2008).

1.3.4. Bacteriophage

Bacteriophage (phage) are viruses that infect bacteria and are thought to be one of the most abundant organisms on Earth. The name bacteriophage literally translates as bacteria eater (phage is from the Greek 'to eat'). Phage have a very specific host range which can be either narrow and restricted to just a few cell types or broader and restricted to either specific species or genera. For example, the well-studied bacteriophage *Lambda* only infects members of the *Escherichia coli* species (Appleyard et al., 1956) whereas the phage which is used in this study, D29, infects many member of the genus *Mycobacterium* (Rybniker et al., 2006). Bacteriophage are generally grouped into families depending on three characteristics: capsid structure, absence/presence and structure of the tail and nucleic acid type. These features are used as the basis of morphological characterisation of phage and the majority of phage used to develop diagnostic methods fall into two morphological groups: the *Myoviridae* and the *Siphoviridae*. Both of these groups have double-stranded DNA genomes packaged into an icosahedral capsid. Ninety-six percent of all bacterial viruses possess tails and various tail structures have been described (Brussow and Hendrix, 2002). The *Siphoviridae* have simple, long, non-contractile tails, and the *Myoviridae* possess rigid, contractile tails and additional tail fibres. Phage structure is not indicative of either host range or life cycle (see Section 1.2.4.1 below); for instance both *Lambda* and D29, are members of the *Siphoviridae* family but infect completely different types of host cell (Gram negative and acid-fast, respectively; and phage *Lambda* is lysogenic whereas D29 is a lytic phage. The two main mycobacteriophage used in this study are both well described lytic Siphoviruses specific for members of the *Mycobacterium* genus: D29 and TM4 (Figure 1.5).

Figure 1.5. Structure of Bacteriophage



Upper diagram: generalised structure of Myovirus and Siphovirus (taken from Rees et al., in press). Shown below are EM images of two *Siphoviridae* bacteriophage, used in this project. Images A (B. Swift) and B (PhagesDB.org) are bacteriophage D29 and image C is phage TM4 (PhageDB.org) where the genetic material is encased in a protein capsid (or head). Structures in the tail baseplate attach to specific receptors on the host's cell surface. The Siphoviridae have non contractile tails and the genetic material travels through the tail sheath as it enters the host.

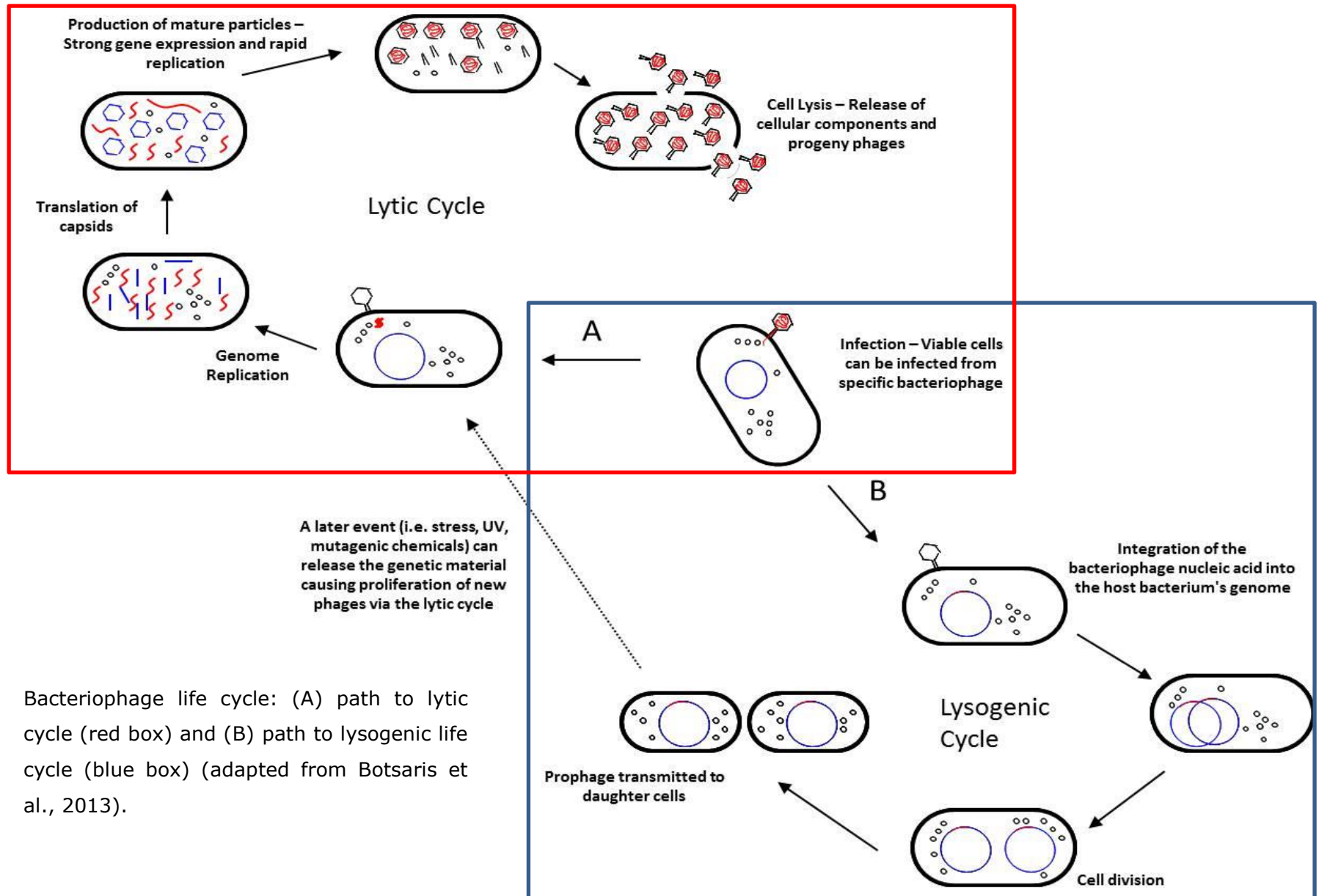
1.3.4.1. Phage life cycles

Bacteriophage can also be separated into two groups according to their life cycle. The simplest are lytic bacteriophage. Like many eukaryotic viruses, these phage take over their host cell and use its cellular machinery to replicate themselves many times and eventually the progeny phage are released from the cell by inducing cell lysis (hence they term lytic phage; Fig. 1.6). Once obligate lytic phage comes into contact with their host cell, they are committed to the lytic replication pathway. After inserting their genomic material into the host cells, the first step is to produce additional copies of the phage genome. Next the structural proteins for the head and tail are then made, and the phage DNA is then packaged into the capsids and the mature phage is assembled. Finally the bacteriophage then expresses proteins required for them to lyse the host cell (holins and lysins). The expression of these proteins is controlled, so that they act like a molecular clock for the phage, to enable them to keep their host intact until all the new phage particles are formed and can be released at the right time (Shi et al., 2012). Holins, as their name suggests, create holes in the membrane that allow the lysins to access the cell wall and break open the cell. Lysins are enzymes that attack the host cell peptidoglycan and generally consist of cell wall binding domain and a cutting domain (Hagens and Loessner, 2007). The cell wall binding domain directs the cutting domain to the correct site of action in their host's cell wall allowing rapid destruction and lysis of the host. The number of phage particles released is variable, but generally up to a hundred progeny phage are released per infected host cell. The time taken for the phage, once inside their host, to replicate and lyse is known as the eclipse phase.

The second are temperate or lysogenic bacteriophage that can either act as lytic phage and lyse their host cell after replication or can become dormant within the cell, forming a prophage (Fig. 1.6). In the prophage state, the phage does not harm the host cell and the phage genome is replicated along with that

of the host so that more copies of the virus are produced at each cell division of the host. This relationship can be beneficial to the host by aiding bacterial survival, giving it immunity against infection by similar phage, as well as increasing virulence (e.g. botulinum toxin) by providing additional genes that allow the bacterium to infect new animal hosts (Jackson et al., 2011).

Figure 1.6. The lytic and lysogenic life cycle of bacteriophage



Bacteriophage life cycle: (A) path to lytic cycle (red box) and (B) path to lysogenic life cycle (blue box) (adapted from Botsaris et al., 2013).

1.3.4.2. Bacteriophage-based detection

The discovery of bacteriophage at the turn of the 20th century has led to many applications for phage being developed. Initially they were applied as therapeutics, but their use in the western world was eclipsed by the discovery of antibiotics and further research in the area was limited. However recently, mounting concerns about drug-resistant pathogenic bacteria have rekindled interest in alternative treatments of bacterial infections (Bull et al., 2002).

More promising has been the use of bacteriophage as novel agents to detect bacteria. The ability to specifically bind to cells and infect them has led to many technologies being developed that have provided a wide range benefits to be generated from phage. The first application to be developed was phage typing. Here the specific host range of phage has been shown to be beneficial for developing a system of identifying different strains of bacteria from within the same species or genus. Although laborious with the need to use agar plates and to maintain phage stocks, phage typing for many years has proved invaluable in epidemiological studies, and has been used extensively to map certain strains of *M. tuberculosis* and to help determine contamination potential within reference laboratories (Jones et al., 1982, Snider et al., 1984). Although a very powerful tool, the use of phage typing and other phenotypic typing methods have become overshadowed by molecular tools used to type bacteria, and even now with cost reduction of DNA sequencing it is possible that this will become the sole laboratory diagnosis (Schurch and van Soolingen, 2012).

1.3.4.3. Reporter phage technology

Reporter bacteriophage detection uses phage that have been engineered to carry a reporter gene, this produces a signal that can be measured. A variety of different reporter genes have been used, including luciferase, fluorescent proteins, and more common enzymatic reporter genes, such as beta-

galactosidase (Goodridge and Griffiths, 2002). Generally the technology works on the principal that when the reporter-engineered bacteriophage infects their target it will express the reporter gene to indicate that infection has occurred. If the phage are able to replicate, they will reproduce and the signal should be amplified as the number of phage increases thus increasing the sensitivity of the result. The system will only work on viable hosts, which is why much of the technology has been used to target food borne pathogens (live-dead differentiation is vital to determine efficacy of food safety processing). However, there are draw-backs to using the technology. The signal to noise ratio will always have to be optimised to distinguish infected hosts and many substrates produce background levels of fluorescence that reduce the sensitivity of the tests.

Several different species of bacterium have been detected by reporter phage technology, such as: *Listeria* (Loessner et al., 1996), *E. coli* (Goodridge et al., 1999), *Salmonella* (Turpin et al., 1993) but the majority of studies have been on developing reporter phage to detect mycobacteria (Riska et al., 1999, Sarkis et al., 1995). The LRP developed for the detection of mycobacteria contained firefly luciferase as the reporter gene (Jacobs et al., 1993). The lytic phage TM4 was initially used, however the limit of detection was only 1×10^4 mycobacterial cells (Jacobs et al., 1993). A LRP based on the temperate phage L5 (where D29 is genetically derived from), prolonged expression and accumulation of the luciferase protein which improved the sensitivity of detection to 1×10^2 cells after a 40 h incubation period. This is because of the temperate nature of L5, where it's genome (along with the reporter gene) are integrated and subsequently amplified allowing an increase in the light signal (Sarkis et al., 1995). The LRP assay when optimised (removal of phage inhibitors and improving L5 stability within their host) has been shown to successfully detect mycobacteria in smear-positive sputum samples within 24-48 hours as well as

being able to detect the mycobacteria as sensitively as standard microbiological testing methods such as MGIT (Riska et al., 1997, Bardarov et al., 2003).

1.3.4.4. Phage amplification detection

Phage amplification technology is based on the ability of the bacteriophage to increase in number after infecting their target cell. However unlike the reporter phage, in this case the phage particles are detected rather than genes expressed by the infected phage. In the phage amplification assay, a positive indication of the presence of bacteria is the formation of plaques (zones of clearing) at the end of the assay, and in theory each plaque represents one target bacterium originally infected. The use of phage amplification has been used to detect antibiotic resistant *Staphylococcus aureus* from blood cultures (MicroPhage KeyPath MRSA/MSSA Blood Culture test). The test works by detecting the amplification of *S. aureus* specific bacteriophage in the presence of an antibiotic. If the phage are detected the bacteria is resistant to antibiotics as they are metabolically active (phage can only infect and replicate within an active host; Bhowmick et al., 2013).

One particular form of phage amplification technology was developed to detect mycobacteria, as a commercial product, the *FASTplaqueTB*TM (FPTB) assay and, as this forms the basis of the research described in this thesis, this assay will be reviewed in more detail.

The FPTB assay was originally developed to detect Mtb cells in the sputum of individuals suffering from tuberculosis. It is a rapid test that can detect viable mycobacteria within 48 h and does not require a skilled operator or specialised equipment, making it an ideal assay to use in developing countries where TB is still a major problem.

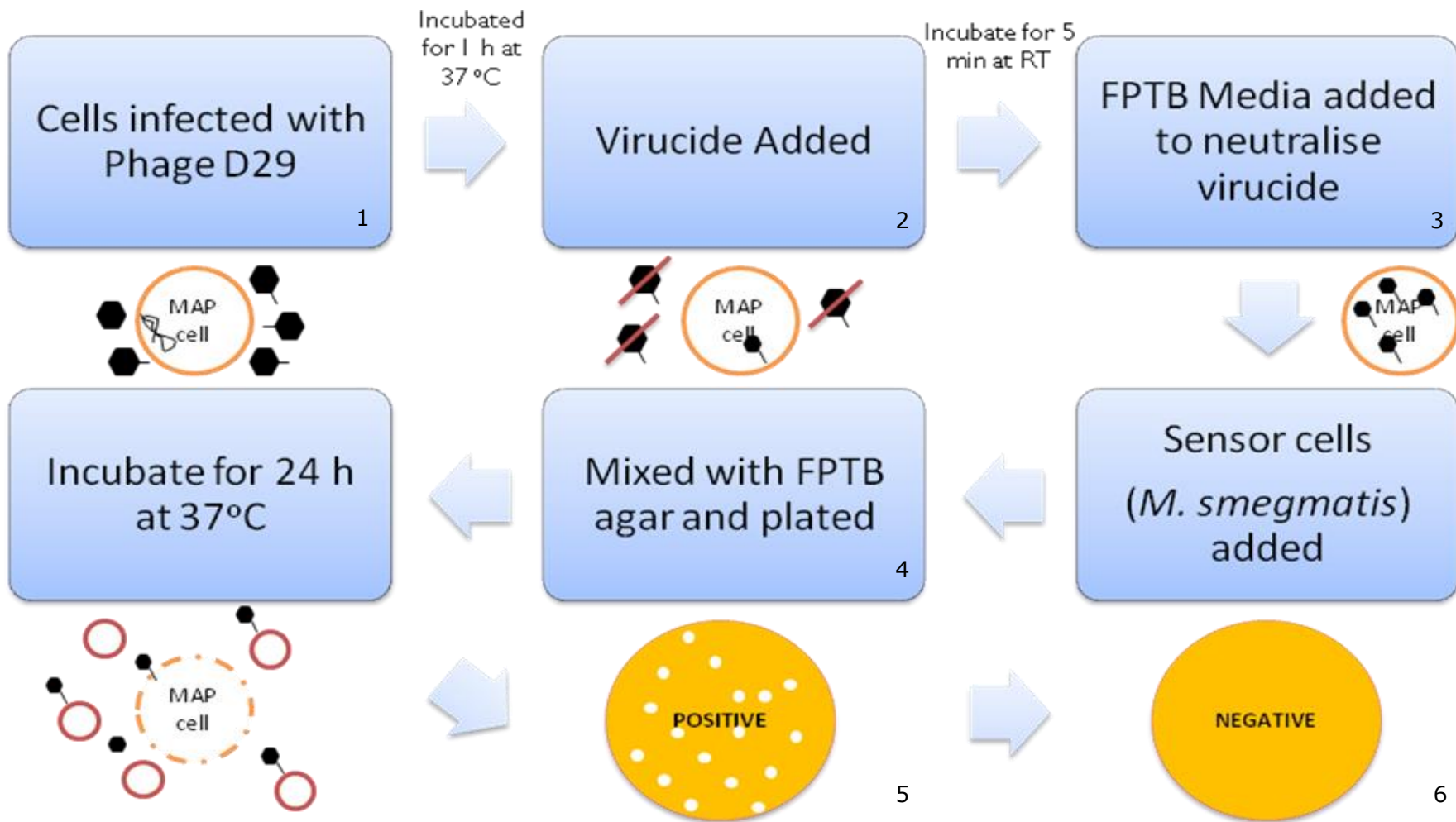
This assay uses mycobacteriophage D29 (Fig. 1.5) and this phage is closely related to a well-documented temperate phage L5 (Hatfull and Sarkis, 1993).

However deletions in the D29 genome mean that its ability to enter the lysogenic cycle has been lost (Ford et al., 1998). Thus mycobacteriophage D29 is an obligate lytic phage that infects both fast and slow-growing mycobacterial species (Ford et al., 1998). An interesting attribute of phage D29 is that it has the ability to infect a wide range of organisms from the genus *Mycobacterium* (Rybniker et al., 2006) and this has been exploited when developing the FPTB assay. As Mtb grows so slowly, forming a lawn to support the growth of phage plaques to detect the infection event is not practicable. Since phage D29 is also able to infect fast growing species of mycobacteria, such as *M. smegmatis*, this is used to form lawns of bacteria on agar plates to detect infected Mtb cells within 24 h.

The FPTB assay (Fig. 1.7) is performed by firstly mixing a sputum sample suspected to contain Mtb with mycobacteriophage D29 and then incubating to allow phage infection. After this any extracellular phage that have not infected a susceptible host bacterium, are destroyed by a virucide (in the case of the FPTB assay ferrous ammonium sulphate is used, however other virucides have been described for use in such assays; de Siqueira et al., 2006). The sample containing an infected Mtb cells is then diluted, which reduces the concentration of the virucide to below the effective concentration, and then pour plated with *M. smegmatis* cells that will form the mycobacterial lawn to support the growth of phage plaques. If Mtb cells are present in the sample, they will lyse that cell and infect the growing *M. smegmatis* cells in the lawn, such that plaques are produced, indicating that an infected Mtb cell was present (a positive result; Fig. 1.7). If no viable Mtb cells are present in the sample, no plaques are formed. The FPTB assay proved to be a sensitive, low cost relative to the PCR offering more rapid diagnosis in comparison with culture-based methods (Marei et al., 2003).

The assay has been adapted to perform a range of different functions other than just detection of Mtb. With drug resistant Mtb becoming more prevalent, the need to identify these strains quickly is extremely important. Resistance to rifampicin (a frontline bactericidal antibiotic used to treat TB) involves alterations of the *rpoB* gene that codes RNA polymerase (Telenti et al., 1993) and the resistance to rifampicin is considered as a surrogate marker for the identification of multi-drug resistant Mtb (Lemus et al., 2005). The FPTB assay has been modified to produce a rapid test for identifying rifampicin resistance, enabling rapid and appropriate management of patients with drug-resistant TB (Albert et al., 2004). The principle is the same as that for the Microphage MRSA *S. aureus* test. The Mtb cells were exposed to rifampicin, and if resistant would remain metabolically active, whereas if they were sensitive they would die. Only the metabolically active cells support phage replication so if original Mtb cells are resistant plaques will form at the end of the assay. The antibiotic resistance assay only works with bactericidal antibiotics, and does not work well for bacteriostatic antibiotics such as isoniazid (INH) as only the mycobacterial cell growth is arrested, so phage will infect both sensitive and resistant strains.

Figure 1.7. Overview of the *FASTPlaqueTB*TM assay



The *FASTPlaqueTB*TM assay was originally designed for the identification of Mtb from human sputum samples. It is executed by firstly inoculating a suspected sample with mycobacteriophage D29 [1]. This is incubated for 1 h at 37 °C. A virucide is then added to destroy any extracellular phage [2]. Phage that have infected their host are protected by the cell wall. The virucide is then neutralised by the addition of Media Plus [3]. The sample is then plated with sensor cells (*M. smegmatis*) and *FASTPlaqueTB-Agar*TM [4]. This is then left to set and incubated at 37 °C for 24 h. Mtb cells infected with phage will lyse and progeny phage will infect the sensor cells forming plaques on the lawn [5]. Samples with no Mtb cells will not form plaques and a lawn of sensor cells is seen [6].

1.3.4.5. The FASTPlaqueTB™ Assay and MAP

The broad host range of mycobacteriophage D29 allows the assay to be adapted for use with other pathogenic mycobacteria such as *M. bovis* and MAP. The use of the assay to detect viable MAP in a veterinary setting has been investigated. However due to the broad host range of D29, when testing samples especially from a farm setting, detectable environmental mycobacteria may present, more so than in a sputum sample of an individual with TB. Thus an additional step had to be taken introduced to confirm the identity of cell being detected. A MAP specific PCR has been used routinely to determine the identity cell detected from the phage assay when testing milk and cheese (Stanley et al., 2007, Altic et al., 2007, Botsaris et al., 2010). Stanley et al. (2007) described a plaque-PCR, which involves picking a plaque that has formed from the FPTB assay, extracting the DNA and subjecting it to PCR. The plaque formed would have the DNA of the original mycobacteria infected preserved in the middle. The FPTB assay with the PCR was able to detect and specifically identify viable MAP cells within 48 h.

Further developments to the assay have been on going and there have been many improvements. Rees and Botsaris (2012) described how the FPTB assay can be used to enumerate MAP to be used as a tool in the laboratory and in the field, giving investigators valuable insight into the viable bacterial load of MAP infected samples, which is especially useful in potentially identifying super shedders in a herd. By being able to detect the number of viable cells released in to their milk could help control the vertical spread of the disease (Aly et al., 2012).

The FPTB assay has also been developed to be used in conjunction with a specific peptide mediated magnetic separation (PMMS) to remove MAP cells from a phage inhibitory environment to one where phage infection is supported. Peptides initially identified by Stratmann et al. (2002, 2006) using phage display

have been bound to magnetic beads, the beads were then mixed with samples to capture MAP cells in them. MAP cells had then been taken from milk and faecal samples gently, using a magnet and resuspended in a better environment. This enables the vast majority of contaminating microorganisms and inhibitors to be removed and the phage amplification assay enables rapid enumeration of viable MAP cells within 24 h (Foddai et al., 2010). The great benefit of using the magnetic beads, means that decontamination of samples does not need to happen, as cells bound to the beads can be washed to remove as much background microflora as possible. What is more, the ability to capture cells on beads allows samples to be concentrated (Foddai et al., 2011). This is important when it comes to the sensitivity of tests, as by having more sample to test increases the chances of detecting cells in low numbers.

In combination these very different methods of detection offer novel ways to rapidly detect MAP in many different matrices. These advances have allowed the identification of viable MAP to be made rapidly and can potentially be used to control the spread of the disease on farms. However the fact remains the tests used on their own are poor at identifying sub-clinically infected animals. Fast and early identification is required to combat this endemic disease and reduce its impact on agriculture. Therefore more work into better, sensitive diagnostics needs to be carried out.

1.4. AIM

From a survey of the literature, one of the main problems with MAP is that it is very difficult to detect with a high sensitivity. The long incubation period between infection and clinical disease means MAP cells can be contaminating the environment for years before detection, possibly infecting a large proportion of the herd. The financial losses from lower milk yield, meat quality and general price per head can be detrimental to a farmer. Therefore a rapid reliable test for

Johne's disease is required. It is known that MAP cells can be shed in milk and can become systemic and can be cultured from blood (Bower et al. 2010). The best way of testing for MAP cells is by using a combination of tests.

Thus the first aim is to develop a rapid test to detect viable MAP within 48 h that will offer a better alternative method for detecting Johne's disease, as the phage assay will detect whole viable cells rather than an immune response by way of ELISA testing. We aim to initially optimise the FPTB assay for use on MAP cells combined with a plaque-PCR to rapidly, sensitively and specifically detect the organism experimentally in blood. Once optimised, the assay will be used to determine whether MAP cells are circulating in blood samples of clinically infected cattle and if so determine how early, at what stages of the disease and how many MAP cells can be detected. By using a phage assay we hope to be able to detect viable cells within 24 h and confirm their identity with a PCR within 48 h.

The second aim is to use the MAP-specific peptides used for PMMS to construct recombinant fluorescent fusion peptides that will specifically label MAP cells so they can be visualised with fluorescent microscopy. The hypothesis we wish to test is that the fluorescent peptides will bind to the MAP cells specifically and not interact with other mycobacteria, whereas insensitive acid-fast staining methods such as the ZN stain will detect all acid-fast mycobacteria.

CHAPTER 2

MATERIALS, METHODS AND STANDARD PROCEDURES

2.1. GENERAL MEDIA AND REAGENTS

2.1.1. Culture and growth conditions

2.1.1.1. In house Herrold's Egg Yolk Media (HEYM)

One litre of this media was made by; dissolving 9 g of peptone (Oxoid, UK), 4.5 g sodium chloride (Fischer Scientific, UK), 1 ml of 10% sodium hydroxide (Fischer Scientific, UK), 2.7 g of Lab-lemco (Oxoid, UK), 25 ml of glycerol (Fischer Scientific, UK) and 9 g of agar (Fischer Scientific, UK) in 870 ml of sterile RO water. This was sterilised at 121 °C for 15 min. A 10 ml solution of 400 g/l sodium pyruvate was made and sterilised at 121 °C for 15 min. The yolk of six eggs (approximately 150 ml) was mixed well with 5.1 ml of 2 % malachite green dye. This was slowly heated in a water bath to 56 °C and held at this temperature for 1.5 h. These components were all mixed together under sterile conditions at 56 °C.

Several supplements were prepared. Penicillin G (Duchefa Biochemie, Germany) at a final concentration of 200 units ml⁻¹, Chloramphenicol (Sigma, UK) at final a final concentration of 50 µg ml⁻¹, Amphotericin B (Sigma, UK) at a final concentration of 50 mg ml⁻¹ and Mycobactin J (Synbiotic Corporation, France) at a final concentration of 2 µg µl⁻¹. These were aseptically mixed thoroughly with the previously prepared media. To act as a control HEYM without Mycobactin J was made. MAP requires this supplement to grow and therefore if nothing grows on the HEYM without Mycobactin J but on the HEYM with Mycobactin J, then the organisms growing can be assumed confidently that they are MAP.

The supplements were mixed with the sterilised mixture. The molten HEYM, with all the components, with and without Mycobactin J was then dispensed into either vials at a slant to make up slopes or into Petri dishes and left to set. This was all carried out in a laminar flow cabinet.

2.1.1.2. Commercial HEYM (Becton Dickinson, France)

Quality tested HEYM slopes purchased from Becton Dickinson were also used as a comparison to the in-house made HEYM. This was to confirm the HEYM made in-house was made up to the right specification. This was because the potential 16 week incubation period where the organisms grow is a long time. Thus the media used would have to be at a good standard.

2.1.1.3. HEYM inoculation

The prepared HEYM slopes were inoculated with 100 µl of MAP cells in a class 2 biosafety cabinet under strict aseptic conditions. The caps of the slopes were loosely placed on the HEYM slopes and left in the 37 °C for one week. After this time if no colonies had formed contamination could be ruled out and the lids tightened and Nesco film placed around the lids to prevent dehydration of the media. The sealed tubes were placed back in the 37 °C incubator. After a month the slopes were removed every week within a 16 week period to check for growth. If small 'cauliflower' shaped colonies formed the sample was positive for MAP cells.

2.1.1.4. Middlebrook 7H10 and 7H9 mycobacteria culture

All mycobacteria were sub-cultured and maintained every two months on Middlebrook 7H10 agar and Middlebrook 7H9 media (Becton Dickenson, France) by dissolving 9 g of media in 1 L of RO water and sterilised by autoclaving at 121 °C for 15 min. When culturing MAP, the media was supplemented 2 mg ml⁻¹ of Mycobactin J (Synbiotic Corporation, France). All cultures were incubated statically at 37 °C.

2.1.1.5. Slope wash

When trying to detect whether extremely slow growing organisms are present on agar, a slope wash and then PCR can be performed to detect the genomic DNA of any organisms that may be present. To perform the slope wash, 1.5 ml of PBS was added to the slope of the agar. Using a transfer loop, the surface of the agar was gently scraped. This was then vortexed 30 s. The liquid was removed and sample centrifuged at 16000 x *g* for 10 min. The pellet was then suspended in water for crude cell lysis and PCR.

2.1.2. FASTPlaqueTB™ assay media and reagents

2.1.2.1. Media Plus

The Media Plus (Middlebrook 7H9-based medium) was prepared by dissolving one sachet of FASTPlaqueTB™ Media Plus (MP) into 270 ml of RO water. This was sterilised by autoclaving at 121 °C for 15 min.

2.1.2.2. Virusol

One tablet of Virusol (virucidal component is ferrous ammonium sulphate) was dissolved under aseptic conditions into 5 ml of sterile RO water.

2.1.2.3. Actiphage

Free-dried mycobacteriophage D29 was reconstituted by adding 1.1 ml sterile MP. This was agitated until a uniform suspension of phage was achieved.

2.1.2.4. Sensor cells

Free-dried Sensor cells (*M. smegmatis*) were reconstituted with 11 ml of sterile MP. This was agitated until a uniform suspension of cells was achieved. This resulted in a final concentration of 10⁸ cfu ml⁻¹ and pfu ml⁻¹.

2.1.2.5. *FASTPlaqueTBTM* Agar

One sachet of *FASTPlaqueTBTM* agar was dissolved into 60 ml of RO water. This was sterilised at 121 °C for 15 min. The molten agar was stored at 50 °C until used. The *FASTPlaqueTBTM* agar was cooled to hand temperature before use.

2.1.3. The *FASTPlaqueTBTM* assay

2.1.3.1. Controls

Using the reconstituted Sensor cells, a series of 10-fold dilutions was carried out aseptically into sterile MP to gain a final Sensor cell concentration of 10^{-6} cfu ml⁻¹. This was used as the positive control. The negative control was 1 ml of sterile MP (Fig 2.1).

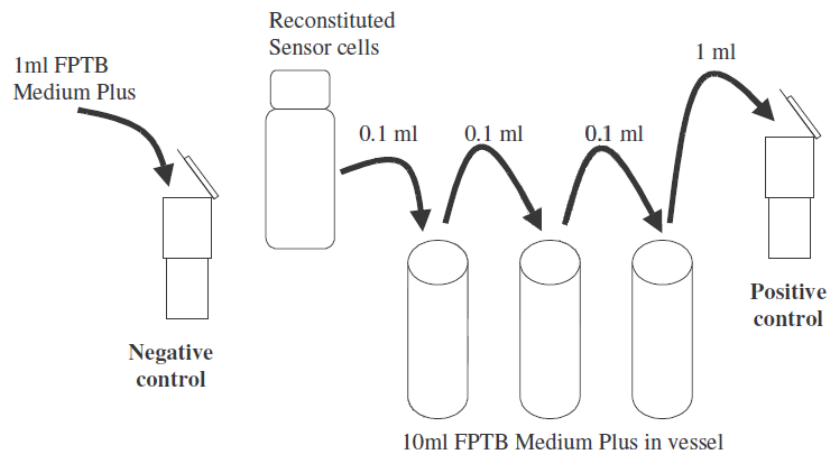
2.1.3.2. *FASTPlaqueTBTM* assay

Sample of 1 ml were used for each FPTB test and samples were placed in reaction vessels. One-hundred micro litres of reconstituted Actiphage (Section 2.1.2.3) was directly added to each sample aseptically to infect any mycobacteria that may have been in the sample, as well as being added to negative and positive control vessels (Section 2.1.3.1). The reaction vessels were incubated for one hour at 37 °C. After the incubation period, 100 µl of Virusol (Section 2.1.2.2) was added to the sample to neutralise any phage in the sample that had not infected any Mycobacteria. The samples were incubated at room temperature whilst rotating to cover the surfaces of the reaction vessel for 5 min. To neutralise the Virusol, 5 ml of MP was added to each sample. After the Virusol neutralisation, each sample was inoculated with 1 ml of reconstituted Sensor cells (Section 2.1.2.4) and these were poured into sterile labelled petri dishes. The samples were mixed gently with 6 ml of FPTB agar (Section 2.1.2.5)

and were left to set at room temperature. The plates were inverted and incubated for 24 h at 37 °C.

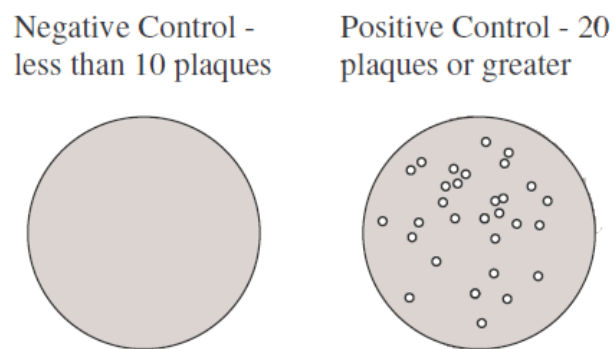
To determine whether the assay and its reagents had worked, the positive control after incubation should have more than 20 plaques (Fig 2.2). The negative control should have less than 10 plaques (Fig 2.2). The number of plaques from the samples was accepted as true and positive if over 20 plaques had formed on the plates. For a schematic representation of the Assay, see Figure 2.3.

Figure 2.1. Schematic diagram of the preparation of controls used in the FASTPlaqueTB™ assay



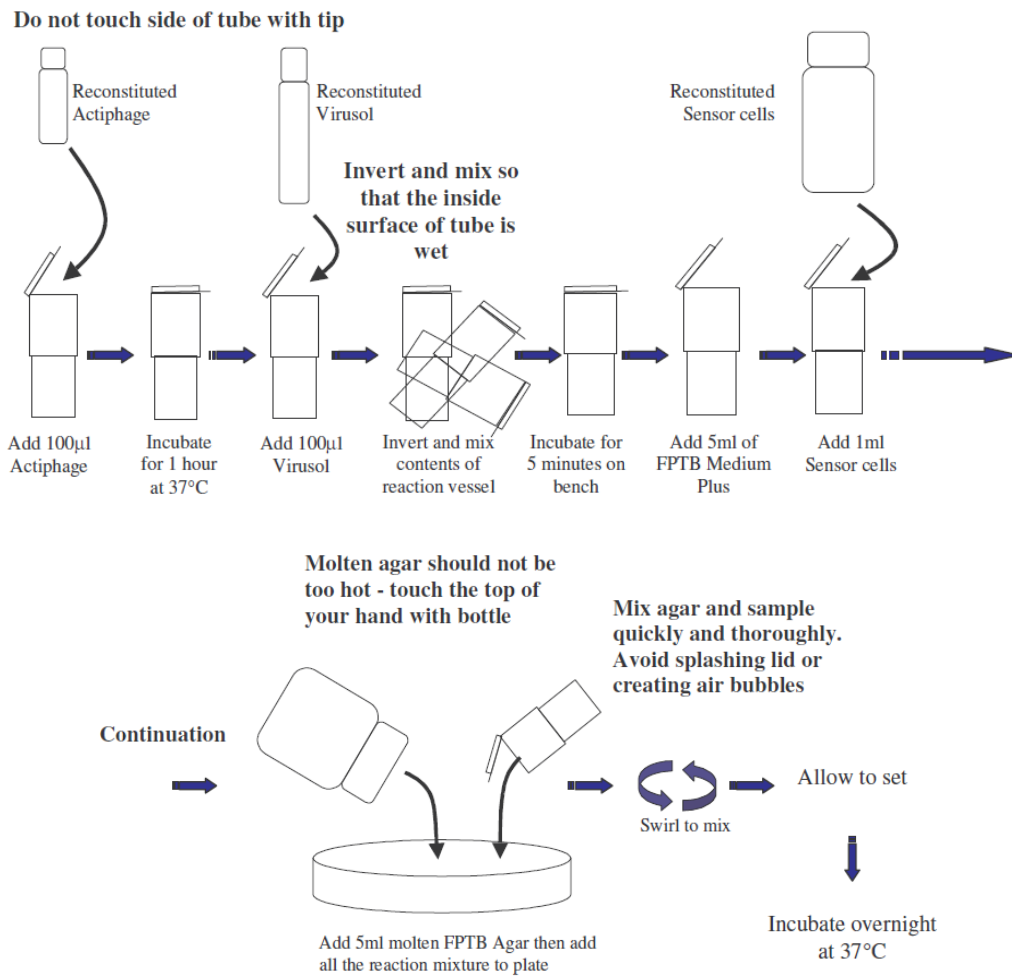
The negative control was prepared by adding 1 ml of FPTB+ into a reaction vessel. The positive control was prepared by diluting down reconstituted sensor cells by factor of 10^{-7} . One millilitre was then used as the positive control. Diagram sourced from *FASTPlaqueTB™* manual.

Figure 2.2. An example of positive and negative control plates



Less than ten plaques must form on the negative control plate and greater than 20 plaques must form on the positive control plate for the results from the assay to be accepted. Diagram sourced from *FASTPlaqueTB™* manual.

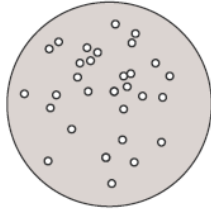
Figure 2.3. Schematic diagram of the *FASTPlaqueTB*TM assay



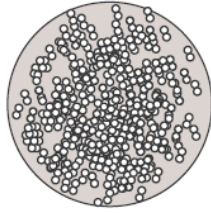
Each sample is inoculated with 100 µl of Actiphage. The sample is then incubated for 1 h at 37 °C. Virusol (100 µl) is added to the sample and incubated at room temperature whilst spinning for 5 min. 5 ml of MP is added to neutralise the virucide and 1 ml of Sensor cells added to the sample. This is poured into a petri dish with cooled molten FPTB agar, mixed and left to set. The plates were incubated for 24 h (48 h if needed) at 37 °C. Diagram sourced from *FASTPlaqueTB*TM manual.

Figure 2.4. Interpretation of the results from the *FASTPlaqueTBTM* assay

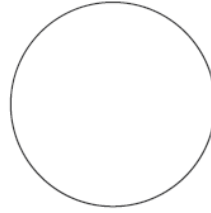
Positive Specimen -
20 plaques or
greater



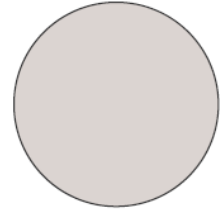
Positive Specimen -
confluent lysis - 20
plaques or greater



Positive Specimen -
complete lysis - 20
plaques or greater



Negative Specimen -
less than 20 plaques



Each plate represents different results that may be gained from the assay. With more than 20 plaques meaning a positive result, less than 20 plaques is a negative result. Diagram sourced from *FASTPlaqueTBTM* manual.

2.1.3.3. *Mycobacteria enumeration using the FASTPlaqueTB™ assay*

An enumeration step was worked into the protocol to allow the plaque forming units (pfu ml⁻¹) to roughly determine the amount of Mycobacteria originally in a sample. This was achieved by either diluting the sample either before carrying out the assay, or after adding the 5 ml of Media plus to the sample to neutralise the Virusol. A series of 10-fold dilutions were carried out to gain a countable amount of plaques (20-100) on one plate. Then using the equation (see below) the pfu ml⁻¹ was calculated.

$$pfu\ ml^{-1} = \frac{\text{Number of plaques} \times \text{Dilution Factor}}{\text{Amount plates (ml)}}$$

This calculation makes the assumption that each plaque that forms on a plate is made from the one cell (similar to cfu ml⁻¹). However it is only estimate as cells may be overlapping or clumping together (which mycobacteria tend to do) thus it was treated as a guide to the cell number.

2.1.4. Bacteria strains

Table 2.1. Table of bacteria strains used during this project

Bacteria	Strain	Ref
<i>Mycobacterium avium</i> subsp. <i>paratuberculosis</i>	ATCC 19851	Type Strain
	DVL 943	National Veterinary Lab, Denmark
	B4	Field Isolate NI
	K10	Type Strain
<i>Mycobacterium bovis</i> BCG	Glaxo	Glaxo Vaccine Strain
	Pasteur	Type Strain
<i>Mycobacterium smegmatis</i>	FPTB strain	Lab21
<i>Escherichia coli</i>	Top10 (Invitrogen)	Cloning Strain
	BL21 (DE3)	Expression Strain
	BL21 (DE3) pLysS	Controlled Expression Strain

2.2. MAGNETIC SEPARATION OF MAP

2.2.1. Preparing magnetic beads

Magnetic beads (Dynabeads - MyOne Tosylactivated, Invitrogen) were prepared and coated with either of the two peptides (supplied by Cambridge Peptides Ltd, UK); aMp3 and aMptD (Stratmann, 2002; 2006 respectively). I.e. half of the beads were coated with aMp3 and the other with aMptD.

The Magnetic beads were stored at 2-8 °C until required. The peptides were kept stored at -20 °C. To coat the beads, 50 mg (final concentration 500 µl/ml) of the uncoated beads were placed in a sterile microcentrifuge tube. The beads were washed with 1 ml of 0.1 M sodium borate, pH 9.5. Using a magnetic rack the beads were separated from the sodium borate for 2 min and sodium borate was removed. This wash step was then repeated. The washed beads were suspended in 100 µl of 0.1 M sodium borate pH 9.5 and mixed thoroughly by vortexing for 30 s. A further 735 µl of 0.1 M sodium borate, pH 9.5 was added to the beads and this was mixed again for a further 30 s. After mixing, 2 mg of biotinylated peptide suspended in 60 µl of sterile distilled water was added to the beads. This was mixed briefly using a vortex. 415 µl of 3 M ammonium sulphate was added to the sample and mixed. The final solution was placed on a DYNAL MPC-5 magnetic particle concentrator rotating mixer at 10 rpm at 37 °C for 24 h. After incubation the coated beads were washed twice with 1 ml of PBS pH 7.4 and separated using the magnetic rack. The washed coated beads were finally suspended in 1 ml of PBS pH 7.4.

2.2.2. Peptide mediated magnetic separation (PMMS)

This method was adapted from Grant *et al.* (2000). Sterile microcentrifuge tubes were filled with 1.5 ml of sample for testing. 10 µl (5 µl of peptide aMp3 and 5 µl of peptide aMptD) of freshly peptide coated magnetic beads (Section 2.2.1) were added to the sample. The sample was incubated in an Invitrogen

Dynal MPC-5 Magnetic particle concentrator, rotating at 18 rpm at room temperature for 30 min.

The microcentrifuge tubes were placed on magnetic rack for 10 min to recover the beads. The racks were agitated after five minutes to improve separation. The supernatant was gently removed; being careful to not disturb the beads adhered to the side of the microcentrifuge tube. The beads were suspended in 1 ml of MP and mixed by vortexing. The tubes were placed on the magnetic rack and the beads separated and supernatant removed again. Finally the beads were suspended in 1 ml of Media Plus and ready to be used in further downstream applications.

2.2.2.1. Magnetic separation from blood

A modification of magnetic separation method was used when capturing MAP cells in blood. Blood samples (1 ml) were diluted with 9 ml of MP. 10 μ l (5 μ l of peptide aMp3 and 5 μ l of peptide aMptD) of freshly peptide coated magnetic beads (Section 2.2.1) was added to the sample. This was centrifuged (15 min; 4500 \times g). The supernatant was removed and the pellet was resuspended in 9 ml of MP. The sample was centrifuged again (4500 \times g for 15 min). The supernatant was removed and the pellet resuspended into 1 ml of MP. The 1 ml sample was placed on a magnetic rack and separation of the cells continued as with the original PMMS method (Section 2.2.2) or for culture (Section 2.1.1.3).

2.3. PHAGE BASED DETECTION OF MAP

2.3.1. Detecting MAP in milk

This method is adapted from Botsaris et al. (2010). Milk samples obtained were placed in a 10 ml centrifuge tube. They were centrifuged (2500 \times g for 15 min). A layer of cream then formed on the top of the sample. Very carefully this was removed using a sterile cotton swab. The supernatant was removed making

sure not to disturb the pellet. 2 ml of MP was used to suspend the pellet. At this point the samples could be refrigerated overnight.

The centrifuged milk samples were washed twice. This was achieved by centrifuging the samples for 15 min at $2500 \times g$. The supernatant was removed and the pellet was resuspended in 2 ml of MP (with 0.2 % glycerol). This was repeated and the pellet was finally resuspended in 1 ml of MP (with 0.2 % glycerol). This suspension could either be frozen at $-20 \text{ }^{\circ}\text{C}$ or processed through the FPTB assay (Section 2.1.3).

2.3.2. Detecting MAP in blood

In each case (where possible) heparinised blood was used. Samples of blood (1 ml) were diluted with 9 ml of MP into 15 ml Falcon tubes. The sample preparation and PMMS procedure on blood (Section 2.2.2.1) was then carried out. The washed separated 1 ml sample resuspended in MP was then processed through the FPTB assay (Section 2.1.3).

2.3.2.1. Buffy coat isolation

The isolation of the white blood cells (buffy coat) from cattle blood was carried out using Ficoll-Paque Plus (GE Healthcare Life Sciences, UK). The buffy coat layer from 2 ml of whole heparinised blood was mixed with 2 ml of PBS. Using aseptic technique, 3 ml of Ficoll-Paque Plus was added to 15 ml falcon tube. The 4 ml of PBS-blood mixture was then carefully layered onto the Ficoll-Paque Plus, ensuring the samples did not mix. The samples were then centrifuged ($400 \times g$, for 30 min at $18 \text{ }^{\circ}\text{C}$). After centrifugation the upper layer (plasma) of the sample was drawn off using a clean 10 ml pipette and saved for later use. The buffy coat layer was then carefully removed ensuring the minimal amount of Ficoll-Paque Plus is removed. The buffy coat layer was then washed with 6 ml of PBS. The samples were then centrifuged ($100 \times g$ for 10 min at $18 \text{ }^{\circ}\text{C}$). The supernatant

was removed and the pellet resuspended and centrifuged again. The supernatant was finally removed and the pellet resuspended in 1 ml of MP for the phage assay.

2.4. MAP SPECIFIC POLYMERASE CHAIN REACTIONS (PCR)

2.4.1. Genomic DNA preparation and purification

2.4.1.1. Heat extraction

Under aseptic conditions, one colony was picked using a sterile loop. It was suspended into 200 μ l of sterile RO water. The sample was heated at 95 °C for 20 min, cooled and centrifuged (13,000 $\times g$ for 3 min). For each PCR reaction 10 μ l of sample was used as template reaction.

2.4.1.2. DNEasy™ DNA extraction kit (Qiagen, UK)

Colonies of suspected MAP grown on HEYM agar were grown in MP to a concentration of approximately 10^6 pfu ml⁻¹ (as defined by the FPTB assay). One and a half millilitre of this was placed in a microcentrifuge tube and centrifuged (11,000 $\times g$ for 60 s). The supernatant was removed and discarded. The pellet was suspended in 180 μ l lysis buffer (25 mM Tris-HCl; pH 8.0, 10 mM EDTA and 50 mM sucrose). Lysozyme was added at a concentration of 20mg ml⁻¹ and incubated for 30 min at 37 °C.

After the incubation 25 μ l of proteinase K and 200 μ l of buffer AL (lysis buffer, no composition given) was added and mixed. The tube was incubated at 95 °C for 15 min and then 200 μ l of ethanol was added to the solution and mixed.

The DNA was purified from the sample by pipetting the solution into a DNeasy™ mini spin column. The spin column was placed in a 2 ml collection tube. This was centrifuged at 4,000 g for 60 s. The flow through and collection tube were discarded. The column was placed in a new collection tube and 500 μ l of buffer AW1 (composition not given) was added to the spin column. This was

centrifuged for 60s at 4,000 x *g*. The flow through and collection tube were again discarded. The DNeasy™ spin column was placed in a new collection tube and buffer AW2 (composition not given) was added on top of the spin column. To dry the spin column membrane, the spin column was centrifuged (12,000 x *g* for 3 min) and the flow through and collection tube were again discarded.

The spin column was placed in a new microcentrifuge tube and 200 µl of buffer AE (composition not given) was then placed on the spin column membrane. This was incubated for 60 s at room temperature. After incubation the sample was centrifuged for 60 s at 4,000 *g* to elute the DNA. This was repeated with 100 µl of buffer AE instead of 200 µl. Purified DNA was left in the microcentrifuge tube, and could be used as template for the PCR reactions.

2.4.2. Plaque DNA preparation

2.4.2.1. Plaque extraction

This method is adapted from a method described by Stanley et al. (2007). It was used to confirm the identity of the mycobacteria that had formed plaques from the *FASTPlaqueTB™* assay (Section 2.1.3).

The central area of a plaque was picked out using a sterile plastic loop and placed in a 0.2 ml PCR tube. Ten micro-litres of sterile RO water was placed in the PCR tube and this was heated (~50 °C) in a PCR block until melted. The solution was pulse centrifuged to bring down any agar and cell debris to the bottom of the PCR tube. This was placed in a -80 °C freezer for 1 h. The sample was thawed at 37 °C and then centrifuged at 13,000 x *g* for 5 min. Ten micro-litres of the supernatant was then used as template DNA in a PCR reaction.

2.4.2.2. ZymoResearch™ Gel DNA extraction

To gain a higher quality of DNA yield from the plaques the ZymoResearch™ Gel DNA Recovery Kit was used. Buffers in the kit first had to be prepared. To

the 'DNA wash Buffer', 24 ml of absolute ethanol was added, which gave the final concentration needed in the DNA wash buffer solution (composition not given). To purify DNA from the plaques, the central area of five plaques were picked out using a sterile plastic loop. This was placed in a microcentrifuge tube. A ratio of three to one of the amount of the Agarose Dissolving Buffer (ADB; composition not given) was added to the amount of agarose removed from the plate. This was briefly mixed and left in an incubator at 37 °C until the agar had dissolved. The solution was placed in a Zymo-Spin I™ Column which was in a collection tube. This was centrifuged at 10,000 $\times g$ for 60 s. The flow through was discarded and 200 μ l of Wash Buffer was added to the spin columns and this was centrifuged again at 10,000 $\times g$ for 30 s. This wash step was repeated. The column was then placed into a new sterile microcentrifuge tube and 10 μ l of sterile water was placed in it. This was centrifuged at 10,000 $\times g$ for 60 s. Pure DNA was in the water, ready to be used in PCR reactions.

2.4.2.3. ZymoResearch™ DNA concentration

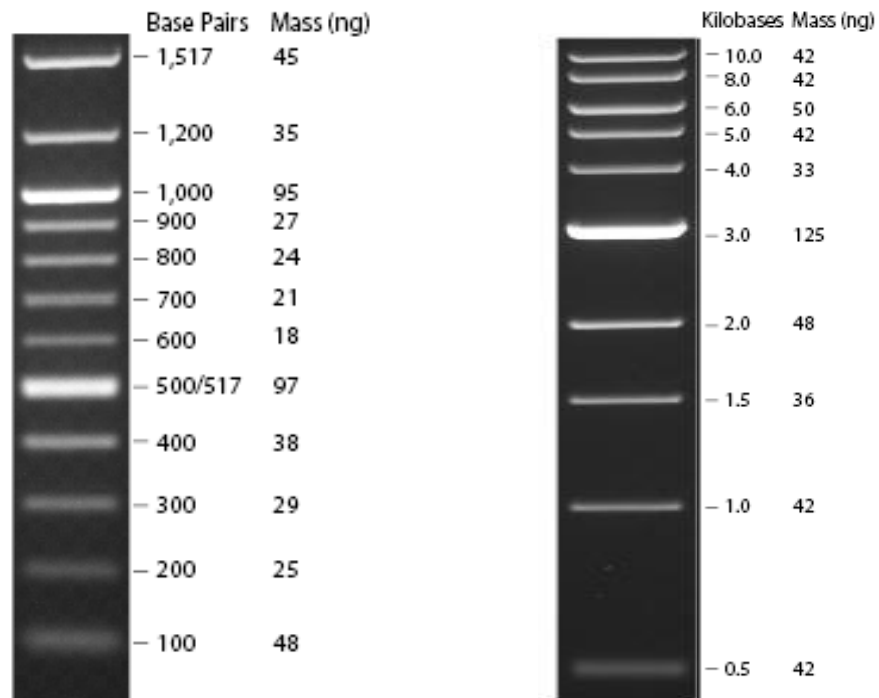
Samples containing DNA were mixed with DNA binding buffer (ratio of 2:1 – DNA binding buffer : sample) in a microcentrifuge tube. The mixture was then transferred into a Zymo-Spin Column which was then placed in a collection tube. The samples were centrifuged (30 s; 13000 $\times g$) and the flow-through was discarded. DNA wash buffer (200 μ l) was added to the spin column and centrifuged (30 s; 13000 $\times g$). This wash was then repeated. After washing 10 μ l of DNA elution buffer or water was placed directly on top of the column matrix and incubated at room temperature for at least 1 min. The spin column was finally placed into a fresh microcentrifuge tube and sample was centrifuged (30 s; 13000 $\times g$) to elute the purified concentrated DNA.

2.4.3. DNA molecular weight marker

Five micro-litres of 100 base pair (bp) DNA ladder (New England BioLabs™ Inc.) was placed in a well on the gel. The ladder ranges from 100 to 1,500 bp. The ladder consists of eleven fragments that range in size from 100–1,000 bp in 100 bp increments (Fig. 2.5), plus an additional fragment at 1,500 bp. The 500 bp fragment is present at increased intensity to allow easy identification. A Blue Loading Dye is provided to visualise the migration.

Each gel that required a larger marker was loaded with 5 µl of the 1 kilo base (kbp) DNA ladder (New England BioLabs™ Inc.). This was used as a molecular weight marker for larger DNA products. The ladder ranged from 10 kbp to 0.5 kbp (Fig. 2.5). The 3 kbp band is at a higher intensity to allow easy identification of the sizes.

Figure 2.5. Molecular DNA markers



Example of 100 bp and 1 kbp DNA ladder. The bands have formed on a 2% agarose gel after 1 h of separation. The 100 bp has the bands 1000 and 500 bp at higher intensities to aid in identifying the size of bands. The 1 kbp ladder has the band at 3 kb at a higher intensity to aid in the identification of the size bands.

2.4.4. Primers used in PCR reactions

Table 2.2. Primer sequences

Primer Name	Primer Sequence	Target DNA
f57f	5'-GGTCGCGTCATTCAGAATC-3'	MAP f57 gene
f57r	5'TCTCAGACAGTGGCAGGTG-3'	MAP f57 gene
P90	5'-GAAGGGTGTTCCGGGGCCGTCGCTTAG-3'	MAP <i>IS900</i> Sequence
P91	5'-GGCGTTGAGGTCGATCGCCACGTGAC-3'	MAP <i>IS900</i> Sequence
TJ1	5'-GCTGATGCGCTTGCTCAT-3'	MAP <i>IS900</i> Sequence
TJ2	5'-CGGGAGTTTGGTAGCCAGTA-3'	MAP <i>IS900</i> Sequence
TJ3	5'-CAGCGGCTGCTTTATATTCC-3'	MAP <i>IS900</i> Sequence
TJ4	5'-GGCACGGCTCTTGTTGTAGT-3'	MAP <i>IS900</i> Sequence
M56	5'-GCGTGAGGCTCTGTGGTGAA-3'	MAP <i>IS1311</i> Sequence
M94	5'-CAGCGATCGTCGACAGTGTG-3'	MAP <i>IS1311</i> Sequence

2.4.5. PCR reactions

2.4.5.1. IS900-PCR

This method used the primers P90 and P91 (Table 2.2) It was described by Whittington et al. (1998). The PCR reaction amplified DNA specific for *M. paratuberculosis*. DNA (10 µl) extracted from cells or plaques (Sections 2.3.2. and 2.3.1) was used in each of the PCR reactions. The 25 µl reaction mixture consisted of: 12.5 µl of Qiagen HotStarTaq Master Mix plus (Qiagen, UK), 250 ng of each primer; P90 and P91 (Table 2.2) and sterile molecular grade water to top up to the final 25 µl reaction volume.

The mixture was briefly pulse centrifuged to bring all the contents to the bottom of the 0.2 µl PCR tubes and placed in a thermo-cycler (Techne TC-3000). The parameters of the thermo cycler were set at an initial denaturing step of 94 °C for 5 min. This was followed by 37 cycles of; 94 °C for 30 s, 62 °C for 30 s and 72 °C for 60 s. This was followed by a final extension step of 72 °C for 4 min.

The PCR products were resolved on a 2 % agarose gel containing 5 % (v/v) ethidium bromide. Two micro-litres of 5 x loading dye (25 mg bromophenol blue, 4 g of sucrose, and H₂O to 10 ml) was added to each PCR product and 15 µl of each dyed product was placed in separate wells on gel. The products were separated for 1 h using 70 V. The gels were visualised under ultra-violet (UV) light. The expected product size was a single 400 bp band.

2.4.5.2. Nested IS900-PCR

This nested-PCR was adapted from (Bull et al., 2003). Two 25 µl PCR reaction volumes were used for this nested PCR. The initial PCR mixture consisted of 10 µl of template plaque DNA (see Section 2.3.2). The 25 µl reaction mixture consisted of: 12.5 µl of Qiagen HotStarTaq Master Mix plus (Qiagen, UK), Each primer used in this reaction was reconstituted to 100 pmol (Section 2.3.4 for primer list). 2 µM of primers TJ1 and TJ2 were used in the first round. Sterile

molecular grade water was placed in the tube to top up the reaction mixture to 25 μ l.

The mixture was pulse-centrifuged and the tubes were placed in thermo cycler (Techne TC-3000). The initial cycling conditions were as follows; 94 °C for 5 min, ten cycles of; 94 °C for 1 min, 59 °C for 1 min and 72 °C for 3 min. This was followed by a final extension of 72 °C for 7 min.

For the nested step, 10 μ l of the PCR product from the first round of PCR was placed in a new 0.2 μ l PCR tube. The 25 μ l reaction mixture consisted of: 12.5 μ l of Qiagen HotStarTaq Master Mix plus (Qiagen, UK), 4 μ M of primers TJ3 and TJ4 (Table 2.2) was placed in the tube. Two units of *Taq* DNA polymerase was placed in the PCR tube. Sterile molecular grade water was placed in the tube to top up the reaction mixture to 25 μ l.

The PCR cycling conditions was the same as the first round parameters; however there were 30 cycles instead of ten and the annealing temperature was 60 °C and not 59 °C.

The PCR products were resolved on a 1.5 % agarose gel containing 5 % (v/v) ethidium bromide. Two micro-litres of 5 x loading dye (25 mg bromophenol blue, 4 g of sucrose, and H₂O to 10 ml) was added to each PCR product and 15 μ l of each dyed product was placed in separate wells on gel. The products were separated for 1 h using 70 V. The gels were visualised under ultra-violet (UV) light. The expected product size was a single 294 bp band.

2.4.5.3. MAP-specific F57 PCR

This method used the primers f57f and f57r (Table 2.2) It was described by Coetsier et al. (2000). The PCR reaction amplified DNA specific for MAP. DNA (10 μ l) extracted from cells or plaques (Sections 2.3.2. and 2.3.1) was used in each of the PCR reactions. The 25 μ l reaction mixture consisted of: 12.5 μ l of Qiagen HotStarTaq Master Mix plus (Qiagen, UK), 250 ng of each primer; f57f and f57r

(Table 2.2) and sterile molecular grade water to top up to the final 25 µl reaction volume.

The mixture was briefly pulse centrifuged to bring all the contents to the bottom of the 0.2 µl PCR tubes and placed in a thermo-cycler (Techne TC-3000). The parameters of the thermo cycler were set at an initial denaturing step of 94 °C for 5 min. This was followed by 37 cycles of; 94 °C for 30 s, 58 °C for 30 s and 72 °C for 60 s. This was followed by a final extension step of 72 °C for 7 min.

The PCR products were resolved on a 1.5 % agarose gel containing 5 % (v/v) ethidium bromide. Two micro-litres of 5 x loading dye (25 mg bromophenol blue, 4 g of sucrose, and H₂O to 10 ml) was added to each PCR product and 15 µl of each dyed product was placed in separate wells on gel. The products were separated for 1 h using 70 V. The gels were visualised under ultra-violet (UV) light. The expected product size was a single 329 bp band.

2.4.5.4. Quantitative real-time PCR

A commercial assay developed Tetracore™ was used called VetAlert Johne's Real Time PCR. The 1 ml sample of bacteria separated during the IMS procedure (Section 2.2.2) was placed in a Disruption tube that contained glass beads, this was thoroughly mixed by vortexing. The sample was bead-beated (MagNa-Lyser, Roche) for 5 min at 4800 rpm. The sample was centrifuged for 10 minutes at 16,000 x *g*. The supernatant was placed in a sterile microcentrifuge tube. The DNA from the cells was now extracted and ready to be used with the real-time PCR.

The Tetracore™ system uses a primers targeted at the specific *HspX* gene found in MAP cells (see Section 1.2.3.4). The probe (TaqMan) was used to generate the fluorescent signal which was detected during the real-time PCR process.

A master mix supplied in the kit was used during the PCR reaction. It contained the necessary primers, probes, DNA polymerase and PCR reaction mixture (dNTP's, buffer, MgCl₂). An inhibition control and positive control was also supplied with the kit. The inhibition control is used in each reaction to determine whether there are any inhibiting substances in the sample that could give rise to false results. The positive control contains a non-infectious synthetic portion of the *HspX* gene of MAP. It contains 25000 gene copies per 2.5 µl. A positive control was used in each of the reactions. A negative control was not supplied with kit, thus sterile RO water was used as the template.

For each 25 µl reaction, 2.5 µl of inhibition control was combined with 20 µl of the master mix into separate wells of the 48-well plate. 2.5 µl of each sample was added to each well. The plate was pulse-centrifuged and inspected to ensure there were no bubbles. The samples were placed in a real-time thermo cycler (ABI PRISM). The cycling parameters were: an initial 95 °C for 10min then 45 cycles of; 95 °C for 15 s, and 62 °C for 60 s. The thermo cycler settings were set as: no quencher, reference dye as ROX, FAM as dye layer and exposure time was 10-25 ms. If no inhibition was found in the samples the samples were put through the PCR.

A series of two-fold dilutions were carried out on the positive control. This was carried out to be able construct a standard curve. In a 25 µl reaction, 22.5 µl of master mix was placed into separate wells on the 48-well plate. Triplicates of the 2.5 µl samples, the serially diluted positive control and a negative control were added to each appropriate well. The plates were covered and pulse centrifuged. They were then placed in real-time thermo cycler (ABI PRISM). The same cycling conditions as the inhibition assay were used.

2.5. GENERAL CLONING, TRANSFORMATION AND EXPRESSION OF PROTEINS IN *E. COLI*

The mycobacteria and *E. coli* strains used in this study are listed in Table 2.1. The plasmids used to clone and express proteins are listed in Table 2.3. *E. coli* were grown at 37 °C and 30 °C in LB-broth (Fisher BioReagents, UK) for growing cells after transformation and during protein expression respectively. Ampicillin (Sigma; 100 µg ml⁻¹) was used to select for cells containing the appropriate plasmid.

Table 2.3. Plasmids

Plasmid	Ref
pET-23a*	Novagen, Expression Vector
pCR -2.1Topo*	Novagen, Cloning Vector
pET -101DTopo*	Novagen, Expression Vector

*plasmid maps can be found in the Appendix

2.5.1. PCR amplification of GFP-fusion peptides

The GFP-fusion peptides were initially amplified using a PCR mastermix (Qiagen, UK). The PCR reaction (25 µl reaction volume) consisted of designed primers (Section 7.2) and GFP template DNA (from the plasmid pDONOR-P4-P1R). The PCR reaction was carried out on a Techne Thermocycler 3000. The PCR parameters were; one cycle of 95 °C for 3 min, 30 cycles of 95 °C for 30 s, 55 °C for 30 s, 72 °C for 1 min and a final extension of 72 °C for 7 min.

2.5.1.1. Amplifying gfp-peptide fusion

The four primers (Table 7.2) used for cloning were diluted to 100 pmol. On ice, 1 µl of each primer was added to a PCR tube corresponding to different n and c-terminal fusions (Table 7.3). Template *gfp* DNA (1 ng/µl) was put into the PCR tube. Dimethyl sulfoxide (DMSO) was added at a concentration of 3 % to the final PCR reaction volume. Finally 10 µl of the proof-reading enzyme, Phusion – High Fidelity DNA Polymerase mastermix (New England Biolabs) was added to each PCR tube. Each PCR reaction was topped up with nuclease free water to a volume of 25 µl.

Each PCR reaction was placed in a thermo-cycler (Techne TC-3000). The PCR cycling conditions were as follows: an initial denaturing step of 95 °C for 30 s. Then 30 cycles of 95 °C for 10 s, 53 °C for 30 s and 72 °C for 30 s. There was a final extension step of 72 °C for 10 min.

A small sample of each PCR product was visualised using electrophoresis on a 1% agarose gel and compared to a positive *gfp* control. A band at around 800 bp confirmed the PCR was successful.

2.5.1.2. Gel-DNA extraction and Restriction Digests

The bands on the gel were placed on a transilluminator. At long ultra-violet (UV) wavelength the bands were visualised and cut with a sterile scalpel. The cut

out gel fragments were placed in microcentrifuge tubes and the DNA was extracted using the ZymoResearch Gel DNA extraction kit (2.4.2.2). The concentration was measured using the Nano-drop (Section 2.5.2). The plasmid vector (pET 23a, Novagen) was also digested.

A double restriction digest was carried out using the enzymes; *Bam*HI and *Nde*I. In a reaction volume of 50 μ l, 1 μ g of extracted DNA was placed into a 0.2 μ l PCR tube. Five microlitres of NEB Buffer number 3 (100 mM NaCl, 50 mM Tris-HCl, 10 mM MgCl₂, 1 mM Dithiothreitol, pH 7.9) was added to the tube. Bovine Serum Albumin (BSA) was added to a concentration of 100 μ g ml⁻¹. 10 units of each restriction enzyme was added. Finally nuclease free water was used to top up the reaction volume to 50 μ l. The restriction digest reaction was carried out at 37 °C for one hour.

The restriction digests were visualised by agarose gel electrophoresis. A slight shift in the bands suggested the digest had been a success. The bands were cut out and the DNA extracted (see Section 2.4.2.1).

2.5.1.3. Ligation Reaction

The concentration of the digested PCR products and vector was measured using the Nano-drop. A ratio 1:3 vector to insert was then prepared and placed in a 0.2 ml PCR tube. One micro-litre of Ligase buffer (50 mM Tris-HCl, 10 mM MgCl₂, 1 mM ATP, 10 mM Dithiothreitol, pH 7.5; New England Biolabs) was placed in the PCR tube. One unit of T4 DNA Ligase (New England Biolabs) was added. Then sterile nuclease free water was used to top the reaction volume up to 10 μ l. The samples were incubated at 15 °C overnight.

2.5.1.4. Preparing chemically competent *E. coli*

E. coli was grown up overnight in 20 ml of LB broth at 37 °C. Fresh LB broth was then inoculated with the overnight culture to an optical density (OD) A_{600nm}

0.05. The cells were then grown at 37 °C in an incubator, shaking at 200 rpm. The cells were diluted further with 20 ml of pre warmed LB broth. This was then incubated at 37 °C for 20 min in an incubator shaking at 200 rpm.

After incubation the culture was cooled on ice for 10 min. The culture was placed in a cooled 50 ml centrifuge tube. The cells were recovered by centrifuging at 3000 $\times g$ for 10 min at 4 °C. The supernatant was removed and the cells resuspended in 10 ml of ice-cold 0.1 M MgCl₂. This was incubated on ice for 1 h. The cells were recovered by centrifugation as before and the pellet resuspended in 1 ml of ice-cold CaCl₂. The cells were packed in ice and incubated overnight.

2.5.1.5. Transformation of chemically competent cells

Four microlitres of the ligation reaction (Section 2.5.1.3) was placed into the fresh chemically competent *E. coli* cells (Section 2.5.1.4). The mixture was then incubated in ice for 1 h. The sample was then heat shocked for 1 min in a static 42 °C water bath. The tubes were then immediately transferred onto ice for five minutes. Two-hundred and fifty microlitres of room temperature LB broth was added to the cells carefully. The tubes were then placed in a 37 °C incubator shaking at 200 rpm for 1 h. 50 μ l and 100 μ l of each transformation was spread onto pre warmed selective amp and Isopropyl β -D-1-thiogalactopyranoside (IPTG)-LB plates. The plates were inverted and incubated at 37 °C for 24 h.

White or light blue colonies that formed were considered positive were picked and patch plated on an amp-LB plate. These were inverted and incubated at 37 °C for 24 h. In parallel a sample of 10 white or light blue colonies were picked and placed in 10 μ l of nuclease free water. This was then used as template DNA. The PCR carried out in Section 2.5.1.1 was then carried out using the GFP primers (see Table 7.2). The patch plate was then placed under blue light to determine whether any of the colonies fluoresced green.

2.5.1.6. Protein extraction

Induced *E. coli* containing an expressed protein of interest was centrifuged (10,000 $\times g$; for 10 min) and the supernatant removed. The pellet was resuspended in 1 ml of ice cold 20 mM Tris-HCl (pH 7.4) and transferred to microcentrifuge tube. The sample was then centrifuged (13,000 $\times g$; for 3 min) and the supernatant was removed and the pellet was washed again in fresh 20 mM Tris-HCl (pH 7.4). The sample was then placed in a 15 ml Falcon Tube and 0.5 g of glass beads (106 μm ; Sigma, UK) was added into the sample. The mixture was vortexed at max-speed for 4 min. The tube was placed on ice for 5 min to allow the glass beads to settle. The supernatant was transferred to a fresh microcentrifuge tube and centrifuged (13,000 $\times g$; 3 min). A sample (20 μl) was removed as crude extract for SDS-page analysis (Section 2.5.1.8). The rest of the sample was removed for purification (Section 2.5.1.7).

2.5.1.7. Protein purification

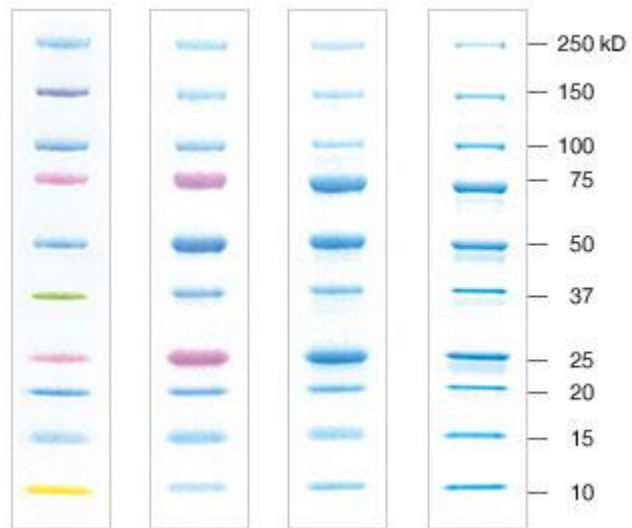
The crude protein extracted in Section 2.5.1.6 was purified using ion exchange chromatography. A 5 inch chromatography column (Evergreen, UK) was washed with 1.5 ml of 70 % ethanol. The column was then loaded with DEAE-Sepharose (Sigma, UK) and left to settle, with excess buffer left to drain off the column. The column was equilibrated with 20 mM Tris-HCl (pH 7.4). The crude protein extracted from Section 2.5.1.6 was carefully loaded onto the column and left to drain through the column. The column was then washed twice with 1 ml of 20 mM Tris-HCl (pH 7.4). Specific proteins were then eluted off the column using 1ml of 20 mM Tris-HCl (pH 7.4) buffers with increasing salt concentrations (50, 100, 150, 200 and 250 mM – NaCl₂). Each fraction was collected and analysed by SDS-page, to determine purity of the protein extracted and by the Bradford Assay to quantify the amount of protein expressed.

2.5.1.8. SDS-page analysis

To analyse the purity of extracted proteins SDS-page analysis was carried out. Protein samples were mixed with 2 x protein sample buffer (Laemmli buffer, Biorad; supplemented with 1 % 2- β mercaptoethanol). The samples were mixed by vortexing and then boiled for 10 min at 100 °C. After boiling the samples were then centrifuged (16000 x *g*; 1 min) and supernatant was used for analysis.

The SDS-page gels (Mini-PROTEAN® TGX™ Precast Gels; 4-20 %) were removed from the packaging and placed in a clamping frame. The gels were placed in an electrophoresis tank with SDS-running buffer (10 x: 30 g Tris-base, 144 g glycine, 10 g SDS; TGS, Biorad). Protein markers (Fig 2.6) were placed in the initial and final well of the gel and the boiled samples (20 μ l) were loaded into the gel and subjected to electrophoresis (200 V; 40 min). After electrophoresis the gels were removed from the clamp and stained with Coomassie blue staining solution (10 % glacial acetic acid, 0.006 % Coomassie Blue dye, 90 % RO water) for 30 min on an orbital shaker. The stain was then removed and the gels were treated with a destaining solution (10 % glacial acetic acid, 90 % RO water) for 5 min on an orbital shaker. The destaining solution was removed and fresh solution was poured over the gels and this was incubated at RT overnight. The destaining solution was then removed after incubation and analysed.

Figure 2.6. Protein markers



Protein markers (Biorad) used with SDS-page gel analysis to determine the approximate size of extracted proteins.

2.5.1.9. Bradford Assay

To quantify the amount of protein purified from Section 2.5.1.7, the Bradford assay was performed. Initially a protein standard was made using a stock (0.1 mg ml⁻¹) of bovine serum albumin (BSA; Sigma). Protein samples (20 µl) from Section 2.5.1.7 were mixed with 1580 µl of water and a series of 2-fold dilutions were carried out to give a final volume of 800 µl. Bradford Reagent (200 µl; Sigma) was added to every samples (diluted protein and BSA standards) and left to equilibrate for 5 min. After the incubation period the absorbance (595 nm) of the samples were measured. A standard curve of the BSA standards was then created and the quantity of protein sample plated on the linear part of the standard curve to determine the approximate quantity of protein in the sample.

2.5.2. TOPO-Cloning (Invitrogen)

A TOPO Cloning Kit (Invitrogen) was used to clone PCR products generated by Taq polymerase for sequencing. PCR products were generated with the required single base 3'-A overhang by Taq polymerase. The PCR products were gel-purified using Zymo-Gel DNA Recovery (Section 2.5.1.2). The vector supplied in the TOPO TA Cloning Kit (pCR2.1-TOPO[®] vector) was supplied linearized with a single 3'-T overhang and has a topoisomerase covalently bound to the vector. The TOPO TA Cloning Kit vector together with the One Shot[®] Chemically Competent E. coli were used in accordance with manufacturer's instructions. Briefly, 1 µl of PCR product was mixed with 1 µl of TOPO salt solution, 3 µl of SDW and 1 µl of TOPO plasmid vector. The mixture was incubated at RT for 5 min and stored on ice. For the transformation 2 µl of the cloning reaction mixture was mixed with one vial of One Shot[®] Chemically Competent E. coli and incubated on ice for 15 min. The reaction mixture was heat shocked for 30 s at 42 °C and transferred onto ice. To the reaction 250 µl of SOC medium was added and the sample incubated at 37 °C for 1 h (200 rpm). To screen for

putative clones 40 μl X-gal (40 mg ml^{-1}) was spread onto each LB agar plate (containing 50 $\mu\text{g ml}^{-1}$ of ampicillin) and 50 μl of the sample was spread onto the selective agar and incubated overnight at 37 $^{\circ}\text{C}$. Putative clones were identified by their white to pale blue colony pigment and their DNA extracted using a QIAprep[®] Spin Miniprep Kit (Qiagen) (Section 2.9.7).

2.5.3. Plasmid DNA extraction

Plasmid DNA was extracted from *E. coli* using Zymo Plasmid-MiniPrep Kit (ZymoResearch). 600 μl of fresh overnight culture of *E. coli* grown in LB media was placed into a 1.5 ml microcentrifuge tube. The bacterial culture was centrifuged for 30 seconds at 16,000 $\times g$. The supernatant was removed and more culture was placed and the centrifuge step repeated. Water (600 μl) was added to the pellet and resuspended completely. 100 μl of 7X Lysis Buffer was then mixed into the sample by inversion (4-6 times). After the solution changed from opaque to clear blue, which indicated complete lysis, 350 μl of chilled Neutralisation Buffer was mixed with the sample. The sample was inverted to ensure complete neutralisation of the lysis buffer. The sample was then centrifuged at 16,000 $\times g$ for 4 min. The supernatant was then removed and placed into a Spin-column. The column was then placed into a collection tube and centrifuged for 15 seconds. The flow-through was discarded and column was placed back into the collection tube. Endo-Wash Buffer (200 μl) was then added to the column. This was centrifuged for 30 s. Zippy[™] Wash Buffer (400 μl) was then added to the column and was centrifuged for 1 min. The spin columns were then transferred to a clean microcentrifuge tube and the 30 μl of elution buffer was added to the column. The column was left to stand for 1 min at room temperature before being centrifuged for 30 s at 16,000 $\times g$. The eluted plasmid DNA could then be used for downstream processing.

2.5.4. DNase I (NEB) treatment

Samples (10 µg) were mixed with n 1X DNase I Reaction Buffer (NEB, UK) in a final volume of 100 µl. Two units of DNase I, was then added to the sample and mixed thoroughly. This was then incubated at at 37°C for 10 minutes. To inactivate the DNase I enzyme, either 1 µl of 0.5 M EDTA (to a final concentration of 5 mM) was used or simply diluting the enzyme with MP to inactivate it.

2.6. PREPARATION OF CELLS FOR SCANNING ELECTRON MICROSCOPE (SEM)

Cells (1 ml) were mixed onto a polymer scaffold in (or enough to cover scaffold; Millipore 0.22 µm filter) with 3% glutaraldehyde (Sigma) and this was left overnight at 4 °C in a sealed container. To further fix the samples the glutaraldehyde was removed and the samples washed with PBS three times for 15 minutes. 1% osmium tetroxide solution was then placed on the samples and incubated at RT for 2 h. After incubation the samples were washed three times for 15 minutes with SDW. The samples were then dehydrated using a series of ethanol concentrations (25, 50, 70, 90, 95 and 100 % for 10 min). To chemically dry the samples HMDS (hexamethyldisilazane) was added and incubated for 5 min and then washed with SDW. The samples were left to dry overnight at RT. Samples were then sputter-coated with gold nanoparticles and ready for SEM.

2.7.1. GFP-fusion peptide binding protocol

MAP strain K10 was used as the standard strain and *M. smegmatis* as a negative control. Approx. 1×10^4 pfu ml⁻¹ of each organism was harvested from liquid culture in MP by centrifugation (13,000 $\times g$ for 3 min). Cells were resuspended in 100 µl of PBS-T (pH 8.0, 0.01 % Tween 20). The cells were then vortexed for 3 min to reduce their clumping. Cells suspended in PBS-T were

treated with BSA (4 % w/v) to block non-specific protein binding. This was then incubated whilst mixing at 18 rpm for 20 min. Each GFP-peptide fusion peptides were then added and incubated with the sample and agitated on an orbital shaker for 10 min. The cells were then recovered by centrifuging at $16,000 \times g$ for 1 min. The supernatant was removed and residual GFP levels determined using a fluorimeter (Genios Pro, Tecan). Labelled cells were resuspended in 50 μ l of PBS-Tween and 20 μ l samples were mounted onto a microscope slide. The slides for microscopy were then air dried and fixed by glutaraldehyde. The sample was flooded with PBS to sustain the GFP fluorescence and a cover slip was placed on top. Cells were then washed with DAPI stain (0.2 ng ml^{-1} ; Sigma) and incubated for 5 min. Excess stain was then removed by washing twice with PBS. Samples were visualised by Confocal fluorescence microscopy and images manipulated using Leica software.

2.7.2. Cell capture assay

The streptavidin coated black 96-well microtitre plates (Nunc) were prepared by coating the wells with biotinylated peptides ($5 \mu\text{g ml}^{-1}$) in a solution of 0.2 M sodium carbonate (pH 9.4). Peptides used for capture were placed into the wells and incubated for $37 \text{ }^{\circ}\text{C}$ for 1 h. After incubation the samples were washed three times with 300 μ l of PBS-T (0.05 % Tween-20). Bovine Serum Albumin (BSA; 4 %) was used to block the samples and incubated for 30 min at $37 \text{ }^{\circ}\text{C}$. After blocking PBS-T (0.05 % Tween-20) was used to wash the samples three times.

Dilutions of cells for capture were then diluted in PBS-T (0.05 % Tween-20) and placed in the wells and incubated for 60 min at $37 \text{ }^{\circ}\text{C}$. After incubation GFP-fusion peptides (20 ng ml^{-1}) were added to the sample and incubated for 60 min. After incubation, samples were washed with PBS three times. The prepared microtitre plates were then analysed using a fluorimeter (Tecan, Genios Pro).

2.8. ZIEHL-NEELEN (ZN) STAINING

The ZN stain was carried out using the Kit Quick-TB cold stain kit (RAL Diagnostics, France). Carbolic Fuchsin was covered on to heat-fixed smears of mycobacteria on microscope slides for 5 min. Tap water was then used to rinse away the initial stain and the slide was covered with Armand Solution for 1 min. After 1 min the slide was rinsed with tap water and left to dry. The samples were then visualised with a x100-immersion objective to look for pink stained cells on a blue background.

2.9. DETECTION AND ENUMERATION OF MAP USING PHAGE TM4 INSTEAD OF D29

When using mycobacteriophage TM4 in the phage detection assay instead of D29 and new virucide was needed as TM4 was resistant to FAS. Gunpowder Green Tea (Whittards of Chelsea, UK) was prepared, by adding sufficient RO water to the tea solids (7 % w/v) and the sampled were boiled for 10 min. The infusion was then filtered (Whatman Grade No. 2 Filter Paper, Whatman International Ltd.), autoclaved and stored at 4 °C. The phage was then treated with 100 µl of tea infusion and incubated for 15 min. The FPTB assay was then carried out (Section 2.1.3).

2.10. INDUCING STATIONARY PHASE IN MYCOBACTERIA

To induce stationary phase in MAP, cells were incubated in screw capped glass vial (25 mm diameter; 10 ml volume) in liquid culture with a ratio of head space : liquid volume = 0.5, and allowed to grow whilst gently shaking at 80 rpm for six months using the method described by Wayne and Hayes (1996). Cells were aerated by opening the cap and increasing the speed of rotation (200 rpm) allowing oxygen to diffuse through the culture. For *M. smegmatis*, cells were

treated in the same way however cells only required 10 d incubation to reach stationary phase – as defined by the bacteria growth curve.

2.10.1. Phage attachment assay

The effect of phage attachment on mycobacteria in the oxygen deprived phase was performed using a method by Spears et al (2008). Briefly cells (10^5 pfu.ml⁻¹) were harvested by centrifugation (13000 x *g* for 3 min) and resuspended in 900 µl of MP. The samples were then inoculated with 100 µl phage D29. Samples were then incubated at 37 °C. After, 0, 30 and 60 min, the samples were removed and centrifuged (1300 x *g* for 4 min). The supernatant (containing unbound phage) were titrated. The pfu ml⁻¹ at time point zero was taken as 100 % of the number obtained over time. As a control, phage were incubated in the presence of no bacteria.

2.10.2. Effect of inhibition of RNA synthesis on phage infection

The effect of the mycobacteria's ability to synthesise RNA after phage infection was determined by centrifuging (13000 x *g* for 3 min) the MAP cells grown in anaerobic and aerobic environments, and resuspending them in rifampicin (Mast Diagnostics, UK; 5 µl ml⁻¹). The cultures were incubated whilst shaking at 200 rpm at 37 °C in an aerobic environment. At daily intervals starting at day zero, samples were taken and washed twice with fresh MP by centrifugation (13000 x *g* for 3 min) to remove the rifampicin. The cells were then resuspended in 1 ml of MP and the FPTB assay with enumeration was carried out.

2.11. STATISTICAL ANALYSIS

All statistical analysis was carried out using SPSS (Version 16) or Excel (2007). The mean and median average was carried out for each set of data. If these values equalled the same or were similar, the data was considered to have

a normal distribution. The standard deviation was carried out for all the data. However the mean and median average were different from one another, the data was considered to have a not normal distribution.

When comparing two groups of data the t-test was used. The t-test enabled a comparison between the means of the two sets of data (control against variable). The t-test performed a calculation that yielded a 't' number. Depending on the degrees of freedom within the data, the computer programme determined whether there was a significant difference between the means or not using a confidence interval of 95% ($P=0.05$).

If analysing more than two sets of data a one-way analysis of variance (ANOVA) was used. This was where each set of data was compared to one another. The calculation was made to determine whether there was a significant difference between their means. The confidence interval was again set at 95% ($P=0.05$). If a significant difference was detected within the data set and post-hoc test was carried out. If there was a control data set to compare the variables against then a Dunnett's post-hoc test was executed. This allowed the identification of variable(s) that were significantly different to the control. Where no control group was used the Tukey's post-hoc test was carried out. This test compared the means of all the data sets to each other and determines where the differences were.

CHAPTER 3

**DEVELOPMENT AND EVALUATION OF A RAPID PHAGE-BASED METHOD
FOR DETECTION OF VIABLE *MYCOBACTERIUM AVIUM* SUBSP.
PARATUBERCULOSIS IN BOVINE BLOOD**

3.1. INTRODUCTION

The current 'gold standard' method for detection of MAP requires cultivation of viable organisms from faeces or intestinal tissue on Herrold's Egg Yolk Medium (HEYM), but this requires long periods of incubation (8–16 weeks; Stabel, 1997). As an alternative, organisms present in faeces have been detected by PCR-based methods, but these methods only detect DNA of the organism and give no indication of the viability of the cell detected. Using faeces to test for Johne's disease has benefits as it is a universal sample, however on the downside, PCR is susceptible to inhibitors that may be present in faeces that act as a barrier to PCR detection without rigorous DNA extraction methods (Chui et al., 2004). Commercial ELISA tests that detect sero-conversion of animals have been developed for milk and blood as a rapid alternative method to culture-based techniques. These tests are inexpensive and can be easily automated for processing large numbers of samples (Juste et al., 2005). The ELISA tests have a better sensitivity in animals that have entered the phase of infection where high numbers of organisms are being shed in the faeces (75% detection rate), however the sensitivity of the assays is poor for animals still in the subclinical phase (15% detection rate; Whitlock et al., 2000). Hence diagnosis of Johne's disease is often based on repeat test results, increasing both costs and the time taken before infection is confirmed. It can also increase the number of false positive results, due to the limited specificity of the assays. Despite these limitations it has been shown that the ELISA tests are consistently better at detecting Johne's disease than faecal culture or faecal-PCR (Pinedo et al., 2008).

The identification of MAP in the blood of animals susceptible to Johne's disease has been carried out using techniques such as PCR and culture (Gwozdz et al., 2000, Naser et al., 2004, Whittington et al., 2010). However, inhibitors present in the blood have limited the effectiveness of these methods to detect MAP cells. As described in Chapter 1, The *FASTplaqueTBTM* assay (FPTB; Lab21, UK) is a phage-based detection method originally developed to detect *M.*

tuberculosis cells in human sputum samples for the diagnosis of tuberculosis. The use of the assay to detect viable MAP in milk and cheese has already been reported (Stanley et al., 2007, Altic et al., 2007, Botsaris et al., 2010). It was found during the development of these new assay formats that the samples can contain inhibitors that reduced the efficiency of phage infection, and therefore sample processing is required to ensure that these are removed. Magnetic separation is a very simple method of capturing and concentrating cells from a matrix using a magnet beads coated with a specific binding agent (either antibody or peptide). MAP-specific binding peptides coupled to magnetic beads have been described by Stratmann et al (2002, 2006) and have been used to recover MAP cells from milk samples (Foddai et al., 2010) and therefore this method is a good candidate for separating MAP cells from the different matrices before performing the FPTB assay.

The FPTB assay use the broad host range phage D29 that can infect both the target slow growing organism (in this case MAP) and also the fast-growing members of the groups, such as *M. smegmatis*, that are used to form the lawn for plaque growth (Monk et al., 2010). Thus the plaque result alone does not indicate the presence of MAP since the presence of any other viable mycobacteria can lead to plaque formation. When the FPTB assay is used to test human sputum a cut off value (20 plaques) is applied and only samples producing more plaques than this are considered to be positive, as sputum does not normally contain high levels of other mycobacteria. However when using the FPTB assay to detect mycobacteria in samples other than sputum, other non-pathogenic mycobacteria may be present and hence identification of the cell detected is achieved by amplification of genomic signatures sequences from the plaques that form at the end of the assay (plaque PCR assay; Stanley et al., 2007). In previous studies, this has been achieved by amplification of the multi-copy IS900 element from individual plaques, although amplification of the f57 single copy gene has also been demonstrated (Botsaris, 2010).

The limitations of using milk samples with the FPTB assay are that only animals that can be milked can be sampled, in cattle, beef herd testing is reliant on faecal and blood testing. In sheep, milk may not be routinely tested and again, only milking animals can be tested with the FPTB milk assay. Hence the aim of this study was to develop a novel methodology that would allow the isolation of viable MAP cells from blood for detection by the FPTB assay. If successful, the next aim was to develop an optimised, robust plaque-PCR method to confirm the identity of the detected cells.

3.2. RESULTS

3.2.1. Initial detection of MAP in blood

As the FPTB assay has been found to be inhibited by milk, the first experiment was designed to determine whether blood has similar inhibitory effects on the assay. Throughout this study, titres of MAP cultures used for the inoculum were determined using a modification of the FPTB assay described in Section 2.1.3.3 that allows enumeration of the number of viable MAP cells present in a culture and hence values are expressed as pfu ml⁻¹. To determine if blood inhibited phage infection, 1 ml of horse blood (Oxoid, UK) was inoculated with 1 x 10⁴ pfu ml⁻¹ of MAP (K10) and the FPTB assay was performed to detect the cells present in the sample. Unspiked blood samples were used as negative controls in addition to the standard FPTB assay controls (Section 2.1.3.2). The results showed no plaque formation on the spiked or any of the negative controls plates indicating that the presence of blood inhibited phage infection in some way.

To overcome the inhibition of phage infection when developing the phage assay for milk samples, centrifugation and subsequent washing steps were introduced to separate the cells from the inhibitory components in the sample matrix (Botsaris, 2010). The same logic was applied to the development of a method to test blood samples. That is, the cells needed to be separated from inhibitory components of the blood before the phage assay was performed. In

this experiment samples (1 ml) of both horse and sheep blood were inoculated with 1×10^4 pfu ml⁻¹ MAP (K10) and then the sample was centrifuged (15 min at 2500 x g) and the pellet washed twice with FPTB Media Plus (MP). Finally the recovered cells were resuspended in 1 ml MP and the FPTB assay performed. Once again control unspiked blood samples were prepared and the standard positive and negative FPTB controls were also carried out. Again no plaques were formed from the spiked samples, whereas the positive control which did not contain any blood did produce plaques, indicating that the assay components were all working. Thus that whatever may have inhibited the FPTB assay in whole blood was carried over during the centrifugation and washing steps.

3.2.2. Optimising bead capture efficiency in Media Plus

Although methods have been developed to remove MAP cells from a milk sample using magnetic beads and then using the FPTB assay to detect the recovered cells (Foddai et al., 2010), this method had not been attempted before using blood samples. Hence two types of commercially available paramagnetic beads, Pathatrix (Invitrogen, UK) and MyOne Tosylactivated Dynabeads (Invitrogen, UK) that have been previously evaluated for capture of MAP from milk (Foddai et al., 2010) were tested for their ability to capture MAP from blood samples. To capture the MAP cells, magnetic beads coated with the MAP-specific peptides (Section 2.2.1) were added to the blood samples and incubated (10 min) for them to bind to their targets. Using a magnetic rack, the beads (with MAP attached) were gently separated from the rest of the blood and resuspended in MP before the FPTB assay was carried out.

Initially to compare the capture efficiency of each type of magnetic bead, MAP cells (K10; 1×10^4 pfu ml⁻¹) were prepared and recovered using the peptide-mediated magnetic separation (PMMS) method (Section 2.2.2) in triplicate. After the final wash stage, each sample was resuspended in 1 ml MP. The FPTB enumeration method (Section 2.1.3.3) was used to detect the recovered cells

and the results showed that the Dynabeads were able to capture approximately $1 \log_{10}$ more MAP cells compared to the Pathatrix beads (Table 3.1). However the Dynabeads were still not very efficient at capturing cells and were only able to capture 28% of the MAP cells initially inoculated into the MP.

One possible reason for the low capture efficiency may have been that the MAP cells in the sample may have saturated the available binding sites on the beads, resulting in lower numbers of cells being detected as plaques. To determine whether more beads would improve the capture efficiency, the number of beads used in the PMMS procedure to capture the MAP cells was increased from 10 μl to 20 μl and 50 μl . The results showed that increasing the amount of beads actually had an adverse effect on the capture efficiency of the Pathatrix beads. In contrast there was no change in the capture efficiency of the Dynabeads (Table 3.2). This suggested that the beads were not saturated and also indicated that the Dynabeads were the most suitable magnetic bead to use for further assay development.

Table 3.1. Capture efficiency of Pathatrix and Dynabeads after the FPTB assay

Approx. N ^o . of MAP cells in inoculum (pfu)	Average No. of Plaques ^a	
	Pathatrix	Dynabeads
10 ⁰	260	Confluent
10 ⁻¹	15	279
10 ⁻²	0	42
10 ⁻³	2	0

Confluent: Denotes confluent lysis of the lawn

^a n= 3

Table 3.2. Effect of increasing beads concentration on the capture efficiency of Pathatrix and Dynabeads

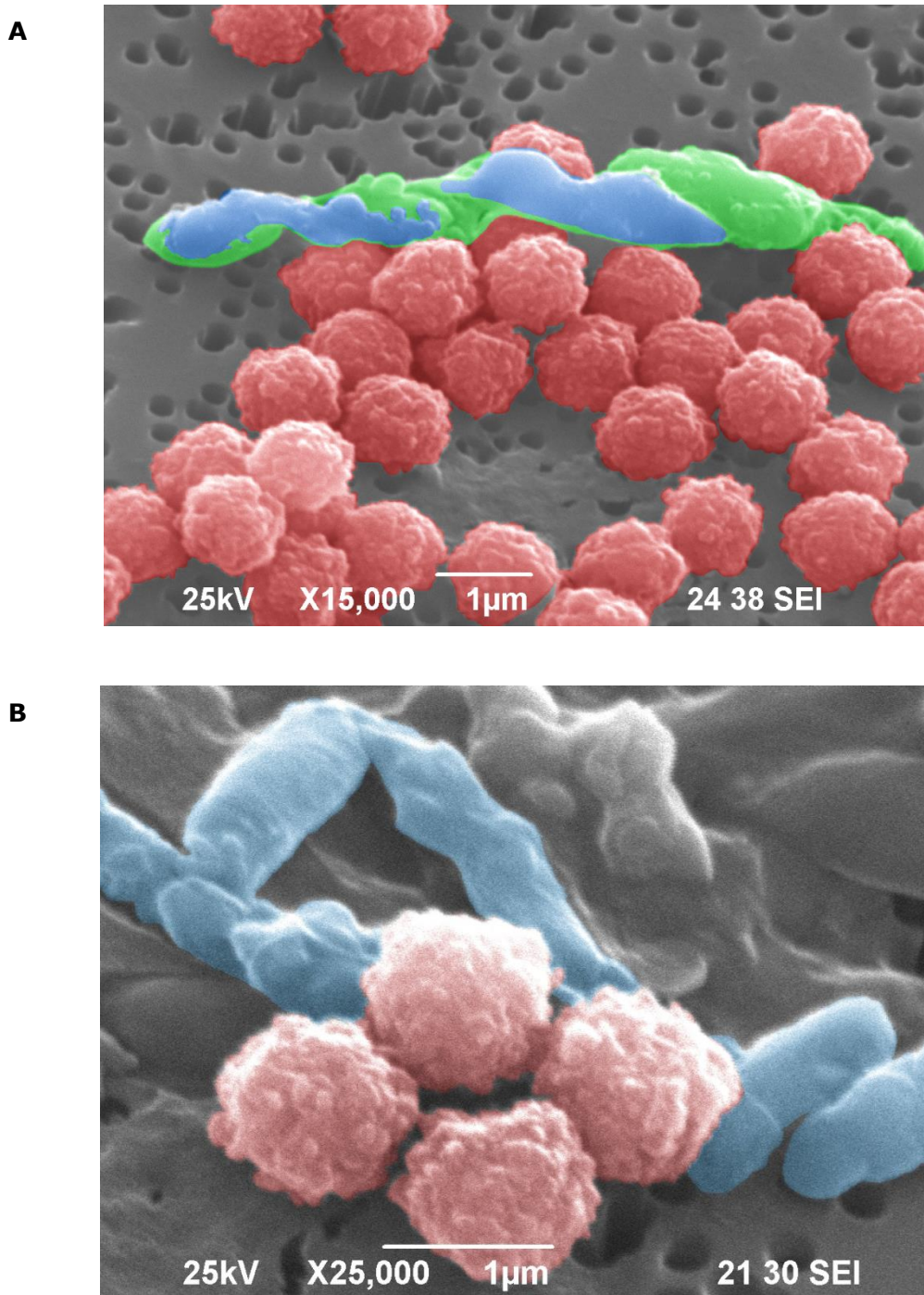
Amount of Beads (µl)	Average No. of Plaques	
	Pathatrix	Dynabeads
10	2.6 x 10 ³	TNTC
20	2.1 x 10 ³	TNTC
50	1.6 x 10 ³	TNTC

TNTC: indicates that the number of plaques that formed on the lowest dilution was greater than countable range (>300 x 10³) but lysis was not confluent.

To confirm that the drop in recoverable MAP cells was not due to bead saturation, 1×10^8 pfu ml⁻¹ MAP cells were captured on beads and visualised using Scanning Electron Microscope (SEM). Figure 3.1 shows false-colour images of MAP cells bound to beads. Figure 3.1A clearly shows that the beads were not saturated with MAP cells. In both images it is also shown that many cells can attach together around only a few beads. MAP cells are known to form clumps (Grant et al., 2003), therefore the reduced plaque number recorded after capture could be due to the clumping of cells. As the cells are held close together, in this case bacteriophage infection of a clump of cells would only lead to the formation of one plaque.

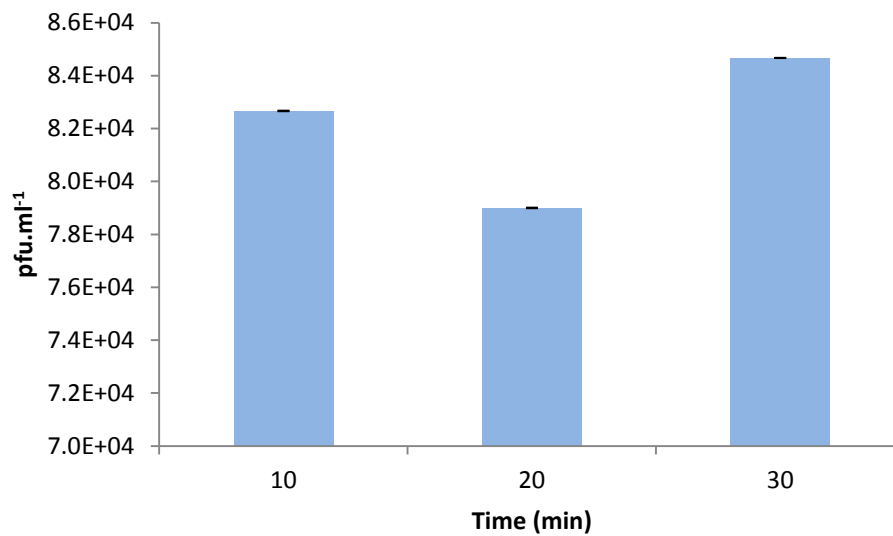
Since the SEM figures confirmed that the beads were not becoming saturated by the MAP cells, the optimal binding time for the beads to bind to the MAP cells was then investigated. The standard protocol recommended 10 min incubation of the beads with the sample. This time was increased from 10 min to 20 min or 30 min to determine if this improved the capture efficiency of the MAP cells. The results show that increasing the capture time did not improve capture efficiency significantly ($P > 0.05$) as the time was increased from 10 to 30 min. However, although the differences were not statistically significant, there was a slight increase in the number of plaques that had formed from the FPTB assay when 30 min capture time was used (Fig. 3.2). Therefore a 30 min incubation period was adopted as the standard time for the cell capture protocol.

Figure 3.1. SEM of MAP cells bound to paramagnetic beads



False colour images show MAP cells (1×10^8 pfu ml⁻¹) bound to magnetic beads following the magnetic separation method (Section 2.2.2.1) and prepared for SEM (Section 2.6). Images on panel A and B show the 1 µm magnetic Dynabeads beads (red). Panel A shows the large number of beads that suggest they do not become saturated by MAP cells (green/blue). Panel B is a higher magnification showing the clumping MAP cells (blue) and beads.

Figure 3.2. Effect of capture time on capture efficiency of MAP cells



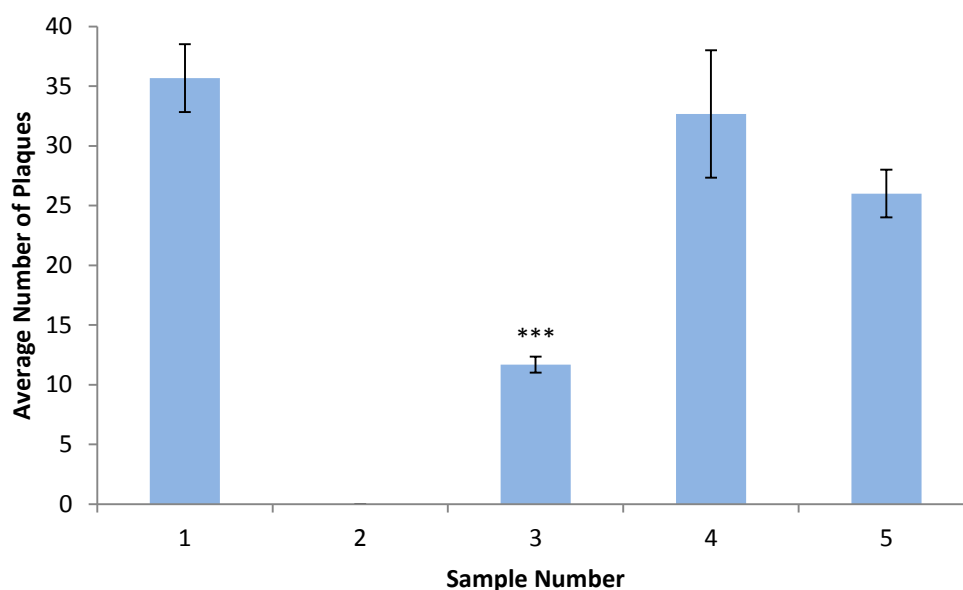
Graph showing plaque numbers recovered after performing the PMMS and phage assay on approx. 1×10^4 pfu.ml⁻¹ MAP cells incubated with the magnetic beads for 10, 20 or 30 min. A One-way ANOVA was carried out to analyse the significance of any differences in the results. Error bars represent the standard deviations of the means of number of plaques recovered from the phage assay (n=3).

3.2.3. Optimising PMMS-MAP detection in blood

The optimised PMMS process adopted was rotation of the blood samples with beads for 30 min before twice separating and washing the beads on a magnetic rack, then finally suspending the sample in 1 ml of MP (Section 2.2.2.1). This was then used as a basis to further investigate the factors affecting the efficiency of the assay and to improve the use of the method to detect MAP in blood. The MAP cells were inoculated into samples of commercially available blood (horse and sheep). To determine the efficiency of the PMMS recovery, 3.5×10^1 pfu ml⁻¹ MAP K10 was inoculated into 1 ml of horse and sheep blood (Oxoid, UK). Both bloods were used as they were readily available in the laboratory and the sheep blood was used as it is clinically relevant to Johne's disease. Magnetic recovery of beads directly from undiluted horse and sheep blood samples was found to be inefficient (0% and 33% of the cells were recovered, respectively; Fig 3.3). Assuming that some component of the blood was inhibiting either the peptide binding or the phage assay, it was clear that some sample processing was needed to either remove or reduce the concentration of the inhibitor.

Therefore the magnetic recovery step was preceded by recovery of cells by centrifugation ($4500 \times g$ for 15 min), after which the pellet was washed and resuspended in MP and the centrifugation step carried out again. As horse blood was not clinically relevant to Johne's disease, only sheep's blood was used going forward for the optimisation experiments. After dilution, the magnetic separation step was carried out. The number of MAP cells detected from samples was significantly higher ($P < 0.01$) than that recovered from the undiluted blood, resulting in 92% recovery of MAP for a 1 in 10 dilution and 73% when a 1 in 50 dilution of the sample was used (Fig. 3.3). Accordingly, a 1 in 10 dilution was adopted as the standard method as it resulted in the most efficient recovery of MAP cells.

Figure 3.3. Effect of blood on detection of MAP by PMMS-phage assay



Graph showing plaque numbers recovered after performing the PMMS and phage assay on: Sample 1; MAP in 1 ml Media Plus. Sample 2; MAP in 1 ml of horse blood. Sample 3; MAP in 1 ml of sheep blood. Sample 4; MAP in 1 ml of sheep blood diluted 1:10 Media Plus. Sample 5; MAP in 1 ml of sheep blood diluted 1:50 Media Plus. A One-way ANOVA, followed by the Dunnett's test was used to analyse significance ($*p < 0.001$) in the reduction in plaque number detected when compared to results gained for Sample 1. Error bars represent the standard deviations of the means of number of plaques recovered from the phage assay ($n = 3$).

3.2.4. Determining limit of detection of PMMS-phage method

After optimising the protocol to recover MAP cells from blood for detection using the FPTB reagents, the next step was to determine the limit of detection of the complete assay protocol. The number of MAP cells in a liquid culture was first determined using the modified FPTB assay (Section 2.1.3). These cultures were then diluted and inoculated into sheep blood at different levels in the range of approximately 1×10^4 pfu ml⁻¹ to 1 MAP pfu ml⁻¹. The optimised method, incorporating the optimised bead capture and sample preparation, was then carried out. Briefly, MAP cells were inoculated into sheep blood and the whole sample was then diluted 1:10 with MP. The samples were centrifuged (4500 *x g* for 15 min) and resuspended into 1 ml of MP. This step was then repeated and the optimised PMMS method was then carried out (Section 2.2.2.1). Using this protocol it was found that the new assay procedure was able to reproducibly detect 10 MAP cells per ml of blood (Table 3.3).

Table 3.3. Limit of detection of phage assay in spiked sheep blood

Approx. N^o. of MAP cells in inoculum (pfu)	Average number of MAP detected (pfu)^c
10⁴	Confluent ^a
10³	TNTC ^b
10²	151
10¹	9
10⁰	0

^a Confluent: lysis of 80 to 90% of the lawn of *M. smegmatis* cells.

^b TNTC: Too numerous to count; merging of plaques.

^c n = 3

3.2.5. Molecular identification of MAP

Since the FPTB assay uses a broad spectrum mycobacteriophage, the plaques from the blood assay may arise from other mycobacteria present in the clinical blood samples. This is addressed by using the MAP-specific plaque-PCR method that was developed to determine the identity of the cell detected by the phage assay in when testing milk samples by Stanley et al. (2007). There are several MAP specific DNA sequences that can be detected by PCR. MAP cells harbour a specific multi-copy genetic element named *IS900*. This insertion sequence occurs in the MAP genome between 14-18 times (Bull et al., 2000) which makes it an ideal target for PCR detection. There are other MAP-specific single copy genetic elements within the genome which have been used as targets for PCR and the *F57* and *HspX* genes are routinely used to specifically detect MAP. However they are only single-copy genetic elements, which make the detection of very low levels of DNA difficult and reduces the sensitivity of the PCR assay. Other insertion elements similar to *IS900* have been found in other *Mycobacterium* subsp. (Englund et al., 2002), which had led to questions about the specificity of using this as a MAP-specific PCR test. However simple methods have since been used by researchers to ensure the specificity of the PCR is maintained. Therefore, as the *IS900* signature sequence offers the best chance of very sensitive detection of genomic DNA extracted from plaques, this PCR assay was chosen for the further optimisation to detect MAP DNA in plaques.

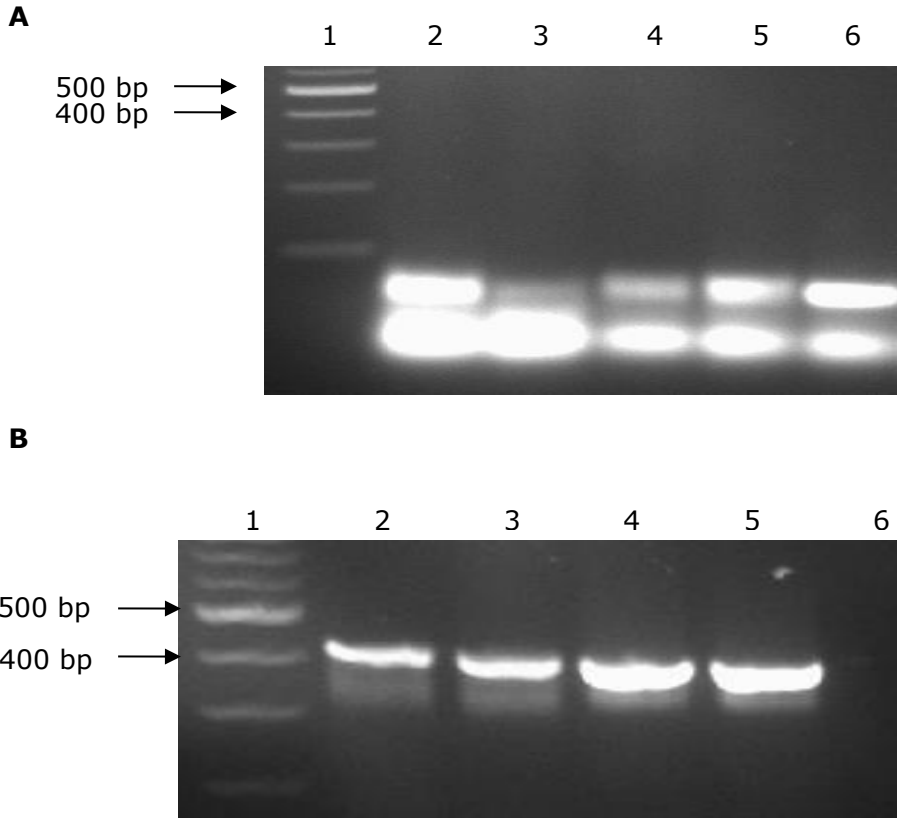
3.2.5.1. Detection of MAP specific DNA from plaques

Initially in this study an *IS900* PCR was carried out using the primers, P90 and P91 (Section 2.4.4) and PCR thermo-cycler parameters described by Miller et al. (1996). DNA was extracted from MAP cells (K10, ATCC 19851, B4 and DVL 943) by the crude boil lysis method (Section 2.4.1.1) and this was used as template DNA for the amplification of *IS900* by PCR and the Qiagen PCR mastermix was used to prepare the PCR reaction (Section 2.4.5.1). However using this method

no MAP genomic DNA was detected from any of the samples (Figure 3.4A). This suggested that either the PCR failed, or there was a problem with the PCR reaction.

The crude method for extracting the MAP DNA may have been the limiting factor since PCR inhibitors may have been present in the crude DNA preparation. Therefore DNA was extracted using the boil and lysis method, and then the DNA samples were centrifuged twice and washed in nuclease free water (Qiagen). The DNA was then diluted 1 in 100 for use as a DNA template. In the initial experiment it was also noted that there was a lot of primer dimer in the PCR samples, including in the negative control sample that only contained water rather than template DNA. This could be indicative of too high a primer concentration in the reaction mixture, therefore the primers concentration in the PCR reaction was reduced to 0.2 μ M. The PCR was then carried out again and this time the results show that there was good amplification of the 400 bp product indicating successful detection of the MAP specific *IS900* sequence from the DNA of each of strains tested (Figure 3.4B). This experiment confirmed that all of the PCR reagents were working correctly and formed a base line for further development of the plaque PCR method used following the phage assay to confirm the identity of the cell detected by the phage assay.

Figure 3.4. Development of the IS900 PCR amplification assay



PCR amplification products were analysed using a TAE agarose gel (2 %) which was run for 1 h at 70 V. The MAP *IS900* band was expected to be approximately 400 bp. Panel A; Amplification of the *IS900* PCR on four strains of MAP DNA was performed using method described by Miller et al. (1996). Panel B; PCR was performed using a modified DNA extraction method (section 2.x) and a lower primer concentration. Lane 1 contains the 100 bp molecular weight marker; the position of the 500 bp and 400 bp bands is indicated by the arrows (see Figure 2.5 for marker details). Lanes 2-5 the template added to the PCR reaction was (1) MAP DNA; (2) K10; (3) ATCC 19851; (4) B4; and (5) DVL 453. Lane 6 is negative control sample where the template DNA was replaced with RO water.

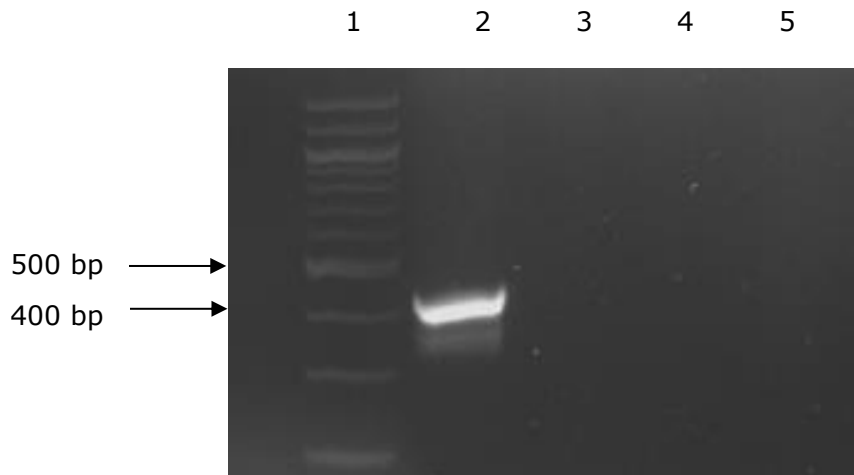
In the method described by Stanley et al. (2007), and later by Botsaris et al. (2010), a single plaque was picked and the DNA extracted using a simple manual squeeze-freeze method (Qian and Wilkinson, 1991) and the DNA extracted from the plaque used as the template for the MAP specific IS900-PCR assay. The theory of this method is that one MAP cell leads to the formation of one plaque and therefore the PCR needs to be sensitive enough to detect one cell.

To establish this method, the FPTB assay was carried out using MAP K10 cells and DNA extraction carried out on the plaques that formed (Section 2.4.2). The P90 IS900 PCR described by Stanley et al. (1997) was then used to detect MAP DNA extracted from one plaque. Two samples of DNA extracted from MAP-plaques, along with a negative (water) control and a positive control containing genomic MAP DNA (K10 or ATCC 19851) prepared as described above. However only genomic MAP DNA was detected, producing a band at 400 bp (Figure 3.5) whereas no amplification of the IS900 element occurred from the DNA extracted from one plaque, suggesting that the PCR assay was not sensitive enough to detect one MAP cell from one plaque. The freeze squeeze DNA extraction method may result in some DNA loss in the agar pellet and this may limit the sensitivity and robustness of the PCR identification assay.

There are different methods that can be used to extract DNA from an agarose gel-based sample. Gel-DNA recovery kits are used frequently to purify DNA from agarose gels after separation by electrophoresis. The principle of these kits is to dissolve the agar (by chemical or enzymatic treatments) and then using affinity spin-columns, extract, clean and concentrate the DNA. Although the agar used in petri dishes is a cruder form of agarose, and potentially of lower quality, the same purification method can be applied to the extraction of DNA within agar extracted from the centre of plaques. The spin columns generally need large amounts of 'carrier DNA' to improve the efficiency of extraction. As each plaque arising from the assay mainly contains the DNA from lysed *M. smegmatis* cells,

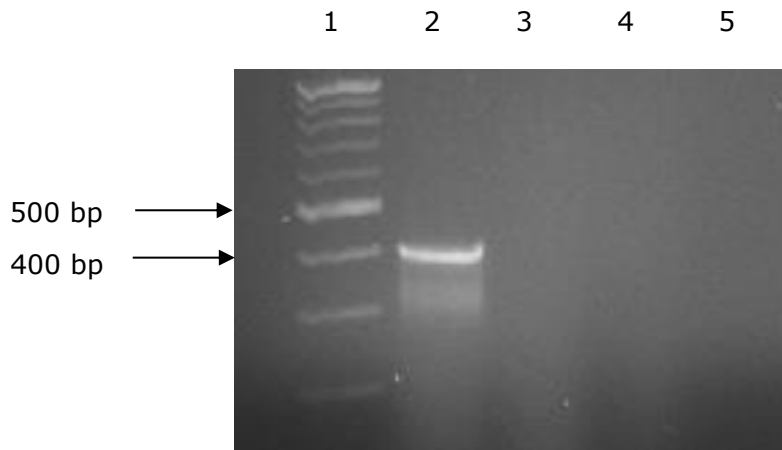
there would be a sufficient amount of carrier DNA present to be compatible with the use of these spin columns. Hence to improve the efficiency of DNA extraction, plaques were picked from plaques derived from infected MAP cells formed using the FPTB assay. The DNA was extracted using Gel-DNA recovery spin columns (ZymoResearch, Cambridge Biosciences, UK; Section 2.4.2.2). The MAP-specific PCR was then carried out to compare the DNA extracted by the spin columns with DNA extracted by the 'freeze and squeeze' method. Genomic MAP K10 DNA was as a positive control. The results show however, that once again no bands were visualised on the agarose gel (Figure 3.6).

Figure 3.5. Establishing the P90-P91 plaque-PCR assay



PCR amplification products of *IS900* were analysed on a 1.5 % agarose gel separated for 1 h at 70 V. Lane 1 is the 100 bp molecular weight marker (Figure 2.5). The template DNA used in each PCR reaction was Lane 2; MAP chromosomal DNA, lane 3 and 4; MAP plaque DNA (strains K10 and ATCC 19851, respectively) and lane 5; negative control (water).

Figure 3.6. Developing DNA extracted method using Zymo-spin columns



PCR amplification product specific for MAP (*IS900*), which were expected to be approximately 400 bp, were analysed on a 1.5 % TAE agarose gel separated for 1 h at 70 V. Lane 1 is the 100 bp molecular weight marker (Figure 2.5). The template DNA used in each PCR reaction was Lane 2; MAP chromosomal DNA (K10), Lane 3; MAP DNA extracted using the manual 'freeze and squeeze' DNA extraction method (Section 2.4.2.1), Lane 4; DNA extracted from a plaque using Zymo-spin columns and Lane 5; negative control (water).

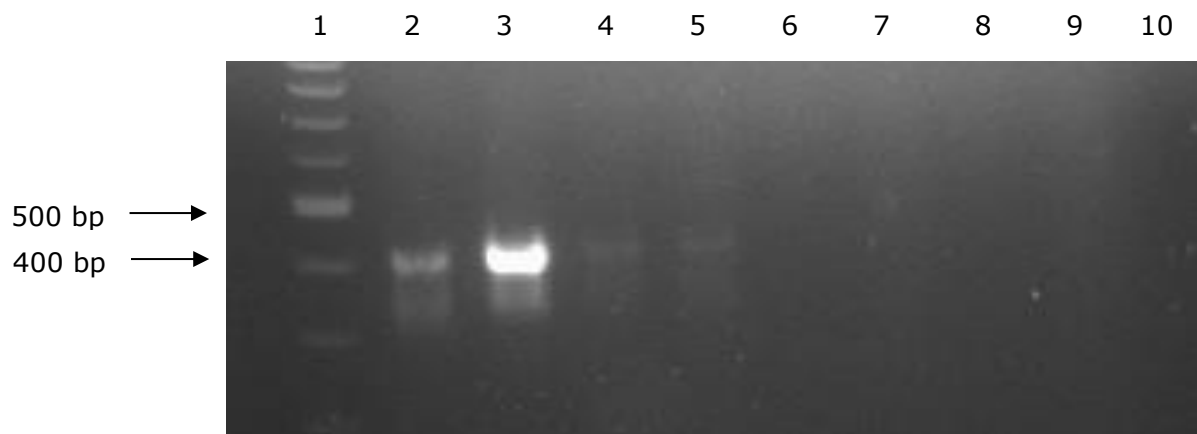
To determine the sensitivity of the PCR reaction, the concentration of a sample of chromosomal MAP DNA was measured using the Nano-drop (Section 2.5.2). The concentration of the DNA was $36.4 \text{ ng } \mu\text{l}^{-1}$, and from this a series of 10-fold dilutions were prepared until the DNA concentration was less than $10 \text{ fg } \mu\text{l}^{-1}$ to represent the amount of target DNA predicted to be present in one cell (the minimum amount that would be present in one plaque). The *IS900* PCR assay was then repeated (Section 2.4.5.1). The results showed that the PCR, prior to optimisation could only detect around 30 pg of DNA (Figure 3.7), which was not sensitive enough for this application.

3.2.5.2. Nested-PCR amplification of signature MAP DNA

Nested PCRs can be used to sensitively and specifically detect regions in DNA that may be hard to amplify. The principle of the nested-PCR is that the PCR reaction is split into two rounds of amplification. The initial round amplifies a region of DNA that contains the specific PCR target of interest. This results in amplification of the amount of template DNA containing that PCR target sequence, and this is then further amplified in the second round of the PCR using primers that target a sequence that lies within (or are nested within) the original amplicon.

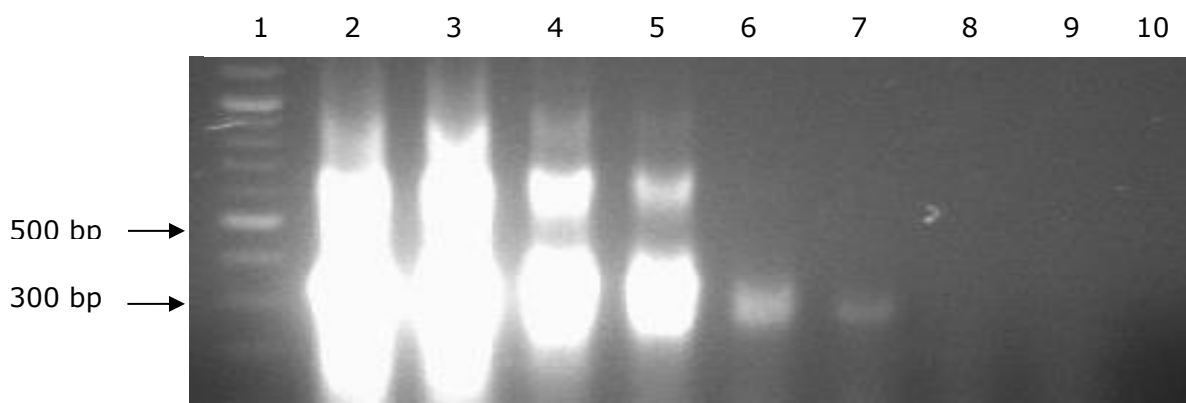
In this study the nested-PCR described by Bull et al. (2003) was used to amplify the same *IS900* element found in MAP DNA (Section 2.4.5.2). Experiments were first performed using dilutions of purified MAP genomic DNA to determine whether the nested-PCR would be sensitive enough to detect the *IS900* target sequence present in one MAP cell. The results showed that the nested-PCR method was more sensitive than the *IS900* PCR that had been used before and that around 300 fg of DNA could be detected (Figure 3.8).

Figure 3.7. Determining the sensitivity of the IS900 PCR assay



A MAP (K10) chromosomal DNA preparation was diluted in 10-fold steps from $36.4 \text{ ng } \mu\text{l}^{-1}$ to $3.6 \text{ fg } \mu\text{l}^{-1}$. This was used as template for the PCR amplification of IS900 product specific for MAP using primers P90/91. The expected PCR product was approximately 400 bp and the products were analysed on a 1.5 % TAE agarose gel separated for 1 h at 70 V. Lane 1 contains the 100 bp molecular weight marker (Figure 2.5), In lane 2 to 9 is the concentration MAP chromosomal DNA (K10) reduced from $36.4 \text{ ng} \cdot \mu\text{l}^{-1}$ to $3.6 \text{ fg} \cdot \mu\text{l}^{-1}$. In Lane 10 the template DNA was replaced by water (negative control).

Figure 3.8. Determining the sensitivity of the nested IS900-PCR assay



A MAP (K10) chromosomal DNA preparation was diluted in 10-fold steps from $36.4 \text{ ng } \mu\text{l}^{-1}$ to $3.6 \text{ fg } \mu\text{l}^{-1}$. This was used as template for the PCR amplification of IS900 product specific for MAP using nested primers TJ1-TJ4. The expected PCR product was approximately 300 bp and the products were analysed on a 1.5 % TAE agarose gel separated for 1 h at 70 V. Lane 1 contains the 100 bp molecular weight marker (Figure 2.5), In lane 2 to 9 is the concentration MAP chromosomal DNA (K10) reduced from $36.4 \text{ ng} \cdot \mu\text{l}^{-1}$ to $3.6 \text{ fg} \cdot \mu\text{l}^{-1}$. In Lane 10 the template DNA was replaced by water (negative control).

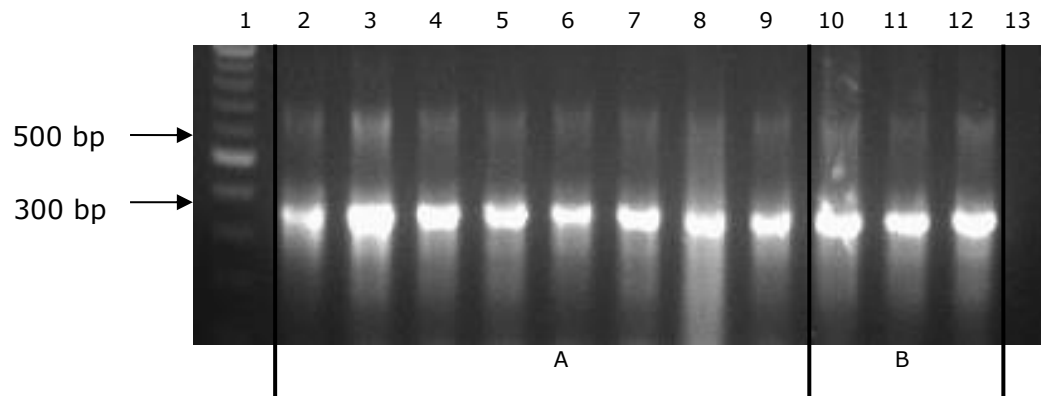
However this was still not sensitive enough to be able to reliably detect MAP DNA if only one cell is present in the sample. The MAP K10 genome is 4,829,781 bp (Li et al., 2005) and given that the average weight per base pair is 652 Daltons and 1 Dalton is equal to 1.67×10^{-24} g, the weight of the MAP K10 strain genome can be calculated to about 5.26 fg (Botsaris, 2010). In addition the PCR the protocol described by Bull et al. (2003) was extremely time consuming, taking around nine hours to complete, which was not ideal when the aim was to develop a rapid identification method. Hence the PCR parameters described by Bull et al. (2003) were re-optimised to reduce the amount of time required for each cycle. Section 2.4.5.2 describes the final set of conditions that were established as being optimal to achieve sensitive amplification of the DNA sequence. By optimising the PCR thermo-cycling parameters, the time taken to carry out the PCR was reduced from 9 h to 3 h, thus increasing the speed of the assay. A greater volume of PCR product from the initial round of the PCR was also used in the nested portion of the PCR (10 μ l instead of 5 μ l). The results demonstrated that using these optimised PCR conditions that the method was now sensitive enough to detect extremely low concentrations of DNA equivalent to that present in one MAP cell (Figure 3.11).

In the studies by Stanley et al., (2007) and Botsaris et al., (2013), DNA was extracted from individual plaques. It was often the case that not all plaques proved to be *IS900* positive (as to be expected when sampling milk, since it is known that non-pathogenic mycobacteria will be present in the sample). For the purposes of developing a blood assay, it was less likely that non-pathogenic mycobacteria would be present and therefore the ratio of pathogen to non-pathogen plaques was of less concern. Therefore to increase the sensitivity and robustness of the PCR identification step, multiple plaques were picked and pooled together and then the DNA was extracted from this pooled sample.

To evaluate the effectiveness of this method and to determine the optimum number of plaques that could be pooled together and still allow efficient DNA

extraction, different numbers of plaques (five, ten and fifteen) were picked following detection of MAP cells using the FPTB assay. The DNA from the plaques was then extracted using the spin-column DNA extraction method (Section 2.4.2.2). The modified nested-PCR was then carried out and the signature IS900 MAP DNA was detected for all samples tested (Figure 3.9). This suggested that the optimised nested-PCR was able to detect plaque DNA.

Figure 3.9. Optimised nested-PCR sensitivity (A) and its ability to detect MAP plaque DNA (B)

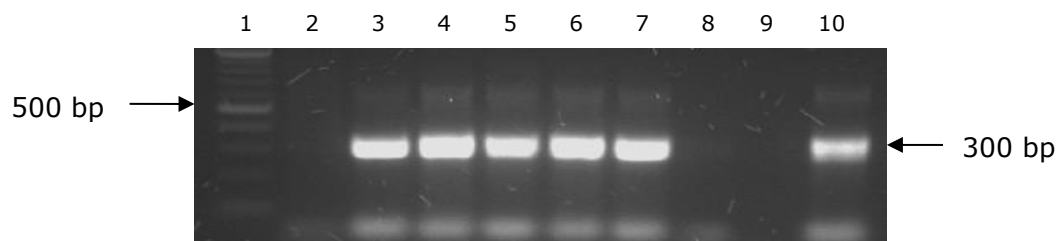


A MAP (K10) chromosomal DNA preparation was diluted in 10-fold steps from $36.4 \text{ ng } \mu\text{l}^{-1}$ to $3.6 \text{ fg } \mu\text{l}^{-1}$. This was used as template for the PCR amplification of IS900 product specific for MAP using nested primers TJ1-4. The expected PCR product was approximately 300 bp and the products were analysed on a 1.5 % TAE agarose gel separated for 1 h at 70 V. Lane 1 contains the 100 bp molecular weight marker (Figure 2.5), In lane 2 to 9 Section A) is the concentration MAP chromosomal DNA (K10) reduced from $36.4 \text{ ng} \cdot \mu\text{l}^{-1}$ to $3.6 \text{ fg} \cdot \mu\text{l}^{-1}$. In lanes 10-12, DNA from 5, 10 and 15 MAP plaques were present. In lane 13 the template DNA was replaced by water (negative control).

There are no good estimates of numbers of cells present in the blood of an infected animal, but the general consensus is that it is likely to be low (for instance see Bower et al., (2011)). To confirm that it was still possible to detect the DNA from a single MAP plaque within this sample, agar extracted from one MAP-positive and four MAP-negative (*M. smegmatis* only) plaques were mixed together. Even at this low concentration of target DNA, the nested PCR assay was able to detect the MAP DNA after extraction even in samples that contained the lowest MAP DNA concentration (1 plaque MAP: 4 *M. smegmatis* plaques) (Figure 3.10).

Since the FPTB assay will detect any mycobacteria present in a sample, it is possible that some plaques in the sample may arise from non-MAP cells. It is also possible that inefficient inactivation of the bacteriophage by the virucide can lead to some plaques being formed due phage that are not inactivated and replicate on the *M. smegmatis* again leading to plaques that do not contain MAP DNA. Thus by increasing the number of plaques picked, this decreases the likelihood of performing the PCR assay on a MAP-negative plaque and simplifies the assay by reducing the number of PCR assays needed, while at the same time retaining the sensitivity of being able to detect the DNA arising from a single MAP cell.

Figure 3.10. Sensitivity of the optimised nested-PCR using mixed MAP and *M. smegmatis* plaques



Nested-PCR amplification of the 300 bp IS900 DNA region specific for MAP. Lane 1; DNA extracted from 5 *M. smegmatis* plaques. Lanes 2; DNA extracted from 5 MAP plaques. Lane 3; 4 MAP plaques mixed with 1 *M. smegmatis* plaque. Lane 4; 3 MAP plaques mixed with 2 *M. smegmatis* plaques. Lane 5; 2 MAP plaques mixed with 3 *M. smegmatis* plaques. Lane 6; 1 MAP plaque mixed with 4 *M. smegmatis* plaques.

3.2.5.3. Quantitative Real-Time PCR

Once the optimal method for the PMMS-plaque-PCR method had been established, a method was needed to be able to compare the efficiency of the assay with another method for detecting MAP cells. Ideally this would be culture, but the high failure rate of culturing MAP from clinical samples meant that this could not be relied upon. Therefore to act as a comparison for the PMMS-phage assay being developed, a quantitative real-time PCR (qRT-PCR) method was established using the commercial assay produced by Tetracore (Section 2.4.5.4) which is reported to be designed to rapidly detect MAP cells in faecal, tissue and liquid samples.

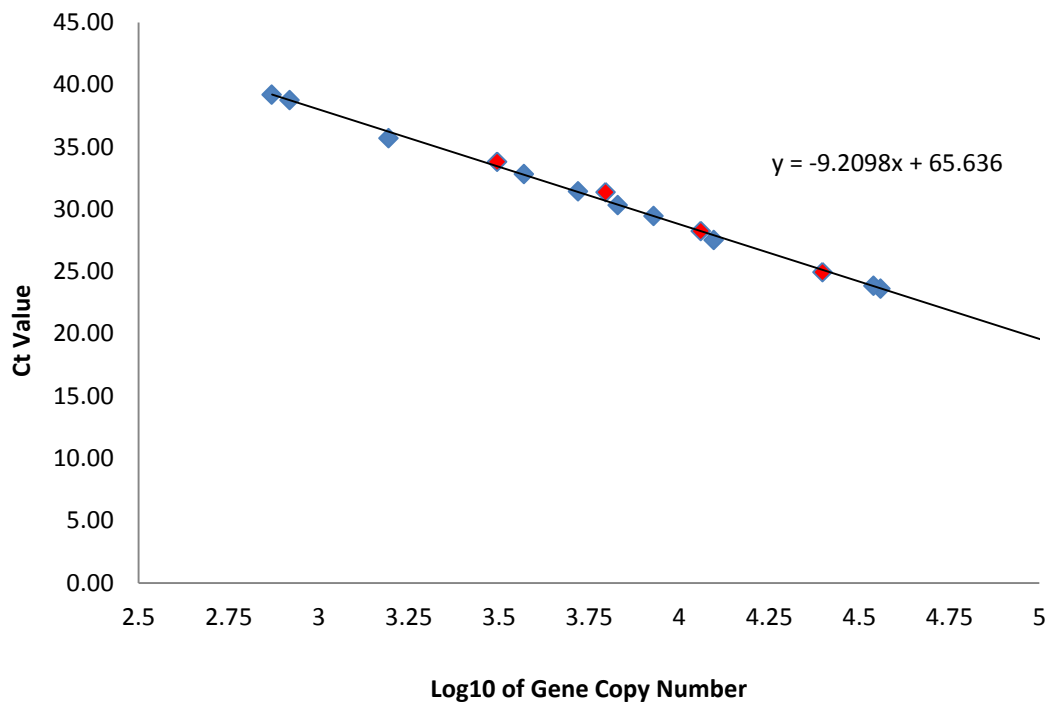
The target MAP DNA sequences targeted by the Tetracore assay is the MAP-specific, single copy gene *hspX*. Provided in the kit is a positive control that contains the equivalent of 2.5×10^4 copies of the MAP genome. To establish the method, and determine the limit of detection of the PCR assay, the control, DNA sample from the Tetracore kit was diluted in 2-fold steps to allow a standard curve to be constructed (Figure 3.11).

To determine the limit of detection of this kit, DNA was extracted from cells using the manufacturer's protocol (Section 2.4.5.4). The number of cells in each sample was estimated using the enumeration modification of the phage assay (Section 2.1.3.3). This culture was diluted into sheep blood to give an initial inoculum of 1×10^4 to 1×10^1 pfu ml⁻¹, to give samples with the lowest inoculum of approximately 10 cells per ml. The PMMS-phage assay was then performed on these samples to determine the number of cells that were recovered from the blood sample.

The results showed that the limit of detection of the qRT-PCR was lower (741 cells per ml) than that of the phage assay alone (10 cells per ml) when the qRT-PCR results were plotted on the standard curve (Figure 3.11), and that of the combined optimised nested-PCR used after PMMS and phage detection which was able to detect the genomic DNA from single cells. This difference may have

been due to fact that the *hspX* gene was used as the target for the qRT-PCR assay. Although highly specific to MAP, the *hspX* gene is found only in single copies in the genome, whereas the target for the nested PCR, IS900, can be present in between 14 and 20 copies in the MAP genome (Enosawa et al., 2003). Although the ability to detect and enumerate the MAP cells present in samples by applying the qRT-PCR assay as confirmation of the results gained using the FPTB assay would be an advantage, the limited sensitivity of the Tetracore qRT-PCR when it was used in this study limits its usefulness when trying to validate the results gained using the FPTB assay.

Figure 3.11. Sensitivity of the Tetracore qRT-PCR MAP detection assay



Graph of different concentrations of the positive control MAP genomic DNA supplied in the Tetracore kit (red diamonds) against Ct value used to construct a standard curve. Blue marker diamonds indicate Ct values gained for dilutions of MAP K10 DNA recovered from a culture of cells that was enumerated using a modification of the phage detection assay to determine the limit of detection of the qRT-PCR assay.

3.3. DISCUSSION

During the development of the phage-based detection method it was found that inhibitors in the blood prevented the *FASTPlaqueTBTM* assay from detecting MAP cells. The use of PMMS to recover cells from the sample has two benefits; it allows concentration of cells and does not affect the viability of MAP. Initially optimising the cell capture method was required. There are many different magnetic beads and binding protocols that could be used and many factors which may affect the binding of MAP cells present in a blood samples. Two types of beads; Pathatrix and Dynabeads (Invitrogen, UK) were tested in this study. It was found that the Dynabeads reproducibly captured more cells than the Pathatrix beads, but the number of cells detected was always lower than the original inoculum. Differences in the characteristics of the beads can affect cell capture, such as: composition, size, concentration, and surface modification (Foddai et al., 2010). Dynabeads being smaller (1 μm) and tosylactivated may have resulted in less bead clumping and resulted in a greater available surface area to bind MAP compared to the Pathatrix beads which are larger (>5 μm) and coated with antibodies. The SEM images also may help explain the apparent loss in capture efficiency, as the MAP cells tended to clump around the beads. Thus in the phage assay, a clump of infected cells constrained on the bead surface would give rise to just one plaque after the phage assay. When this is applied to blood samples from infected animals, it is unlikely that cell concentrations in these clinical blood samples would be high enough to result in clumping, so this result – which may be an artefact of the high cell numbers achieved in the inoculum culture ($\sim 10^8$) – may not be significant when the assay is applied to real blood samples.

In addition to the different properties of the beads it was seen that the properties of the sample affected the efficient capture of MAP cells in the blood sample. When using horse blood no recovery of MAP was achieved whereas low levels of recovery was achieved using sheep blood. The viscosity of horse's blood

is much higher than that of sheep and cattle blood (Windberger et al., 2003) and therefore limitation of bead movement in the sample may have hindered capture of MAP cells. Diluting the sample using modified Media Plus (modified 7H9 media) improved recovery of MAP cells from spiked blood samples. This may be because the beads could then move more easily through the sample or perhaps inhibitors that interfered with the peptides binding to the cells may have been diluted below a critical concentration. Diluting the sample more than 1 in 10 reduced the capture PMMS efficiency, presumably due to the fact that the low number of cells in the sample became more dispersed. Interestingly it was noted that the addition of Media Plus to the blood samples induced lysis of the blood cells. While this was not important during the development of the assay using samples inoculated with cultured MAP, it would be important when using the assay to test clinical blood samples, since the MAP cells are believed to be mainly intracellular when they are present in blood and therefore would be inaccessible for both PMMS and phage infection.

Once capture had been achieved, it was found that further washing of the captured cells was required to remove any bacteria that were not tightly bound to the beads and to remove inhibitors of the phage assay. This is consistent with observations made during the development of other assay formats for use with other sample types (Botsaris et al., 2010).

MAP has been detected in blood samples by PCR-based methods (Gwozdz et al., 2000, Naser et al., 2004, Whittington et al., 2010). However the limitation of these PCR methods is that the viability of the MAP cells cannot be determined. Although viable cells can be cultured, the time taken makes this of limited diagnostic value, since the need for decontamination before culture may reduce the number of viable cells present in a sample (Gumber and Whittington, 2007, Grant et al., 2003, Reddacliff et al., 2003). The results gained here indicated that the combined PMMS-FPTB-PCR assay can achieve rapid and sensitive detection of viable MAP in spiked blood samples within 24 h to overcome this

problem. The next step is to determine whether it would be possible to detect viable MAP in the blood of clinically infected Johne's diseased animals.

CHAPTER 4

APPLICATION OF THE PHAGE ASSAY ON FIELD SAMPLES

4.1. INTRODUCTION

In Chapter three, the development of a phage-based method was described which was able to successfully detect MAP in blood with a limit of detection estimated to be 10 pfu ml⁻¹. A robust plaque-PCR method was also developed using pooled plaques that allowed the IS900 element to be routinely identified in DNA extracted from these samples. The next natural step was to determine whether the assay could be used to detect viable MAP cells in clinical blood samples. Generally blood testing for mycobacteria revolves around tests that measure the immune response, with detection of either antigens to MAP or antibodies as either ELISA or interferon-gamma tests (Robbe-Austerman et al., 2006). The last reported use of culture of mycobacteria as a diagnostic of infection was by (Kiehn et al., 1985). Blood cultures were used to diagnose *Mycobacterium avium* complex (MAC) infection, and it was shown using this method that it had the ability to cause disseminated infection in AIDs patients. The method was found to be most reliable when detecting MAC following a cell lysis step (Kiehn et al., 1985).

Generally the use of MAP cell detection by blood culture to confirm disease is no longer used. Most recently, Naser et al. (2010) attempted to culture MAP from patients suffering from ulcerative colitis (UC) and Crohn's disease (CD). Despite some variability in the results gained from different sites of testing, individuals suffering from CD and UC did give rise to positive blood cultures, suggesting a role of MAP in human infection. However there is no definitive diagnosis that can be gained from the culture alone, as the presence of the organism has not yet been proven to be an indicator of Crohn's disease. With MAP, the only study based on culture from blood reported in the literature (in this case of experimentally infected animals) is that reported by Bower et al. (2010 and 2011), but here again the ability to culture MAP in blood is only taken to be suggestive of disseminated infection and is not used as a definitive diagnosis of disease.

As explained in Chapter three, the time it can take for MAP to form colonies severely limits the information that can be gained about disseminated MAP infection using culture-based methods of diagnosis. The ability to be able to detect MAP cells in blood samples from animals and get results within days (rather than within months), may aid the understanding of disseminated infection with regards to immune responses during disease progression and development of clinical disease.

The aim of this investigation was to apply the phage assay to clinical blood samples to determine whether MAP cells could be detected in the animals and then compare this with results gained from standard ELISA test results. In addition, as it can be assumed that presence of this organism in the blood of the animal indicates that it has crossed the gut and disseminated infection has been established, the results would be used to try and determine if evidence of disseminated infection correlates with the immune response of an animal.

4.2. ETHICAL APPROVAL FOR THE COLLECTION OF BLOOD SAMPLES

Blood samples were provided as superfluous material collected under the Veterinary Surgeons Act as part of an on-going herd health screening programme. The study protocol was approved by the School of Veterinary Medicine and Science ethical review panel prior to sample usage.

4.2.1. Initial trial of the phage assay using field samples

As an initial evaluation of the ability of the assay to detect MAP in clinical samples rather than in spiked laboratory samples, the phage assay was used to test samples from cattle that were most likely to be infected with MAP based on recurrent positive milk-ELISA test results. Blood samples were obtained from nine cows which had produced positive Johne's milk ELISA test results on the last three separate occasions of testing as part of a herd health monitoring programme (Set A; Table 4.1). To act as a negative control for the assay, blood

samples were also obtained from five cows that belonged to an accredited Johne's disease-free herd (Set B; Table 4.1). Before sampling, the site of venipuncture was cleaned twice with alcohol. So that the results from the phage assay could be compared to the blood ELISA status of the animal, blood was drawn into sterile sodium heparin Vacutainer tubes (BD, UK) for the phage assay and into plain Vacutainer tubes (BD, UK) for blood ELISA. The Johne's disease blood ELISA, which detects the presence of antibodies that cross react with MAP, was performed by the Animal Health and Veterinary Laboratories Agency (AHVLA).

To give an indication of the reproducibility of the phage assay methodology, the assay was repeated twice, independently, on parallel 1 ml blood samples. As an independent test to detect the presence of MAP cells, samples of the blood were also screened for the presence of MAP DNA using a commercial real-time PCR kit (Tetracore; Section 2.4.5.4).

The results from the initial study yielded encouraging results. Eight out of the nine animals from Set A gave a positive blood ELISA test result, while the remaining animal (#8), despite the fact that it had previously given three positive milk ELISA tests, produced a negative blood ELISA result (Table 4.1) but indicated that the majority of the animals chosen for the study in this group were likely to be infected with MAP. Interestingly the results from the phage assay detected viable mycobacterial cells in all of the blood samples from the animals in Set A (nine animals, 18 duplicate tests), including animal #8 that gave a negative blood ELISA assay result (Table 4.1). The number of plaques formed using the phage assay ranged from 7 to 32 pfu ml⁻¹, indicating that only low numbers of cells were detected in each sample. There was a good agreement ($r^2 = 0.81$) between the number of plaques generated for the two independently tested samples indicating that the phage assay method was able to reproducibly detect the mycobacterial cells present in each sample.

Since plaque number alone only indicates the presence of viable mycobacteria, to determine the identity of the cells detected by the phage assay the optimised MAP specific-PCR detection method was used. DNA was extracted from five combined plaques and in each case the PCR assay detected IS900 DNA sequences in the samples from the animals in Set A, indicating that they contained viable MAP cells (Fig. 4.1). This result confirmed that the sample from animal #8 did contain detectable levels of MAP in its circulating blood, despite the fact that the blood ELISA result was negative and the sample to positive ratio (S/P) value (S/P = 1.47) well below the cut off value defined for a positive result (S/P= >55). Hence this was not a marginal ELISA test result. In contrast to the phage assay and blood ELISA results, the commercial quantitative real time-PCR assay was unable to detect MAP DNA in any of these blood samples (Table 4.1), however the plaque numbers indicated that the number of cells present in these samples was below the detection limit previously determined for this assay (Section 3.2.6.3).

The five negative control samples from an accredited Johne's disease-free herd (Set B) were also all negative for Johne's disease when tested using the blood ELISA assay (Table 4.1). When using the phage assay three of these samples produced no plaques (i.e. no mycobacteria detected), however one sample produced two plaques and another produced one plaque. PCR analysis of DNA extracted from these plaques indicated that they did not contain MAP genomic DNA (Figure 4.1). As described in Section 3.2.6, the PCR assay using DNA extracted from combined plaques was known to be able to routinely detect DNA extracted from only one plaque, so this negative result would not be due to the low number of plaques used. Hence this negative PCR results indicated that these plaques arose either as phage 'break through' and contained only *M. smegmatis* DNA or were due to the presence of other viable mycobacterial cells in the sample (although this seems less likely).

Table 4.1. Results of phage, milk & blood ELISA and real-time PCR assays from Set A and B

Cow Number	Milk ELISA Status (3 tests)	Blood ELISA Status^a	Phage Assay^b	IS900 Plaque PCR	Blood Q-RT-PCR^c			
Set A	1	+	+	(190)	35	27	+	-
	2	+	+	(>227)	15	13	+	-
	3	+	+	(221)	19	25	+	-
	4	+	+	(111)	31	31	+	-
	5	+	+	(>227)	11	25	+	-
	6	+	+	(>227)	10	10	+	-
	7	+	+	(>227)	35	29	+	-
	8	+	-	(1.47)	10	18	+	-
	9	+	+	(193)	5	9	+	-
Set B	10	-	-		0	0	NR	-
	11	-	-		2	0	-	-
	12	-	-		0	0	NR	-
	13	-	-		1	0	-	-
	14	-	-		0	0	NR	-

Numbers 1-9 represent Set A, numbers 10-14 represent Set B.

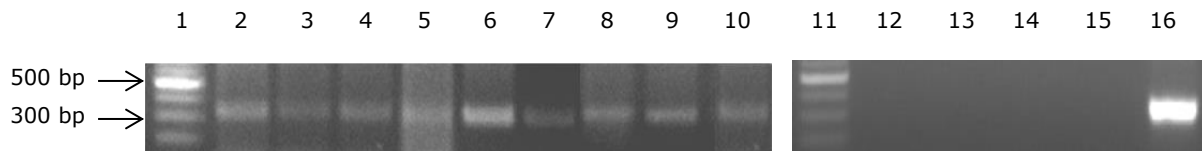
NR - 'not required' shows there were no plaques formed, therefore no PCR required.

^a Numbers in brackets give ELISA S/P values recorded; positive value cut off = >50

^b Values show the numbers of plaques obtained in two independently tested samples.

^c See Section 3.2.6.3 for the details of the lab optimisation of this commercial test.

Figure 4.1. Detection of IS900 by nested PCR from plaque DNA



The nested-PCR of Bull et al. (2003) that amplifies a 300 bp DNA region from IS900 was used. Lanes 1 and 11 contain the 100 bp ladder. Lanes 2-10; plaque PCR results for cows 1-9 (Set A). For these samples 5 plaques were picked and combined together before DNA extraction using a Zymo DNA gel extraction kit (section 2.5.1.2). Lanes 12-14 contain the results for samples from animals 11 and 13 (Set B) and contain DNA extracted from 2 plaques and 1 plaque, respectively. Lane 15 is the negative control (DNA template replaced with sterile water). Lane 16 is the positive PCR control sample (DNA template is MAP K10 genomic DNA).

As expected all the blood samples from animals in Set B were also negative when tested for MAP DNA using the real-time PCR assay, but this was not surprising giving the failure of this method to detect the presence of MAP DNA from those samples which were known to contain viable MAP cells.

4.2.2. Use of the phage assay on Johne's milk ELISA positive, negative and inconclusive animals

The animals in Set A (Section 4.2.1) were chosen for a first trial of the new phage assay results based on three consecutive repeat-positive milk ELISA test results that suggested that they were highly likely to have disseminated MAP infection, and hence it was encouraging - but not surprising - that the phage assay was able to detect MAP in these blood samples. As a more critical evaluation of the test, blood samples from a different herd to those used in Section 4.2.1 were examined using the phage assay (Set C). In this case the animals selected included individuals that (1) had given positive milk ELISA test results over the last three times of testing (Red), (2) those that had given positive, negative and inconclusive milk ELISA test results over the last three tests (Amber) and (3) those animals that had given three negative milk ELISA test results (Green; Table 4.2). Again, to allow comparison with the phage assay results, samples were also commercially tested using the blood ELISA, but given the failure of the commercial qRT-PCR assay to detect any MAP in the previous blood samples, this test was not performed in this trial. Instead, culture of samples (both whole blood and isolated buffy coated) was performed using the method described in section 2.2.2.1.

The results from the blood ELISA showed that antibodies for MAP were detected in 4 out of the 10 animals (Table 4.2). In contrast, eight out of the ten samples gave a positive result for MAP using the phage assay, indicating that there was a poor agreement ($r^2 = -0.2$) between the two assay results.

Table 4.2. Results of analysis of blood samples from animals with different milk ELISA status

Cow Number	Milk ELISA Status ^a	Blood ELISA Status	Plaque Number				Plaque PCR	Culture (WB & BC) ^c
			Whole Blood ^b		Buffy Coat ^b			
Set C	1	Red	-	20 25	38 42	+	-	
	2	Red	+	3 7	22 21	+	-	
	3	Red	+	22 15	28 32	+	-	
	4	Red	+	12 3	17 12	+	-	
	5	Red	-	13 23	15 5	+	-	
	6	Red	+	8 6	9 5	+	-	
	7	Amber	-	21 11	32 31	+	-	
	8	Green	-	22 26	22 22	+	-	
	9	Green	-	1 1	2 0	-	-	
	10	Green	-	3 5	2 5	-	-	

^a Based on most recent three Milk-ELISA results.

Red: Individual animals that had tested milk ELISA positive over the last three times of testing.

Amber: Individual animals that had tested positive, negative and inconclusive over the last three tests.

Green: Individual animals that had three negative milk ELISA readings.

^b Values show the numbers of plaques obtained in two independently tested samples.

^c WB denotes 'whole blood'; BC denotes 'buffy coat'

While none of the samples from the milk ELISA-negative (Green) or milk ELISA-inconclusive (Amber) animals gave positive blood ELISA test results, two of the milk ELISA-positive (Red) samples (animal # 1 and 5, Set C) gave negative blood ELISA test results (Table 4.2), showing that these two commercial assays also did not produce results with complete agreement.

The phage assay detected MAP in all of the Red animals, but also detected MAP cells in the blood of the one Amber animal; this animal (#7) was scored as inconclusive based on the results of the milk ELISA test and negative based on the Blood ELISA test results. MAP was also detected using the phage assay in one of the Green animals that was both milk- and blood ELISA- negative (animal #8). Animals 9 and 10 gave negative test results for all three assays (Table 4.2).

4.2.3. Comparison of MAP detection from whole blood and the buffy coat

The method developed for isolation of the MAP cells using PMMS (Section 2.2.2) includes the fortuitous lysis of the host cells in the blood sample, enabling any intracellular bacteria to be exposed to the peptides and allowing capture by the magnetic beads. However by treating whole blood in this way it was possible that some MAP cells located inside the white blood cells (WBC) may not be efficiently detected. Hence it was thought that isolation of the WBC's prior to lysis for the PMMS step may increase the number MAP cells detected by the phage assay.

To determine whether the number of MAP cells detected could be improved by isolation of the buffy coat layer, parallel blood samples obtained from animals in Set C were processed to isolate the buffy coat layer (Section 2.3.2.1). The buffy coat was then diluted into MP (200 µl buffy coat into 800 µl of MP) and the PMMS cell capture and phage assay then carried out. The results (Table 4.2) show that there was no significant difference ($P > 0.05$) between the number of plaques isolated for the same sample from whole blood or from the buffy coat layer, and accordingly there was no difference in the interpretation of the phage assay

result in terms of which animals were MAP-positive (Table 4.2). When isolating the buffy coat, the plasma fraction and red blood cells are also isolated. The PMMS-phage assay was also performed on these fractions after dilution into Media Plus to determine whether any detectable MAP remained in these fractions. No plaques were detected in any of these other fractions (data not shown), confirming that the majority of the MAP cells were present in the buffy coat layer.

4.2.4. Culture of MAP following PMMS of blood

Culture of the MAP cells from the Set C blood samples was performed to provide a definitive comparison of the phage test results with a recognised gold standard method of detecting viable MAP cells. If successful this would also have provided useful information by allowing the MAP strains that were causing infections in these particular animals to be typed. For culture, both the whole blood and the buffy coat samples were treated in the same way as the samples prepared for the phage assay by first diluting them into Media Plus to lyse the host cells. However after the PMMS was carried out, the beads were finally resuspended in 0.1 ml of MP instead of the 1 ml volume used for the phage assay samples. The liquid (including the beads) was transferred onto HEYM slopes supplemented with Mycobactin J (Section 2.1.1). To decrease the chance of reducing the number of viable MAP cells in the samples, no chemical decontamination was performed. A caveat of using this approach is that contamination of samples might occur, leading to sample loss. Despite the fact that in this case no contamination was observed of any of the samples tested, no growth of MAP occurred on any of the slopes after 30 weeks of incubation (Table 4.2). The absence of any detectable MAP growth was confirmed using the slope-wash method described by Williams and Monif (2009; Section 2.1.1.5) followed by a direct IS900 PCR of the cell suspension (Section 2.4.5) so that even any growing cells in microcolonies would be detectable.

4.2.5. Statistical analysis of results

For the four animals that gave positive blood ELISA test results in set C, the average plaque number was 20.1 (SD = 5.4), and for the four animals that gave negative blood ELISA test results (irrespective of milk ELISA status) the average plaque number was 9.5 (SD = 6.5; the two samples [#9 and #10] where plaques were obtained but no MAP DNA was detected were excluded from this analysis). This result shows a general trend that samples with a higher plaque number occur in those animals that are blood ELISA-positive.

If this analysis is extended to include all samples tested (including animals in Sets A and B, but still excluding phage-PCR negative samples) the same general trend is seen. The average plaque number for tests performed on blood samples from animals that were blood ELISA-positive was 20.5 (SD = 8.8, n = 24), and for the animals that were blood ELISA-negative the average plaque number was 10.4 (SD = 6.3, n = 10) and these values are significantly different ($P < 0.01$).

Despite this correlation, within the blood ELISA-negative group in Set C (#8), one sample contained 22 plaques and in Set A one animal (# 9) that was blood ELISA-positive only produced low numbers of plaques (5 and 9 plaques). Therefore although a general correlation can be seen between the number of MAP cells detected by the phage assay and the likelihood that an animal is blood ELISA-positive, plaque number alone does not seem to be a completely reliable predictor of the blood ELISA status of the animals.

Similarly, a comparison of plaque number results and milk ELISA status for all of the tests performed (Sets A, B and C) shows that the average plaque number for Red animals is 17.2 (SD = 9.6, n = 30) and for Green animals is 3.8 (SD = 8.8, n = 16) showing an overall significant ($P < 0.01$) trend for higher number of MAP cells detected in the blood of Red animals, but the SD values are large due to the fact that each group contains samples with either very low or very high plaque results, so again plaque number alone does not show a direct correlation with milk ELISA status.

4.2.6. Use of the phage assay on blood samples from experimentally infected animals

From the data presented in Section 4.2.2 it has been shown that MAP can be detected in clinical blood samples using the phage assay. However the only positive animals tested in both Sets A and C were those from a farm with a known Johne's disease problem. All of these animals on the farm may have come into contact with MAP being shed by animals in the clinical stage of the disease and may be sub-clinically infected. Thus, from these results, it could not be deduced how early during infection MAP can be detected in blood samples. Hence a lack of information about the infection of the animals (when infected, how much the animals were challenged with, what strain, what age they were infected at etc.) limits the analysis that one can carry out from these results collected in terms of the use of the method to monitor disease progression. Therefore the next stage of the experiments was to use the phage assay to test samples from experimentally infected animals, and also from control groups, so that these specific questions may be addressed.

4.2.7. Detection of early infection in experimentally infected calves

In 2012, a trial was being undertaken by Dr Jayne Hope (Roslin Institute, UK) and Dr Tim Bull (St. George's, University of London, UK) to investigate adenovirus vectors expressing MAP-specific antigens as a potential vaccine candidate for protection of calves against MAP infection. A cohort of eleven calves (Set D) were experimentally infected with a cattle strain of MAP. Six were treated with an experimental viral vaccine and five were not treated, as a control group. Six months post-infection, for a period of three months, blood samples were obtained for parallel testing with the phage assay and by a direct MAP-specific PCR assay (Scanu et al., 2007). After nine months the animals were culled to determine whether any MAP lesions could be detected post-mortem.

In month six the direct blood-PCR assay detected MAP DNA in samples from animals 4, 7, 10 and 11. In contrast the phage assay detected viable MAP cells only in samples from animals 2, 3, 4 and 11 (Figure 4.2). At month seven, the blood-PCR detected MAP in five samples; 5, 7, 9, 10 and 11 whereas the phage assay detected MAP in seven samples; 2, 3, 4, 5, 7, 10 and 11 (Figure 4.2). Hence only 4 samples gave positive results for both assays, but the results for another three animals (1, 6, and 8) both gave negative test results using both methods. In month eight (the final month of testing) the blood-PCR detected MAP in five samples; 5, 7, 9, 10 and 11 and the phage assay also detected MAP in three of these (7, 10 and 11). The phage assay however also detected MAP in a further two samples (2 and 3) (Figure 4.2).

Overall the tests agreed with each other 61 % of the time each for all parallel tests performed. However the results show some discrepancies and discontinuity between the blood-PCR results and the phage assay results. Sample eleven was the only one to give positive results with both tests at all 3 sampling points. Samples 7 and 10 consistently gave positive PCR results but the phage assay results were only positive in months 7 and 8. Samples 1 and 8 both gave consistently negative blood-PCR and phage results. However in samples 2 and 3, the phage assay consistently detected MAP, whereas the blood-PCR did not. In sample 6 MAP was not detected at any time by either assay.

Figure 4.2. Detection of MAP by direct blood-PCR and the phage assay in blood samples from experimentally infected calves

<u>Set D</u>	Month 6		Month 7		Month 8	
Sample Number	Blood-PCR	Phage Assay	Blood-PCR	Phage Assay	Blood-PCR	Phage Assay
1	Blue	Blue	Blue	Blue	Blue	Blue
2	Blue	Red	Blue	Red	Blue	Red
3	Blue	Red	Blue	Red	Blue	Red
4	Red	Red	Blue	Red	Blue	Blue
5	Blue	Blue	Red	Red	Red	Blue
6	Blue	Blue	Blue	Blue	Blue	Blue
7	Red	Blue	Red	Red	Red	Red
8	Blue	Blue	Blue	Blue	Blue	Blue
9	Blue	Blue	Red	Blue	Red	Blue
10	Red	Blue	Red	Red	Red	Red
11	Red	Red	Red	Red	Red	Red

All animals were infected with MAP but animals 1-6 were given a trial vaccine, whereas animals 7-11 were not vaccinated.

Blue: negative MAP test result

Red: Positive MAP test result

Table 4.3. Comparison of test results by the phage assay and direct PCR

PCR test result	Phage test result	Number of samples		%	% agreement/ disagreement
-ve	-ve	12		33.4	60.7%
+ve	+ve	9		27.3	
+ve	-ve	5	(4 UV /1 V)	15.2	36.4%
-ve	+ve	7	(all V)	21.2	
Total		33			

UV = unvaccinated

V = vaccinated

If the overall number of times this latter pattern of results is compared (i.e. PCR -ve, phage +ve result; Table 4.3) it is interesting to note that this pattern occurred 7 times in total, but only in the vaccinated group of animals. Similarly the preponderance of test results where the blood-PCR consistently detected MAP DNA but the phage assay did not was in the unvaccinated group (4/5 cases; Table 4.3). Animal nine (unvaccinated group) consistently gave this result and hence accounted for 3/5 times this pattern was seen.

With regards to plaque number, generally the number of cells detected was low (<14 pfu ml⁻¹) and this is within the range expected for blood ELISA-negative animals determined in section 4.2.5 (10.4 ± 6.3). However 63 plaques were detected in the blood sample from animal #7 after 8 months, and this was well above the average number of plaques recorded for blood ELISA-positive animals (20.5 ± 8.8). Interestingly, when this animal was culled, many lesions were seen and it was the only animal that histopathologically positive signs of the disease.

4.2.8. Use of the blood assay on experimentally infected subclinical cattle

Cattle infected with MAP may not show clinical signs of infection until years after exposure. Sub-clinical animals may shed MAP cells into the environment in their faeces and MAP cells can also be present in their milk, but both milk and blood ELISA testing on sub-clinical animals is notoriously insensitive (Whitlock et al., 2000). It is also true that an immune response may not be indicative of active infection, rather just that the animal has been exposed to the organism, and it is not known whether all animals that give a positive ELISA test result will go on to develop clinical Johne's disease. This is especially pertinent since the results in this study show that naturally infected animals with variable blood ELISA status can harbour viable MAP in their blood. Hence it is clear that more

data is required to better understand the relationship between the immune response and disease progression.

A collaboration with the University of Sydney, Australia, who were undertaking a MAP infection trial, was used to investigate the ability of the phage assay to detect MAP cells in the blood of cattle that were experimentally exposed to MAP (Set E). In this trial 30 calves (aged 2 - 4 months) were age matched then randomly allocated into a group of 20 to be experimentally infected (Numbers; 11 - 30, Table 4.4) along with a group of 10 animals that were used as uninfected controls (Numbers; 1-10, Table 4.4). Control animals were housed separately from the inoculated animals, in paddocks where no MAP infected livestock cattle had been housed in the past. The animals were not used for dairy produce and raised in a manner that minimised stress. The blood samples taken for the experiments described here was at a time point 3.5 years after the animals had been infected and at this stage they were not showing clinical signs of Johne's disease, although at the time of testing animal #23 had previously been found to be shedding MAP in its faeces (Dr K. Plain, University of Sydney, pers. comm.).

All the tests described here were performed in Australia using reagents that were prepared and tested on site before being used to test the clinical samples. Unfortunately, due to the time constraints of the visit, it was not possible to optimise the efficiency of the PMMS bead capture fully (data not shown) and thus for all these experiments the sensitivity of the assay was not as high as the optimised assay procedure used for other experiments in this thesis. In addition, a modified PCR detection assay was used, based on a published real-time PCR assay for MAP IS900 routinely used at the University of Sydney (Plain et al., 2014).

The phage assay was used to test blood samples taken from animals in Set E. The results (Table 4.4) show that two of the control animals (animals #3 and #10;) produced plaques after the phage assay was performed, however none of

these gave a positive result when the IS900 PCR was performed, indicating that these plaques represented either breakthrough or detection of a mycobacteria other than MAP. Therefore the phage results agreed with all other tests performed. Thus none of the control (not exposed to MAP) animals were positive for viable MAP by the phage assay.

There was no correlation between when the phage assay detected MAP in blood and when the PCR detected MAP DNA in faeces or the positive serum ELISA animals. Seven out of the twenty (35 %) of the inoculated subclinical animals gave positive phage-PCR results indicating that MAP cells were detected in their blood, although only very low numbers of plaques (2-5) were produced from these assays.

Two animals were found to be shedding MAP in their faeces by culture (#17 and 23) and this result was confirmed by a faecal PCR assay (Plain et al., 2014). Animal 23 was also positive for Johne's disease by serum ELISA and animal 17 was suspected as having Johne's disease as the OD value of the serum ELISA was just below the cut-off value for a positive test result. However MAP was not detected in the blood using the phage assay of these animals that were shedding MAP and had evidence of systemic immune response to the disease, but this does not mean that the disease was systemic (or disseminated) as a localised infection can lead to this.

Based on their serum ELISA results, none of the other animals were classed as infected or suspected of having clinical Johne's disease, however animals 20 and 27, which were positive for the presence of MAP in their blood according to the phage assay, had relatively high (although classed as negative) ELISA readings.

Table 4.4. Results for sub-clinical, experimentally infected cattle

Set E	Tag #	Breed	MAP exposure status ^a	Results			Serum Ab ELISA (%) ^d
				Phage assay ^b	Faecal culture	Faecal PCR ^c	
1	614	Holstein	Control	- (0)	-	-	1.00
2	618	Holstein	Control	- (0)	-	-	29.34
3	623	Holstein	Control	- (2)	-	-	3.85
4	625	Holstein	Control	- (0)	-	-	5.92
5	630	Holstein	Control	- (0)	-	-	5.42
6	634	Holstein	Control	- (0)	-	-	3.14
7	638	Holstein	Control	- (0)	-	-	17.49
8	641	Holstein	Control	- (0)	-	-	10.49
9	717	Red/Holstein	Control	- (0)	-	-	3.50
10	734	Red/Holstein	Control	- (3)	-	-	4.57
11	615	Holstein	Inoculated	- (0)	-	-	2.57
12	616	Holstein	Inoculated	+ (2)	-	*	3.28
13	617	Holstein	Inoculated	- (0)	-	-	5.00
14	620	Holstein	Inoculated	# ^e	# ^e	# ^e	# ^e
15	621	Holstein	Inoculated	- (5)	-	-	14.49
16	624	Holstein	Inoculated	+ (5)	-	-	3.28
17	626	Holstein	Inoculated	- (0)	+	+	48.68
18	627	Holstein	Inoculated	+ (2)	-	-	8.57
19	628	Holstein	Inoculated	- (0)	-	-	6.21
20	629	Holstein	Inoculated	+ (2)	-	-	35.62
21	631	Holstein	Inoculated	- (2)	-	-	12.63
22	632	Holstein	Inoculated	- (0)	-	-	3.50
23	635	Holstein	Inoculated	- (0)	+	+	118.77
24	636	Holstein	Inoculated	- (0)	-	-	6.50
25	637	Holstein	Inoculated	- (0)	-	*	4.64
26	779	Red/Holstein	Inoculated	+ (4)	-	-	5.21
27	640	Holstein	Inoculated	+ (5)	-	*	41.11
28	642	Holstein	Inoculated	- (0)	-	-	2.00
29	722	Red/Holstein	Inoculated	+ (3)	-	-	13.28
30	755	Red/Holstein	Inoculated	- (0)	-	*	1.50

^a Inoculated – animals experimentally exposed to MAP; Control – animals not exposed to MAP

^b (+/-) indicates result of combined PMMS-phage –PCR assay. Plaque numbers for each sample given in brackets.

^c (*) indicates inconclusive test result

^d Serum Ab ELISA (IDEXX); Positive value > 55%, suspected value 45 - 55%

^e (#) Animal 14 was culled due to other illness unrelated to Johne's disease before sample collection.

4.2.9. Using the phage assay on experimentally infected sheep

Cattle are not the only animals that are affected by Johne's disease, and sheep are also susceptible to MAP infection. Sheep generally show clinical signs of disease faster than cattle, suggesting the pathogenesis of the disease in sheep may be different (Begg and Whittington, 2010). Sheep strains of MAP have also been found to differ from cattle strains, showing a much slower rate of growth in culture and a tendency to be pigmented. It is known that viable MAP cells can be cultured from the blood of infected sheep, but it is not known whether sheep strains of MAP can be captured using PMMS or whether they are as efficiently infected using the bacteriophage D29. The phage based blood assay was originally optimised in commercially supplied sheep's blood (Section 3.2), so when planning to test clinical samples from sheep no optimisation of the methodology of the assay procedure was needed.

Frozen blood samples of culled animals from a previous trial carried out at the University of Sydney involving sheep experimentally infected with MAP were available for testing. Recovery of MAP cells after freezing had been carried out and is reviewed in Chapter 6. The results show that a 3 d recovery period is required to recover all the MAP cells in sample after freezing. However due to time restraints, only a recovery period 24 h at 37 °C was carried out for the MAP cells, which limited the effectiveness of the phage assay. In this study samples from twenty-eight sheep (Set S1) were tested; eight had been experimentally infected with between 1×10^7 and 1×10^8 cfu ml⁻¹ MAP (Telford Sheep Strain; Marsh et al., 2006; according to a validated model by Begg et al., 2010). Samples from twenty other sheep were used as the unexposed control animals; these animals had been kept on adjacent pasture, separate from the infected animals, in groups in small paddocks where no MAP-infected sheep were kept or had been kept in the past. Five of these 20 animals were vaccinated with Gudair™ paratuberculosis vaccine (inactivated strain of MAP; Dr K. Plain, pers. comm.).

Twelve months post-infection each animal was culled and faecal culture, faecal PCR and sheep serum ELISA's assays were carried out to detect the presence of, or exposure to, MAP (data summarised in Table 4.5). During the trial one unexposed, unvaccinated animal (# 3; Set S1) gave a positive MAP serum ELISA test result, suggesting the group of control animals (numbered 1-5) may have been exposed to low levels of MAP from the environment, however at the time of culling none of them showed any clinical signs of MAP infection after post-mortem.

In all the other groups the unexposed sheep gave negative faecal culture and serum ELISA test results, apart from the vaccinated control animals which - as expected - gave a positive serum ELISA result. In contrast, all eight of the exposed animals were positive for MAP by faecal PCR and five of the samples (excluding the vaccinated samples; # 6-10) were positive for MAP by serum ELISA.

At the end of the trial the animals were culled and at that time whole blood samples were taken and frozen at -80 °C and the collaborative visit to the group in Australia occurred three months after culling. To test these samples using the phage assay, the blood samples were first thawed at room temperature and left for a further 24 h at 37 °C to allow as many MAP cells to recover as possible from the freeze injury. After this the blood samples were diluted into Media Plus and the (un-optimised) PMMS-phage assay was performed. The results show (Table 4.5) that out of the twenty-eight samples tested, only 5 gave positive results using the phage assay; 3 from the exposed animals and 2 from the unexposed animals (highlighted in red in Table 4.5).

The fact that two of the control animals (#4 and #10) gave positive results for MAP using the phage-PCR assay was unexpected. However, as mentioned above, the group of animals numbered 1-5 (Set S1; blue text Table 4.5), had given some positive indications of MAP infection during the trial and #4 that gave a positive phage-PCR blood test result belonged to this group. However

both faecal culture and serum ELISA test results were negative. The other unexposed animal that gave a positive test result (#10) came from a vaccinated flock (inactivated MAP strain), hence although these animals gave positive serum ELISA test results (due to the vaccine), they consistently gave negative faecal culture test results for MAP. Hence the positive phage assay test result for this animal is difficult to explain.

Three of the eight sheep exposed to MAP produced positive phage-PCR results, however only very low numbers of MAP cells were detected (1-3 plaques). All of the animals in this group were positive for MAP by faecal culture, and therefore the phage assay agreed with the faecal PCR for three samples exposed to MAP. Interestingly only four of the group gave positive serum ELISA results (>55 %) although another two gave test results in the range designated as being suspect samples (45-55 %). In this case one of the serum ELISAs test results agreed with the phage assay results.

Hence the failure to detect MAP in the blood of all of these exposed animals may indicate that there was a problem with the methodology. Lack of recovery of the MAP cells from the effects of freezing may have caused low bacteriophage infection efficiency. Alternatively, as the coating of the beads with the peptides was not fully optimised, inefficient PMMS capture may have occurred. Alternatively the ability of the peptides used to coat the beads to bind to sheep strains of MAP has not been fully characterised and this may have affected the results gained.

Despite the limitations of this study, the fact that the majority of positive results were achieved in the exposed group is encouraging, since if these results all represented a random problem with the test it would be expected that an equal number of positive results would have been seen when testing the samples from the other negative control animals.

Table 4.5. Results of MAP detection for experimentally infected sheep

Set S	Sheep			Results		
	Tag #	Breed	MAP exposure status	Phage assay	Faecal culture	Serum Ab ELISA ^a (%)
1^b	405	Merino	Unexposed	- (0)	-	0.31
2^b	406	Merino	Unexposed	- (0)	-	0.05
3^b	407	Merino	Unexposed	- (0)	-	0.36
4^b	408	Merino	Unexposed	+ (2)	-	0.1
5^b	409	Merino	Unexposed	- (2)	-	9.88
6	124	Merino	Unexposed	- (0)	-	132.5*
7	125	Merino	Unexposed	- (2)	-	163.3*
8	126	Merino	Unexposed	- (0)	-	165.8*
9	128	Merino	Unexposed	- (6)	-	149.5*
10	129	Merino	Unexposed	+ (1)	-	150.7*
11	167	Merino	Infected	+ (2)	+	35.47
12	181	Merino	Infected	- (0)	+	145.09
13	186	Merino	Infected	- (0)	+	36.3
14	187	Merino	Infected	- (0)	+	55.02
15	188	Merino	Infected	- (1)	+	110.92
16	193	Merino	Infected	- (0)	+	45.81
17	195	Merino	Infected	+ (1)	+	61
18	198	Merino	Infected	+ (3)	+	100.26
19	2176	Merino	Unexposed	- (0)	-	1.02
20	2177	Merino	Unexposed	- (0)	-	0.28
21	2178	Merino	Unexposed	- (0)	-	0.19
22	2197	Merino	Unexposed	- (2)	-	0.74
23	2180	Merino	Unexposed	- (0)	-	0.19
24	2181	Merino	Unexposed	- (0)	-	0.09
25	2182	Merino	Unexposed	- (0)	-	0.83
26	2183	Merino	Unexposed	- (0)	-	0.46
27	2184	Merino	Unexposed	- (0)	-	-0.09
28	2185	Merino	Unexposed	- (1)	-	0.87

* - High ELISA result is due to vaccination not exposure

^a Serum Ab ELISA (IDEXX) - Positive value > 55%, Suspected value 45 - 55%. Positive test results in Bold

^b Animals number 1-5 (blue text) had potentially been exposed to MAP as MAP was detected in a faeces sample from one animal (#3) by PCR during the trial.

4.3. COMPARISON OF OVERALL TEST RESULTS

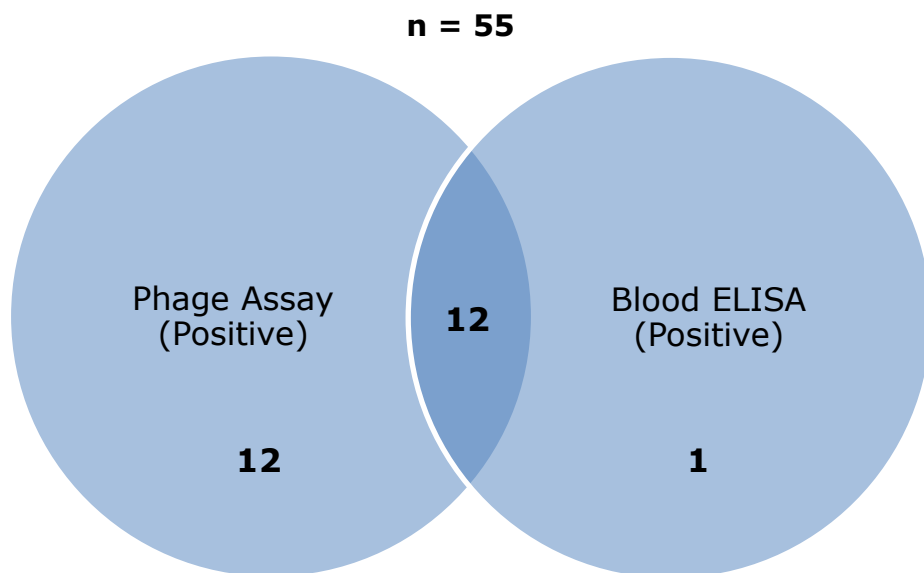
There are shortcomings when it comes to comparing efficacy of the phage assay to detect Johne's disease with other tests like ELISAs and PCR due to the variability in sensitivity and specificity of these assays. As the number of animals tested in all of the experiments was also quite low, this limits the power of the tests performed and the significance of any analysis that can be carried out. Finally Johne's disease is chronic disease and in this study a longitudinal examination of the phage assay compared to other the tests has not been carried out in a defined experimentally controlled way due to limitations in sample collection, thus any analysis that is carried out will have limited power. However, while recognising these limitations, it is worth comparing the results gained for all of the field trials to see if any patterns emerge that might inform future studies.

The data from tables 4.1, 4.2 and 4.3 for the phage assay results and the blood ELISA assays gave the largest number of samples for comparison. When examining the samples that were MAP-positive by any one of the assay results, Figure 4.3 shows that the phage assay detected viable MAP in the blood of 24 out of the 55 (44 %) of the samples, whereas the blood ELISA was positive in only 13 of these samples (24 %), suggesting a lower sensitivity for the blood ELISA assay. Interestingly, when the blood ELISA was positive the phage-PCR test results agreed 92 % of the time. However when the phage assay positive results was compared with the positive ELISA results, MAP infection was only detected 50 % of the time by the blood ELISA assay (Fig. 4.3), which may suggest the phage assay is more sensitive than the blood ELISA.

When all the data is analysed (comparison between detection of MAP and no detection of MAP), there is a very significant difference ($P < 0.001$) between detection rate using the phage-PCR assay and that given by the blood ELISA test (Table 4.6). However to reiterate, there are limitations with using these sample sets comparison. The blood ELISAs have highly variable sensitivity and

specificity, especially in animals with subclinical MAP infection, which the majority of the animals tested were, thus the blood ELISA tests are not a reliable gold standard for comparison of tests. If however, the phage assay is used as the gold standard, the sensitivity of the ELISA tests is seen to be 50 % and the specificity 96 %. Interestingly, these results are very similar to the published sensitivities and specificities of the blood ELISA assay (Table 4.6; Whitlock et al., 2000) and suggest that the phage-PCR assay has a similar detection rate to other methods used as the Gold standard for such analyses.

Figure 4.3. Comparison of the distribution of positive results using phage-PCR assay and the blood ELISA tests



Venn diagram showing the relationship between positive phage-PCR test results and blood ELISA test results based on data in Tables 4.1, 4.2 and 4.4.

Table 4.6. Contingency table of phage assay and the blood ELISA test results for comparable cattle samples

	Phage Assay +ve	Phage Assay -ve	Total
Blood ELISA +ve	12	1	13
Blood ELISA -ve	12	30	42
Total	24	31	55

Variable	Value	95% Confidence Interval
Sensitivity	0.50	0.29 to 0.70
Specificity	0.96	0.83 to 0.99
Positive Predictive Value	0.92	0.63 to 0.99
Negative Predictive Value	0.71	0.55 to 0.84
Likelihood Ratio	15.50	

The two-sided P value is < 0.0001, considered extremely significant.

The row/column association is statistically significant.

Sensitivity: The fraction of those with the disease correctly identified as positive by the test.

Specificity: The fraction of those without the disease correctly identified as negative by the test.

Positive predictive value: The fraction of subjects with positive tests who actually have the condition.

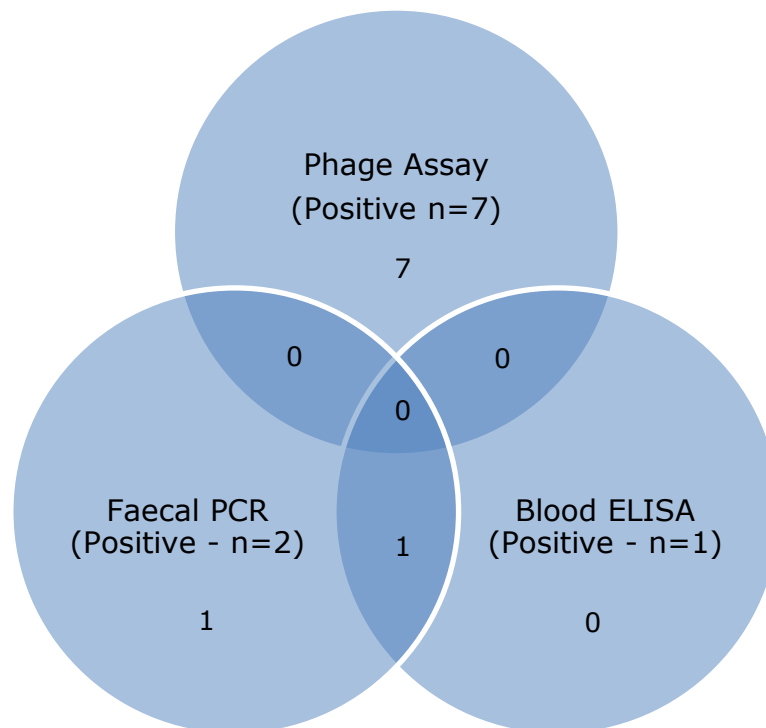
Negative predictive value: The fraction of subjects with negative tests who actually don't have the condition.

Likelihood ratio: If positive, it is how many times more likely are you to have the disease. i.e. the likelihood ratio equals 15.5, then an animal with a positive test is 15.5 times more likely to have the disease than an animal with a negative test.

The smaller data set (30 samples) generated from the collaborative work using samples from experimentally infected cattle (Set E; Table 4.4) were analysed to see if there was a correlation between the results gained using any of the tests used (i.e the phage assay, Blood ELISA and faecal PCR). Again although a very small sample set was used, seven out of the 19 surviving challenged animals (37 %) gave a positive result with the phage assay. This indicated the presence of MAP cells in the blood, but none of these samples came from animals that gave a positive faecal PCR result and or a positive blood ELISA test result. Indeed agreement between the different test results was only seen for one sample that was blood ELISA positive and faecal PCR positive (Fig. 4.7).

Figure 4.4. Relationship between positive phage assay, faecal PCR and blood ELISA results

n = 19 (Inoculated)



Venn diagram showing the relationship between positive results gained from the phage assay, blood ELISA and faecal PCR for samples in Set E (Table 4.3). Overlapping areas show the agreements from each test.

4.4. DISCUSSION

The initial task in this study was to try and detect viable MAP in animals from a farm with a known Johne's disease problem. The first set of animals were selected using standard current diagnostic criteria for Johne's disease which requires repeat testing over a period of six months, and an animal is only considered positive if it has given three consecutive positive milk ELISA test results in that time. As a control, five animals from a different herd that had been accredited as Johne's disease-free were tested. To validate the phage test results in this initial trial, blood ELISA tests were carried out in parallel to determine whether the detection of MAP antibodies in the blood corresponded to the detection of MAP cells using the phage assay.

The blood ELISA results for the initial nine presumed infected animals agreed with the diagnosis of the milk ELISA's in all but one case (animal #8; Set A) which gave an indeterminate test result. Discrepancies between milk and blood ELISA's have been reported before and do not always correspond with one another (Hardin and Thorne, 1996). In contrast the phage assay detected viable organisms in blood samples from all of the infected animals (Set A; Table 4.1), and this result agreed with the milk ELISA results. In the presumed Johne's negative herd (Set B; Table 4.1), two samples (animals #11 and 13) produced MAP DNA-negative plaques, which may be because the virucide did not destroy all the phage before the sample was plated on the lawn of *M. smegmatis*. Break-through has been reported before when performing the FPTB assay (Botsaris et al. 2013), but the introduction of the PCR identification step overcomes this problem (Stanley et al. 2007). Hence in this study samples were not scored as MAP-positive unless the IS900 sequence can be amplified from the plaque.

In the second set of animals from a separate Johne's disease-affected farm, the animals tested were chosen with variable milk ELISA statuses (Set C). Three of the animals from Set C gave negative milk and blood ELISA test results and two of these were also negative for MAP using the phage assay. However the

phage assay detected viable MAP in the blood from one animal (Set C; animal #22), and the plaque numbers were equivalent to those of the majority of the other milk ELISA-positive animals. This indicates that results gained using a method that directly detects the viable organism can differ from test results based on the immune response of the animal to infection. This is a phenomenon that has been described before with MAP cell detection being followed by a spike in the immune response seen by ELISA tests six months post infection in cattle (Kawaji et al., 2012). Further work is now needed to understand the relationship between the immune response of the animal and the presence of viable organisms in the blood.

When phage assay-MAP positive samples were cultured, no growth was detected. Since the plaque number indicates that there were fewer than 42 MAP cells per ml in all of these samples, the lack of growth is to be expected as this number is below the limit of detection for the culture method used. MAP has been detected in blood samples by PCR-based methods and by culture (Gwozdz et al., 2000, Naser et al., 2004, Bower et al., 2010, Bower et al., 2011). Although viable cells can be cultured from these samples, the time required makes this of limited practical value and the need for decontamination before culture may reduce the number of viable cells present in a sample (Reddacliff et al., 2003). Interestingly here, following PMMS of blood samples, no contamination of cultures was seen suggesting that the selectivity of the PMMS followed by the extensive washing used in this method is sufficient to remove contaminating microflora from the sample without the need to apply chemical decontamination.

The phage assay was next carried out on calves experimentally infected with MAP (Set D). This was to determine how early during infection the phage assay could detect MAP compared to a blood-PCR. Early immune response has been detected before as early as four months post-infection when using interferon-gamma tests (Waters et al., 2003). Sensitivities and specificities of milk and

blood ELISA's in the early stages of MAP infection have been reported as being poor (Nielsen and Toft, 2008). The results in this study showed that both the phage assay and the direct blood-PCR were able to detect MAP six months post-infection but this was not as early as the reported interferon-gamma test. However the measurement of interferon-gamma is an indicator of exposure to MAP or its antigens and does not differentiate between dormant infection and active infection, thus it is difficult to identify those animals that may go onto clinical disease compared to those that would not (Jungersen et al., 2011).

Some of the discrepancies between the phage assay and PCR assay may be explained by the ability of bacteriophage D29 only to infect viable, actively growing cells (see Chapter 6). Therefore when the direct blood-PCR assay used in the study of Set D detected MAP DNA in a sample (e.g. set D samples 5, 7, 9 and 10); the DNA detected may have been from dead/non-viable MAP cells which would not have been detected by the phage assay. However in samples # 2, 3 and 4 from Set D the phage assay detected the presence of viable MAP cells whereas the blood-PCR gave negative results, which cannot be explained in the same way. Limitations to the sensitivity to both the blood-PCR and the phage assay may have resulted in the discrepancies between the tests, especially as only small volumes (1 ml) were available for sampling which then can limit the sensitivity of detection.

Analysing the data for Set C (Table 4.2), MAP infection was detected in animals with both inconclusive and negative blood and milk ELISA test results. Many of the animals tested were not exhibiting clinical manifestations of Johne's disease, but MAP was still detected circulating in their blood using the phage assay. In Set E, the animals were infected 3.5 years before blood samples were taken for testing and were not showing clinical symptoms for Johne's disease. The results showed that although plaques were detected in two of the unexposed animals in these studies, no positive MAP DNA was detected. In the MAP-exposed animals, 35 % (7/20) had viable MAP in their blood that was detectable

by the phage assay. In this set, two animals were shedding MAP in their faeces, however no MAP was detected in the blood of these animals. This was interesting as it would have been assumed, if the disease had progressed to shedding, the animals would be more likely to have viable MAP in their blood. However the results gained suggest that this was not the case. In infected sub-clinical animals especially, faecal shedding is intermittent (Crossley et al., 2005). If the failure to detect MAP using the phage assay was a true result it may in fact reflect the fact that the phage assay was not carried out over several time points and the presence of viable MAP cells in the blood may also be intermittent relative to when the animals are found to be shedding MAP in their faeces. Another factor that may have affected the results gained when testing the experimentally infected animals compared to those obtained with commercial dairy cattle (Sets A-C) is that the animals in Set D were not exposed to the same stresses that dairy animals are exposed to, and the effect of this on the progress of the disease means that perhaps the results gained would be different to those obtained with naturally infected dairy herds (Mortensen et al., 2004). However, despite these differences, the ability to detect viable MAP in these animals is an encouraging step forward for this novel assay. A longitudinal study testing the blood, milk and faeces of animals would allow us to gain a better understanding of disease progression and to determine when systemic infection becomes established in animals and how this relates to the milk ELISA and faecal culture or PCR results.

The results obtained using the phage assay could not be compared statistically with any power to those gained using faecal culture, PCR or milk ELISA, due to the lack of number of samples and difference in size of samples in each test group. However in total 55 samples were tested using both with the phage assay and blood ELISA, so basic statistical comparisons can be made between them. Within these 55 samples, when the phage assay gave a positive result, only half as many blood ELISA results were also positive. However when

the phage assay did not detect any viable MAP cells in the blood samples, the majority of the blood ELISA results were also negative. These differences were statistically significant ($P < 0.001$) and, interestingly, when the phage assay was used as the Gold Standard test result, the sensitivity and specificity values of the blood ELISA test were very similar to previously published values (Table 4.6; Whitlock et al., 2000). The blood ELISA test is notorious for having variable sensitivity, especially when testing sub-clinically infected animals where the sensitivity has been found to be as low as 26 % (Alinovi et al., 2009). The pool of samples from Sets A, B, C and E where blood ELISA results were available represent animals at completely different stages of infection and, in two cases (Sets A and C), it was not known how much MAP they were infected with or challenged with, or what strains they were infected with. These variables further reduce the power of the analysis carried out on the small sample set, but the overall pattern of results gained was encouraging. To really evaluate the performance of the phage assay, and to better understand what the results tell us about disease progression, ideally a longitudinal study needs to be carried out, testing a cohort that has been experimentally infected with MAP and performing all the different diagnostic tests (ELISAs, PCR and culture) so that the results can be compared to those gained using the phage assay with a greater degree of power.

MAP can affect many different animals other than cattle. Sheep, camelids, rabbits, deer and many others have all been found to be affected by MAP (Nielsen and Toft, 2009). Although Johne's disease has a larger impact on cattle farms in the UK, throughout the world, the effect of Johne's of disease can have a bigger role on the economics of farming other animals. In Australia, for example, the impact of Johne's disease on sheep farming is by far a bigger issue than its effect on cattle farming (Reddacliff et al., 2003). Developing a test that can detect MAP in different species is very important. During the work described in Chapter 3 to optimise the phage assay, sheep blood was used. With this

knowledge it was known that the phage assay could be used for detection of MAP in clinical samples of sheep blood, so no further optimisations of the methodology was needed before a trial was initiated. There were, however, other variables in the samples provided for the work here that had to be considered. Previously MAP had been detected using the phage assay in milk samples from sheep and goats in milk and in cheese made from these animals (Botsaris et al., 2010), so – despite their different culture characteristic - there was evidence that the bacteriophage should be able to detect the sheep strains of MAP. However the PMMS method has never (to date) been used to recover sheep strains of MAP and the ligand recognised by the peptide may be different to that found on cattle strains of MAP.

The results gained when testing the blood from sheep experimentally infected with MAP were variable. Out of the five animals that gave positive MAP test results using the phage assay, only three had been experimentally infected with MAP. The animals in this group were clinical for ovine Johne's disease and had positive faecal culture, but despite this, only five gave positive (definitive or suspect) serum ELISA test results. One animal that gave a positive MAP test result using the phage assay was from a small group of animals held together that had given a positive MAP ELISA test result in the past, and so could have encountered the organism in the environment. However in the other control cohort (animals 19-28; Set S1), none of these animals had encountered MAP and had shown no positive reactions in any of the other tests performed throughout the experiment. This suggests that either the test was detecting viable MAP in the blood of the sheep through natural infection that was not detected by any of the other tests, or some sort of contamination had occurred, resulting in a false-positive result. As these animals were already culled by the time the phage assay was performed, determining whether they would go on to develop Johne's disease cannot be determined. However, as emphasised previously, a larger study over a long period time is really required to determine

how effective the phage assay can be in identifying infection compared to the other tests, and also to provide a better understanding of disease progression; perhaps low level infection can be cleared by some animals and therefore the presence of MAP in the circulating blood at any one time point may not be indicative of established infection.

Overall in all of these trial studies, the number of samples tested was too low to be able to develop powerful analysis of the performance of the phage assay and its ability to detect and diagnose Johne's disease. Using Mead's Resource Equation (Appendix 4.1), the number of samples used in the initial experiments was adequate to get preliminary data on the phage assay as a detection method for MAP. However as mentioned before, a larger cohort of animals, with many parallel tests are needed to be able to test the efficacy of the phage assay as a detection method or diagnostic for Johne's disease. However the results gained to date suggest that the test has promise to be a good tool for rapidly detecting disseminated MAP infection, to allow more information about the pathogenesis of Johne's disease to be gained.

CHAPTER 5
DEVELOPMENT OF A NEW HIGH-THROUGHPUT ASSAY FORMAT FOR THE
DETECTION OF VIABLE MAP

5.1. INTRODUCTION

The results presented in Chapters 3 and 4 have demonstrated that MAP cells can be detected in the blood of animals exposed to MAP, even in those that are suffering from the sub-clinical stage of Johne's disease. The rapid and reliable detection of this organism within a herd is very important to controlling this disease (Benedictus and Kalis, 2003). The existing *FASTPlaqueTBTM* assay format can detect and enumerate viable MAP in blood within two days (Swift et al., 2013). However although the blood assay is cheap and relatively easy to perform and does not require specialist equipment, the method is labour intensive and therefore it is difficult to test large numbers of samples. In a veterinary setting, where samples from a whole herd need to be taken, often over hundreds of animals would need to be tested and would require the capacity of a high-throughput assay format, as using a labour intensive method would become challenging. If the blood assay can be shortened and concentrated by using just one tube, the process can be automated.

The use of peptide-mediated magnetic separation (PMMS) in developing the phage based blood detection method (Chapter 3) was introduced to isolate MAP cells from the sample matrix, which was potentially inhibitory for phage infection, so that further downstream assay steps could be carried out. PMMS allowed MAP cells to be captured and placed in a medium that enables bacteriophage infection of the cells to occur. However the binding of multiple cells to the surface of the beads (Fig. 3.1) reduces the ability of the assay to accurately enumerate the number of MAP cells present in the sample. This type of method has been described before when MAP cells were isolated from milk using Immuno-Magnetic Separation (IMS) and subsequently lysed to release DNA which was then detected using MAP-specific *IS900* PCR (Grant et al., 2000). But in this case the assay result just reported on the presence or absence of MAP and did not quantify the number of cells detected.

There are several published methods for enumerating MAP cells using quantitative real-time PCR (qRT-PCR; Rodriguez-Lazaro et al., 2005). However this cannot easily be applied to the standard phage assay format after plaque formation and a drawback of using qRT-PCR is that you cannot determine the viability of the cells detected. In the food industry especially, the ability to differentiate between live and dead cells is very important.

The aim of these experiments was to develop a specific and sensitive method of detecting viable MAP, quickly and in a 'single-tube' format that had the potential to be automated. Bacteriophage are natural predators of bacteria and lytic phage have evolved the ability to routinely and efficiently break open cells, hence it was hypothesised that if PMMS was used to isolate MAP cells from blood, the concentrated cells could then be lysed using the lytic mycobacteriophage D29 and then the DNA released from on the infected cells could be detected by PCR. This combination of methods would allow rapid, sensitive detection and provide a method to distinguish between live and dead cells, as the phage will only lyse cells that are able to support phage replication. In addition if combined with qRT-PCR the assay would retain the ability to enumerate the number of cells detected.

5.2. RESULTS

5.2.1 Determining the time taken for bacteriophage D29 to release DNA from MAP

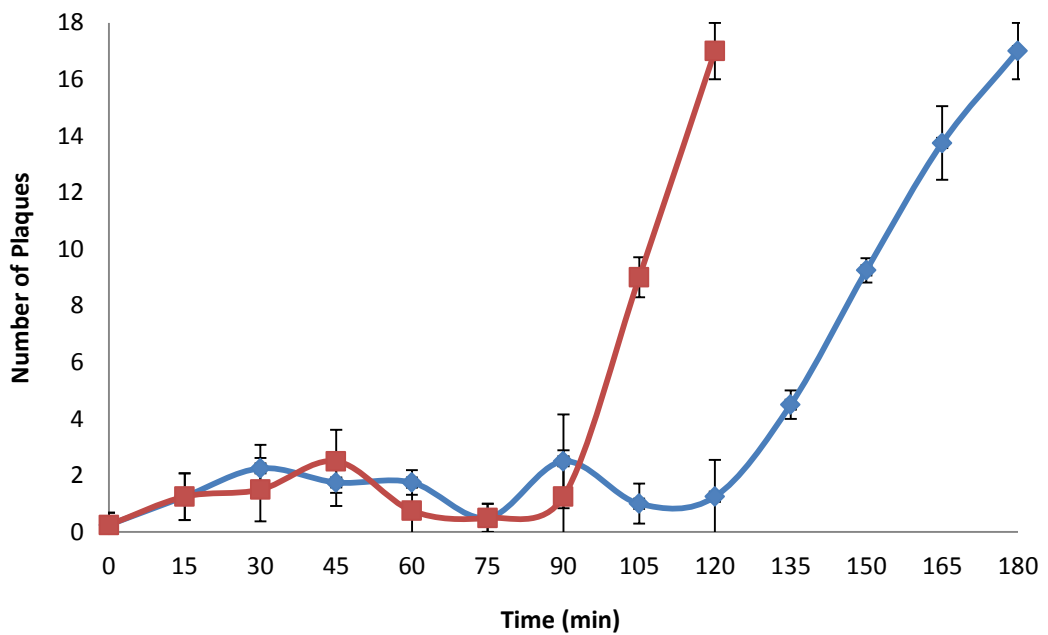
To be able to detect the DNA from MAP lysed by the bacteriophage, knowledge about the life cycle of phage D29 is required. If a sample of the lysis mixture to be used as a template for PCR is removed too early before the cells have lysed, no cells would be detected. In contrast, if left too late, DNA may start to become degraded by nucleases released from the lysed MAP cells. Therefore determining when exactly the cells are lysed by the phage, will enable

successful recovery of template DNA to be used for PCR amplification of signature sequences.

Standard protocols exist to measure bacteriophage growth and replication within a host. Generally the burst size and determining the length of the eclipse phase has to be carried out by a series of dilutions. To measure the eclipse phase of the phage, both host and phage would normally be diluted to a countable and detectable range and both cell number and phage titres monitored over time, which is time consuming and uses a lot of material. As an alternative to this, FAS was used to inactivate extracellular bacteriophage, so that the eclipse phase of D29 could be determined. Briefly; countable MAP or *M. smegmatis* cells (1×10^2 pfu ml⁻¹) were infected with phage D29 (m.o.i. 10) and left to infect for 30 min. The virucide was then added and the sample was plated out over different time points.

Figure 5.1 shows that the eclipse phase of D29 when infecting *M. smegmatis* was around 90 min. However when the eclipse phase was determined for phage D29 when infecting the MAP, the eclipse phase was longer at 120 min. From this it was determined that after infection the samples should be left for at least 160 min to allow bacteriophage to break open their host cell so that the released DNA could be detected.

Figure 5.1. Use of FAS to determine the eclipse phase of bacteriophage D29 infecting *M. smegmatis* and MAP



Graph showing the time taken for new D29 bacteriophage virions to be released from *M. smegmatis* (Red) and MAP (Blue). Samples were taken after an initial incubation of 40 min to allow phage adsorption to the host cells. Error bars represent the standard deviations of the means of number of plaques recovered from the phage assay performed in quadruple. The eclipse phase is defined as the time taken for new particles to be released from the cells after infection, thus the period when no phage are detected outside of the host cell.

5.2.2. Isolating MAP and extracting DNA using bacteriophage

To facilitate MAP cell capture prior to cell lysis, two peptides, aMP3 and aMptD, that bind specifically to MAP, were used as described previously in Chapters 3 and 4. To capture the cells the PMMS method described in Section 2.2.2, was used initially to recover MAP cells (1×10^4 pfu ml⁻¹) from 1 ml of MP. After PMMS, one sample was inoculated with bacteriophage (100 µl of reconstituted FPTB bacteriophage) and one sample was not (100 µl of MP added as a control). Each sample was then incubated at 37 °C for 3 h, to allow for adsorption, replication and release of new bacteriophage from the MAP cells. After incubation the cells were pulse centrifuged to bring the beads and the MAP to the bottom of the tube, and the samples were then placed onto a magnet to separate any intact cells from the MAP chromosomal DNA released by the phage into the supernatant.

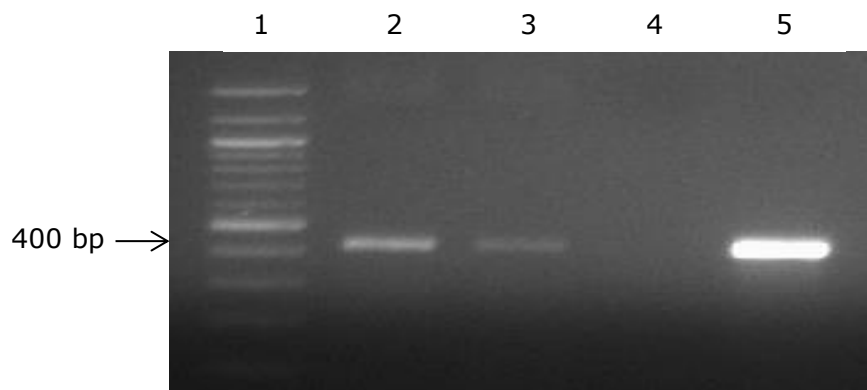
Carefully (to avoid picking up any unlysed cells attached to the beads) 100 µl of the supernatant was transferred into a fresh microcentrifuge tube. Ten microlitres of the sample was then used as template DNA for the MAP specific F57 PCR assay (Section 2.4.5.3) to determine whether any released MAP DNA could be detected. However in this case no PCR products were detected. It was possible that resuspending the MAP cells attached to the beads after PMMS in 1 ml of MP may have diluted the DNA too much, therefore reducing the probability that the PCR assay would be able to detect any released DNA. In addition the F57 PCR only targets a single copy gene, also reduces the sensitivity of the PCR assay compared to the PCR assays that target the multicopy *IS900* PCR assay and this could also have resulted in no DNA being detected.

Taking these factors in to account, the experiment was repeated, however after PMMS, the samples were resuspended in just 100 µl of MP and the amount of phage added was then reduced accordingly to maintain the same final pfu ml⁻¹ concentration. After the 3 h incubation, again the samples were centrifuged to remove the beads and any cells remaining attached to them and to also separate

out any cell debris present in the phage-infected sample. The tubes were then placed on a magnet. Samples (10 μ l) of the supernatant were removed and were again used as template DNA for the MAP specific F57 PCR.

The results show where the phage were added a strong band of the expected size was present at around 400 bp. However in the negative control, where the phage were not added, although there was less PCR product indicating a lower amount of starting template there was still a faint band visible (Figure 5.2). This suggested there could be contaminating free MAP DNA in the sample (although this is unlikely as the water control did not produce a PCR product. Alternatively some MAP cells present in the sample were lysed even though no phage were present. Although the cells were captured on beads, some intact MAP cells may have been released into the supernatant and acted as template DNA for the PCR since the heating during the denaturing step of the PCR may have been lysed the cells and therefore released their DNA for further amplification.

Figure 5.2. Detection of MAP DNA following lysis by bacteriophage



PCR amplification of the 400 bp F57 DNA region specific for MAP following capture of cells by PMMS and lysis by bacteriophage D29. Lane 1, 100 bp DNA ladder (Fig 2.5). Lane 2, template DNA following bacteriophage lysis of MAP cells; lane 3, template DNA from sample without bacteriophage; lane 4, negative control (SDW replaces MAP DNA as template). Lane 5, positive control (purified genomic MAP K10 DNA used as template).

5.2.3. Optimising bacteriophage mediated cell lysis PCR-detection

One of the advantages of the phage-based detection is that it is able to distinguish between the live and dead cells, and it was important to retain this feature of the assay when developing the rapid, one tube format. Since a PCR product occurred in the sample to which no bacteriophage was added further method development was required to overcome this.

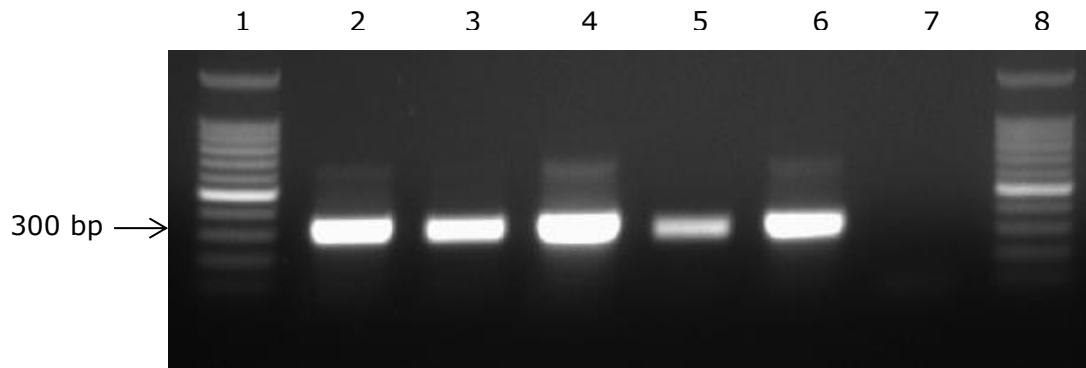
5.2.3.1. Removing potential free MAP DNA

Bacterial cultures grown to high cell density can contain free DNA from cells that have lysed, and this may have resulted in the amplification of the PCR product in the sample that no phage was added to. To investigate this, before repeating the experiment described in Section 5.2.2 cultures of MAP strain K10 and ATCC 19851 were subjected to DNase I (NEB, UK) treatment (Section 2.5.4) to degrade any DNA that may have been carried from the pure cultures into the assay. The washing step used during PMMS would then remove the DNase I from the sample so that after phage lysis only template DNA from viable cells would be present. In this case the P90 IS900 PCR (Section 2.4.5.1) was carried out to increase the sensitivity of the PCR step and to negate the impact of low levels of DNase I remaining in the samples.

The results showed that once again a stronger band was seen when the bacteriophage was used to release the MAP DNA from the strains K10 and ATCC 19851 (Fig. 5.4) indicating that DNase I was not having an adverse effect on the PCR amplification. However a band was still seen on both non-bacteriophage controls suggesting free DNA in the original sample was not the cause of the problem. The use of the more sensitive IS900 PCR also resulted in a much stronger signal from the uninfected sample, which was not desirable. This result suggested the cells were still lysing, either because of bacteriophage contamination or because free cells were released into the supernatant and were being detected during the denaturation steps of the PCR.

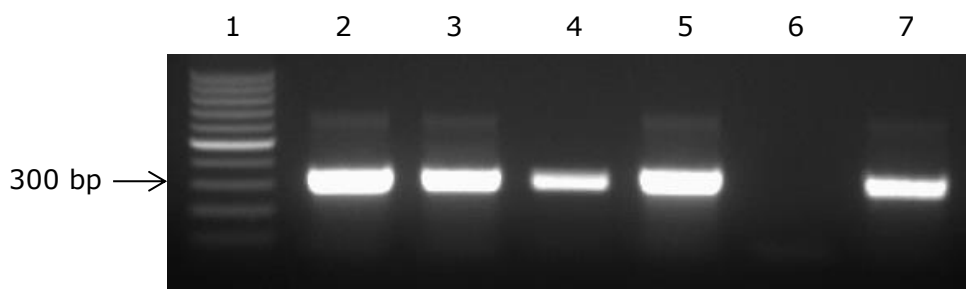
No matter how good the laboratory practice and hygiene are, bacteriophage contamination can occur (Los et al., 2004). To rule out bacteriophage contamination, the experiment above was repeated using fresh pipettes, pipette tips and was performed on a different bench where mycobacteriophage had not been used before. New reagents and equipment were also used. Four samples of MAP cells (K10) ranging from 1×10^6 to 1×10^3 pfu ml⁻¹ were tested but in this case no phage were used to lyse the cells. The IS900 PCR was used again to make sure any DNA released from the MAP cells during the PCR would have been detected. The results show that when no bacteriophage were added, strong PCR signals were still detected in each of the samples (Fig. 5.5). This suggested that the false-positive results were not due to bacteriophage being inadvertently introduced into the negative control samples, and that free cells in the sample may be responsible for the signals from the uninfected controls.

Figure 5.4. The effect of DNase I treatment to remove potential DNA contamination



PCR amplification of the approximately 300 bp IS900 DNA region specific to MAP. Lane 1 and 8, 100 bp DNA ladder (Fig. 2.5). Lanes 2 and 4, template DNA from MAP cells lysed using bacteriophage D29 (K10 and ATCC 19851, respectively); lanes 3 and 5, template MAP cells with no bacteriophage added (K10 and ATCC 19851, respectively); lane 6, positive control (template used was purified genomic MAP K10 DNA); lane 7, negative control (SDW replaced template DNA in PCR reaction).

Figure 5.5. Experiment to rule out bacteriophage contamination of uninfected MAP cells



PCR amplification of the approximately 300 bp IS900 DNA region specific to MAP. Lane 1, 100 bp DNA ladder (Fig. 2.5). Lanes 2 to 5, template DNA from intact MAP cells (K10) added into the PCR tubes. Number of cells added ranged from 1×10^6 to 1×10^3 pfu ml⁻¹. Lane 6, negative control (SDW replaced template DNA in PCR reaction) and lane 7, positive control (template used was purified genomic MAP K10 DNA).

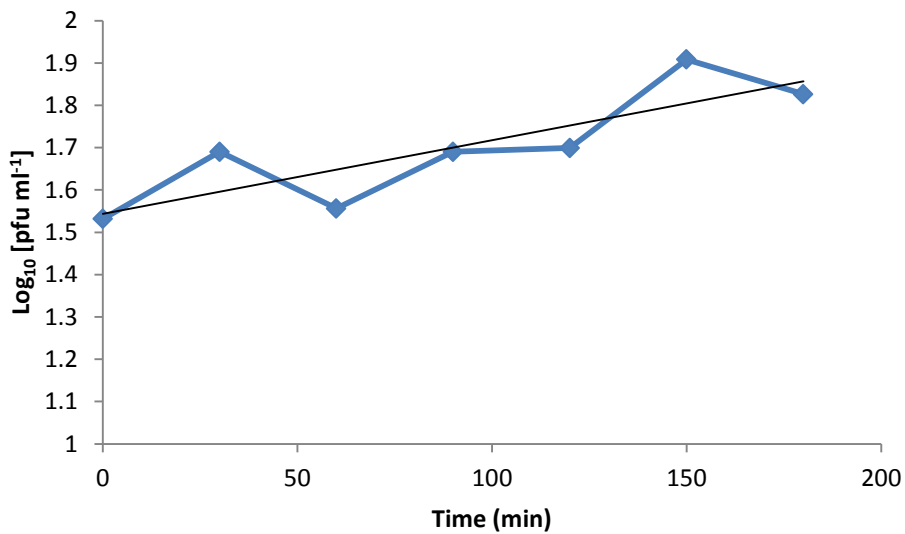
5.2.3.2. Improving peptide-mediated magnetic capture efficiency

As bacteriophage contamination and DNA carry over from the pure cultures had been ruled out as the causes of the strong bands seen in the uninfected control, the capture efficiency and stability of the captured cells was investigated. The FPTB assay was used to determine whether MAP cells may be dissociated from the magnetic beads during PMMS and if so, how many.

The original protocol developed for capturing MAP cells from blood by PMMS only required MAP cell capture for 30 min, and subsequent washing only takes an extra 20 min. Thus MAP cells would only be required to remain on the magnetic beads for a maximum of 1 h. During the one day assay, the cells are required to remain on the beads for almost 4 h, which may give the cells enough time to begin dissociating from the peptides binding them. Therefore an experiment was designed to determine the number of cells that could be detected being released from the beads during a 3 h incubation during which the bacteriophage were lysing the cells.

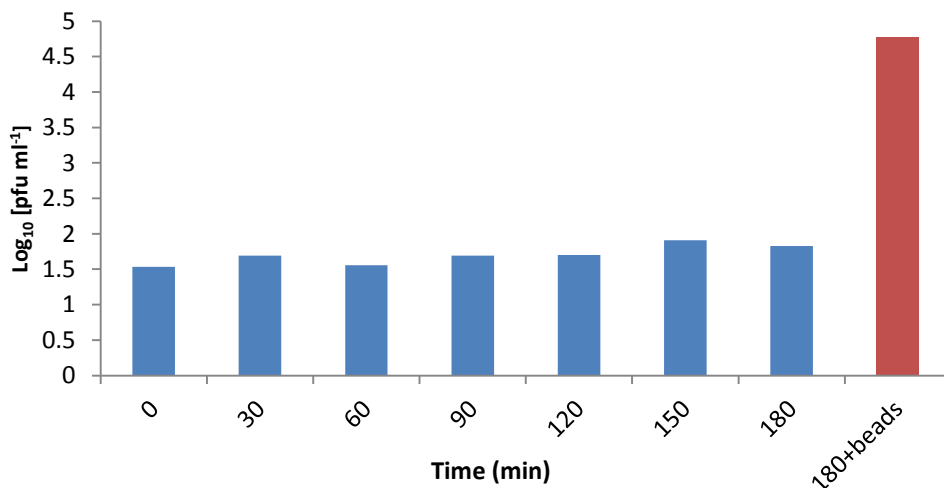
To do this, approximately 1×10^6 pfu ml⁻¹ of MAP cells (K10) were mixed with the magnetic beads for 15 min and PMMS was carried out. The samples were placed at 37 °C and at 30 min intervals the samples were placed on magnetic racks and 100 µl was taken from the supernatant. The number of free MAP cells in this sample was then determined using the FPTB assay. During the 3 h incubation used, as the time increased the number of cells detected in the supernatant almost doubled from the sample taken at time point zero to that taken after 180 min. The highest number of cells was detected at 150 min, when 8.1×10^2 pfu ml⁻¹ was detected, however this fell to 6.7×10^2 pfu ml after 180 min (Figure 5.6)

Figure 5.6. Number of dissociated MAP cells detected in the supernatant during 3 h incubation on magnetic beads



Graph showing the number of plaques numbers recovered from the supernatant of media containing MAP cells bound to magnetic beads by PMMS. Samples were taken every 30 min for 3 h. The trend-line represents the general increase over time in the number of MAP cells dissociating from the beads detected by the FPTB assay.

Figure 5.7. Number of MAP cells dissociated from the magnetic beads during incubation

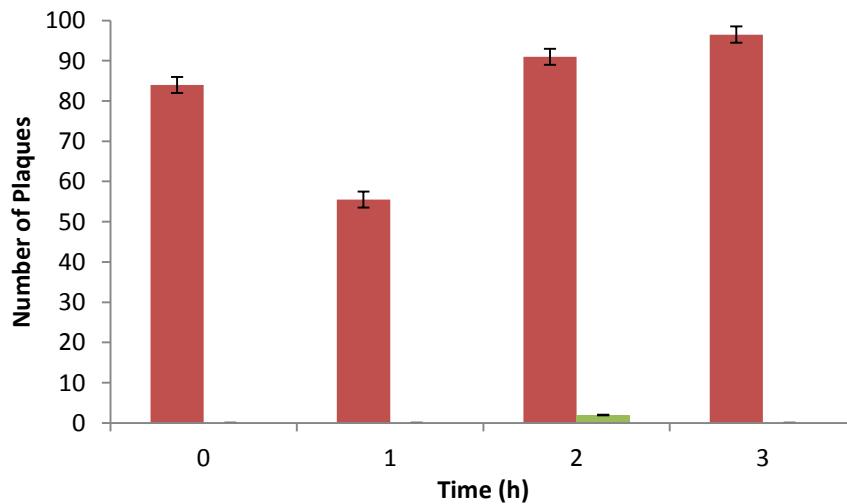


Graph showing log₁₀ of the plaque numbers recovered from the supernatant during PMMS every 30 min for 3 h (blue bars) and from the beads after 3 h of incubations (red bar).

The results from Figures 5.6 and 5.7 show that captured MAP cells can fall off the beads, and these may be detectable by PCR once they are free in the supernatant. Several parameters such as pH, temperature and length of time, can be altered that can increase or decrease the rate of dissociation between binding partners. In this case the length of time is difficult to change as the bacteriophage require a certain amount of time to release their host's DNA (Section 5.1).

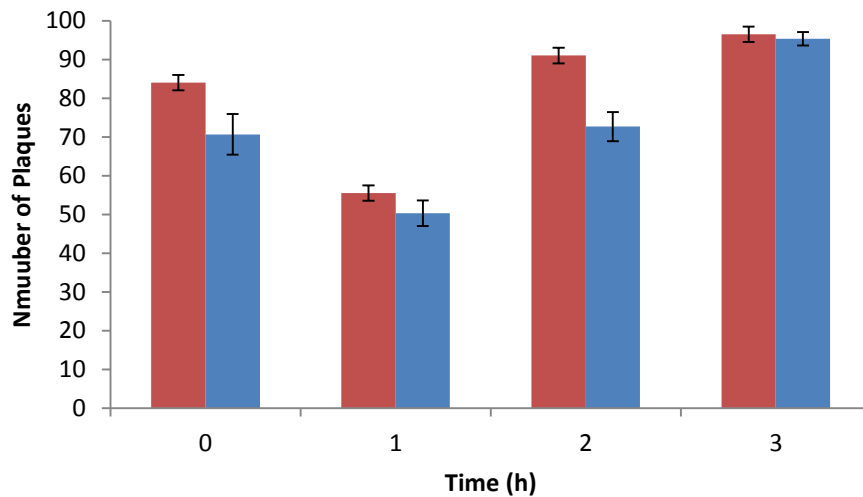
Hence changing the pH of the buffer was initially chosen as a parameter that could be optimised. The original PMMS methods described by Stratmann et al. (2002) used PBS (pH 7.4) to isolate the MAP cells. In the modified protocol used during the blood-phage assay, MP is used instead which has a pH of 6.6. This shift in pH may alter the dissociation constants which resulted in the release of the MAP cells into the supernatant after the magnetic separation. To compare the effect of these two buffers. The experiment described above (Section 5.2.2) was repeated, however this time cells were suspended in either PBS or MP and samples of the supernatant taken every hour. The number of free MAP cells present in these samples was then determined using the FPTB assay. The results (Fig. 5.8) show that when PBS was used virtually no MAP cells were detected in the supernatant at each time point and this was significantly different to the result gained when the cells were in MP ($P < 0.001$). Therefore the pH of MP was adjusted using sodium hydroxide to pH 7.4 and the experiment repeated. In this case the results (Fig. 5.9) showed that there was no significant difference between the number of MAP cells detected in MP at either pH 7.4 or 6.6.

Figure 5.8. MAP cell dissociation in PBS compared to Media Plus



Graph showing the number plaques recovered from the supernatant of MAP cells isolated and suspended in either MP (red bars) or PBS (green bars). Unpaired T-test was used to determine significance of difference between MAP detection in PBS and MP. Error bars represent the standard deviations of the means of number of plaques recovered from the phage assay performed in triplicate.

Figure 5.9. MAP cell dissociation in MP with pH 7.4 compared to 6.6



Graph showing the number plaques recovered from the supernatant of MAP cells isolated and suspended in either MP pH 6.6 (red bars) or MP pH 7.4 (blue bars). Unpaired T-test was used to determine significance of difference between MAP detection in PBS and MP. Error bars represent the standard deviations of the means of number of plaques recovered from the phage assay performed in triplicate.

Since this result showed that pH alone did not result in a tighter binding of the MAP cells to the beads, it was possible that resuspending the cells in PBS made them less infectable by the phage and this would account for the reduced number of cells detected and account for the fact that seemingly no dissociation of MAP cells from the beads when PBS was used as the buffer. To investigate this, the experiment was repeated, however the number of cells remaining on the beads was also determined using the FPTB assay. The results show that when the beads were tested, again no MAP was detected suggesting that PBS does not support efficient phage infection and therefore the difference in pH did not affect the rate of dissociation. However this result did highlight the importance of using a buffer that is compatible with phage infection when using the FPTB assay to detect MAP cells.

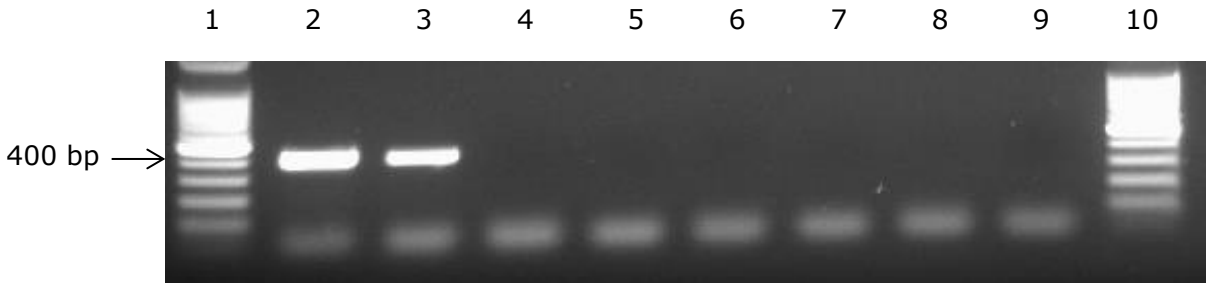
5.2.3.3. Preventing detection of unlysed MAP cells by limiting thermal lysis

The above experiments indicated that uninfected free MAP cells dissociating from the magnetic beads were being detected by the PCR assay. The initial denaturing step at 95 °C during the PCRs is known to lyse bacterial cells and this fact is used when performing direct colony PCR. If the dissociation of the MAP cells from the beads could not be prevented this lysis was not desirable for development of the one tube assay format. To try and reduce cell lysis, the denaturation temperature was reduced. Samples (10 µl) containing 10^2 pfu ml⁻¹ MAP cells (K10) were prepared as template for a PCR reaction. The MAP cells were initially washed with MP by centrifugation to remove as much free DNA in the culture as possible, before being used as template. A non-Hot Start PCR master mix (Qiagen) was used for the PCR reaction. A temperature gradient PCR was used to change the denaturing temperature from 94 °C, to 85.1, 74.8 and 70 °C. Control samples containing Genomic MAP DNA (K10) were prepared to ensure that at the modified temperatures the PCR was still able to amplify the correct PCR products.

The results (Fig. 5.10a) show that only the genomic MAP DNA and the intact MAP cells produced a good PCR product after the MAP-specific F57 PCR when 94 °C was used as the denaturation temperature but no PCR products were produced when lower denaturation temperatures were used. The experiment was repeated using a smaller range of temperatures for denaturation: 95, 92.6, 89.6, 83.1 and 80 °C (Fig. 5. 10b). The results show that the PCR products were only amplified when temperatures of 95 and 92.6 °C were used for the denaturation step, but again both the genomic DNA and whole cell samples gave a positive result showing that altering the denaturing temperature could not be used to overcome the problem of thermal cell lysis.

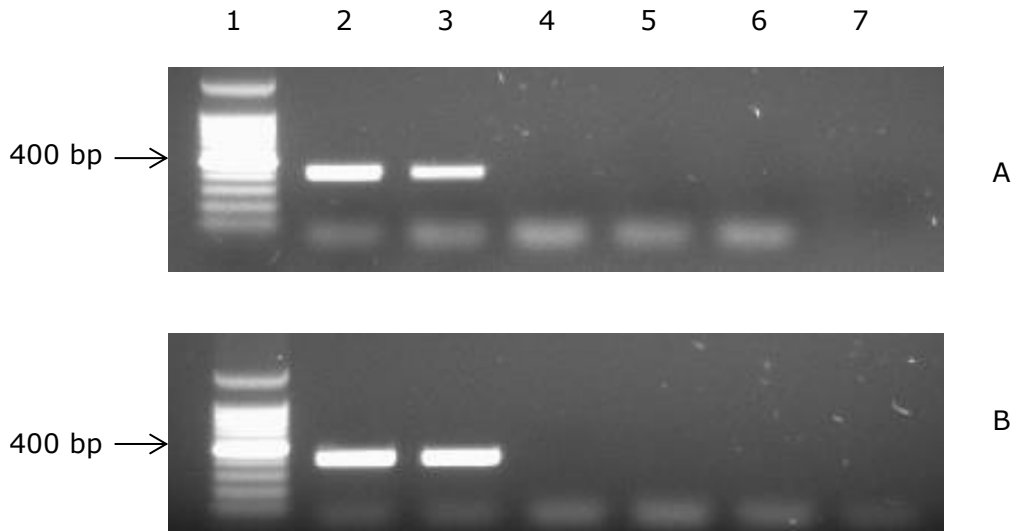
Figure 5.10. Effect of reducing the denaturation temperature on PCR amplification and cell lysis

A



PCR amplification of the 400 bp F57 DNA region specific for MAP. Lane 1 and 10, 100 bp DNA ladder (Fig 2.5). In lanes 2, 4, 6 and 8 the template was purified genomic MAP (K10) DNA. In lanes 3, 5, 7 and 9 intact MAP cells (K10) were added as template. The denaturation temperatures used were lanes 2 & 3, 94 °C; lanes 4 & 5, 85.1 °C; lanes 6 & 7, 74.8 °C and lanes 8 & 9 70 °C.

B



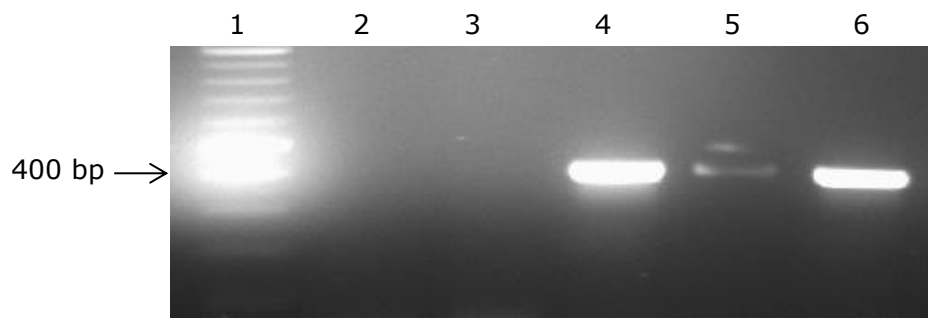
PCR amplification of the 400 bp F57 DNA region specific for MAP. Lane 1 and 10, 100 bp DNA ladder (Fig 2.5). In panel A the template was purified genomic MAP (K10) DNA. In panel B intact MAP cells (K10) were added as template. The denaturation temperatures used were lane 2, 95 °C; lane 3, 92.6 °C; lane 4, 89.6 °C, lane 5, 83.1 °C and lane 6, 80 °C. Lane 7 is a negative control (SDW added as template).

5.2.3.4. Preventing detection of unlysed MAP cells by separation

The next approach tried to prevent the detection of the uninfected cells was to try and remove the dissociated MAP cells from the sample. When performing the PCR identification during the blood assay, spin columns are used to isolate and concentrate DNA. It was hoped that by applying the free DNA from the lysed cells to a spin column these may act as a barrier to the free cells in the supernatant whilst still binding and concentrating the free DNA that would be released from the cells after phage infection.

To investigate this MAP K10 cells (1×10^4 pfu ml⁻¹) were inoculated into MP and recovered using the PMMS protocol (Section 2.2.2). The cells attached to the beads were resuspended in 1 ml of MP and incubated for 3 h at 37 °C with or without the addition of bacteriophage (final concentration - 10^8). After incubation 10 µl was removed from the supernatant of each sample and the rest was passed through the DNA concentrator spin column (ZymoResearch; Section 2.4.2.3). The eluted DNA and the sample were taken directly from the phage lysis tube (10 µl) and were used as template for the MAP-specific F57 PCR (Section 2.4.5.3). In this case neither of the samples taken directly from the lysate gave a positive PCR result indicating that the number of cells released from the beads directly into the supernatant was below the limit of detection of the PCR assay (Fig. 5.11). However the DNA that had been concentrated via the spin column from the sample that had been infected with phage gave a very strong band. Unfortunately the concentrated sample from the non-phage infected sample also gave a band, although it was much weaker.

Figure 5.11. Use of spin column to separate out intact MAP cells



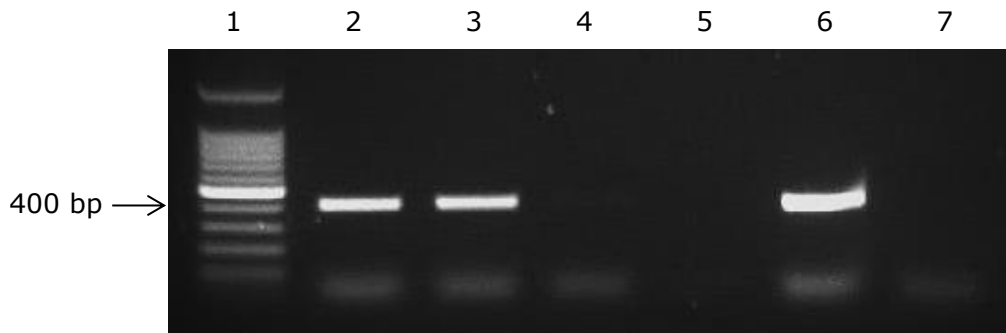
PCR amplification of the 400 bp F57 DNA region specific for MAP. Lane 1, 100 bp DNA ladder (Fig. 2.5). Lane 2 was sample removed from the bacteriophage lysis tube before the spin columns were used to concentrate the DNA; lane 3, template from non-bacteriophage lysed MAP cells before spin column concentration. Lane 4, concentrated template DNA removed from bacteriophage lysed MAP cells. Lane 5, concentrated template from non-bacteriophage lysed MAP cells. Lane 6, positive control (purified genomic MAP K10 DNA).

As this result was encouraging, the experiment was repeated using *M. smegmatis* as well as SDW as negative experimental and PCR controls. The results showed that, as expected, both *M. smegmatis* and the SDW negative PCR control did not support amplification of the F57 band. However both this time the phage-infected and uninfected MAP sample gave strong positive bands, even after purifying the sample using the spin columns (Figure 5.12) suggesting continued contamination by whole cells.

Therefore it was decided to use the beads again after the cell lysis step to try and remove any intact cells from the supernatant. The experiment was repeated, however after the time had been allowed for phage lysis, the beads (and any remaining intact cells) were removed (by pulse centrifugation and magnetic separation) and then the supernatant was transferred into a tube containing fresh magnetic beads. The samples were then incubated at room temperature with rotation for 30 min to allow any free MAP cells to bind to the beads. The samples were then placed back on the magnetic rack and the supernatant was then removed processed through the spin columns and the PCR assay performed.

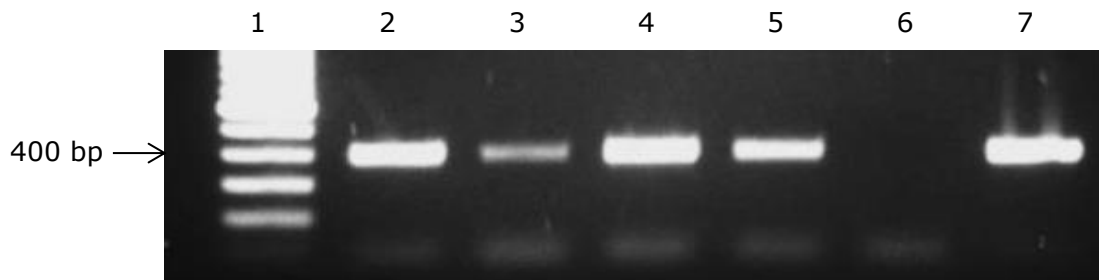
The results show that after the first round of PMMS there was a brighter band from the phage infected sample compared to the uninfected sample. However after the second round of PMMS and DNA concentration, there was still a strong, although fainter, band from the uninfected sample suggesting MAP cell DNA was still finding its way into the columns and being detected by the MAP specific PCR (Figure 5.13).

Figure 5.12. Effect of using spin column to remove intact MAP cells



PCR amplification of the 400 bp F57 DNA region specific for MAP. Lane 1, 100 bp DNA ladder (Section 2.5). Lane 2, concentrated template DNA removed from bacteriophage lysed MAP cells. Lane 3, concentrated template DNA removed from non-bacteriophage infected MAP cells. Lane 4, concentrated template DNA removed from bacteriophage inoculated *M. smegmatis* cells. Lane 5, concentrated template from non-bacteriophage lysed *M. smegmatis* cells. Lane 6, positive control (genomic MAP K10 DNA). Lane 7, negative control (SDW).

Figure 5.13. Effect of using spin columns and PMMS to remove intact MAP cells



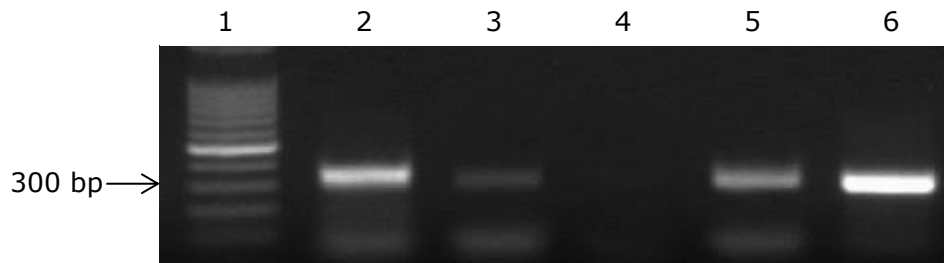
PCR amplification of the 400 bp F57 DNA region specific for MAP. Lane 1, 100 bp DNA ladder (Fig. 2.5). Lane 2, concentrated template DNA removed from bacteriophage lysed MAP cells. Lane 3, concentrated template DNA removed from non-bacteriophage infected MAP cells after one round of PMMS. Lane 4, concentrated template DNA removed from bacteriophage infected MAP cells after two rounds of PMMS. Lane 5, concentrated template from non-bacteriophage infected MAP cells after two rounds of PMMS. Lane 6, negative control (SDW). Lane 7, positive control (genomic MAP K10 DNA).

Once again the PCR amplified signature MAP DNA sequences from the sample containing uninfected MAP cells, even after two rounds of PMMS were used to remove the intact cells. The DNA concentrator uses a DNA binding buffer which may induce lysis of the bacterial cells. Since the components of the kit are not given in the kit MSDS it was difficult to predict the effect of the buffers from their chemical composition, therefore the hypothesis that the buffer may induce cell lysis was investigated empirically. To do this MAP cells (K10) were 10-fold serially diluted from 1×10^4 pfu ml⁻¹ to 1×10^1 pfu ml⁻¹. The samples were then subjected to DNA concentration using the spin columns without any previous cell lysis step and the eluted template amplified using MAP-specific IS900 PCR to determine whether using the spin columns induced MAP cell DNA lysis. DNA was detected from each of the dilutions tested, apart from the sample that contained 10^2 pfu.ml⁻¹ MAP cells, (Figure 5.14). This result appeared to be an anomaly as DNA was detected in the sample that contained 10-fold fewer cells. Therefore it seems that the buffers in the DNA concentrator kit can induce lysis of the intact MAP cells, resulting in release of the genomic DNA, which may explain why PCR products were still being produced from samples that were not infected with bacteriophage.

The experiment with two rounds of PMMS was repeated using 1×10^4 pfu ml⁻¹ of MAP cells (K10). However, this time the spin-columns were not used to concentrate the DNA. The PMMS was carried out to capture the MAP cells then the beads were finally resuspended in 100 µl of MP. The sample was then pulse centrifuged and placed on a magnetic rack. A 10 µl sample of the supernatant was taken as a sample of the unpurified template DNA and the rest of the lysis mixture was placed in a fresh microcentrifuge tube. Fresh magnetic beads were mixed with this and the samples incubated with rotation for 30 min. Finally the beads were separated on a magnetic rack along with any captured intact cells and 10 µl of the supernatant was used as template DNA for the MAP-specific IS900 PCR reaction.

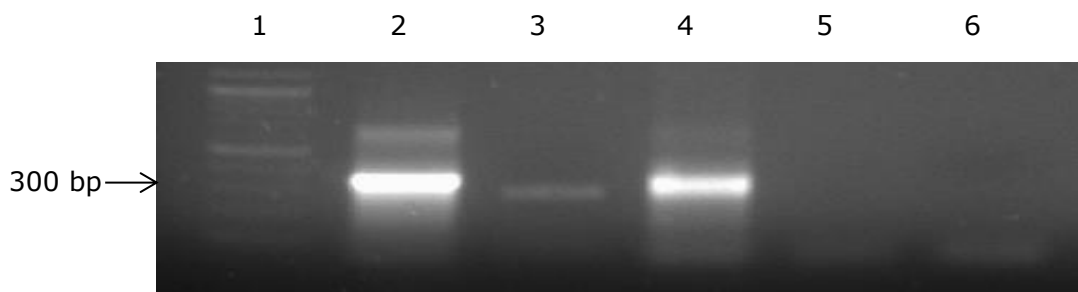
As before, MAP DNA was detected strongly when bacteriophage was used to lyse the cells both in the original lysis mixture after the first round of PMMS and in the second sample after the second round of PMMS to remove any remaining intact cells. However in the uninfected sample only a faint PCR product was amplified after the first round of PMMS and no amplification was seen at all when testing the lysis mixture after the second round of PMMS (Figure 5.15).

Figure 5.14. Determining if spin column buffer can cause the release of MAP DNA from intact cells



PCR amplification of the approximate 300 bp IS900 DNA region specific to MAP. Lane 1, 100 bp DNA ladder (Fig. 2.5). Lane 2 to 5, MAP cells (K10) diluted from 1×10^4 pfu.ml⁻¹ to 1×10^1 pfu.ml⁻¹. Lane 6, positive control (genomic MAP K10 DNA).

Figure 5.15. Effect of removing intact MAP cells from the phage lysis supernatant by PMMS without DNA concentration

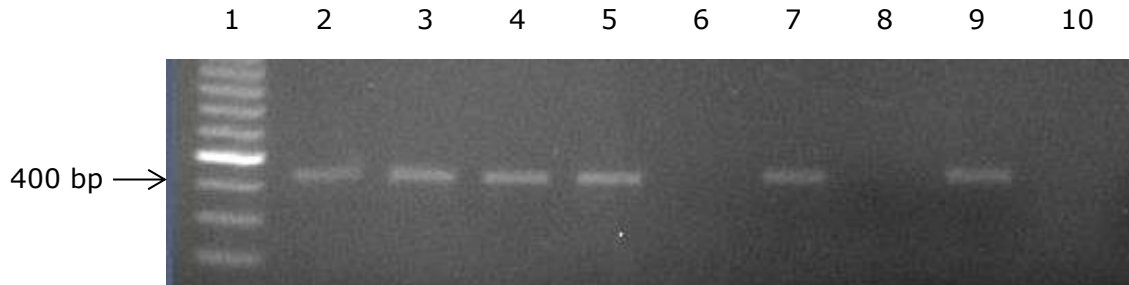


PCR amplification of the approximate 300 bp IS900 DNA region specific to MAP. Lane 1, 100 bp DNA ladder (Fig. 2.5). Lanes 2 and 3 used template DNA after one round of PMMS. Lanes 4 and 5 used template DNA after two rounds of PMMS. Lanes 2 and 4 were phage infected MAP cells (K10) Lanes 3 and 5 were uninfected MAP cells. Lane 6 was negative control (SDW).

The experiment with two rounds of beads was repeated using 1×10^4 pfu ml⁻¹ of MAP strains K10 and also a second strain of MAP (strain B4). In addition the less sensitive MAP-specific F57 PCR assay was used rather than the more sensitive IS900 PCR. The results show positive results for the samples lysed with the phage. However for the non-lysed control samples once again after the first round of PMMS some intact cells remained in the supernatant since a PCR product was amplified (Figure 5.16). After the second round of PMMS however, only the MAP cells infected with bacteriophage were detected and no PCR products were produced from the uninfected samples.

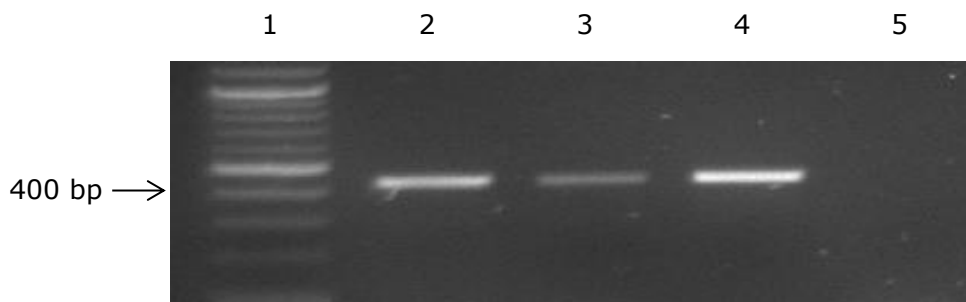
To determine how reproducible this result was the experiment was repeated a third time using another MAP strain, ATCC 19851. However in this case the results show that the MAP DNA was detectable in the uninfected samples even after the second round of PMMS to remove the intact cells, although the band was less intense than that seen in the phage-lysed sample (Figure 5.17). This result indicated that further work was required to fully optimise the one tube assay format.

Figure 5.16. Detection of MAP cells after one or two rounds of PMMS



PCR amplification of the 400 bp F57 DNA region specific for MAP. Lane 1, 100 bp DNA ladder (Fig. 2.5). Lanes 2 to 5, one round of PMMS; Lanes 6 to 9, two rounds of PMMS. Lanes 2, 3, 6 and 7 were strain K10. Lanes 4, 5, 8 and 9 were strains B4. Phage were added to samples in lanes 3, 5, 7 and 9. Lane 10 was negative control (SDW).

Figure 5.17. Detection of MAP ATCC 19851 after two rounds of PMMS



PCR amplification of the 400 bp F57 DNA region specific for MAP. Lane 1, 100 bp DNA ladder (Fig. 2.5). Lane 2, MAP (ATCC 19851) infected with bacteriophage. Lane 3, MAP not infected with bacteriophage. Lane 4, positive control (genomic MAP K10 DNA). Lane 5, negative control (SDW).

5.2.4. Discussion of development of the one tube assay format

The initial experimental design used here was to determine whether MAP DNA could be detected from MAP cells lysed using bacteriophage creating a PCR-based assay that was novel in that only viable cells would be detected. The initial results using cells capture on magnetic beads and simply removing the supernatant for PCR analysis showed that while the phage-lysed samples gave a strong band, a faint MAP specific PCR product was also amplified from the uninfected sample. The possible causes for this (presence of free MAP DNA in the sample, bacteriophage contamination or intact MAP cells dissociating from the beads) were investigated and it was concluded that the problem was caused by MAP cells dissociating from the magnetic beads.

Several factors can affect the binding of ligands, such as time, temperature and buffer composition (Origene Development Guide, USA). As this assay uses bacteriophage, the temperature and time could not be easily altered. When buffer composition was investigated initial results suggested that PBS was a superior buffer compared to MP for capturing and holding the MAP cells over the 3 h period. However, this result proved to be an artefact since it was found that the phage were not able to efficiently infect the cells when resuspended in PBS. Certain components such as calcium ions are required to allow bacteriophage D29 (and other phage) to infect their host (Rees and Botsaris, 2012). Although not generally required for adsorption, the calcium ions are thought allow the phage to approach the cells surface by neutralising negative charge of cell surface molecules and for some phage to be involved in DNA injection to their host (Watanabe and Takesue, 1972). As MP supports bacteriophage infection, the pH was altered to 7.4 to mimic that of PBS. However the difference in pH did not make a difference on the capture efficiency or rate of dissociation.

Being able to distinguish between viable and non-viable host MAP cells is vitally important for the detection assay. In a clinical case of Johne's disease and other general infections caused by mycobacteria, the organisms are taken up by

macrophages and either the cells are killed or survive and persist in the cells. During PCR, temperatures at 95 °C are used to denature DNA and to, if used, activate hot-start *Taq* DNA polymerases. Colony PCR's, that do not use prepared template DNA but intact cells as the template DNA source can be amplified, due to the denaturing step that can release DNA from whole cells (Tsuchizaki et al., 2000). Whole cells free in the sample that are not removed may therefore be detectable. To try and overcome the problem of thermal lysis of the uninfected cells, the denaturing temperature was reduced however it was found that the minimum temperature required for successful amplification of the genomic MAP DNA (92.6 °C) was still hot enough to lyse the whole MAP cells and release DNA that then acted as a template for PCR amplification.

Hence the assay format was modified to try and prevent the detection of the uninfected cells. Physical barriers in the form of DNA purification spin columns were used to separate the whole cells from the released MAP DNA. However the results showed that the DNA binding buffer supplied with the kit lysed intact MAP cells, which again resulted in their detection by PCR. It was noted that although initial binding of MAP to the peptide-coated beads was quite efficient, over time the number of cells dissociating from beads increased. Hence it was decided to use this efficient capture profile to remove any intact cells from the supernatant after bacteriophage lysis of the viable cells. The initial results demonstrated that this method was successful in allowing detection of just the DNA from MAP cells that had been lysed following infection with bacteriophage. While the results were encouraging when using two different cattle strains of MAP (K10 and B4), when the experiment was repeated using a different MAP strain, a faint band was detected indicating that some residual intact cells were not removed by the PMMS. Physical parameters such as the size of the bead and time to capture can affect the efficiency of capture (Kell et al., 2008). For recovery of MAP cells from blood, this had already been optimised (Chapter 3) and thus the choice of small diameter (1 µm) superparamagnetic beads and the time left for bacteria to bind

to these beads was already known to be optimal. However the fact that all of the MAP ATCC 19851 cells were not removed by the second round of PMMS could be due to the fact that different MAP strains bind to the peptides with different affinity and therefore the second round of PMMS did not efficiently capture all of the ATCC 19851 cells from the supernatant.

Therefore it was clear that further optimisation of the method was needed to increase the reliability of the assay. However the assay development work was carried out using pure cultures of MAP grown to high cell number which is known to induce clumping (McDonald et al., 2003). This also means that the beads were capturing more cells than would be expected to be found in clinical blood samples where the number of MAP cells per ml would be very low. Hence, although the assay procedure had not been fully optimised, it was felt that the results were promising enough to allow the assay to be tested on clinical blood samples when they became available.

5.2.5. Testing the non-fully optimised one day assay on experimentally infected calves

The blood samples from the calves in Set D (Chapter 4) were tested using the final test method described in section 5.2.3.4. Surplus blood (1 ml) from the samples were diluted in MP and then subjected to PMMS. Bacteriophage D29 was added to the sample (10^8) and incubated for 3 h. The beads were separated from the samples by pulse centrifugation and then by resting on a magnet and then resuspended in 100 μ l of MP. The supernatant was placed into a new microcentrifuge tube and fresh magnetic beads added before incubating for 30 min with rotation at room temperature to remove any intact cells. Finally the beads were separated from the lysis mixture by pulse centrifugation and resting the samples on a magnet. Ten microlitre samples were then used as template DNA for MAP specific IS900 PCR as low numbers of MAP are likely to be present

therefore the more sensitive PCR was used (See Fig. 5.18 for a schematic of the one assay).

Figure 5.18. Schematic diagram of the one day – one tube format assay

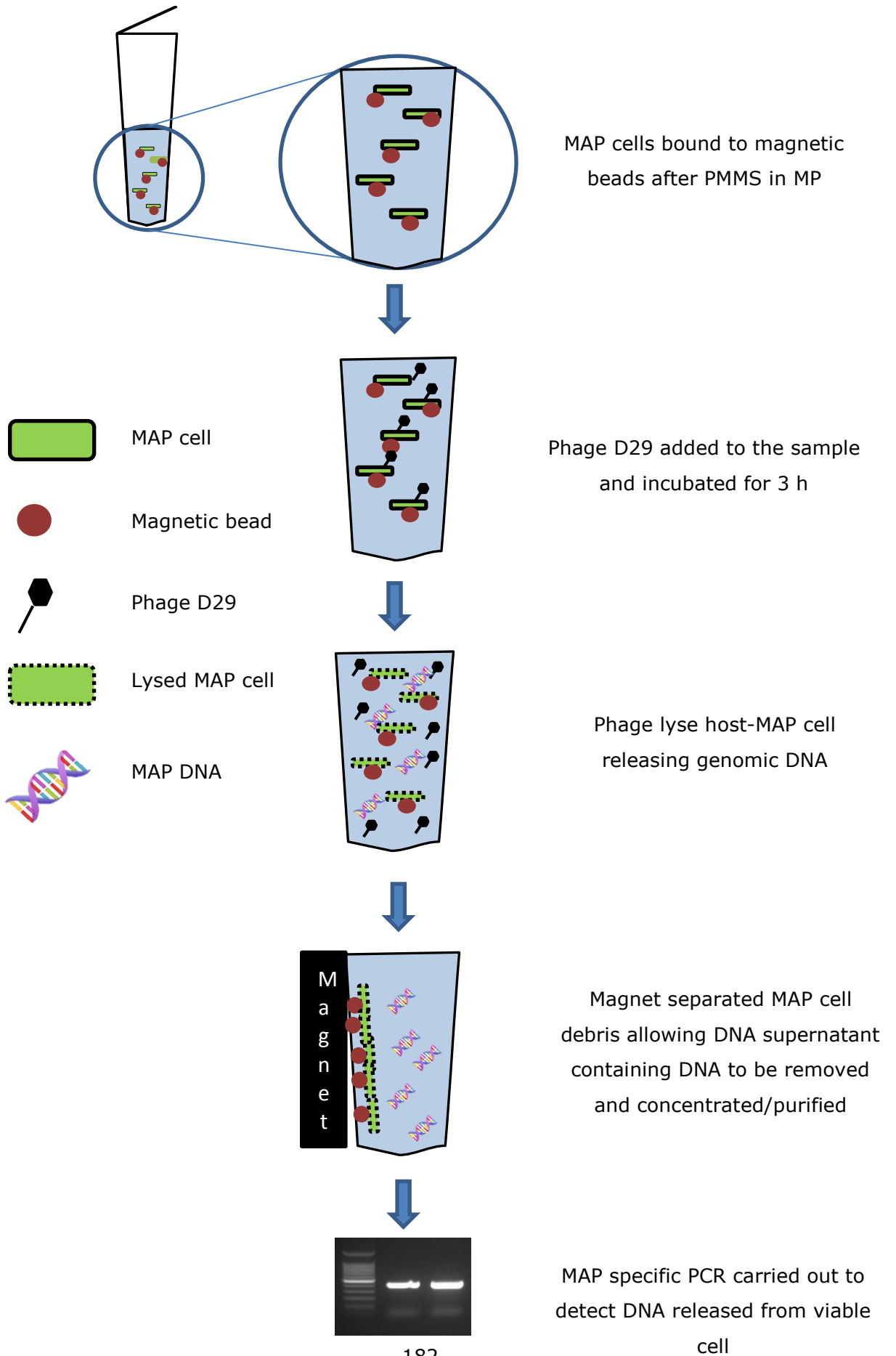


Table 5.1 shows the results gained using the one tube assay compared to the results gained using the original blood phage-PCR assay described in Section 4.2.7. Looking at the overall pattern of results, for 22 out of the total of 33 samples tested, there was agreement between the new one day assay and the phage assay. Of the 11 cases where there was no agreement between the results of the two assay methods, 8 of these were when the phage assay gave a negative result, but the one day tube test gave a positive result. This would suggest that the one tube method is more sensitive. In the plate-based method the lysed MAP DNA has to be extracted from agar after overnight incubation, and there is a possibility that some DNA losses will occur, leading to a negative PCR result. In contrast, in the one tube format all the lysed DNA remains in the lysis mixture and the contaminating intact cells are removed from it before it used as template for the PCR reaction. Therefore this method is less prone to sample loss. In only 3 cases did the plate-based phage-PCR assay give positive results when the one day tube test did not. In these samples the plaque numbers recorded were low (between 3 and 12). Generally these results suggest that the phage-based test results (irrespective of the method) are reproducible (67% agreement of results), and that the one tube method may be more sensitive than the plate-based method.

Interestingly the largest number of results where the test did not agree again fell in the vaccinated group (9 tests did not agree in the vaccinated group, 2 tests did not agree in the unvaccinated group). This was the same pattern seen in the analysis of the results in Section 4.2.7 and suggested that something about these samples was interfering with the assays – irrespective of the test method.

Table 5.1. Comparison of the one tube assay results with conventional phage-PCR results.

	Month 6		Month 7		Month 8	
	Phage	One Tube	Phage	One Tube	Phage	One Tube
1	*	*	*	*		
2			#	#		
3						
4			#	#	*	*
5	*	*			*	*
6	*	*	*	*		
7						
8						
9	*	*				
10			#	#		
11						

* indicates tests where the one tube assay gave a positive result and the plate-based method gave a negative result

indicates tests where the one tube assay gave a negative result and the plate-based method gave a positive result

Blue shading – denotes no MAP was detected.

Red shading - denotes that MAP was detected.

Plate-based method	One Tube assay	Number of samples		%	% agreement/ disagreement
-ve	-ve	9		27.3	66.7%
+ve	+ve	13		39.4	
+ve	-ve	3	(2 V, 1 UV)	9.1	33.3%
-ve	+ve	8	(7 V, 1 UV)	24.2	
Total		33			

UV = unvaccinated
V = vaccinated

If the results of the one tube assay are compared alone with the results of the direct PCR, the percentage agreement or disagreement between two test results is 48.5% and 51.5%, respectively, indicating that there is now little correlation between the two test results (Table 5.2). However the same pattern of discordance of the results for the vaccinated group is seen (11 samples from vaccinated animals, only 1 from the unvaccinated group).

The results from the non-fully optimised one tube assay cannot not be used to definitively confirm the presence of viable MAP cells in the blood of the animals tested. Although anything else concluded from the results would be conjecture, a positive phage-based test result would be indicative of the presence of a MAP cell. Given this limitation, the results gained with both phage-based assays were next compared with the results gained using direct blood-PCR described in section 4.2.7. This analysis (Table 5.3) again suggested that the PCR detection was less sensitive than the phage-based methods (largest group is where the phage results were positive but the PCR results were negative). However the overall agreement between the two tests dropped to 43%. This analysis also revealed a striking pattern where the results for the vaccinated animals were consistently positive for the phage assay but negative for the PCR assay. This result is unexpected but suggests that some interference with the test methods is occurring. This could either be (a) the PCR reaction is being inhibited by something in the blood samples from the vaccinated animals or (b) the phage assay is giving false-positive results. However as both test methods rely on viable cells to support the replication of the phage and then detection of the released genomic DNA by a specific PCR reaction, this latter suggestion is hard to explain.

Table 5.2. Comparison of the one tube assay results with direct-PCR results

	Month 6		Month 7		Month 8	
	Blood-PCR	One Day	Blood-PCR	One Day	Blood-PCR	One Day
1	Blue	Red	Blue	Red	Blue	Blue
2	Blue	Red	Blue	Blue	Blue	Red
3	Blue	Red	Blue	Red	Blue	Red
4	Red	Red	Blue	Blue	Blue	Red
5	Blue	Red	Red	Red	Red	Red
6	Blue	Red	Blue	Red	Blue	Blue
7	Red	Blue	Red	Red	Red	Red
8	Blue	Blue	Blue	Blue	Blue	Blue
9	Blue	Red	Red	Blue	Red	Blue
10	Red	Blue	Red	Blue	Red	Red
11	Red	Red	Red	Red	Red	Red

Blue shading – denotes no MAP was detected.

Red shading - denotes that MAP was detected.

PCR test result	One Tube assay	Number of samples		%	% agreement/ disagreement
-ve	-ve	7		21.2	48.5%
+ve	+ve	9		27.3	
+ve	-ve	5	(5 UV)	15.2	51.5%
-ve	+ve	12	(11 V, 1 UV)	36.3	
	Total	33			

UV = unvaccinated

V = vaccinated

Table 5.3. Comparison of the phage assays results with direct-PCR results

	Month 6		Month 7		Month 8	
	Blood-PCR	Phage Assays	Blood-PCR	Phage Assays	Blood-PCR	Phage Assays
1	Blue	Red	Blue	Red	Blue	Blue
2	Blue	Red	Blue	Red	Blue	Red
3	Blue	Red	Blue	Red	Blue	Red
4	Red	Red	Blue	Red	Blue	Red
5	Blue	Red	Red	Red	Red	Red
6	Blue	Red	Blue	Red	Blue	Blue
7	Red	Blue	Red	Red	Red	Red
8	Blue	Blue	Blue	Blue	Blue	Blue
9	Blue	Red	Red	Blue	Red	Blue
10	Red	Blue	Red	Red	Red	Red
11	Red	Red	Red	Red	Red	Red

Blue shading – denotes no MAP was detected.

Red shading - denotes that MAP was detected.

All results

PCR test result	Phage Assays	Number of samples		%	% agreement/disagreement
-ve	-ve	5		15.2	45.5%
+ve	+ve	10		30.3	
+ve	-ve	4	(4 UV)	12.1	54.5%
-ve	+ve	14	(13 V, 1UV)	42.4	
Total		33			

Unvaccinated group only (#7-#11)

PCR test result	Phage Assays	Number of samples		%	% agreement/disagreement
-ve	-ve	3		20.0	66.7%
+ve	+ve	7		46.7	
+ve	-ve	4		26.6	33.3%
-ve	+ve	1		6.7	
Total		15			

Irrespective of the reason for this pattern, it suggests that the results from the vaccinated group are not appropriate for comparison of the performance of the phage-based methods and PCR. Hence the performance of the two assays was again compared but using only the results for the unvaccinated animals, and comparing the combined phage-assay results with direct PCR (Table 5.4). This analysis showed that there was now a 67% agreement between the test results and – interestingly – the largest group of test results that did not agree were PCR positive, phage-test result negative (4 samples), however the number of samples in this analysis is now too small to draw any strong statistical conclusions.

If the pattern of detection is now considered in the unvaccinated group, the results would suggest infection is never established in animal #8, whereas infection is established in animal #11 so that detectable levels of MAP are present in the blood at all sampling points. The number of MAP cells in the blood of animals #7 and #10 appear to be low at month 6 (hence variable test results) but infection is clearly established by months 8 and 9. Animal #9 only gives positive phage results in month 6, but thereafter the PCR assay can detect DNA but no viable cells are detected. If the results in the vaccinated group are compared to this it might suggest that vaccinated animals maintain low numbers of MAP cells in their blood for a long time, hence the positive phage assay results, but the levels are below the limit of detection of the PCR assay, although the progression seen in animal #5 suggest that a slow infection is developing.

5.3. DISCUSSION

The aim of these experiments was to develop a novel robust method for detecting and enumeration viable MAP within one day, in a format that could be automated. There is commercially available equipment that allows the separation and washing of cells using bead capture technology (Tecan Group; Te-MgS, Life Technologies; Dynabeads-Invitrogen). As long as the detection part of the assay

was kept within a one-tube format, automation would be possible. Capturing and detecting bacteria has been carried out many times before on *E. coli*, *Helicobacter pylori*, *L. monocytogenes* and many more (Nakamura et al., 1993, Su and Li, 2004, Enroth and Engstrand, 1995, Uyttendaele et al., 2000). However the majority of these methods use PCR as an end-point identification which does not differentiate between live and dead cells. It is important to assess the viability status of organisms to determine whether they pose a threat to public health (Keer and Birch, 2003). There are several stains that can be used to determine bacteria viability, however due to the unusual cell wall of mycobacteria these tests tend to be less efficient. Culture is the ideal method for determining viability, however with slow growing mycobacteria such as MAP, it can take several weeks to form colonies and even rapid liquid culture-based methods require up to 40 days incubation (Rees and Botsaris, 2012).

The novelty of the one tube assay format was that MAP cells can then be infected *in situ* with bacteriophage following isolation from a medium (such as blood) on magnetic beads. Since only viable MAP cells will support bacteriophage replication and MAP genomic DNA is released at the end of the lytic cycle, if the DNA is then detected by PCR the assay retains the ability to differentiate between live and dead cells. Lytic bacteriophage infect and break open bacteria efficiently within hours. The FPTB assay was used to determine how long it takes for phage D29, once it had infected the cells, to release progeny phage (eclipse phase) from MAP and *M. smegmatis*. There have been differences in the reported eclipse phase of D29 when infecting different mycobacteria. When using the FPTB assay the eclipse phase of D29 in *M. smegmatis* was 90 min, which is similar to the eclipse phase found by McNerney et al. (1998). In *M. tuberculosis* and *M. aurum* however it has been noted that the length of D29's eclipse phase is much longer at around 120 min (David et al., 1980, McNerney et al., 2004). This corresponds to the 120-135 min eclipse phase found here using the FPTB assay when D29 was infecting MAP cells.

Although further optimisations were required to make the assay reproducible, the results gained were sufficiently encouraging to test the blood samples from calves infected with MAP. The results showed that as the months progressed agreement between all the tests increased, except for the plate-based phage assay and the direct blood PCR, where agreement remained the same at 64 % (Table 5.4). In month 8 the one tube assay agreed with the plate-based phage assay for 82 % of tests. Assuming the assays had that same sensitivity, the two discrepancies in this set of results could be attributed to the one tube assay detecting non-viable MAP that may be present in the blood as it had not been fully optimised, however this cannot be proven outright due to the need for further robust optimisations of the one day assay.

Table 5.4. Agreement between test results over time

	Agreement between each tests (%)			
	One Tube Vs Phage Assay	One Tube Vs Blood PCR	One Tube vs PCR and Phage	Phage Assays vs PCR
Month 6	64	27	27	64
Month 7	55	55	36	64
Month 8	82	64	55	64

Although the early results on clinical experimentally infected animals are very interesting and detection of MAP using a new method of cell extraction from blood is promising, further work is needed to confirm the efficacy of the assay with regards to the differentiation between viable and non-viable cells. To create a fully automatable, high-throughput assay, further work would also require conversion of the DNA detection method into a quantitative real-time PCR assay. This could be used to enumerate the number of MAP cells present (Sidoti et al., 2011) in the sample since in its current format the one tube assay simply gives a presence/absence result. By introducing qRT-PCR the assay results would be both rapid and would have more power for researchers in the field.

CHAPTER 6
AN INVESTIGATION OF FACTORS AFFECTING BACTERIOPHAGE D29
INFECTION

6.1. INTRODUCTION

Mycobacteria are peculiar organisms, grouped into fast- and slow-growers that can take weeks to form colonies (Wayne, 1986). This slow growing attribute is linked to many pathogenic members of the *Mycobacterium* genus (Chacon et al., 2004) and poses one of the greatest threats to treating and controlling diseases due to difficulty in achieving rapid diagnosis of infection by these bacteria. Culturing MAP can take up to 16 weeks (Zimmer et al., 1999) and in some cases it can take up to six months for certain sheep strains to form colonies. Because of these difficulties, several technologies exist that exploit bacteriophage in the detection of mycobacteria. The FPTB assay has been used as a tool to enumerate slow growing mycobacteria as well as determining whether or not they are antibiotic resistant (Rees and Botsaris, 2012). Rifampicin is an antibiotic used regularly in the treatment of mycobacterial infections. Its reversible role in inhibiting RNA synthesis is well known (Nakamura and Yura, 1976). The FPTB-Response™ antibiotic resistance assay works on the principle that if a sample contains rifampicin sensitive mycobacteria, plaques will not form if the antibiotic is added to the sample before performing the phage assay, however if the cells are resistant, plaques will still be formed. In addition to being able to report on the antibiotic resistance of the host cell, mycobacteriophage have also been postulated to be used to provide insights into genetics and physiology of their pathogenic hosts (Hatfull, 2012). Due to a high degree of genetic diversity among sequenced mycobacteriophage, many genes' functions remain unknown. Understanding what they do may provide insight into the host physiology.

Some mycobacteriophage, such as D29, TM4, L5 and Bxz2, have been isolated that have a very broad host range and therefore must bind to receptors found on many different mycobacterial cell types, however there are others that have been found to only infect one host (Rybniiker et al., 2006). While

mycobacteriophage host preferences are expected to be strongly dominated by the availability of specific cellular receptors, few have been identified or studied (Hatfull, 2010) therefore it is difficult to make predictions about the growth conditions needed to ensure that these receptors are expressed to promote good phage infection.

There is little known about of the effect of different metabolic states of the host cells on the ability of bacteriophage to infect mycobacteria. The first observations that led to this study were that, when testing liquid MAP cultures that had been stored over a long period of time (>6 months) with the FPTB assay, the results suggested that no viable MAP cells were detected. However the same phenomenon was observed when this was repeated with fresh cultures, and ZN stain and PCR showed that the cells in the culture were indeed MAP. An initial suggestion was made that the reason that the MAP cells were undetectable by the phage assay was because the MAP cells had been grown in an oxygen limiting environment for long periods of time (>6 months) and that this resulted in some change in the MAP cells which made them uninfected. Hence the aim of this investigation was to use the phage amplification assay as a tool to investigate how different growth and storage conditions of mycobacteria can affect the host cell-phage interaction and thereby affect the efficiency of mycobacteriophage D29 infection.

6.2. RESULTS

6.2.1. Ability of phage D29 to infect mycobacteria in different growth phases

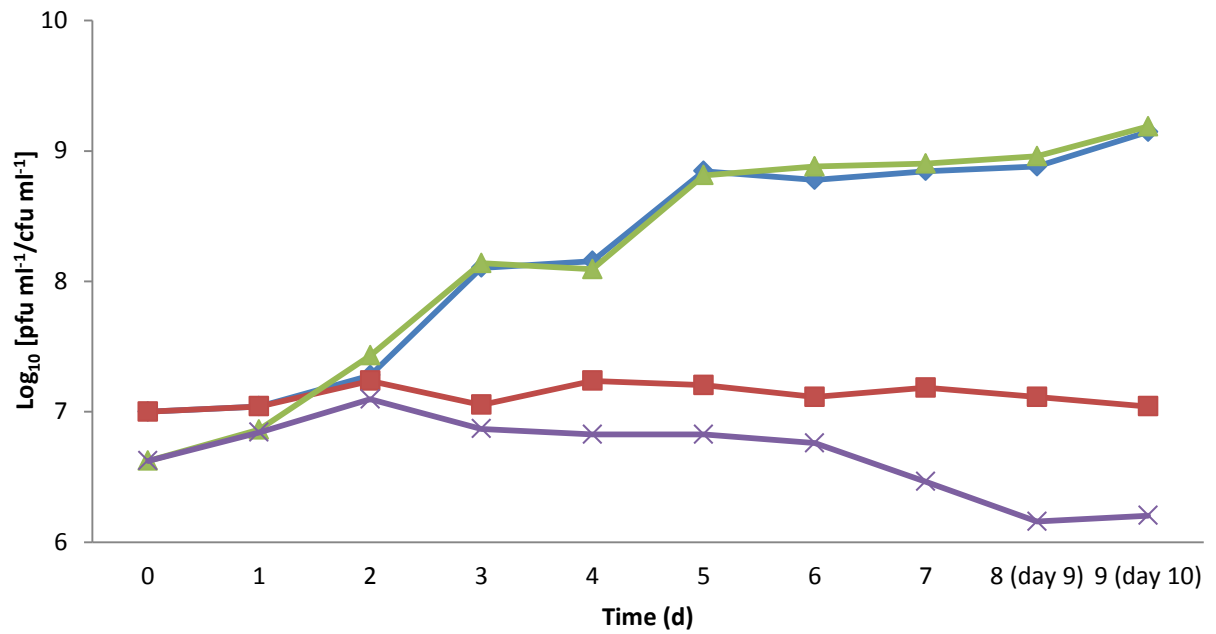
These experiments asked the question why the MAP cells were uninfected and how the cells became infectable. Using *M. smegmatis* as a fast-growing model organism so that cfu values could be determined as well as pfu the implications on the FPTB assays as a tool for looking at mycobacteria was

investigated. First *M. smegmatis* cells were grown aerobically and in conditions where oxygen would become self-limiting as growth occurred. The *M. smegmatis* was grown in glass vials with a screw top lid filled to leave a head space ratio of 1 : 2 (air : liquid) and the tops sealed finger tight. As a control *M. smegmatis* cells were also grown aerobically (with the lid loose) so that the effect of oxygen on the ability of phage D29 to infect mycobacteria could be compared.

The *M. smegmatis* cells (grown to 1×10^7 cfu ml⁻¹) were sub cultured either under oxygen limited conditions mentioned earlier or aerobically for 10 d in a 37 °C incubator shaking at 200 rpm. Each day, samples (100 µl) were removed and the cfu (using Miles and Misra) and the FPTB enumeration assay was carried out.

The initial results show that there was no difference ($P > 0.05$) in the pfu ml⁻¹ and cfu ml⁻¹ results for the culture of *M. smegmatis* when they were cultured aerobically (Fig. 6.1). However after 10 d over the time course, when the *M. smegmatis* was grown in oxygen limiting conditions the pfu ml⁻¹ values were almost one log₁₀ lower than the cfu ml⁻¹ value recorded (Fig. 6.1). When the same *M. smegmatis* culture was further incubated for over one month, no *M. smegmatis* cells were detectable using the phage assay, whereas the number of *M. smegmatis* cells detected by cfu ml⁻¹ remained constant (data not shown). The data shows that the FPTB enumeration compares well with traditional culture when used on aerobically growing *M. smegmatis* cells. However when cultured under self-limiting oxygen conditions, the phage assay is unable to detect the *M. smegmatis* cells efficiently even though the culture method shows the cells are alive.

Figure 6.1. Comparison between the number of *M. smegmatis* cells detected by phage and viable count following growth under self-inducing hypoxia conditions



Graph showing the results of the phage assay (pfu ml^{-1} ; green and purple) viable count (cfu ml^{-1} ; blue and red) for *M. smegmatis* cultured under self-limiting oxygen conditions (red and purple) or under conditions where free oxygen exchange occurred (blue and green) over 10 d.

6.2.2. Determining whether the phage-resistant state is reversible

From the last experiment, where it was found that extended growth under self-limiting oxygen conditions induced an uninfected state in *M. smegmatis*, but the question remained of whether the uninfected state in self-induced oxygen limiting conditions was reversible. To answer this, both the oxygen limited uninfected and infected aerobic *M. smegmatis* cells from the previous experiment (Section 6.2.1) were inoculated separately into 1 ml of fresh MP and incubated aerobically (37 °C; shaking at 200 rpm). A sample (100 µl) from each test was removed each day to determine if the number of *M. smegmatis* cells detected by the phage increased after exposure to oxygen.

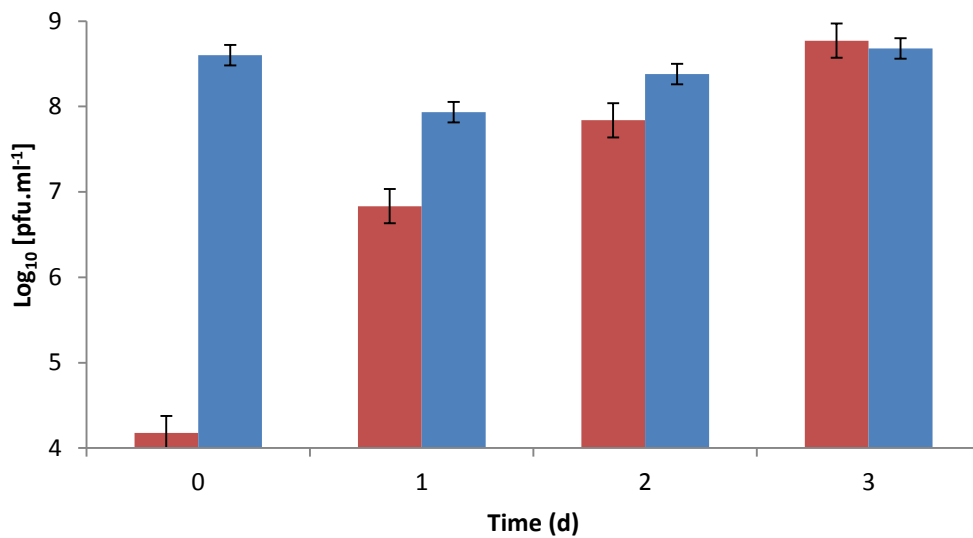
Around 10^4 pfu ml⁻¹ of *M. smegmatis* cells were detected at time point 0. The phage assay was able to detect nearly 10^7 pfu ml⁻¹ after 1 d of aerobic incubation and after 3 d there was no difference ($P > 0.05$) in pfu ml⁻¹ values obtained for both cultures (Fig. 6.2). This suggested that after exposure to air in an uninfected state, the *M. smegmatis* must change to allow successful phage infection and subsequent detection with the phage assay.

As *M. smegmatis* was used as a model for the phage infection, the experiment was repeated using three strains of MAP (K10, DVL 453 and ATCC 19851) which had been grown under the same conditions as the *M. smegmatis* except for a longer time (1 month) to induce the undetectable state (i.e. no MAP cells detected with phage D29) and these were then inoculated into fresh MP at a rate of approximately 1×10^5 pfu ml⁻¹. No Mycobactin-J was added to the media to determine only when recovery has taken place and not growth.

After the MAP cells were allowed to recover for one day with aeration, only cells in the DVL 453 strain were detectable (1.5×10^1 pfu ml⁻¹), while the other two strains did not give any plaques using the FPTB assay (Fig. 6.3). On day 2, a 2-3 log₁₀ increase in the number of cells detected by the phage assay was seen for each strain of MAP tested. This number increased again – but more slowly –

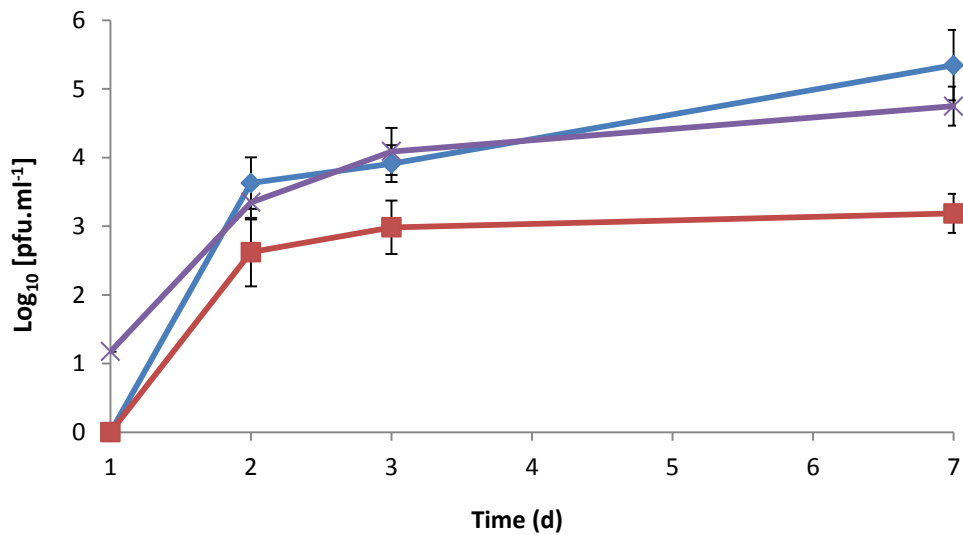
for all strains on day 3 of sampling and after 7 days for the number of MAP cells detected by the phage assay was between 10^2 to 10^5 pfu ml⁻¹. Only for strain ATCC 19851 did the increase in detectable number of cells seem to plateau (Fig. 6.3). The most important conclusion from these results is that the increase in plaque number detected was faster than a predicted growth rate for MAP cultures (as no Mycobactin-J was added), confirming that these results suggested an increase in infectivity rather than an increase in cell number.

Figure 6.2. Recovery of phage D29 infectivity by *M. smegmatis* cells



Graph showing the number of *M. smegmatis* cells detected using the FPTB assay (pfu ml⁻¹). Prior to dilution into fresh medium the *M. smegmatis* cells were either grown under self-limited oxygen conditions (red bars) or aerobic conditions (blue bars). Samples were taken from the fresh cultures over a 3 d period. Error bars represent the standard deviations of the means of number of plaques recovered from the phage assay performed in triplicate.

Figure 6.3. Recovery of phage D29 infectivity by three strains of MAP



Graph showing the number of MAP cells detected using the FPTB assay (pfu ml⁻¹). Prior to dilution into fresh medium the MAP cells were grown under self-limiting oxygen conditions and then samples were taken from the fresh cultures over a 7 d period. The three strains of MAP used were K10 (blue), DVL 453 (purple) and ATCC 19851 (red). Error bars represent the standard deviations of the means of number of plaques recovered from the phage assay performed in triplicate.

6.2.3. Infection with a phage TM4

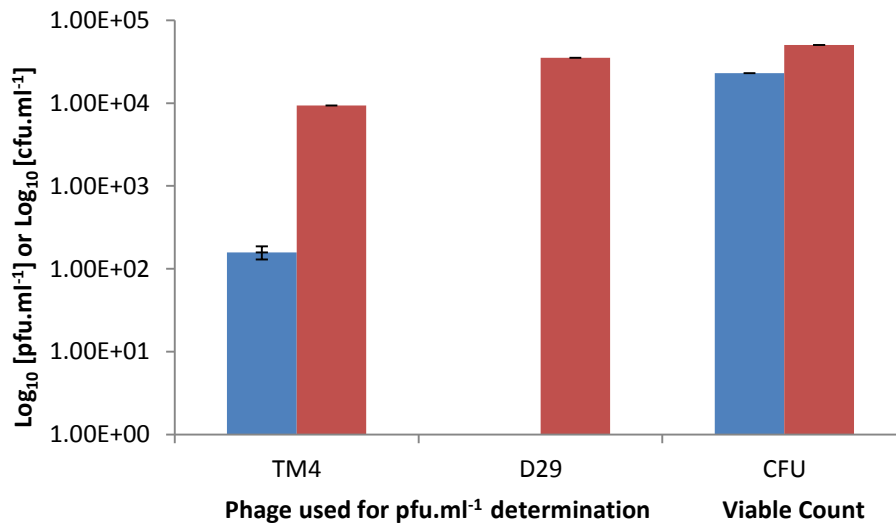
It has been reported that physical changes in the cell surface of *M. smegmatis* as a result of increased expression of a multi-copy phage resistance gene (*mpr*), may prevent bacteriophage D29 infection, by blocking cell receptors or cell penetration (Barsom and Hatfull, 1996). Phage TM4 is another broad spectrum mycobacteriophage, capable of infecting *M. smegmatis* and MAP. It has the ability to infect stationary phase mycobacteria by being able to penetrate the cell wall when it is in a stationary phase (Piuri and Hatfull 2006). The ability to infect cells in different states suggests that phage TM4 may have different binding sites or can activate the dormant cells in some way to allow successful infection and replication within the host. The differences between TM4 and D29's tail may explain why D29 is unable to infect the cells. Hence experiments were designed to replicate the phage infection experiments using phage TM4 instead of D29.

The key to the FPTB assay is the inactivation of the phage with a virucide. When tested, phage TM4 was found to be resistant to Ferrous Ammonium Sulphate (FAS; the virucidal compound provided in the FPTB assay kits). Tea infusions have been used to inactivate other bacteriophage when FAS was not effective (de Siqueira et al., 2006), and therefore a tea infusion was prepared and TM4 was found to be sensitive to this virucide (Section 2.8), producing a 6- \log_{10} kill within 15 min. Another crucial attribute of a good virucide, is that it does not have an adverse effect on the host cell, and it was found that the tea infusion did not affect the viability of the MAP or *M. smegmatis* cells (data not shown).

Once an appropriate virucide had been established *M. smegmatis* and MAP, cells were grown under oxygen limiting conditions (Section 2.9) and were then infected with TM4 before the FPTB assay was performed. As a control, samples of the *M. smegmatis* oxygen limited culture were also then grown with aeration for 3 d before being tested.

The results in Figure 6.4 show that TM4 was able to infect *M. smegmatis* grown under both conditions – although with reduced efficiency (1.58×10^2 pfu ml^{-1} detected) - whereas D29 was not able to infect the cells grown under limiting oxygen conditions at all. The viable count of the two different *M. smegmatis* cultures were very similar (both approx. 1×10^4 cfu ml^{-1}) confirming that the difference in the results obtained was not due to a difference in the number of cells in the cultures grown under different conditions. Interestingly, for the cells growing in the presence of oxygen, the number of cells detected by D29 was not significantly different from the viable count (1.6×10^4 cfu ml^{-1}) of the culture ($P > 0.05$). In contrast the number of cells detected by TM4 was significantly lower ($P < 0.05$), suggesting for cells grown with good aeration, D29 is more efficient at infecting *M. smegmatis* cells.

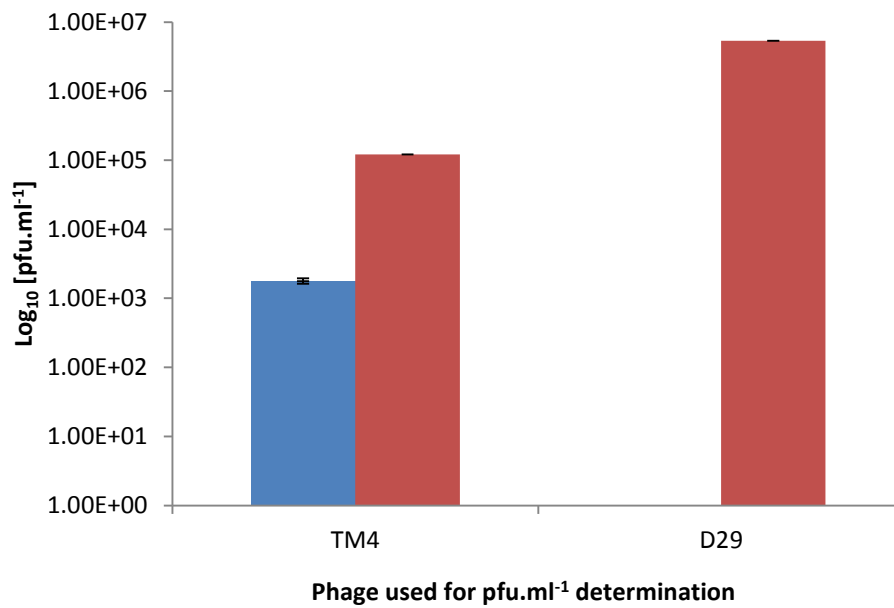
Figure 6.4. Difference in infectivity of *M. smegmatis* by D29 and TM4



Graph showing the number of plaques recovered following the phage assay when using phage TM4 and D29. The *M. smegmatis* cells tested were either grown with limiting oxygen (blue bars) or after these cells had been grown with aeration (red bars). In addition to the phage assay the viable count (cfu ml⁻¹) of both cultures was determined. Error bars represent the standard deviations of the means of number of plaques and colonies recovered from the phage assay and viable count, respectively, performed in triplicate.

The experiment to compare infection of stationary-phase mycobacteria with phage TM4 and D29 was then repeated using MAP cells (K10) but in this case colony counts were not performed due to difficulty of MAP culture. The results show (Fig. 6.5) that for cells grown under oxygen limiting conditions phage TM4 detected 1.8×10^3 pfu ml⁻¹ MAP whereas, once again, D29 did not detect any MAP cells. As seen with the *M. smegmatis* experiment, when these cells were exposed to air for 9 d, phage D29 was able to detect significantly more MAP cells ($1.5 \log_{10}$ pfu ml⁻¹; $P < 0.01$) compared to TM4, confirming that phage D29 seemed able to infect the mycobacteria more efficiently than TM4 when the cells are well aerated and in a more metabolically active state. In contrast when the cells are not actively growing, TM4 was better able to infect both species tested.

Figure 6.5. Difference in infectivity of MAP cells by D29 and TM4



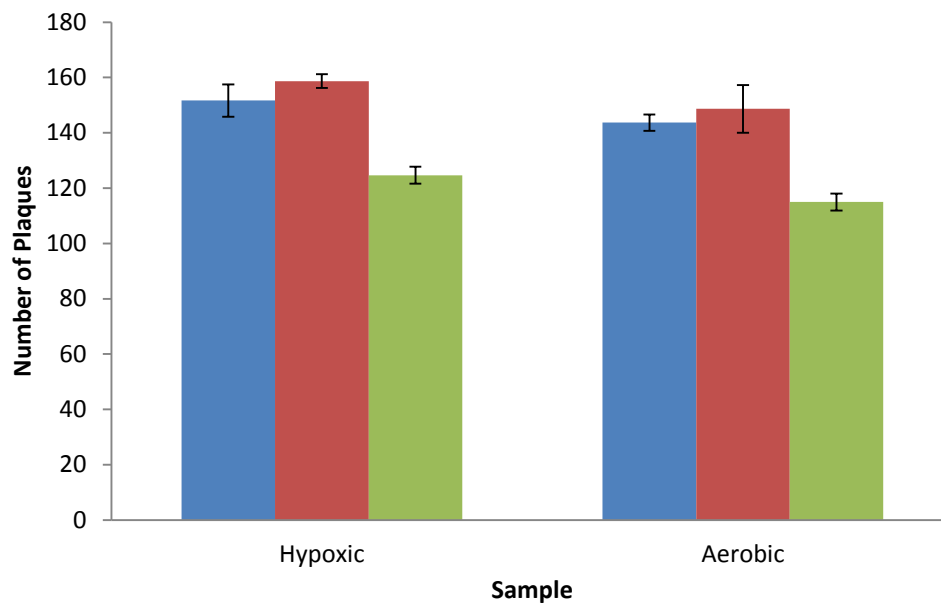
Graph showing the number of plaques recovered following the phage assay when using phage TM4 and D29. The MAP cells tested were either grown with limiting oxygen (blue bars) or after these cells had been exposure to air for 9 days (red bars). Error bars represent the standard deviations of the means of number of plaques recovered from the phage assay performed in triplicate.

6.2.4. Phage attachment to non-infectable MAP cells

It has been reported that mycobacteria can change their cell shape and thickness of their cell wall as they adapt to anaerobic growth conditions. From the results in the last experiments it was not clear whether the D29 phage were not able to attach to the cells surface or whether they were unable to complete the infection process once they had attached to the cells surface. To address this, a phage attachment assay (Section 2.9.1) was carried out to determine whether a change in the cell wall of the MAP cells was preventing the bacteriophage from attaching to the surface. Briefly MAP cells were grown into a stationary phase or cultured to a metabolically active state (Section 6.2.2; Spears et al, 1998). Phage was then added to each samples and left for 0, 30 and 60 min to bind to their host. The samples were then centrifuged to remove the MAP cells from any unbound phage. Phage titres on the supernatants were carried out to determine how many phage particles were bound the MAP cells.

The results show that there was an approximate 20% drop in the number of free phage particles present in the culture supernatant after 60 min of infection for both cell cultures (Fig. 6.6) and there was no statistical difference ($P > 0.05$) in the level of attachment of phage to cells detected for cells grown under oxygen limiting conditions compared to those grown aerobically. As a control the number of bacteriophage present in a sample when they were added to media alone that contained no MAP cells was also monitored and no reduction in phage number was detected, confirming that the reduction of free phage particles in the experiment was due to attachment of the phage to the cells. This result suggests that the receptors that D29 binds to are not altered or lost when the mycobacteria are grown under oxygen limiting conditions, but productive infection is blocked.

Figure 6.6. Effect of stationary phase bacteria on the attachment of phage D29 to MAP cells



Graph showing the number of unbound phage particles to MAP cells that are infectable (aerobic) and uninfected (hypoxic) after 0 min (blue bars), 30 min (red bars) and 60 min (green bars). Error bars represent the standard deviations of the means of number of bacteriophage detected after each time point in triplicate.

6.2.5. Role of RNA synthesis inhibition on phage infection

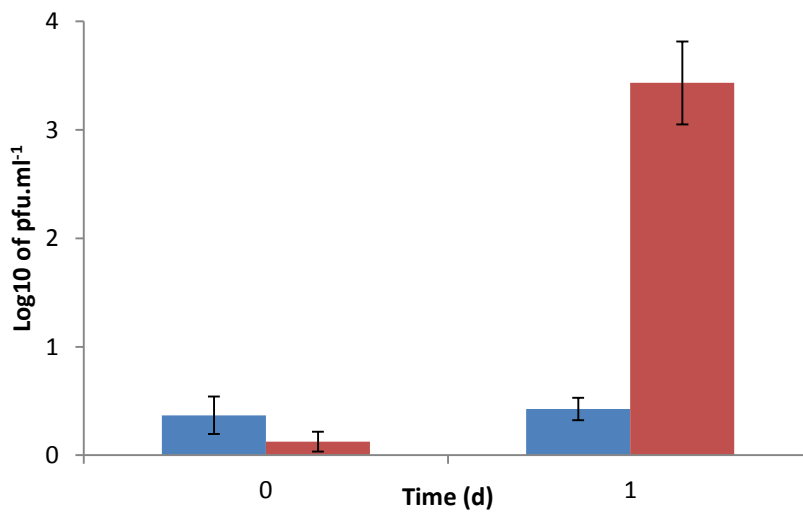
As phage D29 was able to attach to the cells of the stationary phase mycobacteria, this suggested that there was no physical barrier to phage infection, and therefore there was something else blocking productive phage infection other than receptor expression. This could be due to other adaptive changes that are occurring in the cells when the conditions become less aerobic or it could be due to restructuring of existing materials. To determine whether gene expression of proteins was required to allow the phage to infect the mycobacteria after aeration, antibiotics were used to transiently inhibit RNA synthesis in the host mycobacteria. Before the effect of the antibiotic on resuscitation of hosts was investigated, the MAP cells were initially tested to determine their sensitivity to rifampicin (RIF) and then experiments were designed to ensure that the antibiotic could be washed from a sample (i.e. that the RIF inhibition of RNA polymerase was reversible).

As described in the literature review, the FPTB assay can be used to determine whether mycobacteria tested are resistant to bacteriocidal antibiotics using a format of the assay called FPTB-Response™ (Rees and Botsaris, 2012). The samples are treated the same when infecting them with phage, however after the virucide is neutralised, RIF is added. When the mycobacterial cell is resistant to RIF, the phage are able to replicate and lyse their host cell forming plaques on a plate. When the mycobacteria cells are sensitive, the RIF then kills the host, preventing the phage from replicating and lysing their host, which results in no plaque formation. When aerobically grown MAP cells were treated with rifampicin for 1 d, no cells were detected using the FPTB assay. To determine whether the effect of the RIF was reversible the treated cells were centrifuged ($13000 \times g$; 3 min) and the pellet washed with 1 ml of fresh MP. The wash step was then repeated and the cells resuspended in 1 ml of MP so that the FPTB could be carried out. The results showed that the number of MAP cells

detected after RIF treatment was not significantly different ($P < 0.05$) to the number of MAP cells detected before RIF treatment.

Now knowing RIF could be removed from the MAP cells, to determine whether RNA synthesis is needed for the mycobacteria to regain infectivity when exposed to air, uninfected MAP cells (1×10^4 pfu ml⁻¹; K10; Section 2.9) were treated with RIF. Before exposure to air, (time zero), very few MAP cells were detected in either the RIF treated or untreated samples. After one day aeration, there was a significant ($P < 0.01$) three-log₁₀ increase in the number of MAP cells detected from the untreated sample (Fig. 6.7), however no MAP cells were detected from the RIF treated sample when the RIF was washed away. This suggests that there is a role in gene expression, which prevented the bacteriophage from successfully infecting the MAP cells.

Figure 6.7. Investigation of role of gene expression on recovery of sensitivity of MAP to phage D29



Graph showing the number of MAP cells detected by the FPTB assay, after uninfected MAP cells were treated with RIF (blue bars) and without RIF (red bars) before exposure to oxygen (t = 0) and after exposure to oxygen (t = 1). Error bars represent the standard deviations of the means of number of plaques recovered from the phage assay performed in triplicate.

6.2.6. Effect of freezing on phage infection

Freezing MAP cells for storage can have adverse effect on their viability. Ice crystal formation can kill bacteria and stresses on macromolecular structures during thawing the cells can lead to damage that prevents growth (Collins, 2003). However, freezing is often necessary to avoid sample degradation, thus preservation by freezing is very important especially if transport from a farm to a laboratory is not easy and takes a long time (Hasonova et al., 2009). Hence for future applications, freezing of samples for use with the phage assay would probably be necessary and it was not clear what effects this would have on phage infectivity of the host cell. Therefore experiments were carried out to determine the best methods to use when freezing cells to improve the viability of cells post-freezing and to optimise the enumeration and detection of cells when using phage-based assays.

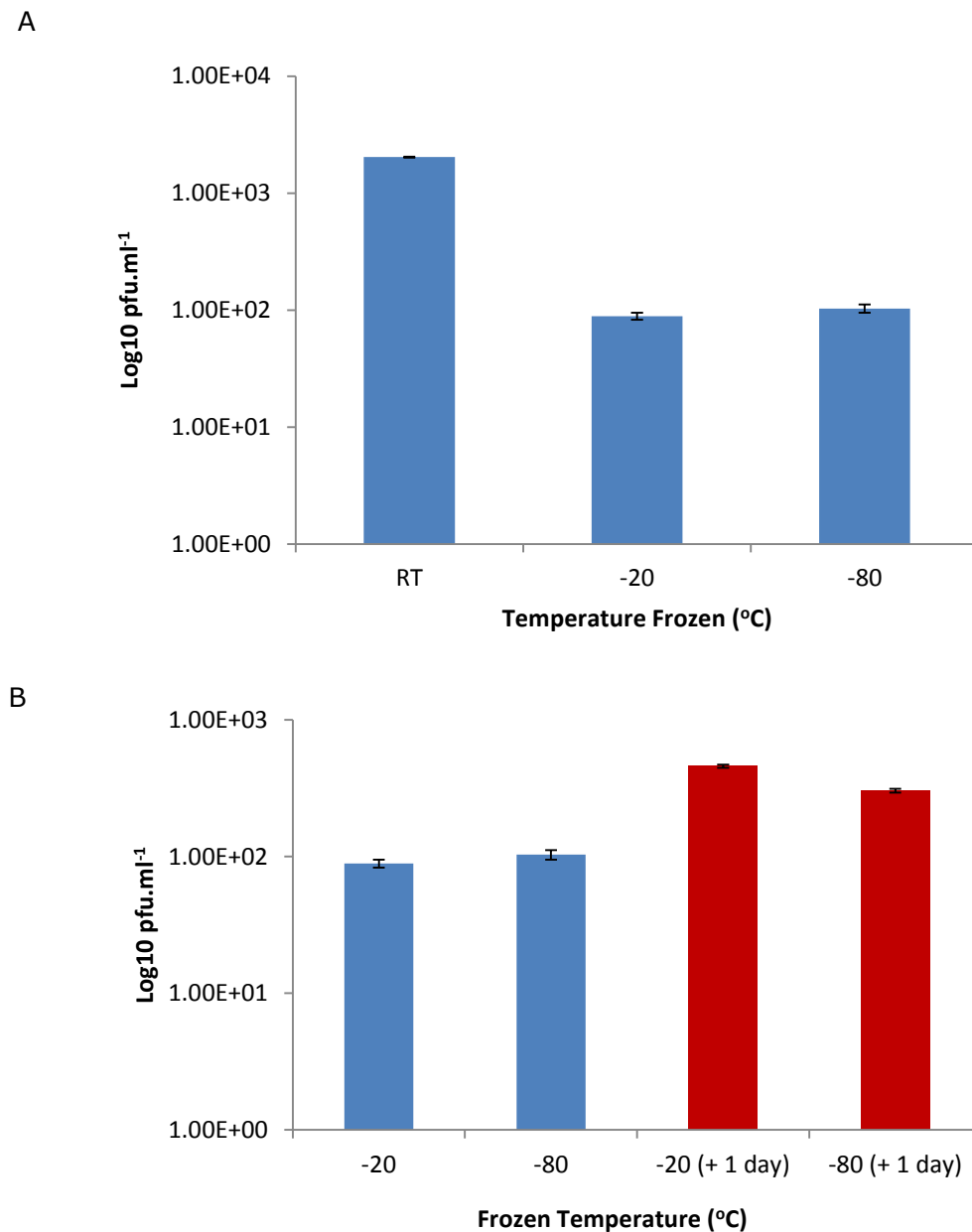
Freezing at different temperatures has been shown to have an effect on the viability of mycobacteria when cultured. The FPTB assay can be used to enumerate the number of detectable mycobacteria present in a sample (Section 2.1.3.3), and this assay format was used to determine whether freezing affected the number of cells detected by the phage-based blood assay.

To perform the experiments, samples of MAP K10 (1×10^4 pfu ml⁻¹) were spiked in triplicate into 1 ml of sheep blood (Oxoid, UK). The samples were frozen at -20 °C and -80 °C and incubated overnight, but the rate of freezing was not controlled. One control sample was left at room temperature. The samples were removed from the freezer and left to thaw at RT and then the MAP cells were recovered from the blood using PMMS. Finally the number of detectable cells was determined using the blood phage detection assay method (Section 2.3.2).

The results (Fig. 6.8A) show that there was a significant drop ($P < 0.05$) of approximate $1.5 \log_{10}$ in the number of plaques detected in the samples after

freezing compared to those left at room temperature, but there was no statistical difference between the samples frozen at -20 °C or -80 °C. The experiment was repeated, but this time the samples that were frozen were left to recover for 24 h at room temperature. The results show that after 24 h, the number of MAP cells detected by the assay increased compared to those without recovery although this difference was not significant ($p > 0.05$; Fig. 6.8B) and again there was no difference seen between cells frozen at the different temperatures.

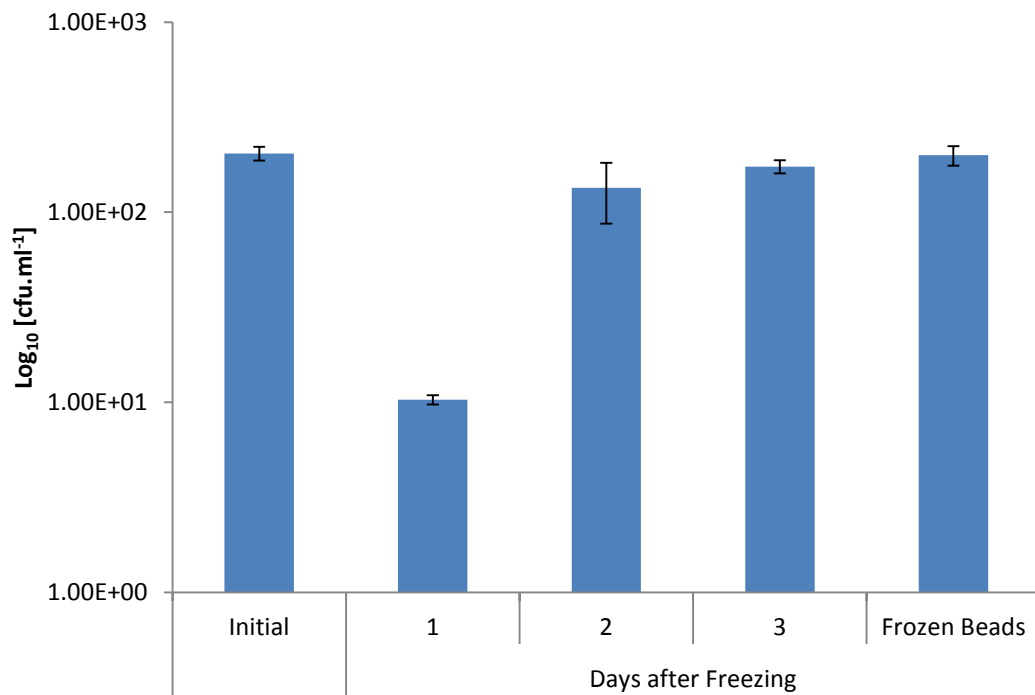
Figure 6.8. Effect of freezing on MAP cell detection



Graph shows the number of plaques recovered by the FPTB assay. MAP cells were frozen in sheep blood over night at -20 and -80 °C. In graph A, MAP cells were frozen in sheep blood over night at -20 and -80 °C and as a control one sample was left at room temperature (RT). In graph B, One set of MAP cells (blue) were tested with the phage blood assay straight away. The other set (red) were kept at RT for 1 day before being processed through the blood phage assay. Error bars represent the standard deviations of the means of number of plaques recovered from the phage assay performed in triplicate.

The number of MAP cells detected increased when left at room temperature, this still did not compare well to the number of MAP cells detected when the blood samples were not frozen. The experiment was repeated again freezing the samples at -20 °C and the length of recovery time was increased further. The samples were then left for 3 d at room temperature after freezing, the cells were recovered by PMMS and the number of detectable cells determined using the phage assay. The results showed that the number of MAP cells detected by the phage assay increased after each day of recovery, and the number of MAP cells detected after 2 and 3 d was not statistically different from the number of MAP cells detected in the samples that were not frozen (Fig. 6.9). To ensure the PMMS was not the factor affecting the recovery of the MAP cells, beads frozen overnight at -20 °C and thawed at RT were used to capture liquid cultures of MAP. The results showed that freezing the magnetic beads did not affect their ability to capture MAP cells (Fig 6.9). This suggested that the MAP cells survived freezing, but were in an uninfected state, until recovery had occurred.

Figure 6.9. Effect of longer recovery periods on number of MAP cells detected after freezing at -20 °C



Graph shows the number of plaques recovered by the FPTB assay. MAP cells were frozen in sheep blood overnight at -20 °C and left to recover at RT for 1, 2 or 3 d before processed through the phage assay. Beads also frozen at -20 °C overnight were thawed as a control to determine the effect of freezing on their capture efficiency of MAP cells. The initial sample was not frozen. Error bars represent the standard deviations of the means of number of plaques recovered from the phage assay performed in triplicate.

6.3. DISCUSSION

The FPTB assay is a powerful tool that can detect, enumerate and determine the antibiotic sensitivity of mycobacteria. However a lack of information about phage-host interactions may lead to inaccurate interpretation of results. Phage D29 was found to be unable to infect both MAP and *M. smegmatis* cells when they were induced into a non-growing phase when oxygen became self-limiting in the growth tubes as described by Wayne and Hayes (1996). However when the cells were reintroduced to oxygen, the ability of the phage to infect the cells was restored almost completely although the time required to achieve this was different for the two organisms tested; three days for *M. smegmatis* and over one week for MAP. This result probably reflects the extremely different growth rates of these two bacterial species.

M. smegmatis, *M. bovis* and *M. tuberculosis* have all been reported to have the ability to enter a 'non-replicating' stationary phase during hypoxic stress (Dick et al., 1998, Hutter and Dick, 1999, Wayne and Hayes, 1996). Hypoxia is predicted to be a key host-induced stress limiting growth of the pathogen *in vivo*. However many studies have indicated that *M. tuberculosis* adapts to oxygen limitation by entering into a metabolically altered state while awaiting the opportunity to reactivate (Rustad et al., 2009). For MAP, Whittington et al. (2004), presented evidence that this organism could enter a dormant stage, similar to that described for *M. tuberculosis*, *M. bovis* and *M. smegmatis*. They also suggested the ability to lie dormant may also aid in the survival of this organism in the environment. A protein, DosR, has been reported to be the primary transcription factor involved in mediating the genetic response to reduced oxygen tension in *M. tuberculosis* and it has been shown to induce expression of nearly all the *M. tuberculosis* genes that respond powerfully to a hypoxic signal (Park et al., 2003). The gene encoding DosR is present in the MAP genome suggesting that MAP also has the ability to respond strongly to hypoxia, although structural

homology does not always infer functional relatedness. However a study by Gumber et al. (2009) confirmed that MAP can enter a dormant, non-replicating phase when exposed to a stressful environment such as hypoxia, and this can involve the regulation of up to fifty proteins, one of which could be the DosR protein.

Due to the many physiological gene expression changes reported when mycobacteria enter their non-replicating phase, the ability of MAP to resist D29 phage infection during hypoxia may be purely coincidental rather than an adaptive resistance to phage D29. It is known that adsorption of D29 to *M. tuberculosis* is more efficient when the bacteria are in exponential phase of growth (David et al., 1980). The reduction in the adsorption efficiency observed by David et al. (1980) was thought to be due to structural changes on the cell wall of the host which occur when they are not in the exponential growth phase, and this in turn may affect the accessibility of D29 to specific phage receptor sites. Structural changes, such as cell wall thickening due to the accumulation of alpha-crystallin chaperone protein, have been reported in *M. tuberculosis* (Cunningham and Spreadbury, 1998, Wayne and Hayes, 1996). Most recently some MAP strains have been reported to have the ability to form spores (Lamont et al., 2012); cell wall thickening due to the accumulation of protein or sporulation could prevent phage D29 from attaching to the cell surface and therefore binding. However the phage attachment assay described in Section 6.2.4 suggests there is no change in the ability of the phage to bind to MAP cells, rather that there could be a barrier to the DNA being delivered into the cell or for productive phage replication to occur inside the host cell.

When MAP - in the non-replicating stationary phase - was treated with rifampicin to prevent *de novo* protein synthesis, the cells were unable to fully revert to an infectable state, suggesting what is affecting productive D29 infection of MAP is not a physical barrier, but rather, they require gene

expression and RNA synthesis. Whittington et al. (2004) found that a homologue of the DNA binding-like protein (Dps), which was first identified in *M. smegmatis* and confers protection by binding to DNA during nutritional and oxidative stress in other bacteria, is present in the *M. avium* genome. Dps has been shown to confer resistance to bacteriophage that infect *E. coli*. Some *E. coli* cells exposed to environmental bacteriophage, isolated from sewage water, were found to be tolerant to phage infection after culture for 24 h. The *E. coli* cells, when subcultured in liquid media began to clump. Dps was found to be present in the cell wall membranes of the phage tolerant cells and was thought to be the reason for the phage resistance. This was confirmed when Dps mutants were created, as the environmental bacteriophage were able to infect the *E. coli* again (Lacqua et al., 2006). Thus resistance to D29 phage infection may be due to an accumulation of proteins such as Dps which would bind to the replicating phage DNA and prevent productive phage replication. What is also interesting is the role of Dps and the clumping in *E. coli*, which may have similar effects in the clumping of mycobacteria. However arguing against this model is that other bacteriophage have been reported to be able to infect stationary phase mycobacteria. This was reported for phage TM4 by researchers exploiting luciferase reporter phage (LRP) technology (Foley-Thomas et al., 1995, Dusthacker et al., 2008). The ability of phage TM4 to infect cells that D29 cannot has been postulated to be due to a peptidoglycan hydrolase motif found on the tape measure protein of TM4 that is not present on the tail of D29. This motif is thought to act in a similar way to resuscitation protein factors (Rpfs) which can induce stationary phase mycobacteria cells into an active growth state (Piuri and Hatfull, 2006). The breakdown of the mycobacteria cell wall peptidoglycan may mimic the signal generated by the Rpfs leading to mycobacteria resuscitation and therefore allowing TM4 phage infection of a metabolically active cell. In this study, although TM4 was able to infect

stationary phase mycobacteria, when infecting aerated metabolically active mycobacteria (defined by phage D29 infection), it was not as efficient at infecting compared to D29 and therefore it would not be a suitable phage to use routinely in the FPTB assay since the ability of phage detection assay to infect all cells present in a sample efficiently is important for use as an enumeration tool (Swift et al., 2013).

Freezing is often used for sample preservation when transporting substances from field to laboratory. However, freezing has been shown to have an adverse effect on mycobacteria viability (Richards and Thoen, 1977, Raizman et al., 2011). This was found to be the case in this study when trying to detect MAP cells in blood samples that had been frozen, where over a 1 log₁₀ drop in the number of MAP cells detected was recorded. While some MAP cells may have died as a result of freeze-thaw injury, others appeared just to not be detectable by the bacteriophage. When Foddai et al. (2009) optimised the phage assay, they determined that an extra day of incubation of MAP cells in media prior to performing the phage assay allowed greater number of MAP cells to be detected. Therefore the idea of introducing a pre-incubation step after thawing was investigated to allow the cells that may be stressed by the freezing and thawing to recover. It was hoped that this would optimise the number of MAP detected after freezing, especially as it had already been demonstrated that when cells are oxygen stressed, phage D29 infection was prevented in a reversible manner. The number of cells detected after just one day resuscitation in media (without Mycobactin-J, therefore no growth) increased significantly, and after two days there was no significant difference to the number of cells detected before freezing. Hence by adding a simple recovery step for frozen samples by incubating the samples for 48 h under conditions that do not allow cell growth would enable sensitive detection of the MAP cells in frozen blood samples. This is very important especially when using the blood assay as very low numbers of

cells would be present. If the blood phage assay was carried out on frozen clinical samples of blood, which have been found in from clinical blood samples from animals tested in Chapter 4 to contain very low numbers of MAP cells, a drop of 1 log₁₀ would be enough to give negative results based on the number of plaques formed.

Many factors can affect the ability for phage to infect their host. Generally bacteria have evolved to avoid or limit infection by bacteriophage, and as a consequence, bacteriophage have co-evolved to overcome barriers to infection. By entering the dormant stationary phase the mycobacteria are able to persist in many harsh environments, including inside their host. Their evolution to enable this survival may or may not have included resistance to bacteriophage infection, but regardless of this, phage TM4 had evolved a mechanism to allow it to infect dormant MAP cells where phage D29 had not. The implications for the FPTB assay when detecting cells from different environments is great, as it may not be able to infect all the cells in a sample if they are lying dormant. Equally when infecting active cells, D29 is much more efficient in infecting mycobacteria than TM4. So a balance could be struck between the two, however unfortunately the same virucide cannot be used for both of these phage that makes the incorporation of TM4 into the assay along with D29 problematic. Fortunately, the studies using the clinical blood samples indicate that the MAP cells inside the macrophage are in a state that allows D29 infection. For the one tube assay format, where all that is required is cell lysis, these results indicated that a combination of both bacteriophage could result in very efficient cell lysis and therefore extend the number of viable cells detected by the assay.

CHAPTER 7

**DEVELOPMENT OF A NOVEL FLUORESCENT PROTEIN FOR LABELLING
MYCOBACTERIUM AVIUM SUBSP. *PARATUBERCULOSIS***

7.1. INTRODUCTION

The unique mycolic acid-rich cell wall characteristic of all mycobacteria described in Chapter 1 (Fig. 1.1) means that traditional staining techniques that rely on the penetration of water soluble dyes, such as the Gram stain, are not effective. A standard method for staining such acid-fast organisms for microscopy is the Ziehl-Neelsen (ZN) stain which differentiates the acid-fast bacteria from bacteria with other cell wall structures that are resistant to the Gram-stain (Fig. 1.2). The use of the ZN stain alone as a method to detect mycobacteria in samples has very low sensitivity as well as limited specificity since the method will stain all members of the genus (Zimmer et al., 1999). In addition the mycolic acid-rich cell wall is not restricted to mycobacteria; other bacteria such as species of *Nocardia*, *Corynebacterium*, and *Rhodococcus* may stain acid-fast (Thoresen et al., 1994). Fluorescent acid-fast stains have been shown to have a limit of detection of 10^4 cfu ml⁻¹ (Hendry et al., 2009), but again these lack specificity and can be less sensitive than other microscopic methods. Therefore, other than revealing cell shape, this method of detecting acid-fast bacteria in a sample is not sufficient to identify the organism (Section 1.2.3.1).

Despite this, because of the limitations of culture methods also described in Chapter 1, microscopy is a commonly used tool to identify mycobacterial infections. Hence researchers have developed alternative methods for staining cells to overcome the limitations of the ZN stain. The Avidin–Biotin Complex peroxidase (ABC) technique uses a primary antibody to bind to the target antigen (MAP cell). A biotinylated secondary antibody, with specificity against the primary antibody is added to bind to the primary antibody. A biotinylated peroxidase is then mixed with free avidin to form large avidin-biotin-peroxidase complex. This solution is then added to the tissue sample, and any remaining biotin-binding sites on the avidin bind to the biotinylated antibody which has already been bound to the target organism. This method is used as it creates a

greater concentration signal at the original antibody and therefore an increase in signal intensity and results in more sensitive detection of mycobacteria when compared to results using the ZN stain (Cancela and Marin, 1993). However the ABC method is more laborious and time consuming compared to the ZN stain (Kheirandish et al., 2009) but its increased sensitivity means that it can be used on very old tissue samples that have been stored for a long time, increasing the type of samples that can be analysed. However, the performance of this technique as a diagnostic still does not rival the use of culture (Martinson et al., 2008, Huntley et al., 2005). Hence, despite the fact that they are routinely applied as diagnostic methods, existing staining techniques for MAP prior to microscopic analysis to identify infection are quite poor.

Fluorescent proteins, like green fluorescent protein (GFP), can be used to label and visualise cells instead of detecting reporter enzymes such as peroxidase. Generally GFP-fusion proteins are created to provide the binding specificity for the GFP moiety, for instance the cell wall binding domains found on some listeriophage fused to GFP have been used to specifically label and detect *Listeria monocytogenes* (Schmelcher et al., 2010).

The aim of the experiments described in this Chapter was to develop a recombinant Gfp protein with the ability to bind to MAP cells to produce a fluorescent MAP-specific label that was far simpler than the ABC method. To do this the MAP-specific peptides described by Stratmann et al. (2002 and 2006) were fused to Gfp to try and develop a new microscopic detection and identification method that would enable MAP specific labelling of cells on a microscope slide. The aim was to create a reagent which could be used as quick and simple method to simultaneously detect and identify the organism and provide a significant advantage over the ZN stain in terms of specificity.

7.2. CONSTRUCTING FLUORESCENT PEPTIDES

7.2.1. Primer Design

To initiate the work, the sequences of the peptides described by Stratmann et al. (2002 & 2006) were converted into codon optimised (for *E. coli*) DNA sequences (Table 7.1). Optimising the codon sequences helps to achieve faster translation rates of the preferred sequences for certain amino acids in *E. coli*. These optimised sequences were then incorporated into the primer sequences that could be used for the amplification of the Gfp protein (Table 7.2). Different primers were designed so that MAP-specific peptides could be joined to either the N- or C-terminal end of Gfp. To facilitate cloning two restriction sites, *SmaI* and *NdeI*, were inserted upstream of the start codon on the forward primers and *SmaI* and *BamHI* restriction sites were inserted upstream of the stop codon on the reverse primers (sites highlighted in primer sequences in Table 7.2). The sites *NdeI* and *BamHI* were included to allow directional cloning of the fusion construct in the vector, so that the insert would be in the correct orientation with respect to the promoter to ensure expression of the recombinant gene.

Table 7.1. Codon optimisation of MAP specific peptides

Peptide - aMP3	N Y V I H D V P R H P A
Codon Optimised	AAT-TAT-GTG-ATT-CAT-GAT-GTG-CCG-CGT-CAT-CCG-GCG
Peptide - aMptD	G K N H H H Q H H R P Q
Codon Optimised	GGT-AAA-AAT-CAT-CAT-CAT-CAG-CAT-CAT-CGT-CCG-CAG

Codon usage optimisation for *E. coli* was determined using the table adapted by Malloy et al. (1996) shown in Appendix 7.1.

Table 7.2. Sequences of primers use to create Gfp fusions

Primer	Sequence (5' – 3')
GFP-Forward	ATGAGTAAAGGCGAAGAAC
GFP-Reverse	GACACATTTATTTGTATAGTTC
aMptD-N-Forward (N-aMptD)	CCCGGGCATATGAATGGTAAAATCATCATCAGCATC ATCGTCCGCAGATGAGTAAAGGCGAAGAAC
aMP3-N-Forward (N-MP3)	CCCGGGCATATGAATTATGTGATTCATGATGTGCCGCGTC ATCCGGCGATGAGTAAAGGCGAAGAAC
N-Reverse	CCCGGGATCCCTTAGACACATTTATTTGTATAGTTC
aMptD-C-Reverse (C-MptD)	CCCGGGATCCCTTACGCTGCGGACGATGATGCTGATGATG ATGATTTTACC GACACATTTATTTGTATAGTTC
aMP3-C-Reverse (C-MP3)	CCCGGGATCCCTTACGCCGATGACGCGGCAGATCAATCAC ATAATTGACACATTTATTTGTATAGTTC
C-Forward	CCCGGGCATATGATGAGTAAAGGCGAAGAAC

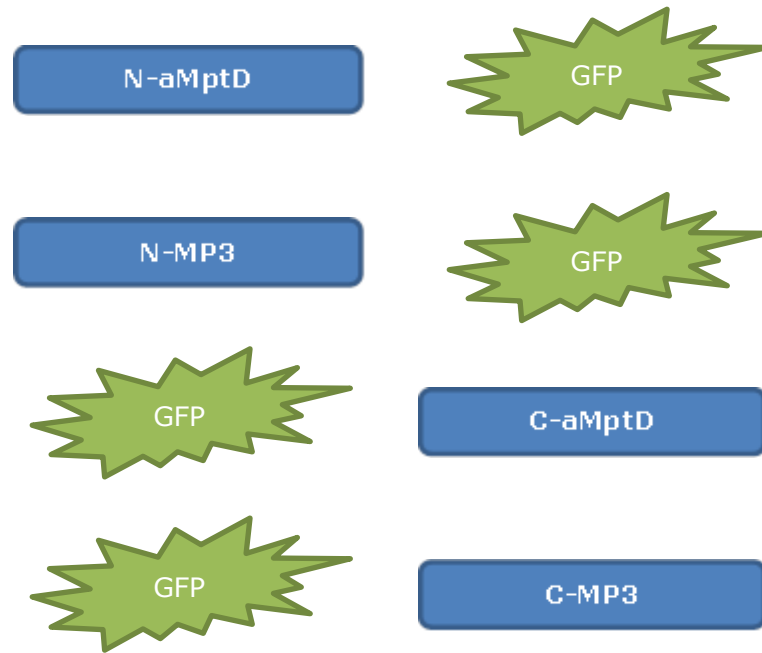
Green: GFP forward and reverse primers (sequence based on Gfp cloned into the plasmid pDONOR-P4-P1R)

Blue: Codon optimised amino acid sequence coding for MAP specific peptide aMptD

Red: Codon optimised amino acid sequence coding for MAP specific peptide aMP3.

Restriction sites are shown as Purple: *Sma*I; Gold: *Nde*I; Grey: *Bam*HI.

Figure 7.1. Schematic of fusion protein construct orientation



A schematic of the cloning strategy to enable the two MAP specific peptides to be bound on the N-terminal (N-aMptD & N-MP3) and C-terminal (C-aMptD & C-MP3) end of the Gfp protein.

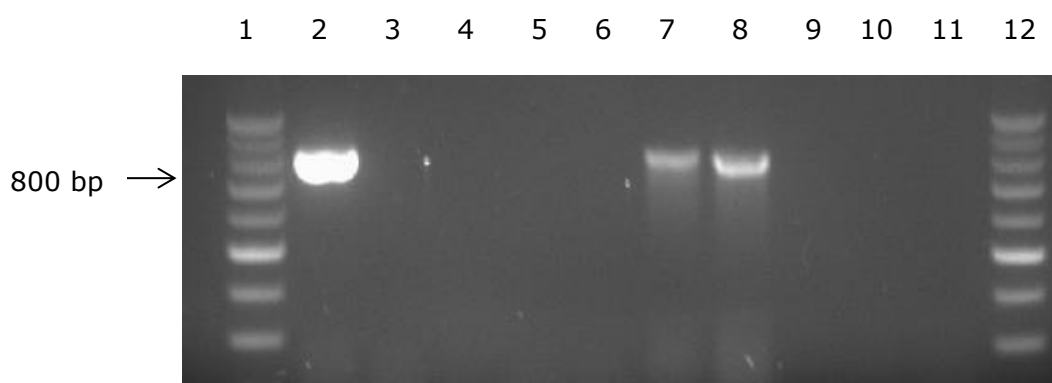
7.2.2. PCR of GFP-fusion peptide

The primers described in Section 7.2.1 were used to amplify GFP-fusion peptide using a proof reading DNA polymerase (Phusion Taq; NEB, UK), using plasmid pDONOR-P4-P1R (Qazi et al., 2001) as template DNA which encodes the *gfp* gene. The expected size of the PCR product was approximately the same as that as the wild type *gfp* gene (800 bp) as the primers only increased the size of the gene product by ~50 bp. Initial attempts to amplify the GFP gene were unsuccessful. Several parameters were changed to try and overcome this problem, including reducing the template DNA concentration and changing the DNA polymerase. Phusion Taq DNA polymerase has been reported to have a lower PCR yield compared to non-proof reading polymerases, therefore the ability of the proof-reading DNA polymerase to amplify the GFP-peptide fusions was compared to a non-proof reading DNA polymerase (Qiagen HotStart-Taq DNA polymerase, UK). The results show that the GFP gene was amplified when the non-proof reading DNA polymerase was used with two of the GFP-fusion peptides (N-aMptD and C-MptD), however no amplification was seen when the proof-reading polymerase was used (Fig 7.2), indicating that for these particular primers the proof-reading DNA polymerase was not sufficiently efficient.

Despite changing the polymerase, a PCR product was not produced using all primer pairs, hence a temperature gradient PCR was carried out for all of the primer pairs using the Phusion Taq DNA polymerase to determine whether the annealing temperature was affecting the amplification of the GFP-fusion peptides. The temperature gradient used ranged between 50 °C and 60 °C, but once again this did not improve amplification of the GFP fusion peptide (data not shown). The Phusion Taq DNA polymerase information sheet recommends using dimethyl sulphoxide (DMSO), which encourages DNA denaturing and can inhibit non-specific primer binding. Therefore the temperature gradient experiment was repeated this time including 3 % DMSO in the PCR reaction mixtures. In this case all four GFP-peptide fusion sequences were amplified consistently over a

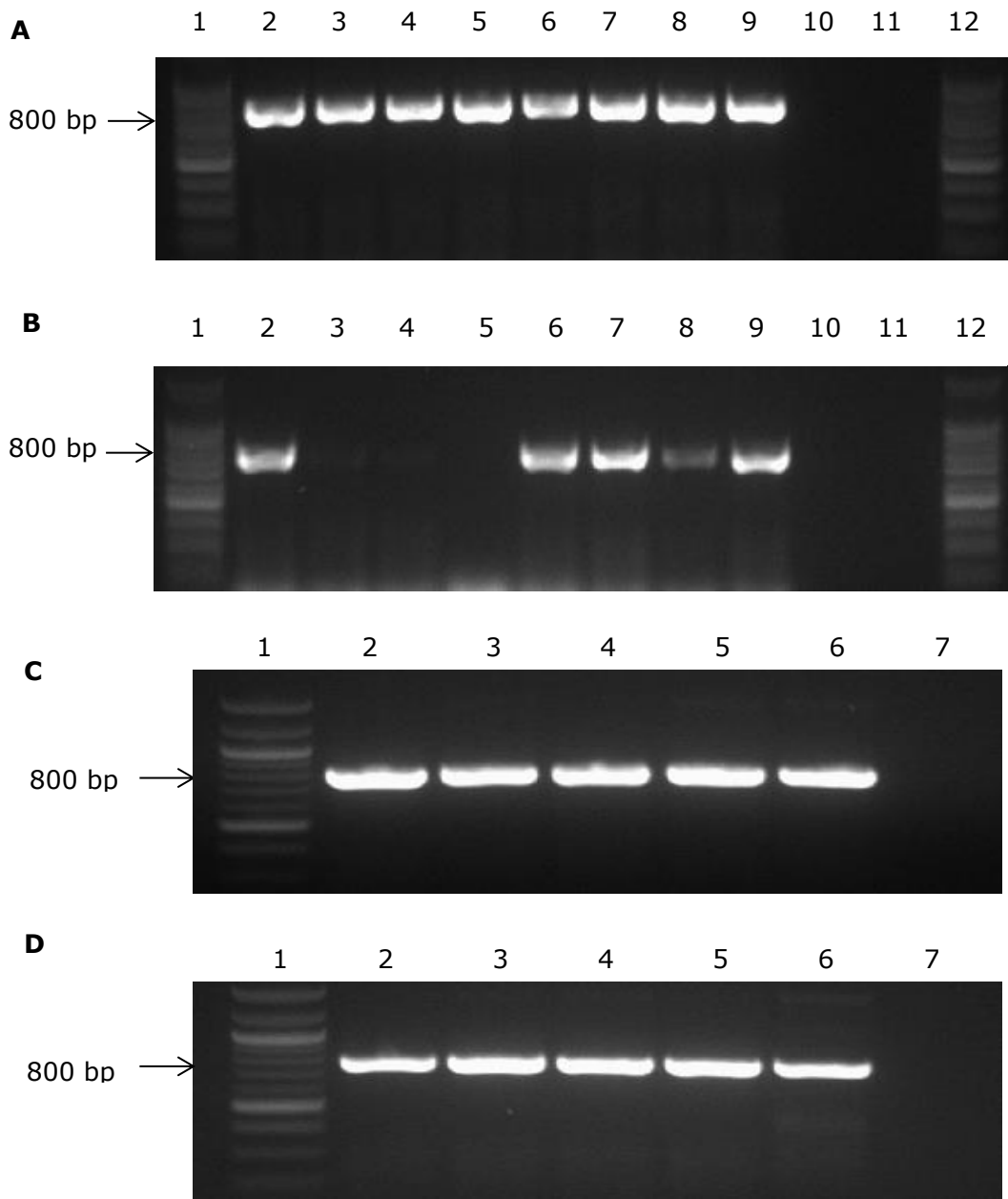
range of different annealing temperatures (56.3 °C to 60 °C; Fig 7.3). Once the correct Gfp-peptide fusion sequences had been successfully amplified, the next step was to clone them into *E. coli*.

Figure 7.2. Comparison of PCR of GFP amplification using a proof-reading and non-proof reading DNA polymerase



Results of amplification of the GFP gene from plasmid pDONOR-P4-P1R (800 bp) using different polymerases and conditions. Image shows the comparison of results gained when using NEB Phusion Taq DNA polymerase and Qiagen HotStart Taq DNA polymerase. Lane 1 and 12; 100 bp Ladder (Section 2.4.3). Lane 2 is a positive control using non-fusion GFP primers (GFP Forward and Reverse; Table 7.2). Lanes 3 to 6 shows results of amplification of GFP using primers: N-aMptD & N-MP3 with reverse primer N-reverse and C-aMptD & C-MP3 with the forward primer C-Forward (Table 7.2) using a proof-reading polymerase. Lanes 7 to 10 show results of amplifying GFP using primers: N-aMptD & N-MP3 with reverse primer N-reverse and C-aMptD & C-MP3 with the forward primer C-Forward (Table 7.2) with Qiagen HotStart Taq DNA polymerase. Lane 10 is a negative control (SDW replaced the plasmid template DNA).

Figure 7.3. Effect of DMSO and annealing temperature on PCR amplification of the GFP-peptide fusion sequence



Results of gradient PCR for the amplification of the *gfp* gene from plasmid pDONOR-P4-P1R (800 bp) with addition of DMSO. Panel A; primer N-aMptD with reverse primer N-reverse, Panel B; primer C-aMptD with the forward primer C-Forward, Panel C; primer N-MP3 with reverse primer N-reverse and Panel D; primer C-MP3 with the forward primer C-Forward. Lanes 2 to 9 annealing temperatures were; 50, 50.7, 52.0, 53.9, 56.3, 58.3, 59.4 and 60 °C, respectively. Lane 10; negative control (SDW replaced the plasmid template DNA). In panels C and D: Lanes 2 to 6 annealing temperatures were; 60, 59.4, 58.3, 56.3, 53.9, respectively. Lane 7 is a negative control (SDW replaced the plasmid template DNA). Marker lanes contain 100 bp Ladder (Section 2.4.3). Poor Amplification of the *gfp* gene in lanes 3-5; panel B, are anomalous results.

7.2.3. Cloning and Analysis of GFP-fusion PCR products

The PCR products were excised from the gel and the DNA was purified and concentrated using a gel recovery spin column (Section 2.5.1.2). The concentration of the DNA was determined using the Nanodrop (Table 7.3). The site for the enzyme *NdeI* had been designed to allow directional cloning into the vector, and an attempt was then made to directionally ligate the insert into the plasmid, however no green colonies formed. Subsequent restriction digest analysis of the plasmid showed that there was an extra unexpected band on the gel (data not shown) indicating that the insert fragment may have been cut more than once. The whole GFP gene was analysed using the NEB-restriction mapping tool (<http://tools.neb.com/NEBcutter2/>) and an additional *NdeI* restriction site was found in the Gfp gene used as a DNA template (Figure 7.4).

However the primer design also included *SmaI* that created blunt ends which could be used. While using this site negated the need to redesign the primers, the orientation of the insert could not be controlled during the cloning, but correct cloning of the *gfp* gene would produce a detectable green fluorescence phenotype which simplified the screening of clones. To clone the PCR products from Section 7.2.2, the purified DNA and the plasmid pET23a (Appendix 7.2) was cut with the restriction enzyme *SmaI* (Section 2.5.1.2). These restriction fragments were then mixed to give a vector : insert ratio of 3:1 and ligated together (Section 2.5.1.3). The ligation mixture was analysed by agarose gel electrophoresis to show that the fragments had been ligated together successfully (data not shown) and were then transformed into chemically competent *E. coli* Top10 (Table 2.1) using the heat-shock method (Section 2.5.1.5). The transformed cells were plated onto ampicillin ($100 \mu\text{g ml}^{-1}$) selective LB-agar. Colonies were isolated and patched onto ampicillin selective agar and colony-PCR targeting the *gfp*-fusion DNA sequence were carried out to confirm that the selected colonies contained the correct gene structure. Colonies

that were positive for the *gfp*-fusion peptide DNA were taken forward for further study.

Table 7.3. Concentration of the purified GFP-fusion PCR amplicons

Primer Pair	DNA concentration (ng.µl ⁻¹)
N-aMptD & N-Reverse	470
N-MP3 & N-Reverse	675
C-aMptD & C-Forward	419
C-MP3 & C-Forward	403

The primer pairs used to generate these PCR amplicons are those presented in Table 7.2. The DNA concentration was measured using a Nanodrop.

Figure 7.4. Predicted restriction enzyme sites in GFP gene

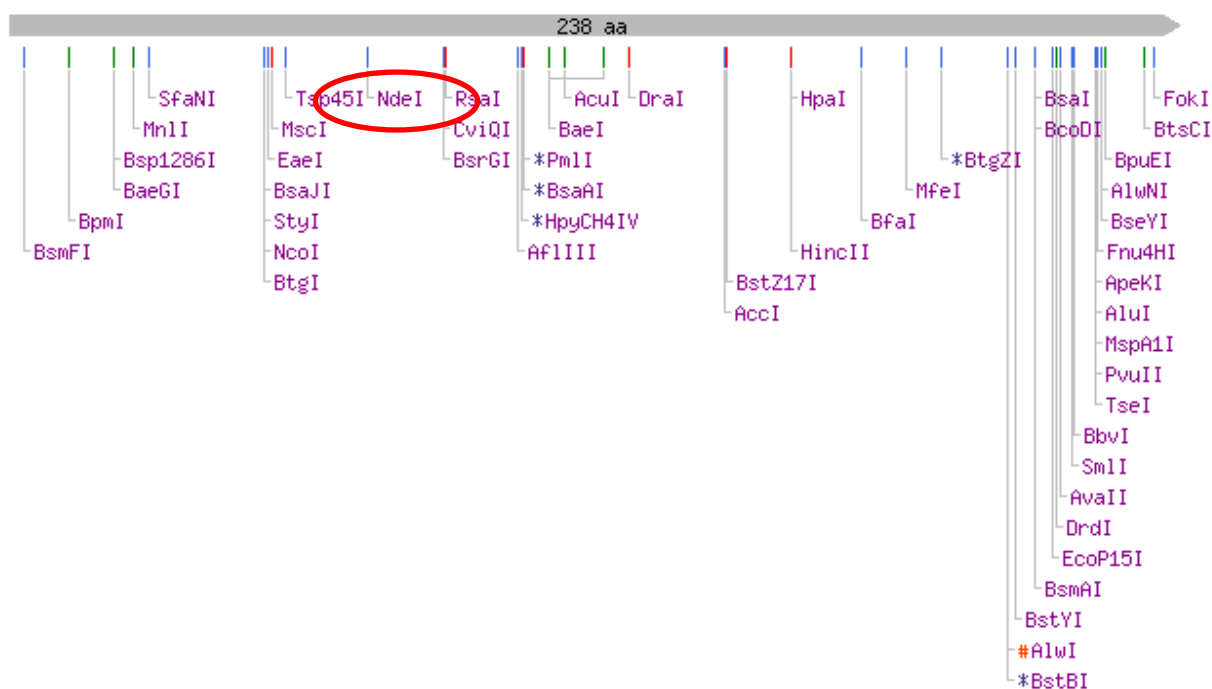


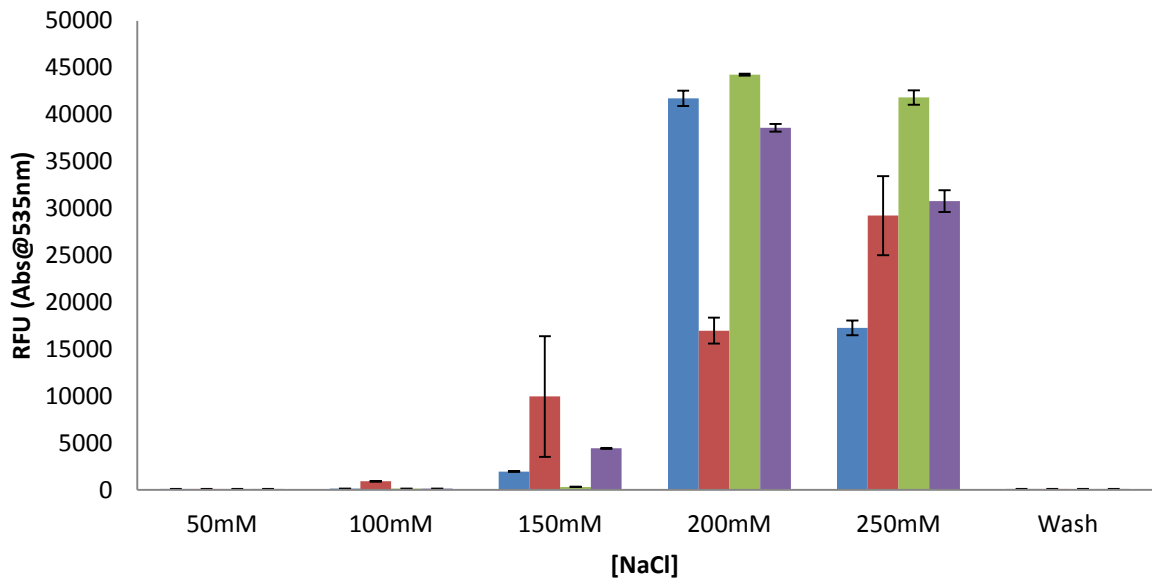
Diagram shows the restriction enzyme sites present in the GFP sequence (NEB online restriction-mapping tool, <http://tools.neb.com/NEBcutter2/>) in plasmid pDONOR-P4-P1R. The red ring shows restriction site *NdeI* which was introduced into the GFP-fusion peptide primers.

7.2.4. Transformation and expression of GFP-fusion peptides

Plasmid DNA was extracted from colonies with the correct phenotype and gene structure using a ZymoResearch mini-prep kit (Section 2.5.3). The concentration and purity of the extracted plasmid DNA was measured using the Nanodrop. The plasmids were then transformed into a chemically competent expression strain of *E. coli* (BL21 DE3; Table 2.1), which was selected due to its ability to express high quantities of recombinant proteins. After transformation, the cells were plated onto selective LB agar supplemented with ampicillin ($100 \mu\text{g ml}^{-1}$) and IPTG (0.5 mM) and incubated overnight at 30 °C. Using a blue light to excite the Gfp, colonies that fluoresced green were selected. These were inoculated into 10 ml of LB media containing ampicillin ($100 \mu\text{g ml}^{-1}$) to prepare the fusion protein. After growth to mid log phase ($\text{OD}_{600\text{nm}} = \sim 0.5$), IPTG was added (0.5 mM) to induce protein expression. The liquid cultures were then incubated for 4 h shaking at 37 °C when they were again visualised using a blue light to confirm that GFP was being expressed.

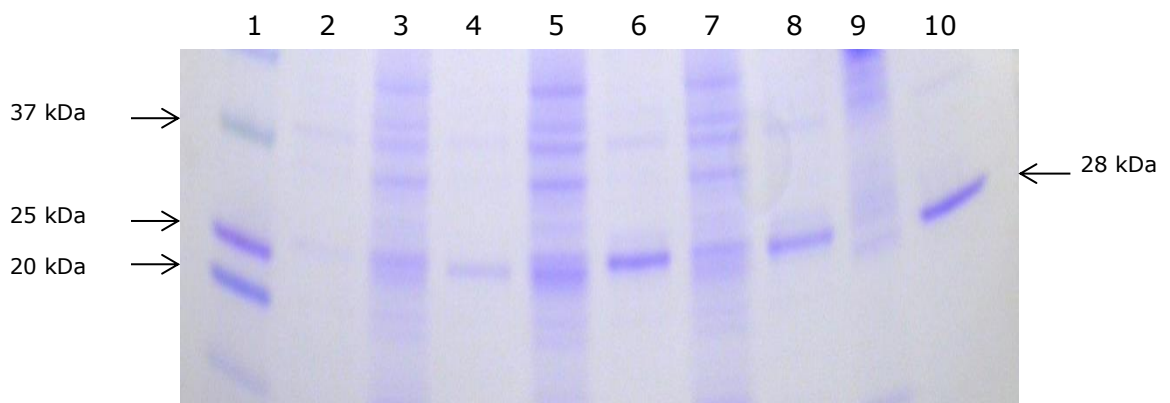
Cell lysis and ion exchange chromatography purification (Sections 2.5.1.6 & 2.5.1.7, respectively) were used to purify the GFP-fusion proteins. Samples from each fraction of the purification column were removed and fluorescence levels measured using a microtitre plate reader (Genios Pro, Tecan). The results showed that for all four constructs the fractions eluted from the columns with 200 and 250 mM NaCl yielded the highest fluorescent activity (Figure 7.5). These samples were also analysed by SDS-PAGE (Section 2.5.1.8) to determine the purity of the fraction containing the GFP-fusion peptide and the Bradford assay was used to determine the concentration of the purified protein (Section 2.5.1.9).

Figure 7.5. Fluorescence of purified GFP fusion-peptides



Relative fluorescent units (RFU) of fractions eluted using different NaCl concentrations containing the GFP-fusion peptides. Blue bars represent peptide N-aMptD. Red bars represent peptide N-MP3. Green bars represent peptide C-aMptD. Purple bars represent peptide C-MP3. Error bars represent the standard deviations of the mean (n=3).

Figure 7.6. SDS-Page analysis of GFP-fusion samples



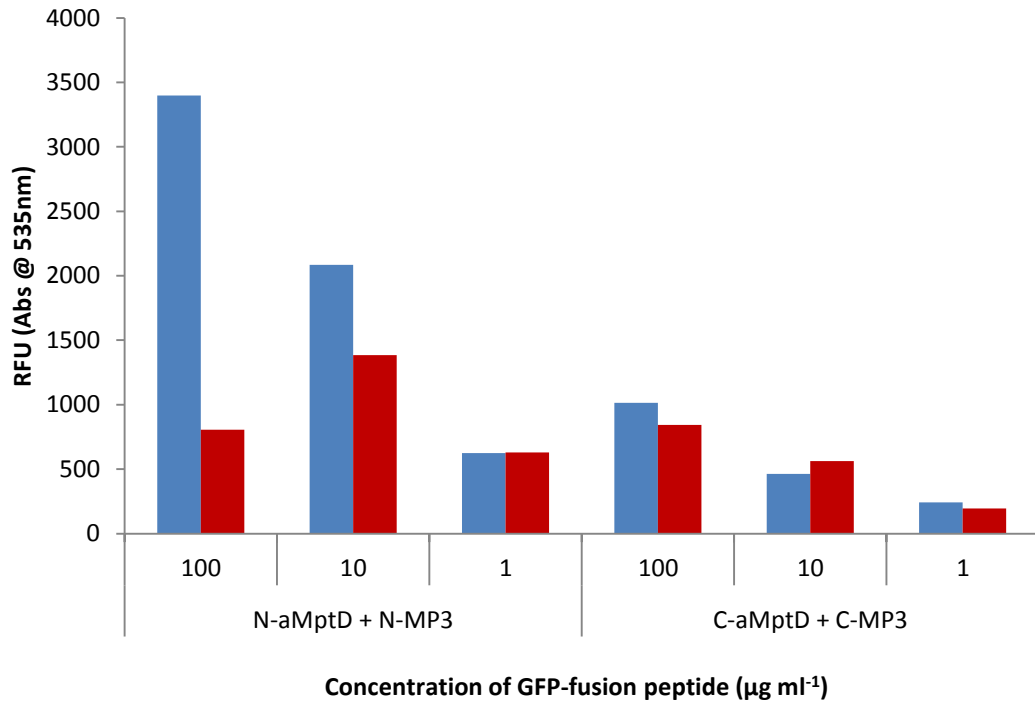
SDS-PAGE analysis of the GFP-fusion protein samples on a 4-20 % gradient acrylamide gel stained with Coomassie Blue. Lane 1 is the protein marker (Fig. 2.6). Lane 3, 5, 7 and 9 contain crude protein extracts of N-aMptD, N-MP3, C-aMptD and C-MP3, respectively. Lanes 2, 4, 6 and 8 are purified GFP-fusion fractions eluted using pooled 200 and 250 mM NaCl. Lane 10 is the positive control containing purified native Gfp protein (28 kDa).

The concentration of each fusion peptide was found to be; 0.17, 0.23, 0.18 and 0.24 mg ml⁻¹ for; N-aMptD, N-MP3, C-aMptD and C-MP3, respectively, and Figure 7.6 shows that all the different the GFP-fusion proteins were successful purified.

7.2.5. Evaluating the ability of the GFP-fusion peptides to bind to MAP cells

To determine whether the purified proteins retained the property of the peptides to bind to MAP cells, a cell binding protocol was developed (Section 2.7.1). Since the peptides were used in pairs to achieve efficient binding of MAP cells when used for PMMS, they were evaluated as mixtures (i.e. mixtures of the two N-terminal peptide fusions or the two C-terminal peptide fusions were prepared before their ability to bind to MAP cells was evaluated). Briefly MAP and *M. smegmatis* cultures were enumerated using the phage amplification protocol (Section 2.1.3.3) and the concentration of cells in the cultures adjusted to 1 x 10⁴ pfu ml⁻¹. To determine which orientation (GFP at the N- or C- terminal end) had better binding capacity and the optimal concentration of the GFP-fusion peptides, the cells were then centrifuged and resuspended PBS (Section 2.7.1) before mixing with the GFP-peptides mixtures (N-aMptD + N-MP3 or C-aMptD + C-MP3) at concentrations of 100, 10 and 1 µg ml⁻¹. The results showed that the highest concentration (100 µg ml⁻¹) of both N-terminal peptide fusions (N-aMptD & N-MP3), when mixed with the different cell types had a significantly (P<0.05) better ability to bind to MAP compared to the C-terminal peptide fusions (C-aMptD & C-MP3), which exhibited little binding capability at all concentrations tested (Fig. 7.7). Even in this first experiment, comparison of the results for the N-terminal fusions binding to the same number of MAP or *M. smegmatis* cells, a relatively low signal to noise ratio was seen indicating that the binding to the MAP cells had some specificity.

Figure 7.7. Binding of mixed GFP-fusion peptides to Mycobacteria



Graph showing relative fluorescent units (RFU) of the GFP-fusion peptides (N-aMptD + N-MP3 or C-aMptD + C-MP3) diluted to different concentrations to bind to MAP (Blue) and *M. smegmatis* (Red).

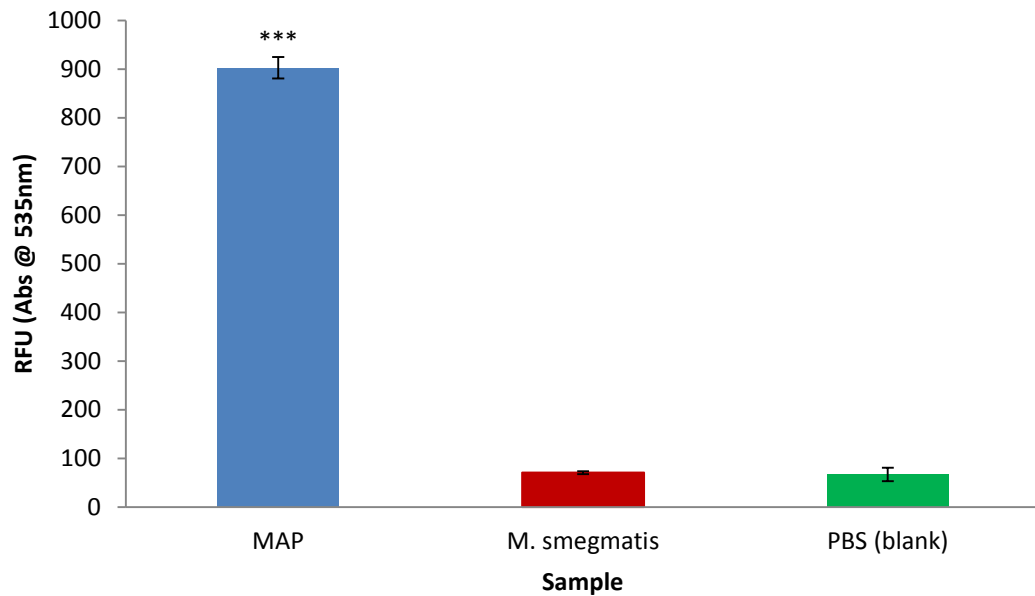
7.2.6. Optimising GFP-fusion peptide binding assay

To try and improve the signal to noise ratio, the mixture of N-terminal peptide fusions (N-aMptD & N-MP3; 100 µg ml⁻¹) was tested again, but this time Tween-20 was included in the wash buffer to try and reduce non-specific binding (Section 2.7.1). An additional negative control sample containing no cells (PBS only) was also included in this experiment as well as the *M. smegmatis* negative control sample. The Gfp fluorescence was again determined and the results show that the GFP fluorescence remaining associated with the MAP cells was now significantly greater ($P < 0.001$) than the level of fluorescence detected associated with either of the negative controls. In addition there was no difference between the level of fluorescence detected in the *M. smegmatis* and the PBS negative control samples suggesting that the non-specific binding of the fusion proteins to *M. smegmatis* seen in the last experiment that resulted in the background level of fluorescence was completely suppressed (Fig. 7.8).

7.2.7. Using GFP-fusion peptides to visualise MAP cells

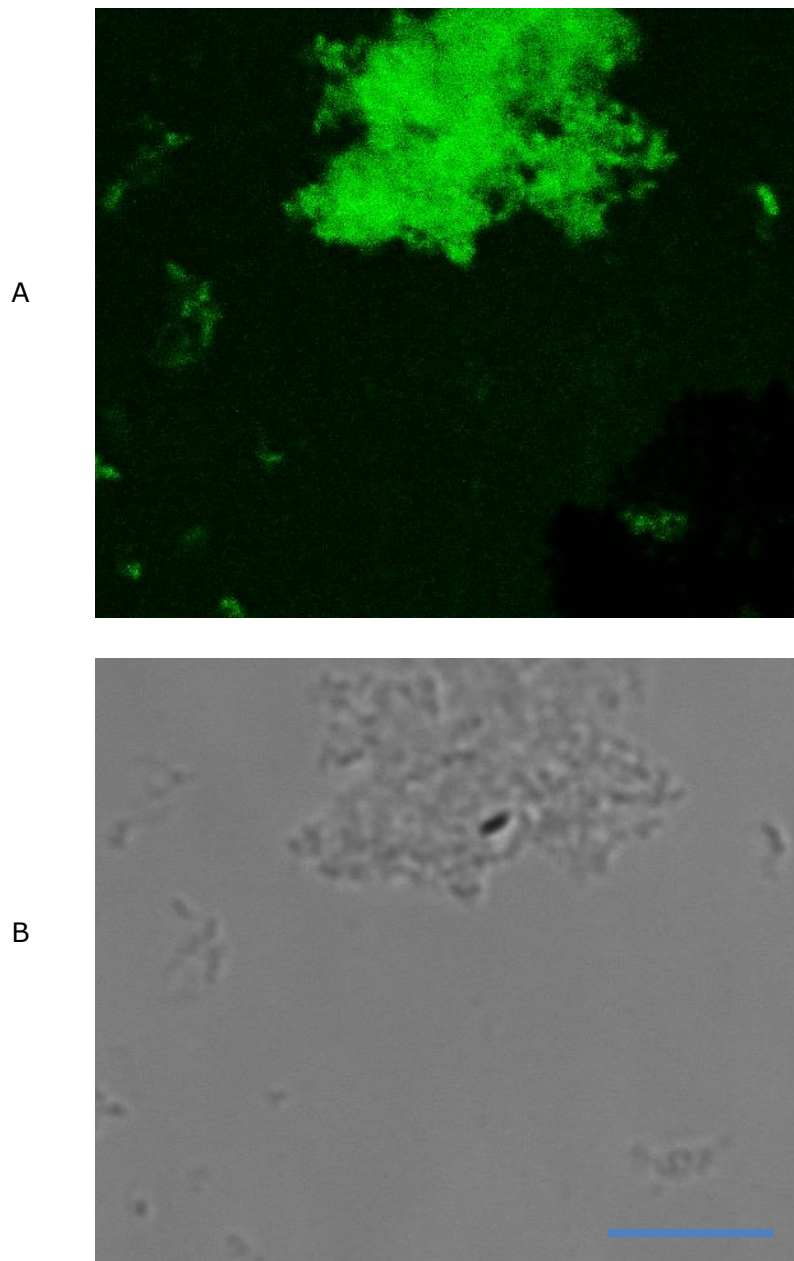
Using the same protocol as described above (Section 7.2.6), MAP cells were labelled with the mixture of N-terminal GFP-fusion peptides and images of the labelled MAP cells were obtained using a Confocal microscope (Leica, SP5). The fluorescence images were compared to brightfield images of the same cells to ensure the GFP-fusion proteins were bound to cells and not to artefacts in the sample or non-specific binding. The results show that the GFP-fusion peptides bound well to the MAP cells, when compared to the brightfield images (Fig. 7.9). However there was an issue with results as there was a lot of background fluorescence from panel A of Figure 7.9, which may have been due to non-specific binding of the fluorescent peptides, or the washing steps were not thorough enough.

Figure 7.8. Specificity of GFP-fusion peptide binding



Graph showing relative fluorescent units (RFU) of the GFP-fusion peptides (N-aMptD + N-MP3) after binding to samples containing MAP (Blue), *M. smegmatis* (Red) or no cells (PBS; Green). Error bars represent the standard deviations of the means (n = 3). A t-Test assuming equal variances was carried out to analyse significance (***) $p < 0.001$) in the difference between RFU levels from the samples containing MAP and *M. smegmatis*.

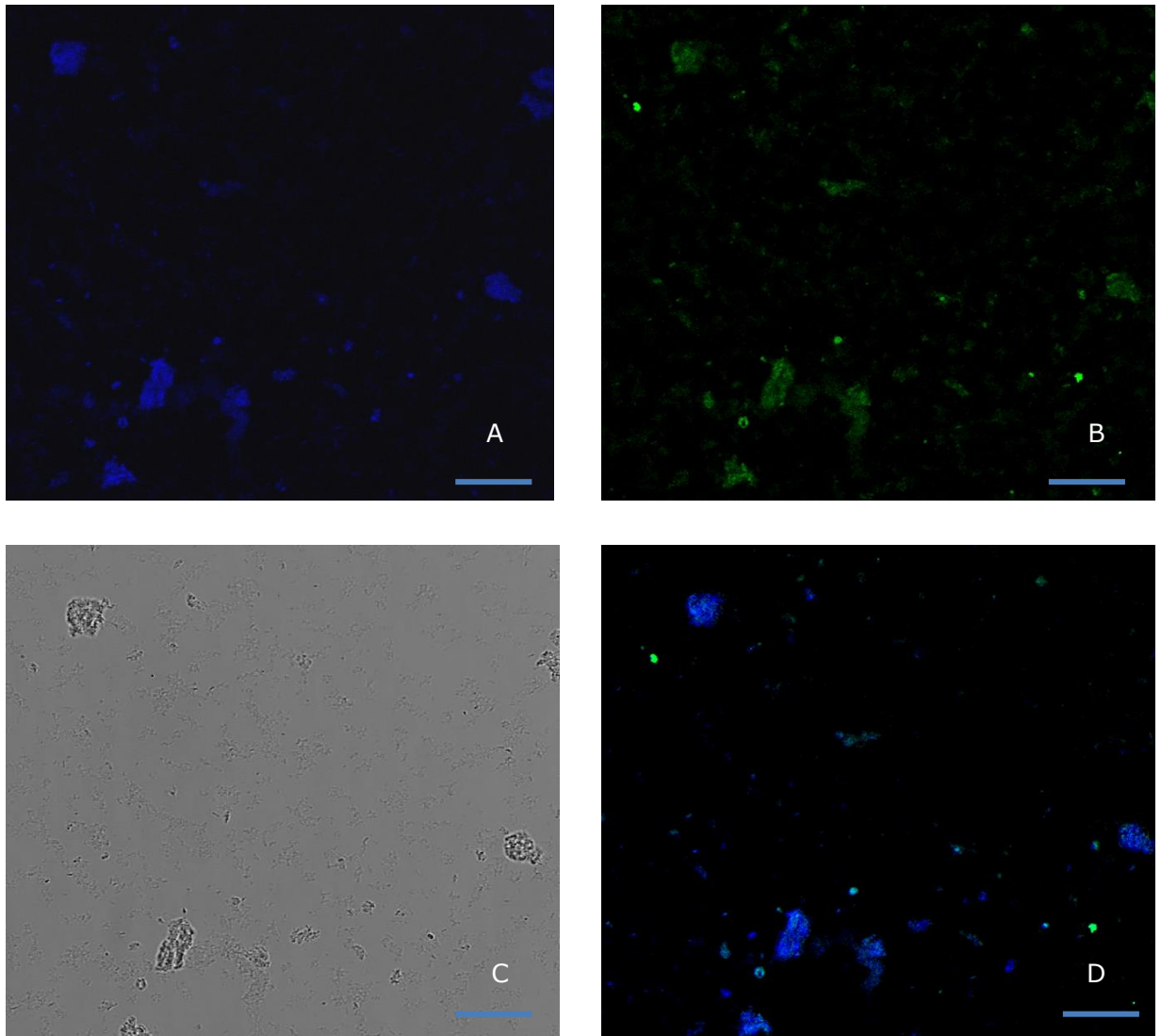
Figure 7.9. Comparison of fluorescent confocal and brightfield images of MAP cells labelled with N-terminal Gfp peptide fusions



Images of MAP cells labelled with the N-terminal GFP-peptides fusions taken using the confocal microscope (x700). Images show (A) fluorescence and (B) the same field using brightfield microscopy (B). The scale bar in each panel represents 10 μm .

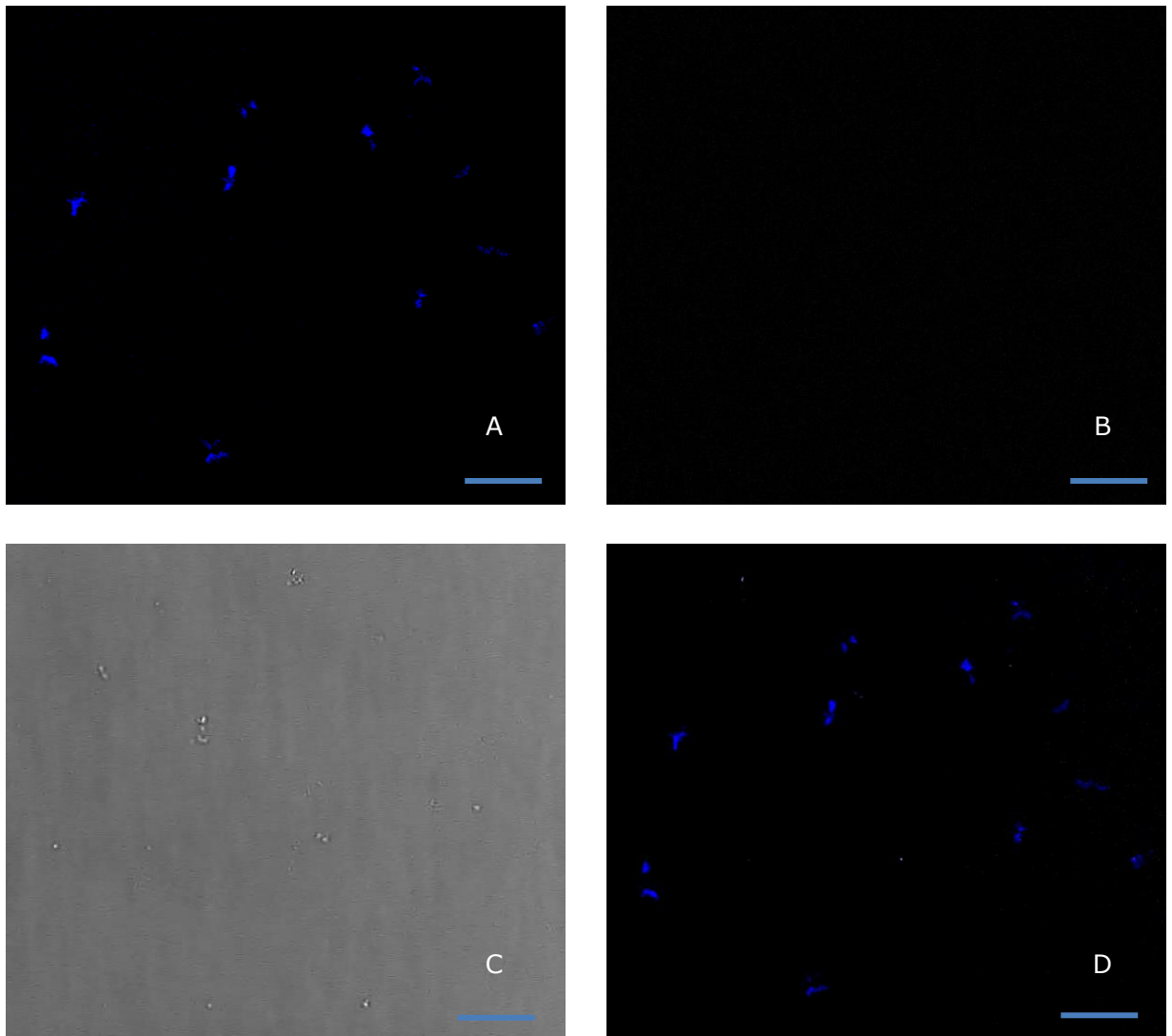
Next the N-terminal Gfp peptide fusions were tested to determine whether they could differentiate between *M. smegmatis* and MAP present within one sample. The cells were prepared and the labelling with the GFP-fusion peptides N-aMptD + N-MP3 was carried out as described before (Section 2.7.1) but this time a sample of *M. smegmatis* was mixed with MAP cells at a ratio of 1 : 1 . To confirm that the brightly fluorescing objects in the images were cells, DAPI staining (Section 2.7.1) was used to identify the DNA within the cells and to allow unlabelled *M. smegmatis* cells to be located when imaged using fluorescence microscopy. The results show that the MAP cells were specifically labelled with the Gfp-fusion proteins whereas the *M. smegmatis* cells were not (Fig. 7.10 & 7.11). This was reinforced by the DAPI stained image which clearly showed the location of the MAP and *M. smegmatis* cells (Fig. 7.10 & 7.11).

Figure 7.10. Comparison of fluorescent confocal and brightfield images of MAP cells labelled with N-terminal Gfp peptide fusions and DAPI



Images of the MAP sample taken using the Confocal microscope ($\times 700$). Panel A shows DAPI stained image (chromosomal DNA detected) of the MAP cells showing that cells are present in the field of view. Panel B shows Gfp fluorescence from cells labelled with Gfp-peptide fusions. Panel C shows the bright field of the image showing some small clumps of cells and individual cells on the surface. Panel D is the over lay image of Panels A, B and C. The scale bar in each panel represents 10 μm .

Figure 7.11. Comparison of fluorescent Confocal and Brightfield images of *M. smegmatis* cells labelled with N-terminal Gfp peptide fusions and DAPI

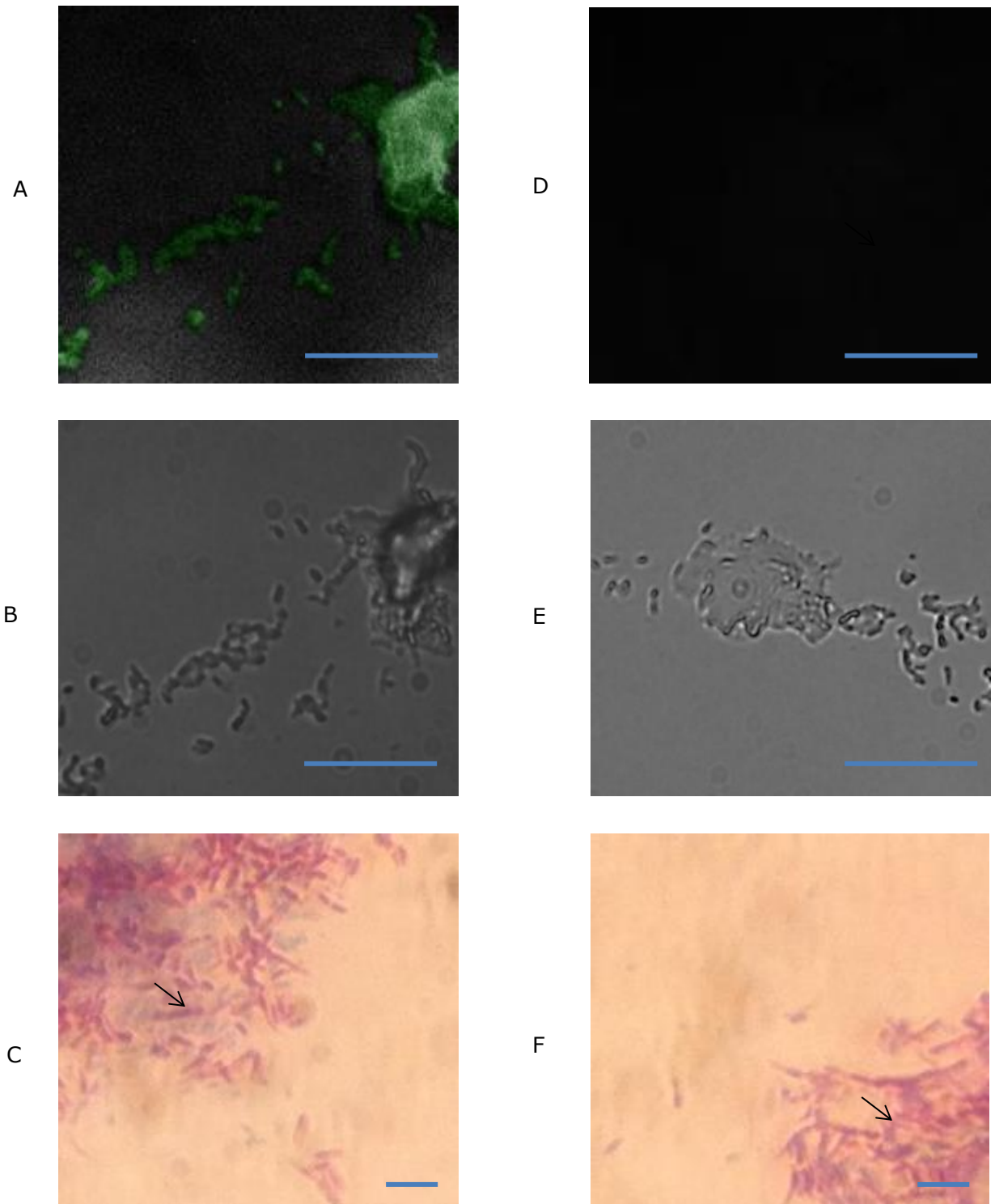


Images of the *M. smegmatis* sample taken using the confocal microscope (x700). Panel A shows DAPI stained image (chromosomal DNA detected) showing that cells are present in the field of view. Panel B shows no Gfp fluorescence detection, where no cells are Gfp-labelled with Gfp-peptide fusions. Panel C shows the bright field of the image showing (some small clumps of cells and individual cells on the surface visible) and panel D is the over lay image of Panels A, B and C. The scale bar in each panel represents 10 μm .

7.2.8. Ziehl-Neelsen staining on fixed MAP samples

When the Ziehl-Neelsen (ZN) stain is routinely using to detect and visualise acid-fast organism under the microscope, specifically on histology samples, they are usually first fixed with glutaraldehyde. To determine the effect of this treatment on Gfp-fusion binding, samples of MAP and *M. smegmatis* were prepared by fixing the samples on glass microscope slides with glutaraldehyde and these samples were then labelled with the mixture of N-terminal GFP-peptide fusions (Section 7.2.6). Samples were then visualised by fluorescent microscopy to determine whether any mycobacteria could be detected. The results show that the MAP cells were detected routinely and, once again, *M. smegmatis* was not detectable under the fluorescent microscope even though cells were clearly visible in the same field using bright field microscopy (Fig. 7.12; panels A-D). The same slides treated with the GFP-fusion peptide were treated with the ZN stain (Section 2.8). In this case both types of mycobacteria were visible after the ZN stain (Fig. 12; panels C and F), showing that the GFP-fusion peptides were equally able to detect the fixed MAP cells but provided a degree of specificity compared to that provided by the routinely used ZN stain.

Figure 7.12. Comparison of fluorescent, Brightfield and ZN stained images of *M. smegmatis* and MAP cells



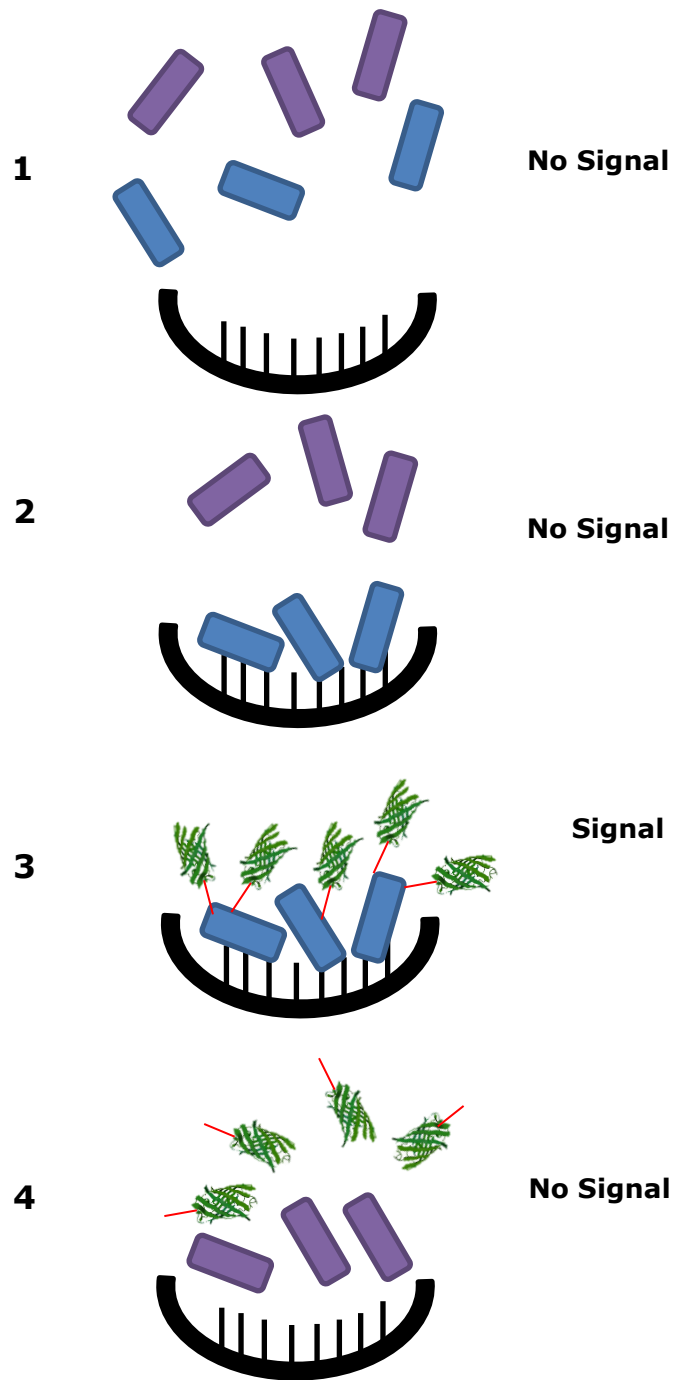
Images of MAP cells (A-C) and *M. smegmatis* cells (D-E) stained by red after ZN (Arrows; C and F) after labelling with GFP-Fusion peptide (B and E) and corresponding brightfield images (B and E). The scale bar in panels C and F represents 2 μm . The scale bar in panels A, B, D and E represents 10 μm . False-colour fluorescent images were manipulated using GIMP2.

7.2.9. Development of fluorescent cell capture MAP detection assay

The peptides described by Stratmann et al. (2002 and 2006) were shown to bind strongly to MAP (association constant of 1×10^9). It was now proposed to use the peptides used for PMMS to capture cells from liquid samples, and then to detect them using the Gfp-fusion proteins (Fig. 7.13). Both the orientations of peptides were used in this study to investigate whether the N- terminal fusions superior binding capacity was consistent when binding to MAP cells fixed to a surface.

To do this the peptides were biotinylated and bound to the surface of an avidin-coated 96-well microtitre plate (Section 2.7.2). Three 10-fold dilutions of MAP and *M. smegmatis* cells estimated to contain 1×10^4 to 1×10^2 pfu ml⁻¹ using the phage enumeration assay (Section 2.1.3.3) were then added into the wells of the prepared microtitre plate (Section 2.7.2.1). Samples were washed twice with PBS-Tween. A sample (100 µg ml⁻¹) of both the N- terminal GFP-peptide fusion mixtures (N-aMptD + N-MP3; Fig. 7.1) and the C- terminal GFP-peptide fusion mixtures (C-aMptD + C-MP3; Fig 7.1) were then added to the wells and incubated for 1 h at 37 °C. As controls MAP and *M. smegmatis* cells were bound to the surface of the peptide coated 96-well plate, and no GFP-fusion proteins added to determine whether the MAP cells contribute to the fluorescent signal (Fig. 7.13). The fluorescence level of each sample was then determined using a fluorimeter (Genios Pro, Tecan).

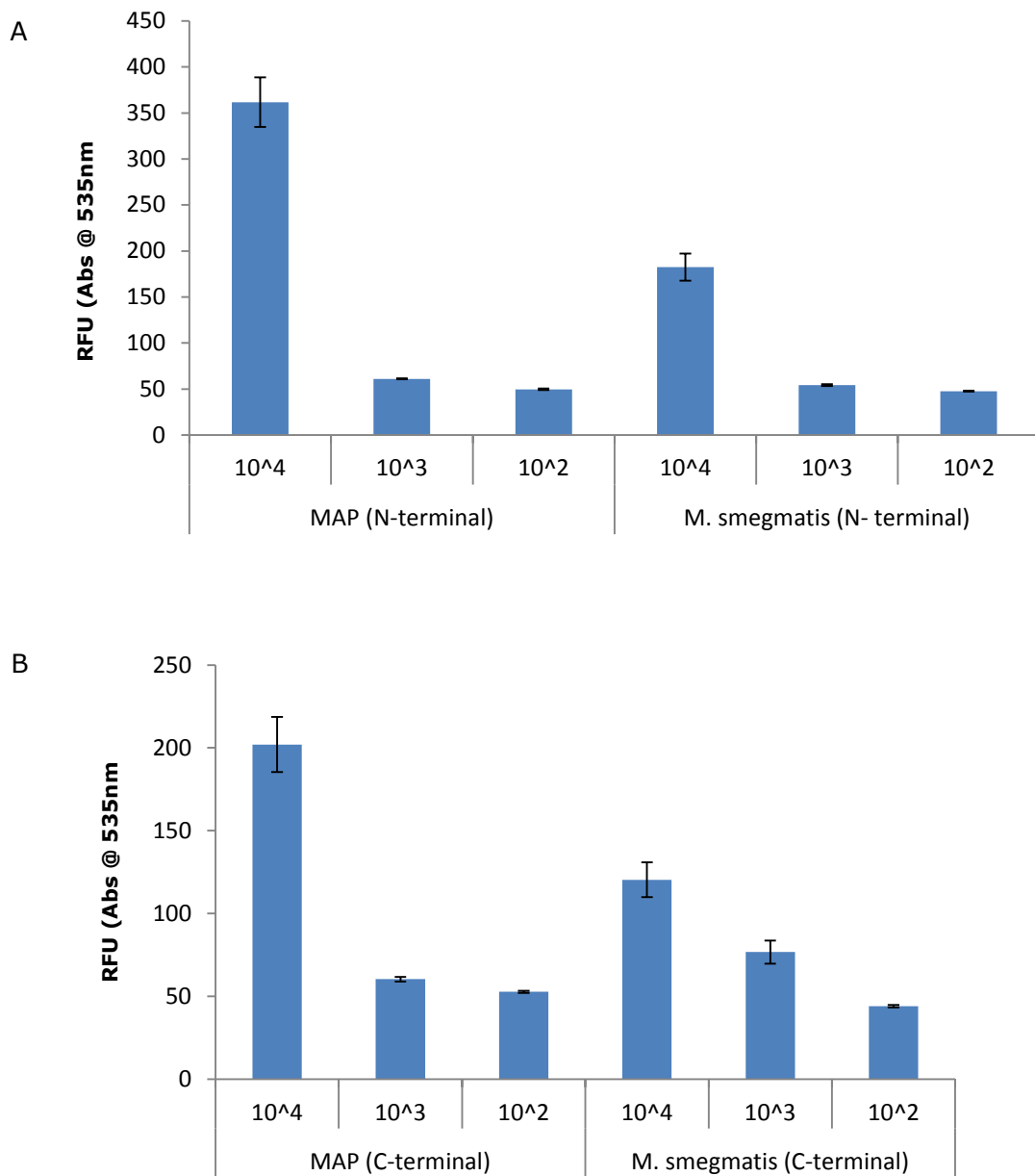
Figure 7.13. Schematic of the ELISA-like cell capture assay



Schematic shows the design of the cell capture assay: (1) a MAP-specific biotinylated peptide-coated well, being washed with MAP (blue) and *M. smegmatis* (purple). (2) MAP cells adhering to the MAP specific peptides, whilst *M. smegmatis* gets washed away. (3) GFP-fusion proteins binding to the bound MAP cells (positive signal). (4) *M. smegmatis* does not bind to the MAP specific peptides and GFP-fusion proteins do not bind (no signal).

The results (Fig. 7.14 A) show that there was significantly higher ($P < 0.05$) fluorescence signal from the highest concentration of MAP cells tested (1×10^4 pfu ml⁻¹) compared to the equivalent sample of *M. smegmatis* cells when the N-terminal fusion peptides were tested. However there was also significant ($P < 0.05$) signal from the sample tested which contained 1×10^4 pfu ml⁻¹ *M. smegmatis* cells when compared to the signal from the sample containing lower numbers of MAP cells (Figure 7.14 A). When the C-terminal GFP-fusion proteins were used, there was no significant difference ($P > 0.05$) between the signal from the highest concentrations of MAP and *M. smegmatis* (Figure 7.14 B). The results also showed that again the N-terminal GFP-fusion proteins were far superior at labelling captured MAP cells compared to the C-terminal proteins. However as there was still a lot of signal from *M. smegmatis* cells, further optimisations would be required to reduce the non-specific binding detected when using this assay format.

Figure 7.14. Microtitre plate cell capture and fluorescent identification with GFP-fusion peptides

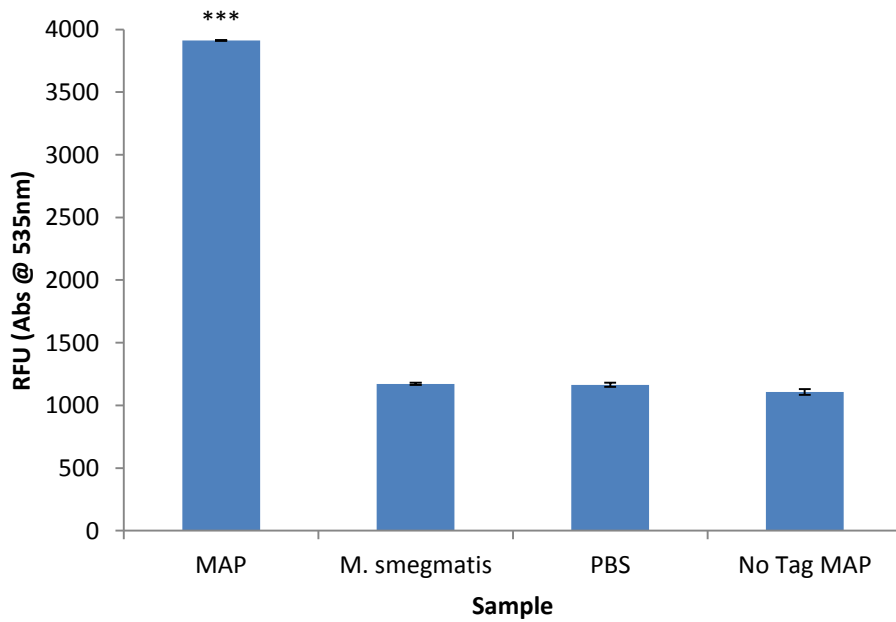


Graphs showing relative fluorescent units (RFU) produced by the GFP-fusion peptides mixtures N-aMptD + N-MP3 (Panel A) and C-aMptD + C-MP3 (Panel B) to binding to 10⁴, 10³ and 10² pfu ml⁻¹ of MAP and *M. smegmatis* captured on the surface of a microtitre dish. Error bars represent the standard deviations of the means (n=3). A t-Test assuming equal variances was carried out to analyse significance (p<0.05) in RFU from the MAP sample compared to *M. smegmatis*.

7.2.9.1. Optimising the cell capture assay

To improve the specificity of the binding of the Gfp-peptide fusion, a higher concentration of BSA (4 % instead of 2 %) was used in the blocking step (Section 2.7.2) of the cell capture assay to help block non-specific binding sites. In addition a small amount of the detergent (Tween-20; 0.05 %) was included in the wash buffer, to help expose the peptide binding sites, to improve the amount of the fusion-peptide actually getting to their target binding site and to inhibit non-specific binding. Once again control samples were prepared containing either *M. smegmatis* or no cells (PBS only). In addition, samples in which MAP cells that were not then labelled with the GFP-fusion peptides were included to determine the background fluorescence levels contributed by the cells themselves. The results (Figure 7.15) shows that there was significantly ($P < 0.001$) more signal from the sample containing the labelled MAP cells compared to the sample containing the captured *M. smegmatis* cells. There was also no difference in the signal from the *M. smegmatis* sample and that containing only PBS and the sample in which the captured MAP cells were not labelled with the fluorescent protein, suggesting that no non-specific binding was occurring. However the signal from the positive MAP control was still not very high, suggesting that either the GFP-fusion peptide was not able to find the right binding sites, or that they were falling off during the washing steps.

Figure 7.15. Effect of BSA concentration on blocking non-specific GFP-fusion peptide binding to MAP and *M. smegmatis*



Graph showing relative fluorescent units (RFU) following binding of the GFP-fusion peptides (N-aMptD + N-MP3) to MAP and *M. smegmatis* after blocking with BSA (4%). As controls samples containing only PBS and MAP cells that were not labelled with GFP-fusion peptides were used. Error bars represent the standard deviations of the means of RFU performed in triplicate. A One-way ANOVA, followed by the Dunnett's test was used to analyse significance (* $P < 0.001$) in the RFU's between each sample.

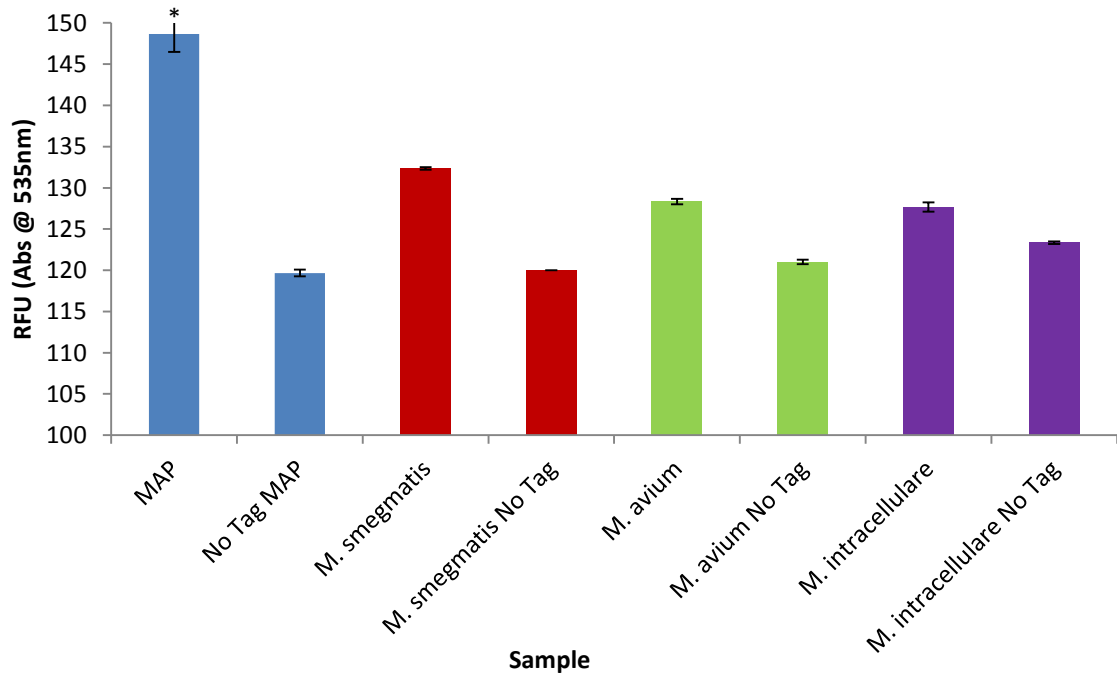
To determine the specificity of the assay, the assay was performed using samples of other mycobacteria that are more closely related to MAP than *M. smegmatis* is. To do this the experiment described in Section 2.7.2 was repeated, using cultures of *M. avium* and *M. intracellulare* in addition to *M. smegmatis*. The results show that although there was a significantly higher signal ($P < 0.05$) from MAP compared to the other mycobacteria (Figure 7.16), the signal to noise ratio was much lower compared to the signal to noise ratio from the results shown in Figure 7.17. This suggests that again the GFP-fusion peptides are not binding sufficiently tightly to MAP.

When developing a fluorescent cell capture assay, the signal to noise ratio needs to be as high as possible. The maximum signal to noise ratio currently achieved was 4:1, hence experiments were designed to try and increase the efficiency of the binding of the peptides to the MAP cells. One factor that can affect peptide binding interactions is temperature. An increase or decrease in temperature can affect the association and dissociation rates of binding which may affect the strength, persistence or specificity of the signal compared to the background noise of the cell capture assay. Thus the temperature that the GFP-fusion peptides were allowed to bind to the MAP cells was changed to 4 °C, 20 °C (room temperature), 25 °C, 30 °C and 37 °C. The results show that the lower temperatures resulted in a lower signal. Only at 30 °C did the signal increase, but at 37 °C the signal was highest.

Another factor that can affect the binding of proteins to their targets is ionic concentration (Pasupuleti et al., 2009). Hence to try and improve the signal to noise ratio from the capture experiments, the concentration of NaCl in the binding buffer was altered from 0 to 0.1, 0.2 or 0.4 M. The cell binding assay was then carried out (Section 2.7.2) using MAP cells. The results (Figure 7.18) show that the increasing concentration of NaCl had an adverse effect on the GFP-fusion peptide binding in that the highest level of fluorescence detected was when no extra NaCl was added and any increase in the salt concentration in the

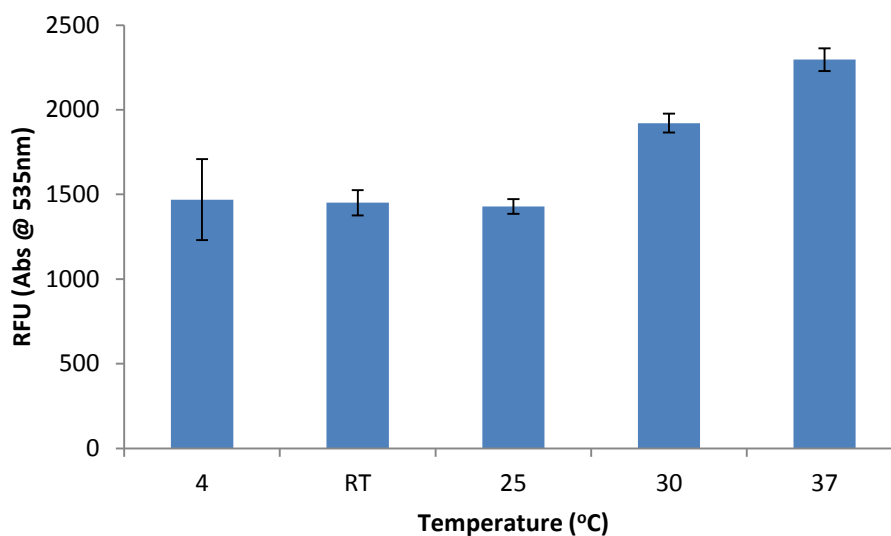
binding and wash buffers reduced the signal detected from samples containing the same number of captured cells.

Figure 7.16. Specificity of GFP-fusion peptide binding to MAP and other closely related mycobacteria



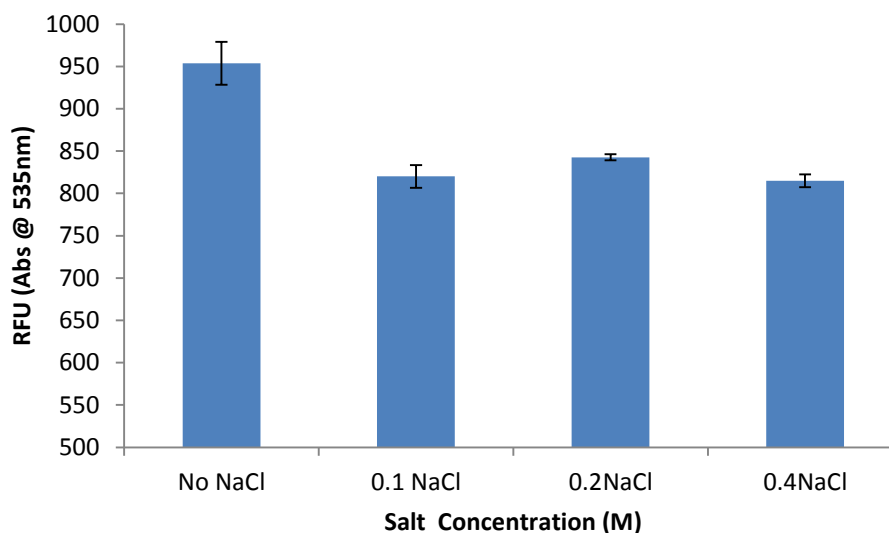
Graph showing relative fluorescent units (RFU) following binding of the GFP-fusion peptides (N-aMptD + N-MP3) to MAP, *M. smegmatis*, *M. avium* and *M. intracellulare* cells. As controls samples containing only PBS and MAP cells that were not labelled with GFP-fusion peptides were used. Error bars represent the standard deviations of the means of RFU performed in triplicate. A One-way ANOVA, followed by the Dunnett's test was used to analyse significance (* $P < 0.05$) in the RFU's between each sample.

Figure 7.17. Effect of temperature on GFP-fusion binding to MAP cells



Graph showing relative fluorescent units (RFU) following binding of the GFP-fusion peptides (N-aMptD + N-MP3) to MAP at different temperatures (4, 20, 25, 30 and 37 -C). Error bars represent the standard deviations of the means of RFU performed in triplicate.

Figure 7.18. Effect of increasing NaCl concentrations on GFP-fusion binding



Graph showing relative fluorescent units (RFU) of the effect different NaCl concentrations (0, 0.1, 0.2 and 0.4 M) on the binding of GFP-fusion peptides to MAP. Error bars represent the standard deviations of the means of RFU performed in triplicate.

7.3. DISCUSSION

7.3.1. GFP-fusion tag expression and purification

Acid-fast stains are used when detecting and diagnosing mycobacteria, in tissue or sputum samples under the microscope. However this method of identification only allows, at best, a genus level of identification. The ability to fuse a fluorescent protein onto to a peptide specific for certain species, would allow differentiation of the different species. The use of fluorescent peptides as labels to specifically target bacteria has been demonstrated many times. In particular fusion proteins have been used to differentiate many species of *Listeria* using fluorescent proteins fused to cell-wall binding domains (CBD) isolated from lysins encoded by listeriphage (Kretzer et al., 2007, Schmelcher et al., 2010). The two MAP-specific peptides described by Stratmann et al. (2002, 2006), had been shown to have a good binding capacity for MAP cells allowing them to be separated from an inhibiting environment by PMMS, and transferred to an environment more suited for downstream processing. Hence these were good candidates to try and created Gfp fusions with specific binding properties.

The results from the studies using microscopy to detect individual cells showed that the GFP-fusion peptides were able to consistently differentiate between MAP and *M. smegmatis* once the blocking steps were optimised.

7.3.2. Cell capture assay development

When visualising the cells looking at the fluorescent image, like the brightfield images, the GFP-fusion peptides did not differentiate between individual cells and clumps of cells (Figure 7.9). This would be a problem when trying to enumerate cells, or to determine how many cells may be present in the clump. The ability to use the microtitre plate enables a relative unit to be given to the number of MAP cells present, which could give an indication of the number of cells present, if a standard-curve was constructed each time the experiment was

carried out. However when observing histological samples, disease status can be categorised on whether there are multibacillary or paucibacillary lesions or a positive or negative observation in the certain tissue samples (Gonzalez et al., 2005).

There are many different strategies that can be used to prevent non-specific binding. Bovine serum albumin (BSA) can be used at varying concentrations to block non-specific binding sites, whereas non-ionic detergents such as Tween, can expose specific binding sites to encourage correct binding. However sometimes when BSA and Tween are used together, they can work against each other resulting in non-specific binding, as Tween can remove the BSA from binding to the cells, so BSA was used at a relatively high concentration (4%) to prevent this (Steinitz, 2000). This resulted in a significant signal to noise ratio when MAP was compared to *M. smegmatis* and PBS (Figure 7.8).

Other ways to increase cell binding were investigated. Peptide and antibody binding can be influenced by the salt concentration (NaCl) of buffers used (Pasupuleti et al., 2009). The results show that a significant signal to noise ratio can be achieved using the cell capture assay format. However optimisations would be needed to produce a more robust system of detection.

7.3.3. Conclusion

As an attempt to make a label that is more specific than the classic ZN stain, the GFP-fusion peptides have shown to be a good alternative for cells from pure cultures, fixed onto microscope slides. The next important step in evaluating the use of this reagent would be to test it on real histology samples, and to determine whether it is possible to specifically identify mycobacteria as MAP cells in these samples. An important part of histology is the ability to maintain tissue samples for a long period of time, and to return to them if needed. So the length of time a sample remains stained for is an important factor. Fluorescent proteins can become bleached and unusable if exposed to too much light (Chalfie et al.,

1994). However if stored correctly, GFP has been known to last for long time, with ability to fluoresce still (Tsien, 1998), therefore it may be possible to store tissue samples for a long time. Other barriers to using the GFP-fusion peptides are that they may not be able to bind effectively onto fixed samples used for histology, as some fixing agents such as the 'aldehydes' cross link proteins to fix them reducing the sensitivity. Other potential problems with the fluorescent peptides binding are that the different components of the tissue being stained may results in non-specific binding, so rigorous optimisation of blocking steps would need to be carried out.

The great potential benefits of the fluorescent probes would be other peptides specific to different mycobacteria could be found and labelled in the same way. Simple phage display and biopanning resulted in the discovery of the MAP specific peptides, and already researchers have found novel peptides that can bind to *M. bovis* (Stewart et al., 2012). Although the efficacy of the peptides alone at capture *M. bovis* cells was poor. However there is definite potential to create different coloured probes that bind to different mycobacteria to rapidly differentiate between them using this method of making a fluorescent fusion peptide.

The attempt to develop a fluorescent cell capture assay was less successful. The signal to noise ratio was quite poor, and the specificity was not as strong compared to labelling the cells *in situ* on a microscope slide. However there was still a significantly stronger signal from MAP, compared to the other mycobacteria used as test samples. Fluorescent detection methods are susceptible to several parameters that can affect the signal output. Detection of fluorescence is susceptible to changes in pH, temperature, ion concentration, detergent concentration, drying, and the solid matrix (Gibbs et al. 2001) although GFP is a very stable, other proteins are not (Tsien, 1998). Further optimisations of these parameters may affect the binding of peptides, which may increase the signal from the MAP cells.

CHAPTER 8
GENERAL DISCUSSION AND FUTURE WORK

Mycobacterial diseases represent some of the most important and ancient diseases known to infect humans and animals. *M. tuberculosis* was the first organism that was definitively shown to be associated with human disease by Koch – given the problems that exist cultivating this organism, this was quite remarkable as it might be expected that it would have been easier to demonstrate this with *V. cholera* or Shigella, which were also big killers at the time of Koch. Despite many years of research, ways to improve the detection of viable slow-growing mycobacterial cells, other than liquid culture systems, have not been found. Not only does the difficulty in culturing these organisms hinder diagnosis, it also handicaps research because determining the number of viable cells is still the most routinely used method to quantify cells in studies of infection and survival in the host.

The FPTB assay was developed to utilise the ability of bacteriophage to infect and replicate faster than their hosts doubling time. Originally developed for the rapid detection of *M. tuberculosis* in human sputum samples, the FPTB assay was a major breakthrough in the detection of viable mycobacteria. However due to the advent of molecular methods such as PCR around the same time, the FPTB assay fell out of favour. The assay in its original format, to detect TB, did not reach its full potential, however as the phage used in the assay can infect a wide range of mycobacteria (Rybniker et al., 2006), work was carried out to determine whether other pathogenic mycobacteria could be detected.

MAP is the causative agent for significant animal disease, called Johne's disease. The economic impact of Johne's disease is of great importance, as Johne's disease is thought to be endemic in many countries around the world (Pradhan et al., 2009). MAP is another organism that is difficult to work with as it can take months to form colonies on agar. The bacteriophage used in the FPTB assay can be used to infect MAP as well as TB. The ability to detect MAP in the blood of animals suffering from Johne's disease could be a crucial step in understanding and controlling the spread of the disease. Johne's disease has a

major economic impact on the dairy and meat industry where significant losses in milk production are seen (Losinger, 2005). The limitations of culture, ELISA and PCR based tests and the difficulties complexities of the different stages of disease, means that there is a definite need for alternative tests.

8.1. THE BLOOD PHAGE ASSAY

The FPTB assay has been applied in a variety of ways to rapidly detect viable MAP in milk and dairy products (Botsaris et al., 2010, Stanley et al., 2007, Foddai et al., 2009). In dairy herds, milk is one of the easiest samples to obtain for Johne's screening as there are no ethical ramifications or other issues to overcome for collection. However a problem with faecal contamination has always been thought to be an issue when using milk to detect viable MAP cells as an indication of disseminated disease. Animals can be passively transmitting MAP cells in their faeces without becoming infected with Johne's disease (Whittington and Sergeant, 2001). This can contaminate milk being tested leading to a false representation of MAP being found in milk. In contrast the use of aseptically collected blood samples reduces this concern about contamination. The site where the blood is removed can be thoroughly cleaned, reducing the likelihood of faecal contamination. In addition, the use of blood as a test sample makes the method applicable to animals of all genders, all ages and all stages of production, rather than being limited to those animals that are producing milk. Having a good blood test that detects whole-viable MAP cells also allows questions about the pathophysiology of disease to be asked. Information about when the MAP cells become systemic and how they get into the milk can be determined leading to a greater understanding of the disease.

8.1.1. Developing phage assay protocols

Whenever new applications of the phage assay have been developed, sample processing has been found to be crucial to allow as efficient phage infection as possible. Pragmatically the approach that has been taken is to use methods that have already been shown to be successful for the culture of mycobacteria for that sample type. This has two benefits; first to speed up the time taken for method development by utilising the knowledge of other experts in the field and second the methods are familiar to other workers which, makes them more likely to be accepted and also allows others to easily compare the results gained to their own. In this case to capture the MAP cells, PMMS that had previously been used to capture MAP cells from milk was used, however variability in the assay with regards to capture and detection rates were found when different animal blood types were used. When PMMS was used on horse blood, cell capture was very poor, however when carried out in sheep blood, cell capture was improved. It was hypothesised that as different animals have different viscosities of blood, bead movement was being impeded (Windberger et al., 2003), and several dilution steps were needed to allow efficient capture of the MAP cells in the blood. Fortuitously, diluting the blood resulted in the lysis of the red and white blood cells; although this was not an intentional part of the method design it meant that any MAP cells in clinical samples, that are believed to be intracellular (Bower et al., 2011), were then accessible to the phage in the FPTB assay. Bower et al. (2012) optimised the macrophage cells lysis step when MAP culture was being optimised from blood.

When developing the original blood assay the emphasis was on establishing the conditions required to make sure the sample would not inhibit phage infection. However, not much thought was given to the state of the cells being detected. It was found in Chapter 6, that mycobacteria cells that are in a stationary non-replicating, dormant phase would resist phage infection with D29. Whether or not this was an evolved strategy by the cells or a coincidence

suggested that the phage assay potentially may not be detecting all of the cells present in this sample and potentially in others that have been tested.

It had been reported before that phage D29 could not infect dormant mycobacteria, but another mycobacteriophage TM4 could (Piuri and Hatfull, 2006). When the mycobacteria were induced into the non-replicating phase, detection of the cells with D29 was arrested. Interestingly this gave information about the metabolic state of the mycobacteria detected in the blood in Chapter 4, as D29 could infect the cells it was suggested that the MAP cells were metabolically active. Furthermore, by changing the components of the FPTB assay to work with TM4 instead of D29, a method to differentiate between dormant and metabolically active mycobacteria was developed, which could be used to gain information about different metabolic states of the cells. Phage TM4 could also be used in the high-throughput assay as a cocktail with D29 or on its own to detect a wider range of mycobacteria cells that may be dormant in different sample types. This would lead to the detection of MAP cells that may be in an unculturable state, improving the whole cell detection sensitivity. It would also give information about the metabolic state of the cells in the blood, and whether some are actively growing whereas others may be dormant, which is all very important information to understand the pathophysiology of Johne's disease.

When testing clinical samples only 1 ml of blood was tested due to ethical sampling reasons. As low numbers of MAP was detected in such small samples, it was thought that the detection method was at the limit of its sensitivity. In Chapter 4, from the sample Set C of animals, the question was asked; where in the blood are the MAP cells. It was hypothesised that because of the intracellular nature of MAP (Ghosh et al., 2013) the cells were most likely to be inside blood macrophages, thus the buffy coat was isolated to concentrate macrophages and therefore the MAP cells. It was found that all the detectable MAP cells were in the concentrated buffy coat layer. This means that when blood sampling, although it

will add another processing step, if more blood is obtained and if the buffy coat is isolated first, there would be a greater concentration of MAP cells from a 10 ml sample, increasing the efficiency of detection by theoretically 1 Log₁₀.

Furthermore, by removing other phage inhibitory components in the blood, such as the red blood cells, the magnetic separation step may not be necessary.

Therefore reducing the cost and time associated with the PMMS method.

Finally the effect of freezing mycobacteria and the implications of detection with the phage assay were investigated. It has been reported that freezing can reduce the viability of MAP (Richards and Thoen, 1977). However, cells that are frozen and thawed may well be sub-lethally damaged and actually still alive, but unable to be cultured. A pre-enrichment step has been used by other researchers to increase the efficiency of the phage assay (Foddai et al., 2009). Thus the effect of a recovery steps for the MAP cells after freezing and thawing was investigated, and it was found that the number of viable MAP cells detected by the phage assay after freeze-thawing was not significantly different after 3 d recovery to the sample before freezing. This finding could have worked well for frozen blood samples from sheep experimentally infected with MAP that had been culled after one year and were showing clinical signs of infection. Again using the sub-optimised phage assay the blood samples were tested. The results showed that three exposed animals harboured viable MAP in their blood, however two animals that were not exposed to MAP also tested positive. The assay showed that there is the potential to detect MAP in sheep blood, but a lot of further optimisations were required with sample preparation and getting the phage assay fully optimised. Because of the slower growing nature of sheep strains of MAP, further recovery from the freezing may have been needed to detect all the MAP cells potentially in the sheep blood.

When the blood phage assay was then carried out on artificially spiked blood samples, it was found that there was a good limit of detection of 10 cells per ml of blood. A good limit of detection was needed as it was anticipated that the

number of MAP cells present in the blood of clinical animals would be low (Bower et al., 2010). By optimising the processing of the samples with different types of blood, this now means that a wide range of different blood types can now be tested with the phage assay and not just cattle. There are many other animals where Johne's disease is a problem, as mentioned before sheep can be infected by MAP. Sheep can suffer from Johne's disease which also had a significant impact on the farming industry, especially in countries like Australia and New Zealand (Begg and Whittington, 2010). If using the phage assay to detect other mycobacteria such as *M. bovis*, other animals could be tested, such as camelids, badgers and now even cats (Garcia-Bocanegra et al., 2010, Tomlinson et al., 2012, Roberts et al., 2014).

8.1.2. Using the phage assay on clinical samples

The development of a robust blood assay meant that new questions could be asked about when and how many MAP cells could be found in the blood of animals. As the phage assay has been shown to detect MAP in the blood of animal with Johne's disease future work will focus on what can be done with the new information. Being able to detect viable MAP cells in blood within 24 h means that an almost real time assessment of the progression of Johne's disease in animals can be carried out. A longitudinal study with a large cohort of animals is required to determine what it means with regards to disease progression when an animal has bacteraemia, how this relates to current tests such as PCR and ELISA, and whether the phage assay could be used as a diagnostic of Johne's disease. Chapter 4 investigated whether the phage assay could detect MAP in clinical blood samples. The results showed great promise in detecting MAP in blood in a number of animals at different stages of the disease. However the number of samples tested was too low to draw too many conclusions, or perform any powerful statistical analyses with. As well as this, the relationship between measuring an immune response and detecting whole viable MAP cells is not

known, that is if an animal has whole MAP cells in their blood does that mean they will go on to develop clinical symptoms of Johne's disease. There has always been variability in the immune response from animals suffering from Johne's disease, especially in those in the subclinical phase of infection (Dennis et al., 2011). Using the rapid phage assay, the relationship between the bacterial load in the blood and the immune response of an animal could be mapped over a period of time, allowing greater understanding of the disease.

In the first investigations described here the animals tested were all naturally exposed to MAP, there was no information about when they were exposed or by how much, limiting the amount of information one could gain about the disease progression. Fortunately samples were obtained from several trials working with experimentally infected animals. A major question asked was how early the phage assay can detect MAP in the blood of experimentally infected animals. The phage assay detected MAP within 6 months which was comparable to when testing experimentally infected calves. Interestingly Kawaji et al. (2012) found that calves infected with MAP launched an innate immune response to after 30 weeks of infection, which may make sense if it takes 6 months for MAP to be found in the blood, the immune response is likely to occur after. This was again encouraging because by detecting the MAP cells sooner, may result in better understanding and therefore control of the disease (Schillinger et al., 2013).

Another major problem with controlling Johne's disease, is that it can take up to 5 years post exposure to MAP for any clinical symptoms to manifest (Collins, 2003). Being able to detect Johne's disease during subclinical infection is very difficult as the diagnostic sensitivities of ELISAs are very poor and can range from 17 to 56 % at an individual animal level (Nielsen and Toft, 2008). The phage assay was used on experimentally infected cows that were not showing any clinical signs of disease and yielded conflicting results compared to the blood ELISA tests. If the phage assay is compared to the blood ELISA as a Gold Standard, it could suggest that the phage assay is not specific and is yielding

more false-negative results. However it should be noted that if a more sensitive test is developed than the existing Gold Standard, one issue is that the new test appears to give rise to a large number of false positive results. Hence all tests should also be evaluated as stand-alone assays compared to the development of clinical symptoms so that the value of the test in terms of diagnosis and management of the disease can be established.

Chapter 6 described factors that affected phage infection. It was found that dormant mycobacteria resisted successful phage D29 infection; however another broad spectrum mycobacteriophage, TM4, was able to infect dormant mycobacteria. This led to a method capable of determining when mycobacteria were lying dormant, by simply changing the phage used in the FPTB assay. MAP and tuberculosis causing mycobacteria have similar characteristic subclinical phases of infection (Burgelt and Williams, 2004). Being able to detect mycobacterial dormancy is hugely important in understanding and ultimately controlling the diseases caused by mycobacteria. Using the blood phage assay with TM4, mycobacteria lying dormant in blood cells could be detected, thus allowing animals in the subclinical stages of infection to be identified and monitored to allow good control of Johne's disease (Lybeck et al., 2011).

8.1.2.1. Future applications for the detection of MAP and other mycobacteria

As the original FPTB assay was developed for the detection of *M. tuberculosis* Complex bacteria, the blood assay would be applicable for the detection of the zoonotic pathogen *M. bovis* which causes bovine tuberculosis (Btb). Interest in Btb has been increasing lately with the implementation of badger cull that has led to a renewed effort to develop novel detection methods for Btb in badgers and the environment (Broughan et al., 2013). A novel blood test that detects the whole Btb cell could be of use as an alternative to the dated skin-test currently used. By simply changing the primers in the end-point PCR, the test can be adapted to detect *M. bovis*. Additionally a major economic issue with bTB is that

vaccines cannot be used on animals that are to be exported. Restrictions on the movement of bTB vaccinated cattle means that UK farmers are not allowed to export to Europe as there is not a reliable test that can differentiate between vaccinated and naturally infected animals (DIVA test). As the phage assay detects most viable mycobacteria, both BCG vaccinated and naturally infected animals with bTB would be detectable. Simply by changing the end-point PCR to a method that can differentiate between *M. bovis* and BCG means that the phage assay could be used as a DIVA test.

As a notifiable disease, when bTB is detected in a cow, the animal is culled and a post mortem is carried out to determine whether the animal had bTB. Often lymph node cultures are taken and these are sent for culture. The long length of time and the expense of culture means that a lot of money is spent determining whether a substandard test has detected bTB infection or not. By using the phage assay on lymph tissue, the time for culture can be reduced from several weeks to a 24 h saving time, space and money.

8.2. DEVELOPMENT OF A HIGH-THROUGHPUT MAP DETECTION PLATFORM

The original FPTB assay was developed to be used as a cheap, low tech assay for use in the developing world. The assay format is laborious as it uses petri dishes and pipettes. For the phage assay to be developed for use, especially in a veterinary setting, where many samples would be taken, the present format is not practical. One of the main benefits of the ELISA based assays is that they can be carried out in large numbers (Schillinger et al., 2013). The basis of the novel one tube high-throughput assay is that the phage are used as a very efficient DNA extraction agent. Lytic phage such as D29 will enter their host cell take over their molecular machinery replicating before lysing the cell. As phage D29 will only infect viable mycobacteria, only viable cells will lyse, resulting in the release of the mycobacterial DNA from a sample which can then be tested

using an end-point method such as PCR. As with the original phage assay sample preparation was key to allow as efficient phage infection as possible. Getting the target mycobacteria cells in a good media for detection is crucial, and so the PMMS method employed during the phage assay was vital to remove the MAP cells from phage inhibiting blood to media. Once this had been achieved the phage the sample can inoculated with phage, and if mycobacteria were present they would lyse releasing their DNA for detection. Enumeration can be carried out with the original phage assay by counting plaques. Enumeration could still be used with the one tube format of the assay, if the end point detection method uses qRT-PCR. When the assay was tested on clinical samples it yielded more positive results than both the phage assay and a blood PCR (Section 5.2.5). By cutting down the amount of steps required to detect the cells, the one tube format speeds up the process of testing compared to the phage assay (results within 8 h rather than 24 h) and allows the testing to be carried out in a high-throughput capacity. This novel assay has been subsequently protected by a patent (Patent Number: GB Patent 1317392.7) to be exploited commercially.

8.2.1. Future developments of the high-throughput MAP detection assay

As the technology is in its infancy it needs to be optimised and developed further so that it can be fully automated. Platform technologies already exist for performing automated magnetic separation and sample processing (Dynabead Automated Separator, Life Technologies and Vidas, Biomerieux respectively), thus incorporating the novel DNA lysis technology would not be difficult.

The next stage of development would be optimising the assay for other mycobacteria. The PMMS method used specifically binds MAP cells, no others. Therefore other methods of cell capture would be required. Novel peptides have been sequenced and produced by phage-display that bind to all mycobacteria (Ngubane et al., 2013). Although this limits the specificity of the PMMS cell isolation, once the mycobacteria cell has been lysed by the phage, the specificity

of the assay would depend on the design and specificity of the end-point PCR being carried out. As with the original phage assay, further studies could be carried out to detect other pathogenic mycobacteria, such as *M. tuberculosis* or *M. bovis*.

8.3. NOVEL MAP-SPECIFIC FLUORESCENT FUSION PEPTIDES

The ZN stain is method commonly used to detect acid-fast organisms such as mycobacteria when looking for *M. tuberculosis* in sputum samples. However the specificity and sensitivity of the method is often very low compared to culture, PCR and the FPTB assay (Marei et al., 2003). The development of a MAP specific fluorescent stain increases the specificity of microscopic methods to detect MAP, however further work needs to be carried out to determine whether the stain will work on histological samples, where microscopic analysis routine takes place.

Other fluorescent peptides that have been found and sequenced that could also be used in the same way as the MAP specific peptides. Future work would be involved in finding novel species specific peptides and using them in the same way as the MAP specific peptides. For example peptides derived from phage display libraries that bind specifically to *M. bovis* have been found (Stewart et al., 2012), which could be used in the same way as the MAP-specific peptides to create a specific fluorescent *M. bovis* stain.

8.4. CONCLUSION

Phage have proved to be a powerful tool to understand other bacteria, and again here the phage are providing us with tools to study this most unmanageable of bacteria. By being able to understand the interaction between the phage and the host, the phage will lead us to develop new insights about the organism and is allowing us now to develop new tools to help combat the diseases caused by mycobacteria.

CHAPTER 9
BIBLIOGRAPHY

- ABUBAKAR, I., MYHILL, D., ALIYU, S. H. & HUNTER, P. R. 2008. Detection of Mycobacterium avium subspecies paratuberculosis from patients with Crohn's disease using nucleic acid-based techniques: A systematic review and meta-analysis. *Inflammatory Bowel Diseases*, 14, 401-410.
- ALBERT, H., TROLLIP, A. P., MOLE, R. J., HATCH, S. J. B. & BLUMBERG, L. 2002. Rapid indication of multidrug-resistant tuberculosis from liquid cultures using FASTPlaqueTB-RIFTM, a manual phage-based test. *International Journal of Tuberculosis and Lung Disease*, 6, 523-528.
- ALBERT, H., TROLLIP, A., SEAMAN, I. & MOLE, R. J. 2004. Simple, phage-based (FASTPlaque) technology to determine rifampicin resistance of Mycobacterium tuberculosis directly from sputum. *International Journal of Tuberculosis and Lung Disease*, 8, 1114-1119.
- ALINOVI, C. A., WARD, M. P., LIN, T. L., MOORE, G. E. & WU, C. C. 2009. Real-time PCR, compared to liquid and solid culture media and ELISA, for the detection of Mycobacterium avium ssp paratuberculosis. *Veterinary Microbiology*, 136, 177-179.
- ALTIC, L. C., ROWE, M. T. & GRANT, I. R. 2007. UV light inactivation of Mycobacterium avium subsp paratuberculosis in milk as assessed by FASTPlaqueTB phage assay and culture. *Applied and Environmental Microbiology*, 73, 3728-3733.
- ALY, S. S., ANDERSON, R. J., WHITLOCK, R. H., FYOCK, T. L., MCADAMS, S. C., BYREM, T. M., JIANG, J. M., ADASKA, J. M. & GARDNER, I. A. 2012. Cost-effectiveness of diagnostic strategies to identify Mycobacterium avium subspecies paratuberculosis super-shedder cows in a large dairy herd using antibody enzyme-linked immunosorbent assays, quantitative real-time polymerase chain reaction, and bacterial culture. *Journal of Veterinary Diagnostic Investigation*, 24, 821-832.
- APPLEYARD, R. K., MCGREGOR, J. F. & BAIRD, K. M. 1956. Mutation to Extended Host Range and the Occurrence of Phenotypic Mixing in the Temperate Coliphage Lambda. *Virology*, 2, 565-574.
- BARDAROV, S., BARDAROV, S., PAVELKA, M. S., SAMBANDAMURTHY, V., LARSEN, M., TUFARIELLO, J., CHAN, J., HATFULL, G. & JACOBS, W. R. 2002. Specialized transduction: an efficient method for generating marked and unmarked targeted gene disruptions in Mycobacterium tuberculosis, M-bovis BCG and M-smegmatis. *Microbiology-Sgm*, 148, 3007-3017.
- BARKSDALE, L. & KIM, K. S. 1977. Mycobacterium. *Bacteriological Reviews*, 41, 217-372.
- BARSOM, E. K. & HATFULL, G. F. 1996. Characterization of a Mycobacterium smegmatis gene that confers resistance to phages L5 and D29 when overexpressed. *Molecular Microbiology*, 21, 159-170
- BAUMGART, D. C. & CARDING, S. R. 2007. Gastroenterology 1 - Inflammatory bowel disease: cause and immunobiology. *Lancet*, 369, 1627-1640.
- BEASLEY, L., TRUYERS, I. G. R., MELLOR, D. J., NORQUAY, R., DUTHIE, S. & ELLIS, K. A. 2011. Prevalence of Johne's disease among cattle in Orkney. *Veterinary Record*, 169, 50A

- BEGG, D. J., DE SILVA, K., DI FIORE, L., TAYLOR, D. L., BOWER, K., ZHONG, L., KAWAJI, S., EMERY, D. & WHITTINGTON, R. J. 2010. Experimental infection model for Johne's disease using a lyophilised, pure culture, seedstock of *Mycobacterium avium* subspecies paratuberculosis. *Veterinary Microbiology*, 141, 301-11.
- BEGG, D. & WHITTINGTON, R. 2010. Paratuberculosis in sheep. In: BEHR, M. A. & COLLINS, D. M. (eds.) Paratuberculosis: organism, disease, control. Wallingford: CABI
- BENEDICTUS, G. & KALIS, C. J. H. 2003. Paratuberculosis: Eradication, control and diagnostic methods. *Acta Veterinaria Scandinavica*, 44, 231-241.
- BERMUDEZ, L. E., KOLONOSKI, P., WU, M., ARALAR, P. A., INDERLIED, C. B. & YOUNG, L. S. 1999. Mefloquine is active in vitro and in vivo against *Mycobacterium avium* complex. *Antimicrobial Agents and Chemotherapy*, 43, 1870-1874.
- BHOWMICK, T., MIRRETT, S., RELLER, L. B., PRICE, C., QI, C., WEINSTEIN, M. P. & KIRN, T. J. 2013. Controlled Multicenter Evaluation of a Bacteriophage-Based Method for Rapid Detection of *Staphylococcus aureus* in Positive Blood Cultures. *Journal of Clinical Microbiology*, 51, 1226-1230.
- BOTSARIS, G. 2010. Development and Evaluation of a Rapid Phage-PCR Assay to Detect *Mycobacterium avium* subsp. paratuberculosis in Dairy Products. PhD, University of Nottingham.
- BOTSARIS, G., SLANA, I., LIAPI, M., DODD, C., ECONOMIDES, C., REES, C. & PAVLIK, I. 2010. Rapid detection methods for viable *Mycobacterium avium* subspecies paratuberculosis in milk and cheese. *International Journal of Food Microbiology*, 141, S87-S90.
- BOTSARIS, G., SWIFT, B. M. C. & REES, C. E. D. 2013. Bacteriophage-based techniques for detection of foodborne pathogens. *Encyclopedia of Food Microbiology*. Second Edition.
- BOWER, K., BEGG, D. J. & WHITTINGTON, R. J. 2010. Optimisation of culture of *Mycobacterium avium* subspecies paratuberculosis from blood samples. *Journal of Microbiological Methods*, 80, 93-99.
- BOWER, K. L., BEGG, D. J. & WHITTINGTON, R. J. 2011. Culture of *Mycobacterium avium* subspecies paratuberculosis (MAP) from blood and extra-intestinal tissues in experimentally infected sheep. *Veterinary Microbiology*, 147, 127-132.
- BRENNAN, P. J. 2003. Structure, function, and biogenesis of the cell wall of *Mycobacterium tuberculosis*. *Tuberculosis*, 83, 91-97.
- BROWN-ELLIOTT, B. A., NASH, K. A. & WALLACE, R. J. 2012. Antimicrobial Susceptibility Testing, Drug Resistance Mechanisms, and Therapy of Infections with Nontuberculous Mycobacteria. *Clinical Microbiology Reviews*, 25, 721-721.
- BRUSSOW, H. & HENDRIX, R. W. 2002. Phage genomics: Small is beautiful. *Cell*, 108, 13-16.

- BUDDLE, B. M., ALDWELL, F. E., DE LISLE, G. W., VORDERMEIER, H. M., HEWINSON, R. G. & WEDLOCK, D. N. 2011. Low oral BCG doses fail to protect cattle against an experimental challenge with *Mycobacterium bovis*. *Tuberculosis*, 91, 400-405.
- BUERGELT, C. D., HALL, C., MCENTEE, K. & DUNCAN, J. R. 1978. Pathological evaluation of paratuberculosis in naturally infected cattle. *Veterinary Pathology*, 15, 196-207.
- BUERGELT, C. D. & WILLIAMS, J. E. 2004. Nested PCR on blood and milk for the detection of *Mycobacterium avium* subsp. paratuberculosis DNA in clinical and subclinical bovine paratuberculosis. *Australian Veterinary Journal*, 82, 497-503.
- BULL, T. J., HERMON-TAYLOR, J., PAVLIK, I., EL-ZAATARI, F. & TIZARD, M. 2000. Characterization of IS900 loci in *Mycobacterium avium* subsp. paratuberculosis and development of multiplex PCR typing (vol 146, pg 2185, 2000). *Microbiology-Uk*, 146, 3285-3285.
- BULL, T. J., LEVIN, B. R., DEROUIN, T., WALKER, N. & BLOCH, C. A. 2002. Dynamics of success and failure in phage and antibiotic therapy in experimental infections. *BMC Microbiology*, 2, 35.
- CANCELA, M. M. G. & MARIN, J. F. G. 1993. Comparison of Ziehl-Neelsen Staining and Immunohistochemistry for the Detection of *Mycobacterium-Bovis* in Bovine and Caprine Tuberculous Lesions. *Journal of Comparative Pathology*, 109, 361-370.
- CHACON, O., BERMUDEZ, L. E. & BARLETTA, R. G. 2004. Johne's disease, inflammatory bowel disease, and *Mycobacterium paratuberculosis*. *Annual Review of Microbiology*, 58, 329-63.
- CHALFIE, M., TU, Y., EUSKIRCHEN, G., WARD, W. W. & PRASHER, D. C. 1994. Green Fluorescent Protein as a Marker for Gene-Expression. *Science*, 263, 802-805.
- CHAMBERLIN, W., GRAHAM, D. Y., HULTEN, K., EL-ZIMAITY, H. M. T., SCHWARTZ, M. R., NASER, S., SHAFRAN, I. & EL-ZAATARI, F. A. K. 2001. Review article: *Mycobacterium avium* subsp. paratuberculosis as one cause of Crohn's disease. *Alimentary Pharmacology & Therapeutics*, 15, 337-346.
- CHATTERJEE, D. 1997. The mycobacterial cell wall: structure, biosynthesis and sites of drug action. *Current Opinion in Chemical Biology*, 1, 579-588.
- CHIODINI, R. J. 1989. Crohn's disease and the mycobacterioses: a review and comparison of two disease entities. *Clinical Microbiology Reviews*, 2, 90-117.
- CHO, J., TAUER, L. W., SCHUKKEN, Y. H., GOMEZ, M. I., SMITH, R. L., LU, Z. & GROHN, Y. T. 2012. Economic analysis of *Mycobacterium avium* subspecies paratuberculosis vaccines in dairy herds. *Journal of Dairy Science*, 95, 1855-1872.
- CHUI, L. W., KING, R., LU, P., MANNINEN, K. & SIM, J. 2004. Evaluation of four DNA extraction methods for the detection of *Mycobacterium avium* subsp. paratuberculosis by polymerase chain reaction. *Diagnostic Microbiology and Infectious Disease*, 48, 39-45.

- COLLINS, D. M., STEPHENS, D. M. & DE LISLE, G. W. 1993. Comparison of polymerase chain reaction tests and faecal culture for detecting *Mycobacterium paratuberculosis* in bovine faeces. *Veterinary Microbiology*, 36, 289-99.
- COLLINS, M. T., GARDNER, I. A., GARRY, F. B., ROUSSEL, A. J. & WELLS, S. J. 2006. Consensus recommendations on diagnostic testing for the detection of paratuberculosis in cattle in the United States. *Javma-Journal of the American Veterinary Medical Association*, 229, 1912-1919.
- COUSINS, D. V., EVANS, R. J. & FRANCIS, B. R. 1995. Use of BACTEC radiometric culture method and polymerase chain reaction for the rapid screening of faeces and tissues for *Mycobacterium paratuberculosis*. *Australian Veterinary Journal*, 72, 458-462.
- COUSINS, D. V., WHITTINGTON, R., MARSH, I., MASTERS, A., EVANS, R. J. & KLUVER, P. 1999. Mycobacteria distinct from *Mycobacterium avium* subsp paratuberculosis isolated from the faeces of ruminants possess IS900-like sequences detectable by IS900 polymerase chain reaction: implications for diagnosis. *Molecular and Cellular Probes*, 13, 431-442.
- COUSSENS, P. M. 2001. *Mycobacterium paratuberculosis* and the bovine immune system. *Anim Health Res Rev*, 2, 141-61.
- CROHN, B. B., GINZBURG, L. & OPPENHEIMER, G. D. 1932. Landmark article Oct 15, 1932. Regional ileitis. A pathological and clinical entity. By Burril B. Crohn, Leon Ginzburg, and Gordon D. Oppenheimer. *JAMA*, 251, 73-9.
- CROSSLEY, B. M., ZAGMUTT-VERGARA, F. J., FYOCK, T. L., WHITLOCK, R. H. & GARDNER, I. A. 2005. Fecal shedding of *Mycobacterium avium* subsp paratuberculosis by dairy cows. *Veterinary Microbiology*, 107, 257-263.
- CUNNINGHAM, A. F. & SPREADBURY, C. L. 1998. Mycobacterial stationary phase induced by low oxygen tension: Cell wall thickening and localization of the 16-kilodalton alpha-crystallin homology. *Journal of Bacteriology*, 180, 801-808.
- DA SILVA, P. E. A. & PALOMINO, J. C. 2011. Molecular basis and mechanisms of drug resistance in *Mycobacterium tuberculosis*: classical and new drugs. *Journal of Antimicrobial Chemotherapy*, 66, 1417-1430.
- DALTON, J. P. & HILL, C. 2013. Survival of *Mycobacterium avium* subsp paratuberculosis in Synthetic Human Gastric Juice and Acidified Porcine Bile. *Applied and Environmental Microbiology*, 79, 1418-1420.
- DARDNI. 2006. Guidance on the control of Johne's disease in dairy herds [Online]. Belfast: DARDNI. [Accessed 11 May 2011 2011].
- DAVID, H. L., CLAVEL, S. & CLEMENT, F. 1980. Adsorption and Growth of the Bacteriophage-D29 in Selected Mycobacteria. *Annales De Virologie*, 131, 167
- DE SIQUEIRA, R. S., DODD, C. E. R. & REES, C. E. D. 2006. Evaluation of the natural virucidal activity of teas for use in the phage amplification assay. *International Journal of Food Microbiology*, 111, 259-262.
- DEFOIRDT, T., BOON, N., SORGELOOS, P., VERSTRAETE, W. & BOSSIER, P. 2007. Alternatives to antibiotics to control bacterial infections: luminescent vibriosis in aquaculture as an example. *Trends in Biotechnology*, 25, 472-479.

- DEFRA. 2013. Bovine TB Research Programme. DEFRA. <https://www.gov.uk/government/policies/reducing-bovine-tuberculosis/supporting-pages/research-and-evidence-about-bovine-tb>. Last accessed 12th May 2014.
- DHEDA, K., BOOTH, H., HUGGETT, J. F., JOHNSON, M. A., ZUMLA, A. & ROOK, G. A. W. 2005. Lung remodeling in pulmonary tuberculosis. *Journal of Infectious Diseases*, 192, 1201-1210.
- DICK, T., LEE, B. H. & MURUGASU-OEI, B. 1998. Oxygen depletion induced dormancy in *Mycobacterium smegmatis*. *FEMS Microbiology Letters*, 163, 159-64.
- DROBNIIEWSKI, F. A., GIBSON, A., RUDDY, M. & YATES, M. D. 2003. Evaluation and utilization as a public health tool of a national molecular epidemiological tuberculosis outbreak database within the United Kingdom from 1997 to 2001. *Journal of Clinical Microbiology*, 41, 1861-1868.
- DUSTHACKEER, A., KUMAR, V., SUBBIAN, S., SIVARAMAKRISHNAN, G., ZHU, G. F., SUBRAMANYARN, B., HASSAN, S., NAGAMAIAH, S., CHAN, J. & RAMA, N. P. 2008. Construction and evaluation of luciferase reporter phages for the detection of active and non-replicating tubercle bacilli. *Journal of Microbiological Methods*, 73, 18-25.
- DWORKIN, M. & FOSTER, J. W. 1958. Experiments with Some Microorganisms Which Utilize Ethane and Hydrogen. *Journal of Bacteriology*, 75, 592-603.
- EDDY, R. G. (ed.) 2004. Bovine Medicine, Oxford: Blackwell Publishing Company.
- ELLINGSON, J. L. E., BOLIN, C. A. & STABEL, J. R. 1998. Identification of a gene unique to *Mycobacterium avium* subspecies paratuberculosis and application to diagnosis of paratuberculosis. *Molecular and Cellular Probes*, 12, 133-142.
- ENGLUND, S., BOLSKE, G. & JOHANSSON, K. E. 2002. An IS900-like sequence found in a *Mycobacterium* sp other than *Mycobacterium avium* subsp paratuberculosis. *FEMS Microbiology Letters*, 209, 267-271.
- ENOSAWA, M., KAGEYAMA, S., SAWAI, K., WATANABE, K., NOTOMI, T., ONOE, S., MORI, Y. & YOKOMIZO, Y. 2003. Use of loop-mediated isothermal amplification of the IS900 sequence for rapid detection of cultured *Mycobacterium avium* subsp. paratuberculosis. *Journal of Clinical Microbiology*, 41, 4359-4365.
- ENROTH, H. & ENGSTRAND, L. 1995. Immunomagnetic Separation and Pcr for Detection of *Helicobacter-Pylori* in Water and Stool Specimens. *Journal of Clinical Microbiology*, 33, 2162-2165.
- FELLER, M., HUWILER, K., STEPHAN, R., ALTPETER, E., SHANG, A., FURRER, H., PFYFFER, G. E., JEMMI, T., BAUMGARTNER, A. & EGGER, M. 2007. *Mycobacterium avium* subspecies paratuberculosis and Crohn's disease: a systematic review and meta-analysis. *Lancet Infectious Diseases*, 7, 607-613.
- FENTON, M., ROSS, P., MCAULIFFE, O., O'MAHONY, J. & COFFEY, A. 2010. Recombinant bacteriophage lysins as antibacterials. *Bioengineered Bugs*, 1, 9-16.

- FISCHETTI, V. A. 2005. Bacteriophage lytic enzymes: novel anti-infectives. *Trends in Microbiology*, 13, 491-496.
- FODDAI, A., ELLIOTT, C. T. & GRANT, I. R. 2009. Optimization of a Phage Amplification Assay To Permit Accurate Enumeration of Viable Mycobacterium avium subsp paratuberculosis Cells. *Applied and Environmental Microbiology*, 75, 3896-3902.
- FODDAI, A., ELLIOTT, C. T. & GRANT, I. R. 2010. Maximizing Capture Efficiency and Specificity of Magnetic Separation for Mycobacterium avium subsp paratuberculosis Cells. *Applied and Environmental Microbiology*, 76, 7550-7558.
- FOOD STANDARDS AGENCY. 2002. Food hygiene: MAP results. http://www.food.gov.uk/safereating/microbiology/mapinmilk/MAP_results. Last Accessed on 2nd April 2014.
- FOLEY-THOMAS, E. M., WHIPPLE, D. L., BERMUDEZ, L. E. & BARLETTA, R. G. 1995. Phage Infection, Transfection and Transformation of Mycobacterium-Avium Complex and Mycobacterium-Paratuberculosis. *Microbiology-Uk*, 141, 1173-1181.
- FORD, M. E., SARKIS, G. J., BELANGER, A. E., HENDRIX, R. W. & HATFULL, G. F. 1998. Genome structure of mycobacteriophage D29: Implications for phage evolution. *Journal of Molecular Biology*, 279, 143-164.
- FREGNAN, G. B. & SMITH, D. W. 1962. Description of Various Colony Forms of Mycobacteria. *Journal of Bacteriology*, 83, 819
- FRIDRIKSDOTTIR, V., GUNNARSSON, E., SIGURDARSON, S. & GUDMUNDSDOTTIR, K. B. 1999. Paratuberculosis in Iceland: Epidemiology and control measures, past and present. *Proceedings of the Sixth International Colloquium on Paratuberculosis*, 105-108.
- FYOCK, T.L., SWEENEY, R.W. & WHITLOCK, R.H. 2005. MGIT, liquid culture system for detection of MAP in bovine faecal samples, *Proceedings of the Eighth International Colloquium on Paratuberculosis* Copenhagen, Denmark, p. 554.
- GAO, L. Y., LAVAL, F., LAWSON, E. H., GROGER, R. K., WOODRUFF, A., MORISAKI, J. H., COX, J. S., DAFTE, M. & BROWN, E. J. 2003. Requirement for kasB in Mycobacterium mycolic acid biosynthesis, cell wall impermeability and intracellular survival: implications for therapy. *Molecular Microbiology*, 49, 1547-1563.
- GENGENBACHER, M. & KAUFMANN, S. H. E. 2012. Mycobacterium tuberculosis: success through dormancy. *FEMS Microbiology Reviews*, 36, 514-532.
- GHOSH, P., WU, C. W. & TALAAT, A. M. 2013. Key Role for the Alternative Sigma Factor, SigH, in the Intracellular Life of Mycobacterium avium subsp paratuberculosis during Macrophage Stress. *Infection and Immunity*, 81, 2242-2257.
- GIBBS J. 2001. Selecting the detection system-colorimetric, fluorescent, luminescent methods. Corning Life Sciences ELISA Technical Bulletin 2001:14.
- GIESE, S. B. & AHRENS, P. 2000. Detection of Mycobacterium avium subsp paratuberculosis in milk from clinically affected cows by PCR and culture. *Veterinary Microbiology*, 77, 291-297.

- GIL, F., GRZEGORZEWICZ, A. E., CATALAO, M. J., VITAL, J., MCNEIL, M. R. & PIMENTEL, M. 2010. Mycobacteriophage Ms6 LysB specifically targets the outer membrane of Mycobacterium smegmatis. *Microbiology-Sgm*, 156, 1497-1504.
- GLICKMAN, M. S., COX, J. S. & JACOBS, W. R. 2000. A novel mycolic acid cyclopropane synthetase is required for cording, persistence, and virulence of Mycobacterium tuberculosis. *Molecular Cell*, 5, 717-727.
- GOMEZ, J. E. & MCKINNEY, J. D. 2004. M-tuberculosis persistence, latency, and drug tolerance. *Tuberculosis*, 84, 29-44.
- GONZALEZ, J., GEIJO, M. V., GARCIA-PARIENTE, C., VERNA, A., CORPA, J. M., REYES, L. E., FERRERAS, M. C., JUSTE, R. A., MARIN, J. F. G. & PEREZ, V. 2005. Histopathological classification of lesions associated with natural paratuberculosis infection in cattle. *Journal of Comparative Pathology*, 133, 184-196.
- GOODRIDGE, L., CHEN, J. R. & GRIFFITHS, M. 1999. The use of a fluorescent bacteriophage assay for detection of Escherichia coli O157 : H7 in inoculated ground beef and raw milk. *International Journal of Food Microbiology*, 47, 43-50.
- GOODRIDGE, L. & GRIFFITHS, M. 2002. Reporter bacteriophage assays as a means to detect foodborne pathogenic bacteria. *Food Research International*, 35, 863-870.
- GRANT, I. R., HITCHINGS, E. I., MCCARTNEY, A., FERGUSON, F. & ROWE, M. T. 2002. Effect of commercial-scale high-temperature, short-time pasteurization on the viability of Mycobacterium paratuberculosis in naturally infected cows' milk. *Applied Environmental Microbiology*, 68, 602-7.
- GRANT, I. R., KIRK, R. B., HITCHINGS, E. & ROWE, M. T. 2003. Comparative evaluation of the MGIT (TM) and BACTEC culture systems for the recovery of Mycobacterium avium subsp paratuberculosis from milk. *Journal of Applied Microbiology*, 95, 196-201.
- GREEN, E. P., TIZARD, M. L. V., MOSS, M. T., THOMPSON, J., WINTERBOURNE, D. J., MCFADDEN, J. J. & HERMON TAYLOR, J. 1989. Sequence and Characteristics of IS900, an Insertion Element Identified in a Human Crohns-Disease Isolate of Mycobacterium-Paratuberculosis. *Nucleic Acids Research*, 17, 9063-9073.
- GREENSTEIN, R. J. 2003. Is Crohn's disease caused by a mycobacterium? Comparisons with leprosy, tuberculosis, and Johne's disease. *Lancet Infectious Diseases*, 3, 507-514.
- GREIG, A., STEVENSON, K., PEREZ, V., PIRIE, A. A., GRANT, J. M. & SHARP, J. M. 1997. Paratuberculosis in wild rabbits (Oryctolagus cuniculus). *Veterinary Record*, 140, 141-143.
- GUMBER, S. & WHITTINGTON, R. J. 2007. Comparison of BACTEC 460 and MGIT 960 systems for the culture of Mycobacterium avium subsp paratuberculosis S strain and observations on the effect of inclusion of ampicillin in culture media to reduce contamination. *Veterinary Microbiology*, 119, 42-52.
- GUMBER, S., TAYLOR, D. L., MARSH, I. B. & WHITTINGTON, R. J. 2009. Growth pattern and partial proteome of Mycobacterium avium subsp. paratuberculosis during the stress response to hypoxia and nutrient starvation. *Veterinary Microbiology*, 133, 344-57.

- GUTIERREZ, M. C., SUPPLY, P. & BROSCHE, R. 2009. Pathogenomics of Mycobacteria. *Microbial Pathogenomics*, 6, 198-210.
- GWOZDZ, J. M., THOMPSON, K. G., MURRAY, A., WEST, D. M. & MANKTELOW, B. W. 2000. Use of the polymerase chain reaction assay for the detection of Mycobacterium avium subspecies paratuberculosis in blood and liver biopsies from experimentally infected sheep. *Australian Veterinary Journal*, 78, 622-624.
- HAGENS, S. & LOESSNER, M. J. 2007. Application of bacteriophages for detection and control of foodborne pathogens. *Applied Microbiology and Biotechnology*, 76, 513-519.
- HARRIS, N. B. & BARLETTA, R. G. 2001. Mycobacterium avium subsp. paratuberculosis in Veterinary Medicine. *Clinical Microbiology Reviews*, 14, 489-512.
- HATFULL, G. F. & SARKIS, G. J. 1993. DNA-Sequence, Structure and Gene-Expression of Mycobacteriophage-L5 - a Phage System for Mycobacterial Genetics. *Molecular Microbiology*, 7, 395-405.
- HATFULL, G. F. 2010. Mycobacteriophages: genes and genomes. *Annual Reviews of Microbiology*, 64, 331-56.
- HATFULL, G. F. 2012. The secret lives of mycobacteriophages. *Advances in Virus Research*, 82, 179-288.
- HPA (2013) Incidents of TB in UK. <http://www.hpa.org.uk/topics/infectiousdiseases/infectionsaz/tuberculosis/>. Last Accessed Online on 1st April 2014.
- HEINZMANN, J., WILKENS, M., DOHMANN, K. & GERLACH, G. F. 2008. Mycobacterium avium subsp paratuberculosis-specific mpt operon expressed in M. bovis BCG as vaccine candidate. *Veterinary Microbiology*, 130, 330-337.
- HENDRY, C., DIONNE, K., HEDGEPEETH, A., CARROLL, K. & PARRISH, N. 2009. Evaluation of a Rapid Fluorescent Staining Method for Detection of Mycobacteria in Clinical Specimens. *Journal of Clinical Microbiology*, 47, 1206-1208.
- HINES, M. E. & STYER, E. L. 2003. Preliminary characterization of chemically generated Mycobacterium avium subsp paratuberculosis cell wall deficient forms (Spheroplasts). *Veterinary Microbiology*, 95, 247-258.
- HUDA, A., JUNGERSEN, G. & LIND, P. 2004. Longitudinal study of interferon-gamma, serum antibody and milk antibody responses in cattle infected with Mycobacterium avium subsp paratuberculosis. *Veterinary Microbiology*, 104, 43-53.
- HUDSON, C. 2008. An outbreak of Johne's disease in a dairy herd. *UK Vet*, 13, 1-4.
- HUNTER, S. W. & BRENNAN, P. J. 1981. A Novel Phenolic Glycolipid from Mycobacterium-Leprae Possibly Involved in Immunogenicity and Pathogenicity. *Journal of Bacteriology*, 147, 728-735.
- HUNTLEY, J. F. J., WHITLOCK, R. H., BANNANTINE, J. P. & STABEL, J. R. 2005. Comparison of diagnostic detection methods for Mycobacterium avium subsp paratuberculosis in North American bison. *Veterinary Pathology*, 42, 42-51.

- HUTTER, B. & DICK, T. 1999. Up-regulation of narX, encoding a putative 'fused nitrate reductase' in anaerobic dormant Mycobacterium bovis BCG. *FEMS Microbiology Letters*, 178, 63-9.
- INDERLIED, C. B., KEMPER, C. A. & BERMUDEZ, L. E. M. 1993. The Mycobacterium-Avium Complex. *Clinical Microbiology Reviews*, 6, 266-310.
- JACKSON, R. W., JOHNSON, L. J., CLARKE, S. R. & ARNOLD, D. L. 2011. Bacterial pathogen evolution: breaking news. *Trends in Genetics*, 27, 32-40.
- JARLIER, V. & NIKAIDO, H. 1994. Mycobacterial Cell-Wall - Structure and Role in Natural-Resistance to Antibiotics. *FEMS Microbiology Letters*, 123, 11-18.
- JAYACHANDRAN, R., SUNDARAMURTHY, V., COMBALUZIER, B., MUELLER, P., KORF, H., HUYGEN, K., MIYAZAKI, T., ALBRECHT, I., MASSNER, J. & PIETERS, J. 2007. Survival of mycobacteria in macrophages is mediated by coronin 1-dependent activation of calcineurin. *Cell*, 130, 37-50.
- JOHNE, H. A., AND J. FROTHINGHAM 1895. Ein eigenthuemlicher fall von tuberculose beim rind. *Dtsch. Z. Tiermed. Pathol*, 21, 438-454.
- JONES, W. D., GOOD, R. C., THOMPSON, N. J. & KELLY, G. D. 1982. Bacteriophage Types of Mycobacterium-Tuberculosis in the United-States. *American Review of Respiratory Disease*, 125, 640-643.
- JUNGERSEN, G., MIKKELSEN, H. & GRELL, S. N. 2011. Use of the johnin PPD interferon-gamma assay in control of bovine paratuberculosis. *Veterinary Immunology and Immunopathology*, 10.1016.
- JUSTE, R. A., GARRIDO, J. M., GEIJO, M., ELGUEZABAL, N., ADURIZ, G., ATXAERANDIO, R. & SEVILLA, I. 2005. Comparison of blood polymerase chain reaction and enzyme-linked immunosorbent assay for detection of Mycobacterium avium subsp paratuberculosis infection in cattle and sheep. *Journal of Veterinary Diagnostic Investigation*, 17, 354-359.
- KAISER, A. D. & JACOB, F. 1957. Recombination between Related Temperate Bacteriophages and the Genetic Control of Immunity and Prophage Localization. *Virology*, 4, 509-521.
- KAWAJI, S., NAGATA, R., WHITTINGTON, R. J. & MORI, Y. 2012. Detection of antibody responses against Mycobacterium avium subsp paratuberculosis stress-associated proteins within 30 weeks after infection in cattle. *Veterinary Immunology and Immunopathology*, 150, 101-111.
- KEER, J. T. & BIRCH, L. 2003. Molecular methods for the assessment of bacterial viability. *Journal of Microbiological Methods*, 53, 175-183.
- KELL, A. J., SOMASKANDAN, K., STEWART, G., BERGERON, M. G. & SIMARD, B. 2008. Superparamagnetic nanoparticle-polystyrene bead conjugates as pathogen capture mimics: A parametric study of factors affecting capture efficiency and specificity. *Langmuir*, 24, 3493-3502.
- KHEIRANDISH, R., TAFTI, A. K. & HOSSEINI, A. 2009. Classification of lesions and comparison of immunohistochemical and acid fast staining in diagnosis of naturally occurring paratuberculosis in goats. *Small Ruminant Research*, 87, 81-85.

- KIEHN, T. E., EDWARDS, F. F., BRANNON, P., TSANG, A. Y., MAIO, M., GOLD, J. W. M., WHIMBEY, E., WONG, B., MCCLATCHY, J. K. & ARMSTRONG, D. 1985. Infections Caused by Mycobacterium-Avium Complex in Immunocompromised Patients - Diagnosis by Blood Culture and Fecal Examination, Antimicrobial Susceptibility Tests, and Morphological and Seroagglutination Characteristics. *Journal of Clinical Microbiology*, 21, 168-173.
- KIMURA, K., REINHARDT, T. A. & GOFF, J. P. 2006. Parturition and hypocalcemia blunts calcium signals in immune cells of dairy cattle. *Journal of Dairy Science*, 89, 2588-2595.
- KNECHEL, N. A. 2009. Tuberculosis: Pathophysiology, Clinical Features, and Diagnosis. *Critical Care Nurse*, 29, 34-43.
- KOHLER, H., GYRA, H., ZIMMER, K., DRAGER, K. G., BURKERT, B., LEMSER, B., HAUSLEITHNER, D., CUSSLER, K., KLAWONN, W. & HESS, R. G. 2001. Immune reactions in cattle after immunization with a Mycobacterium paratuberculosis vaccine and implications for the diagnosis of M. paratuberculosis and M. bovis infections. *Journal of Veterinary Medicine Series B-Infectious Diseases and Veterinary Public Health*, 48, 185-195.
- KRALIK, P., NOCKER, A. & PAVLIK, I. 2010. Mycobacterium avium subsp paratuberculosis viability determination using F57 quantitative PCR in combination with propidium monoazide treatment. *International Journal of Food Microbiology*, 141, S80-S86.
- KRETZER, J. W., LEHMANN, R., SCHMELCHER, M., BANZ, M., KIM, K. P., KORN, C. & LOESSNER, M. J. 2007. Use of high-affinity cell wall-binding domains of bacteriophage endolysins for immobilization and separation of bacterial cells. *Applied and Environmental Microbiology*, 73, 1992-2000.
- LACQUA, A., WANNER, O., COLANGELO, T., MARTINOTTI, M. G. & LANDINI, P. 2006. Emergence of biofilm-forming subpopulations upon exposure of Escherichia coli to environmental bacteriophages. *Applied and Environmental Microbiology*, 72, 956-959.
- LAMONT, E. A., BANNANTINE, J. P., ARMIEN, A., ARIYAKUMAR, D. S. & SREEVATSAN, S. 2012. Identification and Characterization of a Spore-Like Morphotype in Chronically Starved Mycobacterium avium Subsp Paratuberculosis Cultures. *Plos One*, 7.
- LARSEN, A. B., R. S. MERKAL, AND R. C. CUTLIP 1975. Age of cattle as related to resistance to infection with Mycobacterium paratuberculosis. *American Journal of Veterinary Research*, 36, 225-257.
- LEDERER, E. 1977. The mycobacterial cell wall. *Pure Applied Chemistry*. 25:135-165.
- LEITE, F., STOKES, K., ROBBE-AUSTERMAN, S. & STABEL, J. 2013. Comparison of fecal DNA extraction kits for the detection of Mycobacterium avium subsp paratuberculosis by polymerase chain reaction. *Journal of Veterinary Diagnostic Investigation*, 25, 27-34.
- LEMUS, D., MARTIN, A., MONTORO, E., PORTAELS, F. & PALOMINO, J. C. 2005. Rapid Alternative Methods for Detection of Rifampicin Resistance in Mycobacterium tuberculosis. *International Journal of Antimicrobial Agents*, 26, S96-S96.

- LERNER, P. I. 1996. Nocardiosis. *Clinical Infectious Diseases*, 22, 891-903.
- LOEFFLER, J. M. & FISCHETTI, V. A. 2003. Synergistic lethal effect of a combination of phage lytic enzymes with different activities on penicillin-sensitive and -resistant *Streptococcus pneumoniae* strains. *Antimicrobial Agents and Chemotherapy*, 47, 375-377.
- LOESSNER, M. J., REES, C. E. D., STEWART, G. S. A. B. & SCHERER, S. 1996. Construction of luciferase reporter bacteriophage A511::luxAB for rapid and sensitive detection of viable *Listeria* cells. *Applied and Environmental Microbiology*, 62, 1133-1140.
- LOSINGER, W. C. 2005. Economic impact of reduced milk production associated with Johne's disease on dairy operations in the USA. *Journal of Dairy Research*, 72, 425-432.
- LYBECK, K. R., STORSET, A. K., DJONNE, B., VALHEIM, M. & OLSEN, I. 2011. Faecal shedding detected earlier than immune responses in goats naturally infected with *Mycobacterium avium* subsp *paratuberculosis*. *Research in Veterinary Science*, 91, 32-39.
- MANNING, E. J. B. & COLLINS, M. T. 2001. *Mycobacterium avium* subsp *paratuberculosis*: pathogen, pathogenesis and diagnosis. *Revue Scientifique Et Technique-Office International Des Epizooties*, 20, 133-150.
- MAREI, A. M., EL-BEHEDY, E. M., MOHTADY, H. A. & AFIFY, A. F. M. 2003. Evaluation of a rapid bacteriophage-based method for the detection of *Mycobacterium tuberculosis* in clinical samples. *Journal of Medical Microbiology*, 52, 331-335.
- MARSH, I. B., BANNANTINE, J. P., PAUSTIAN, M. L., TIZARD, M. L., KAPUR, V. & WHITTINGTON, R. J. 2006. Genomic comparison of *Mycobacterium avium* subsp *paratuberculosis* sheep and cattle strains by microarray hybridization. *Journal of Bacteriology*, 188, 2290-2293.
- MARTINSON, S. A., HANNA, P. E., IKEDE, B. O., LEWIS, J. P., MILLER, L. M., KEEFE, G. P. & MCKENNA, S. L. B. 2008. Comparison of bacterial culture, histopathology, and immunohistochemistry for the diagnosis of Johne's disease in culled dairy cows. *Journal of Veterinary Diagnostic Investigation*, 20, 51-57.
- MCDONALD, W. L., O'RILEY, K. J., SCHROEN, C. J. & CONDRON, R. J. 2003. Heat inactivation of *Mycobacterium avium* subsp *paratuberculosis* in milk. *Proceedings of the Seventh International Colloquium on Paratuberculosis*, 312-316.
- MCLEOD, R., BUSCHMAN, E., ARBUCKLE, L. D. & SKAMENE, E. 1995. Immunogenetics in the Analysis of Resistance to Intracellular Pathogens. *Current Opinion in Immunology*, 7, 539-552.
- MCNERNEY, R., KAMBASHI, B. S., KINKESE, J., TEMBWE, R. & GODFREY-FAUSSETT, P. 2004. Development of a bacteriophage phage replication assay for diagnosis of pulmonary tuberculosis. *Journal of Clinical Microbiology*, 42, 2115-2120.
- MCNERNEY, R., WILSON, S. M., SIDHU, A. M., HARLEY, V. S., AL SUWAIDI, Z., NYE, P. M., PARISH, T. & STOKER, N. G. 1998. Inactivation of mycobacteriophage D29 using ferrous ammonium sulphate as a tool for the detection of viable *Mycobacterium smegmatis* and M-tuberculosis. *Research in Microbiology*, 149, 487-495.

- MEYLAN, M., NICOLET, J., OPPLIGER, A., BURNENS, A. & MARTIG, J. 1994. Evaluation of 2 Techniques of Elisa for the Diagnosis of Bovine Paratuberculosis. *Schweizer Archiv Fur Tierheilkunde*, 136, 377-381.
- MILLAR, D., FORD, J., SANDERSON, J., WITHEY, S., TIZARD, M., DORAN, T. & HERMON TAYLOR, J. 1996. IS900 PCR to detect Mycobacterium paratuberculosis in retail supplies of whole pasteurized cows' milk in England and Wales. *Applied and Environmental Microbiology*, 62, 3446-3452.
- MOBIUS, P., HOTZEL, H., RASSBACH, A. & KOHLER, H. 2008. Comparison of 13 single-round and nested PCR assays targeting IS900, ISMav2, f57 and locus 255 for detection of Mycobacterium avium subsp paratuberculosis. *Veterinary Microbiology*, 126, 324-333.
- MONK, A. B., REES, C. D., BARROW, P., HAGENS, S. & HARPER, D. R. 2010. Bacteriophage applications: where are we now? *Letters to Applied Microbiology*, 51, 363-9.
- MONTEIRO, L., BONNEMAISON, D., VEKRIS, A., PETRY, K. G., BONNET, J., VIDAL, R., CABRITA, J. & MEGRAUD, F. 1997. Complex polysaccharides as PCR inhibitors in feces: Helicobacter pylori model. *Journal of Clinical Microbiology*, 35, 995-998.
- MORAVKOVA, M., BABAK, V., KRALOVA, A., PAVLIK, I. & SLANA, I. 2012. Culture- and quantitative IS900 real-time PCR-based analysis of the persistence of Mycobacterium avium subsp. paratuberculosis in a controlled dairy cow farm environment. *Applied Environmental Microbiology*, 78, 6608-14.
- MORTENSEN, H., NIELSEN, S. S. & BERG, P. 2004. Genetic variation and heritability of the antibody response to Mycobacterium avium subspecies paratuberculosis in Danish Holstein cows. *Journal of Dairy Science*, 87, 2108-2113.
- MULLER, B., DURR, S., ALONSO, S., HATTENDORF, J., LAISSE, C. J., PARSONS, S. D., VAN HELDEN, P. D. & ZINSSTAG, J. 2013. Zoonotic Mycobacterium bovis-induced tuberculosis in humans. *Emerging Infectious Diseases*, 19, 899-908.
- NAGATA, R., KAWAJI, S. & MORI, Y. 2013. Use of enoyl coenzyme A hydratase of Mycobacterium avium subsp. paratuberculosis for the serological diagnosis of Johne's disease. *Veterinary Immunology Immunopathology*, 155, 253-8.
- NAKAMURA, N., BURGESS, J. G., YAGIUDA, K., KUDO, S., SAKAGUCHI, T. & MATSUNAGA, T. 1993. Detection and Removal of Escherichia-Coli Using Fluorescein Isothiocyanate Conjugated Monoclonal-Antibody Immobilized on Bacterial Magnetic Particles. *Analytical Chemistry*, 65, 2036-2039.
- NASER, S. A., SCHWARTZ, D. & SHAFRAN, I. 2000. Isolation of Mycobacterium avium subsp paratuberculosis from breast milk of Crohn's disease patients. *American Journal of Gastroenterology*, 95, 1094-1095.
- NASER, S. A., GHOBRIAL, G., ROMERO, C. & VALENTINE, J. F. 2004. Culture of Mycobacterium avium subspecies paratuberculosis from the blood of patients with Crohn's disease. *Lancet*, 364, 1039-1044.
- NIELSEN, S. S. & TOFT, N. 2008. Ante mortem diagnosis of paratuberculosis: A review of accuracies of ELISA, interferon-gamma assay and faecal culture techniques. *Veterinary Microbiology*, 129, 217-235.

- NIELSEN, S. S. 2009. Use of diagnostics for risk-based control of paratuberculosis in dairy herds. *In Practice*, 31, 150-154.
- NIELSEN, S. S. & TOFT, N. 2009. A review of prevalences of paratuberculosis in farmed animals in Europe. *Preventive Veterinary Medicine*, 88, 1-14.
- O'FLAHERTY, S., ROSS, R. P. & COFFEY, A. 2009. Bacteriophage and their lysins for elimination of infectious bacteria. *FEMS Microbiology Reviews*, 33, 801-819.
- ORIGENE TECHNOLOGIES. 2012. Origene development guides: ELISA development guide.
http://www.origene.com/assets/documents/Assays/ELISA_Luminex_Development_Guide.pdf. Last accessed on 2nd April 2014.
- PARK, H. D., GUINN, K. M., HARRELL, M. I., LIAO, R., VOSKUIL, M. I., TOMPA, M., SCHOOLNIK, G. K. & SHERMAN, D. R. 2003. Rv3133c/dosR is a transcription factor that mediates the hypoxic response of *Mycobacterium tuberculosis*. *Molecular Microbiology*, 48, 833-843.
- PASUPULETI, M., SCHMIDTCHEN, A., CHALUPKA, A., RINGSTAD, L. & MALMSTEN, M. 2009. End-Tagging of Ultra-Short Antimicrobial Peptides by W/F Stretches to Facilitate Bacterial Killing. *Plos One*, 4.
- PATTERSON, C. J., LAVENTURE, M., HURLEY, S. S. & DAVIS, J. P. 1988. Accidental Self-Inoculation with *Mycobacterium-Paratuberculosis* Bacterin (Johnes Bacterin) by Veterinarians in Wisconsin. *Journal of the American Veterinary Medical Association*, 192, 1197-1199.
- PAYNE, K., SUN, Q. A., SACCHETTINI, J. & HATFULL, G. F. 2009. *Mycobacteriophage* Lysin B is a novel mycolylarabinogalactan esterase. *Molecular Microbiology*, 73, 367-381.
- PINEDO, P. J., RAE, D. O., WILLIAMS, J. E., DONOVAN, G. A., MELENDEZ, P. & BUERGELT, C. D. 2008. Association among results of serum ELISA, faecal culture and nested PCR on milk, blood and faeces for the detection of paratuberculosis in dairy cows. *Transboundary and Emerging Diseases*, 55, 125-133.
- PIURI, M. & HATFULL, G. F. 2006. A peptidoglycan hydrolase motif within the *mycobacteriophage* TM4 tape measure protein promotes efficient infection of stationary phase cells. *Molecular Microbiology*, 62, 1569-1585.
- PLAIN, K. M., MARSH, I. B., WALDRON, A. M., GALEA, F., WHITTINGTON, A. M., SAUNDERS, V. F., BEGG, D. J., DE SILVA, K., PURDIE, A. C. & WHITTINGTON, R. J. 2014. High-throughput direct fecal PCR assay for detection of *Mycobacterium avium* subsp. *paratuberculosis* in sheep and cattle. *Journal of Clinical Microbiology*, 52.
- POHANE, A. A., JOSHI, H. & JAIN, V. 2014. Molecular dissection of phage endolysin: An interdomain interaction confers host specificity in Lysin A of *Mycobacterium* phage D29. *Journal of Biology and Chemistry*.
- POUPART, P., COENE, M., VANHEUVERSWYN, H. & COCITO, C. 1993. Preparation of a Specific Rna Probe for Detection of *Mycobacterium-Paratuberculosis* and Diagnosis of Johnes Disease. *Journal of Clinical Microbiology*, 31, 1601-1605.

QAZI, S. N. A., REES, C. E. D., MELLITS, K. H. & HILL, P. J. 2001. Development of gfp vectors for expression in *Listeria monocytogenes* and other low G+C gram positive bacteria. *Microbial Ecology*, 41, 301-309.

QIAN, L. & WILKINSON, M. 1991. DNA Fragment Purification - Removal of Agarose 10 Minutes after Electrophoresis. *Biotechniques*, 10, 736-8.

RAIZMAN, E. A., WELLS, S. J., GODDEN, S. M., BEY, R. F., OAKES, M. J., BENTLEY, D. C. & OLSEN, K. E. 2004. The distribution of *Mycobacterium avium* ssp paratuberculosis in the environment surrounding Minnesota dairy farms. *Journal of Dairy Science*, 87, 2959-2966.

REDDACLIFF, L. A., VADALI, A. & WHITTINGTON, R. J. 2003. The effect of decontamination protocols on the numbers of sheep strain *Mycobacterium avium* subsp paratuberculosis isolated from tissues and faeces. *Veterinary Microbiology*, 95, 271-282.

REES, C. R. & BOTSARIS, G. 2012. The Use of Phage for Detection, Antibiotic Sensitivity Testing and Enumeration. In: CARDONA, P.-J. (ed.) *Understanding Tuberculosis - Global Experiences and Innovative Approaches to the Diagnosis*. Rijeka: InTech.

REZWAN, M., GRAU, T., TSCHUMI, A. & SANDER, P. 2007. Lipoprotein synthesis in mycobacteria. *Microbiology-Sgm*, 153, 652-658.

RICHARDS, W. D. & THOEN, C. O. 1977. Effect of freezing on the viability of *Mycobacterium paratuberculosis* in bovine feces. *Journal of Clinical Microbiology*, 6, 392-5.

RISKA, P. F., SU, Y., BARDAROV, S., FREUNDLICH, L., SARKIS, G., HATFULL, G., CARRIERE, C., KUMAR, V., CHAN, J. & JACOBS, W. R. 1999. Rapid film-based determination of antibiotic susceptibilities of *Mycobacterium tuberculosis* strains by using a luciferase reporter phage and the Bronx box. *Journal of Clinical Microbiology*, 37, 1144-1149.

ROBBE-AUSTERMAN, S., KRULL, A. C. & STABEL, J. R. 2006. Time delay, temperature effects and assessment of positive controls on whole blood for the gamma interferon ELISA to detect paratuberculosis. *Journal of Veterinary Medicine Series B-Infectious Diseases and Veterinary Public Health*, 53, 213-217.

RODRIGUEZ-LAZARO, D., D'AGOSTINO, M., HERREWEGH, A., PLA, M., COOK, N. & IKONOMOPOULOS, J. 2005. Real-time PCR-based methods for detection of *Mycobacterium avium* Subsp paratuberculosis in water and milk. *International Journal of Food Microbiology*, 101, 93-104.

RUNYON, E. H. 1959. Anonymous *Mycobacteria* in Pulmonary Disease. *Medical Clinics of North America*, 43, 273-290.

RUSTAD, T. R., SHERRID, A. M., MINCH, K. J. & SHERMAN, D. R. 2009. Hypoxia: a window into *Mycobacterium tuberculosis* latency. *Cellular Microbiology*, 11, 1151-1159.

RYBNIKER, J., KRAMME, S. & SMALL, P. L. 2006. Host range of 14 mycobacteriophages in *Mycobacterium ulcerans* and seven other mycobacteria including *Mycobacterium tuberculosis* - application for identification and susceptibility testing. *Journal of Medical Microbiology*, 55, 37-42.

- SARKIS, G. J., JACOBS, W. R. & HATFULL, G. F. 1995. L5 Luciferase Reporter Mycobacteriophages - a Sensitive Tool for the Detection and Assay of Live Mycobacteria. *Molecular Microbiology*, 15, 1055-1067.
- SCANU, A. M., BULL, T. J., CANNAS, S., SANDERSON, J. D., SECHI, L. A., DETTORI, G., ZANETTI, S. & HERMON-TAYLOR, J. 2007. Mycobacterium avium subspecies paratuberculosis infection in cases of irritable bowel syndrome and comparison with Crohn's disease and Johne's disease: Common neural and immune pathogenicities. *Journal of Clinical Microbiology*, 45, 3883-3890.
- SCHMELCHER, M., SHABAROVA, T., EUGSTER, M. R., EICHENSEHER, F., TCHANG, V. S., BANZ, M. & LOESSNER, M. J. 2010. Rapid Multiplex Detection and Differentiation of Listeria Cells by Use of Fluorescent Phage Endolysin Cell Wall Binding Domains. *Applied and Environmental Microbiology*, 76, 5745-5756.
- SCHOOLNIK, G. K., SUMMERS, W. C. & D WATSON, J. 2004. Phage offer a real alternative. *Nature Biotechnology*, 22, 505-506.
- SCHURCH, A. C. & VAN SOOLINGEN, D. 2012. DNA fingerprinting of Mycobacterium tuberculosis: From phage typing to whole-genome sequencing. *Infection Genetics and Evolution*, 12, 602-609.
- SHI, Y. B., YAN, Y. X., JI, W. H., DU, B., MENG, X. P., WANG, H. G. & SUN, J. H. 2012. Characterization and determination of holin protein of Streptococcus suis bacteriophage SMP in heterologous host. *Virology Journal*, 9.
- SIDOTI, F., BANCHE, G., ASTEGIANO, S., ALLIZOND, V., CUFFINI, A. M. & BERGALLO, M. 2011. Validation and standardization of IS900 and F57 real-time quantitative PCR assays for the specific detection and quantification of Mycobacterium avium subsp paratuberculosis. *Canadian Journal of Microbiology*, 57, 347-354.
- SMITH, G. P. & PETRENKO, V. A. 1997. Phage display. *Chemical Reviews*, 97, 391-410.
- SNIDER, D. E., JR., JONES, W. D. & GOOD, R. C. 1984. The usefulness of phage typing Mycobacterium tuberculosis isolates. *American Reviews of Respiratory Diseases*, 130, 1095-9.
- SPEARS, P. A., SUYEMOTO, M. M., PALERMO, A. M., HORTON, J. R., HAMRICK, T. S., HAVELL, E. A. & ORNDORFF, P. E. 2008. A Listeria monocytogenes mutant defective in bacteriophage attachment is attenuated in orally inoculated mice and impaired in enterocyte intracellular growth. *Infection and Immunity*, 76, 4046-4054.
- STABEL, J. R. 1997. An improved method for cultivation of Mycobacterium paratuberculosis from bovine fecal samples and comparison to three other methods. *Journal of Veterinary Diagnostic Investigation*, 9, 375-380.
- STABEL, J. R. 1998. Johne's Disease: A Hidden Threat. *Journal of Dairy Science*, 81, 283-288.
- STANLEY, E. C., MOLE, R. J., SMITH, R. J., GLENN, S. M., BARER, M. R., MCGOWAN, M. & REES, C. E. D. 2007. Development of a new, combined rapid method using phage and PCR for detection and identification of viable Mycobacterium paratuberculosis bacteria within 48 hours. *Applied and Environmental Microbiology*, 73, 1851-1857.

- STEINITZ, M. 2000. Quantitation of the blocking effect of tween 20 and bovine serum albumin in ELISA microwells. *Analysis of Biochemistry*, 282, 232-8.
- STERMANN, M., SEDLACEK, L., MAASS, S. & BANGE, F. C. 2004. A promoter mutation causes differential nitrate reductase activity of *Mycobacterium tuberculosis* and *Mycobacterium bovis*. *Journal of Bacteriology*, 186, 2856-2861.
- STEWART, L. D., MCNAIR, J., MCCALLAN, L., THOMPSON, S., KULAKOV, L. A. & GRANT, I. R. 2012. Production and Evaluation of Antibodies and Phage Display-Derived Peptide Ligands for Immunomagnetic Separation of *Mycobacterium bovis*. *Journal of Clinical Microbiology*, 50, 1598-1605.
- STRATMANN, J., DOHMANN, K., HEINZMANN, J. & GERLACH, G. F. 2006. Peptide aMptD-mediated capture PCR for detection of *Mycobacterium avium* subsp paratuberculosis in bulk milk samples. *Applied and Environmental Microbiology*, 72, 5150-5158.
- STRATMANN, J., STROMMINGER, B., STEVENSON, K. & GERLACH, G. F. 2002. Development of a peptide-mediated capture PCR for detection of *Mycobacterium avium* subsp paratuberculosis in milk. *Journal of Clinical Microbiology*, 40, 4244-4250.
- STROMMINGER, B., STEVENSON, K. & GERLACH, G. F. 2001. Isolation and diagnostic potential of ISMav2, a novel insertion sequence-like element from *Mycobacterium avium* subspecies paratuberculosis. *FEMS Microbiology Letters*, 196, 31-37.
- SU, X. L. & LI, Y. 2004. Quantum dot biolabeling coupled with immunomagnetic separation for detection of *Escherichia coli* O157:H7. *Analysis of Chemistry*, 76, 4806-10.
- SULAKVELIDZE, A. 2005. Phage therapy: On attractive option for dealing with antibiotic-resistant bacterial infections (vol 10, pg 808, 2005). *Drug Discovery Today*, 10, 877-877.
- SWEENEY, R. W. 2011. Pathogenesis of Paratuberculosis. *Veterinary Clinics of North America-Food Animal Practice*, 27, 537-540.
- SWIFT, B. M., DENTON, E. J., MAHENDRAN, S. A., HUXLEY, J. N. & REES, C. E. 2013. Development of a rapid phage-based method for the detection of viable *Mycobacterium avium* subsp. paratuberculosis in blood within 48 h. *Journal of Microbiological Methods*, 94, 175-179.
- TELENTI, A., IMBODEN, P., MARCHESI, F., LOWRIE, D., COLE, S., COLSTON, M. J., MATTER, L., SCHOPFER, K. & BODMER, T. 1993. Detection of Rifampicin-Resistance Mutations in *Mycobacterium-Tuberculosis*. *Lancet*, 341, 647-650.
- THORESEN, O. F., FALK, K. & EVENSEN, O. 1994. Comparison of immunohistochemistry, acid-fast staining, and cultivation for detection of *Mycobacterium paratuberculosis* in goats. *Journal of Veterinary Diagnostic Investigations*, 6, 195-9.
- THORNTON, C. G. & PASSEN, S. 2004. Inhibition of PCR amplification bovine fecal specimens with by phytic acid, and treatment of phytase to reduce inhibition. *Journal of Microbiological Methods*, 59, 43-52.

- TSIEN, R. Y. 1998. The green fluorescent protein. *Annual Review of Biochemistry*, 67, 509-544.
- TSUCHIZAKI, N., ISHIKAWA, J. & HOTTA, K. 2000. [Colony PCR for rapid detection of antibiotic resistance genes in MRSA and enterococci]. *Japan Journal of Antibiotics*, 53, 422-9.
- TURPIN, P. E., MAYCROFT, K. A., BEDFORD, J., ROWLANDS, C. L. & WELLINGTON, E. M. H. 1993. A Rapid Luminescent-Phage Based Mpn Method for the Enumeration of Salmonella-Typhimurium in Environmental-Samples. *Letters in Applied Microbiology*, 16, 24-27.
- UYTTENDAELE, M., VAN HOORDE, I. & DEBEVERE, J. 2000. The use of immuno-magnetic separation (IMS) as a tool in a sample preparation method for direct detection of L-monoctogenes in cheese. *International Journal of Food Microbiology*, 54, 205-212.
- VAN KOOTEN, H. C. J., MACKINTOSH, C. G. & KOETS, A. P. 2006. Intra-uterine transmission of paratuberculosis (Johne's disease) in farmed red deer. *New Zealand Veterinary Journal*, 54, 16-20.
- VORDERMEIER, H. M., COCKLE, P. C., WHELAN, A., RHODES, S., PALMER, N., BAKKER, D. & HEWINSON, R. G. 1999. Development of diagnostic reagents to differentiate between Mycobacterium bovis BCG vaccination and M-bovis infection in cattle. *Clinical and Diagnostic Laboratory Immunology*, 6, 675-682.
- WARD, L. R., DESA, J. D. H. & ROWE, B. 1987. A Phage-Typing Scheme for Salmonella-Enteritidis. *Epidemiology and Infection*, 99, 291-294.
- WATANABE, K. & TAKESUE, S. 1972. The requirement for calcium in infection with Lactobacillus phage. *Journal of General Virology*, 17, 19-30.
- WATERS, W. R., MILLER, J. M., PALMER, M. V., STABEL, J. R., JONES, D. E., KOISTINEN, K. A., STEADHAM, E. M., HAMILTON, M. J., DAVIS, W. C. & BANNANTINE, J. P. 2003. Early induction of humoral and cellular immune responses during experimental Mycobacterium avium subsp paratuberculosis infection of calves. *Infection and Immunity*, 71, 5130-5138.
- WATERS, W. R., NONNECKE, B. J., PALMER, M. V., ROBBE-AUSTERMANN, S., BANNANTINE, J. P., STABEL, J. R., WHIPPLE, D. L., PAYEUR, J. B., ESTES, D. M., PITZER, J. E. & MINION, F. C. 2004. Use of recombinant ESAT-6 : CFP-10 fusion protein for differentiation of infections of cattle by Mycobacterium bovis and by M. avium subsp avium and M. avium subsp paratuberculosis. *Clinical and Diagnostic Laboratory Immunology*, 11, 729-735.
- WAYNE, L. G. 1994. Dormancy of Mycobacterium-Tuberculosis and Latency of Disease. *European Journal of Clinical Microbiology & Infectious Diseases*, 13, 908-914.
- WAYNE, L. G., AND KUBICA G. P. 1986. The Mycobacteria. In: GIBBONS, E. B. A. N. E. (ed.) *Bergey's manual of determinative bacteriology*. 9 ed. Baltimore: The Williams & Wilkins Co.
- WHITLOCK, R. H., WELLS, S. J., SWEENEY, R. W. & VAN TIEM, J. 2000. ELISA and fecal culture for paratuberculosis (Johne's disease): sensitivity and specificity of each method. *Veterinary Microbiology*, 77, 387-398.

WHITTINGTON, R. J., BOWER, K. & BEGG, D. J. 2010. Optimisation of culture of *Mycobacterium avium* subspecies paratuberculosis from blood samples. *Journal of Microbiological Methods*, 80, 93-99.

WHITTINGTON, R. J. 2009. Factors Affecting Isolation and Identification of *Mycobacterium avium* subsp paratuberculosis from Fecal and Tissue Samples in a Liquid Culture System. *Journal of Clinical Microbiology*, 47, 614-622.

WHITTINGTON, R. J., MARSHALL, D. J., NICHOLLS, P. J., MARSH, A. B. & REDDACLIFF, L. A. 2004. Survival and dormancy of *Mycobacterium avium* subsp paratuberculosis in the environment. *Applied and Environmental Microbiology*, 70, 2989-3004.

WHITTINGTON, R. J. & SERGEANT, E. S. G. 2001. Progress towards understanding the spread, detection and control of *Mycobacterium avium* subsp para-tuberculosis in animal populations. *Australian Veterinary Journal*, 79, 267-278.

WINDBERGER, U., BARTHOLOVITSCH, A., PLASENZOTTI, R., KORAK, K. J. & HEINZE, G. 2003. Whole blood viscosity, plasma viscosity and erythrocyte aggregation in nine mammalian species: reference values and comparison of data. *Experimental Physiology*, 88, 431-40.

WINDER, F. G. 1982. Mode of action of the antimycobacterial agents and associated aspects of the molecular biology of the mycobacteria, p. 417-521. In C. Ratledge and J. Stanford (ed.), *The biology of the mycobacteria*, vol. 1. Academic Press, London.

WORLD HEALTH ORGANISATION (WHO). 2011. Leprosy elimination: the microbiology of leprosy. <http://www.who.int/lep/microbiology/en/index.html>. Last accessed online on 2nd April 2014.

WRIGHT, A., HAWKINS, C. H., ANGGARD, E. E. & HARPER, D. R. 2009. A controlled clinical trial of a therapeutic bacteriophage preparation in chronic otitis due to antibiotic-resistant *Pseudomonas aeruginosa*; a preliminary report of efficacy. *Clinical Otolaryngology*, 34, 349-357.

ZIMMER, K., DRAGER, K. G., KLAWONN, W. & HESS, R. G. 1999. Contribution to the diagnosis of Johne's disease in cattle. Comparative studies on the validity of Ziehl-Neelsen staining, faecal culture and a commercially available DNA-Probe (R) test in detecting *Mycobacterium paratuberculosis* in faeces from cattle. *Journal of Veterinary Medicine Series B-Infectious Diseases and Veterinary Public Health*, 46, 137-140.

ZURBRICK, B. G., FOLLETT, D. M. & CZUPRYNSKI, C. J. 1988. Cytokine Regulation of the Intracellular Growth of *Mycobacterium-Paratuberculosis* in Bovine Monocytes. *Infection and Immunity*, 56, 1692-1697.

CHAPTER 10

APPENDICES

Appendix 1. Manuscript in production for submission to Journal of bacteriology

Title: Induction of pigment production in cattle strains of *Mycobacterium avium* subsp. *paratuberculosis*

INTRODUCTION

The research of mycobacterial pigments has often been limited taxonomic and identification purposes. Mycobacterial pigments, especially carotenoids have been clearly associated with cellular photoprotection and survival, the regulation of their production and their physiological role have been largely unstudied (Robledo et al., 2011). Thus any *Mycobacterium's* ability to produce pigmentation is of clinical interest for identification and diagnostic purposes as well as understanding causative of infection. Saviola and Felton (2011) have previously found that pigmentation can be induced in non-pigmented strains of mycobacteria by growth on acidic agar.

Different strains of MAP can infect different hosts. Marsh et al (1996) developed a simple REA-PCR to differentiate between cattle (C) and sheep (S) strains of MAP. Where broadly speaking; C strains generally infect cattle and S strains generally infect sheep, although there have been cases of C strains infecting sheep and vice versa as well as there being evidence of strains being shared between wild and domesticated animal species (Motiwala et al. 2004).

MAP can take several months to culture. The general colony morphology during early growth are small smooth and convex, and most importantly not pigmented (Merkal and Curran, 1974), however as the cultures age the colonies can become differentiated, with rough edged, crenulated colonies described (Fregnan and Smith, 1962). Although MAP is not in the pigmented classes in Runyon's classification, sheep strains of MAP have been reported to be pigmented based on the pathological representation of Johne's disease affected sheep intestine, which appears yellow and orange (Stevenson et al, 2002). These organisms are difficult to culture and they generally take longer to form colonies. There are no reported pigmented cattle strains of MAP.

Observations made in laboratory had shown that cattle strains of MAP cultured on solid agar for over six months in plastic Universal vessels became pigmented whereas those cultured in glass Universal vessels did not.

These investigations were based on whether the pigmented organisms were MAP and if they were previously unknown pigmented cattle strains of MAP. The conditions required for pigment induction was then investigated, on two cattle

strains of MAP, *M. avium*, *M. intracellulare*, *M. bovis* BCG and *M. smegmatis*. Resistance to bacteriophage infection was also investigated as it was found that changes in culture conditions in mycobacteria can result in phage infection resistance (see Chapter 6).

RESULTS

Original observations and molecular analysis

The original pigmented observations were made with MAP cells (K10; reference cattle strain) slopes cultured in 30 ml plastic Universals (Sterilin, UK) for over 3 years. Orange pigmentation can clearly be seen, compared to those cultured in glass at the same time (Fig. 1). Colonies from the slope were subcultured to rule out contamination from other potential pigment causing bacteria. The colonies were also subjected to a MAP specific PCR. The results show that each pigmented colony was positive for the MAP-specific f57 gene, as well as this no contamination was seen from the subculture.

As the organisms were confirmed as MAP, further analysis was carried out to determine whether they were cattle strains or the known potentially pigmented sheep strains of MAP. REA-PCR analysis has been shown to be able to differentiate between and cattle and sheep strains of MAP by the point mutations in the *IS1311* sequences (Marsh et al., 1999) found in the MAP genome. The results show that the pigmented cells were from cattle strains of MAP and not sheep (Fig. 2).

Figure 1. Original pigmented MAP

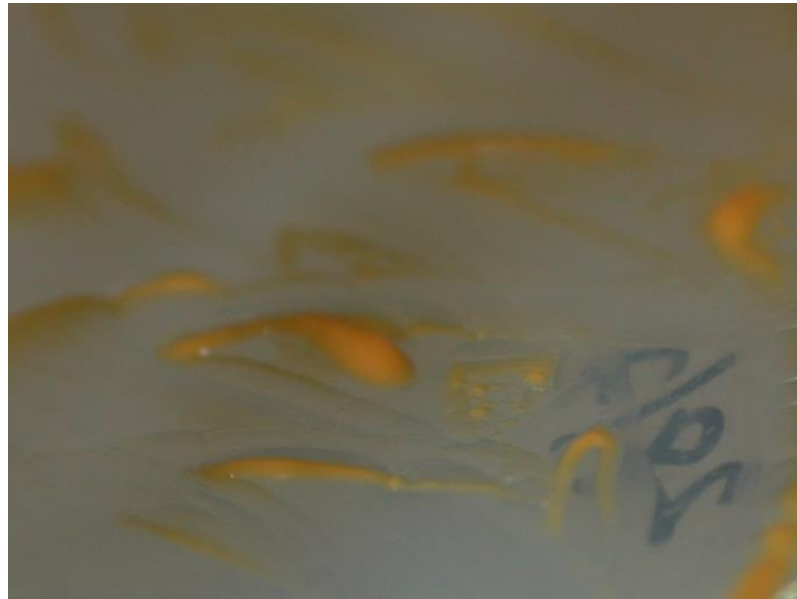
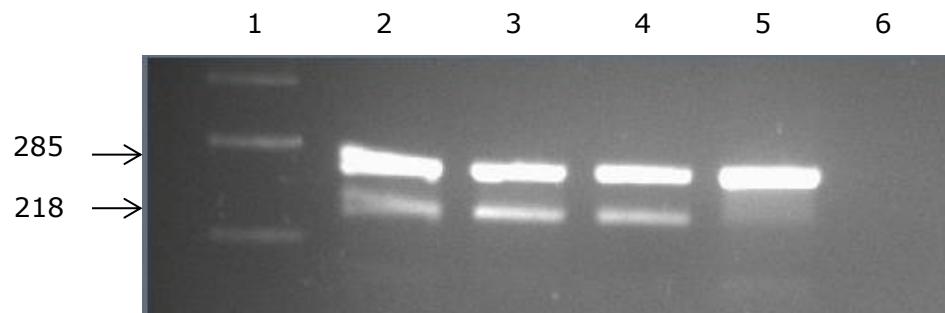


Image shows the original pigmented presumptive MAP colonies cultured on Middlebrook 7h10 (Becton Dickenson) for over 2 years.

Figure 2. REA-Analysis of unknown MAP isolate



REA-PCR analysis of the amplified *IS1311* gene, from two pigmented cattle MAP strains (presumptive K10 and ATCC 19851; lanes 2 and 3 respectively), after treatment with the restriction enzyme *Hinf*I. . Lane 3 is confirmed MAP K10 genomic DNA. Lane 5 is genomic DNA extracted from a pigmented sheep strain DNA (Kindly donated by K. Stevenson). Lane 6 is negative control (SDW). Bands at 285 bp show the presence of the *IS1311* element in all MAP strains. Bands at 218 bp show the point mutation in the insertion element found only in cattle strains of MAP.

Carotenoid operon in cattle strain of MAP (K10)

Many mycobacteria have the ability to produce pigments in response to light or stresses. The carotenoid biosynthesis pathway has been established for a long time in a lot of organisms, including the operon responsible for its synthesis in mycobacteria. Pigment synthesis genes found in *M. tuberculosis* were used to find homologues in the MAP K10 genome using BLAST. The results show that MAP K10 has a same operon for creating carotenoid pigments as *M. tuberculosis* (Figure 3). This shows that the cattle strains of MAP have the genes present to produce pigments, however having the genes does not necessarily mean that are able to use them.

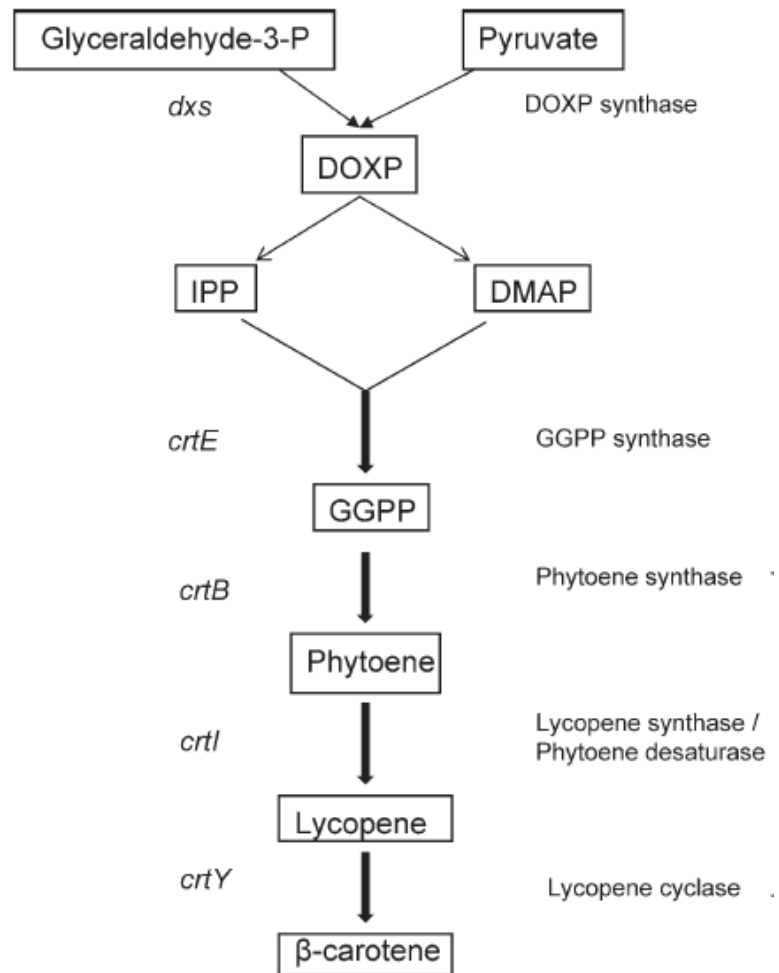
Role of stress on pigmentation in *M. smegmatis* and MAP

The initial observations of pigmentations in MAP could have been because of the length of time since culture. Old cultures of mycobacteria have been known to become pigmented over time (Dworkin and Foster, 1958). To ensure this was not the case, *M. smegmatis* was used as a fast-growing model organisms to determine whether they have the ability to become pigmented. It has already been described by Saviola and Felton (2011) that *M. smegmatis* can produce pigments when grown on acidic agar. When the MAP cells produced pigments, that only did so in plastic universals and not in glass.

Differences between the glass and plastic were postulated, such as permeability to air and what light is let through. If the plastic let more air in, the cells would be less likely to go completely into a dormant state (as seen in Chapter 6). Thus slow steady growth when oxygen is present may result in a drop in pH in the bacterial colonies as they grow, replicating the acidic conditions seen by Saviola and Felton (2011).

Initially the ability of *M. smegmatis* and MAP to produce pigmentation was investigated by repeating the experiments by Saviola and Felton (2011). *M. smegmatis* and MAP were cultured on 7h10 agar slopes, at pH 6.5, pH 5.5 and pH 5. The results show that both MAP and *M. smegmatis* did not produce pigments at pH 7, but did at pH 6 (Fig. 4). No growth was seen by either of the cells at pH 5 (data not shown).

Figure 3. Beta-carotene biosynthetic pathway in mycobacteria



Consensus biosynthesis pathway of beta-carotene in mycobacteria. Genetic precursors found in the MAP K10 genome are listed on the left and the enzymes they make are on the right (Robledo et al., 2011).

Figure 4. Culture of MAP and *M. smegmatis* on 7h10 agar adjusted to pH 6.5 and pH 5.5

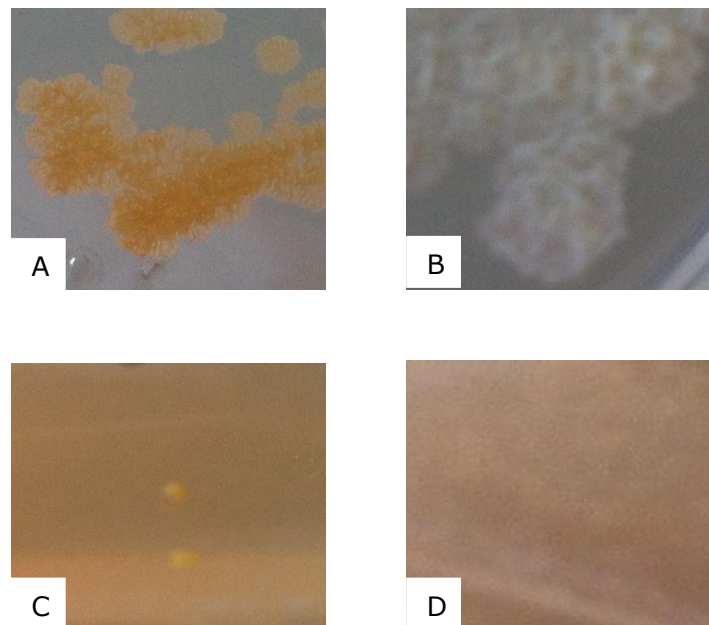


Figure shows *M. smegmatis* (FPTB strain; panel A and B) and MAP (K10; panel C and D) grown on 7h10 agar adjusted to pH 6.5 (panel A and C) or pH 5.5. Orange colonies can clearly be seen after 4 d and 2 weeks incubation at 37 °C for *M. smegmatis* and MAP respectively.

As both MAP and *M. smegmatis* have the ability to produce pigments on acidic agar, *M. smegmatis* was carried forward as a model organisms to determine what physical stresses (that may or may not result in a pH drop) are involved in pigment production. Thus aerobic, anaerobic and limited oxygen liquid cultures of *M. smegmatis* were prepared to determine if a reduction in oxygen decreases the pH. The results show that when grown aerobically there is a drop in pH to 6.3, but there is no pigment production, similarly when the *M. smegmatis* was cultured with less oxygen available, pigmentation did occur, but the pH dropped to the same level as the aerobic culture (Fig. 5). This suggested that pH is not the only factor in pigment production.

As some mycobacteria can form pigment as a response to light, the experiment above was repeat in the light and in the dark, and there was no difference in the results seen (data not shown).

Future Work

The novel observation of MAP being able to produce pigments goes against the Ruyoun classification. As the ability to produce pigments can be used as a diagnostic tool, ensuring culture conditions and the environment is controlled is vitally important. Further work will be carried out in identifying if there is any difference in expression of the pigment biosynthesis genes qRT-PCR.

Figure 5. Effect of oxygen, no oxygen and limited oxygen on pigment production

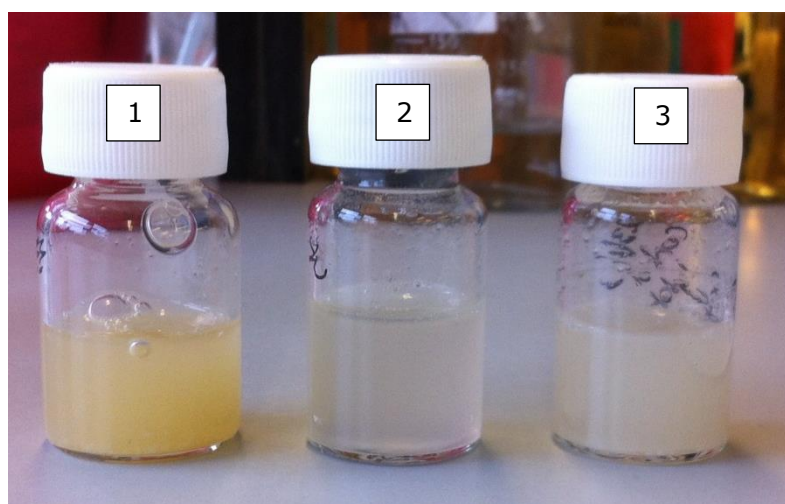


Image shows the effect of limited oxygen availability (1), no oxygen (2) and oxygen (3) on the ability of *M. smegmatis* to produce pigments.

Appendix 2. Manuscript in production for submission to Journal of Applied Microbiology

Title: Cloning and expression of bacteriophage D29 lysins and their application in lysing mycobacteria

INTRODUCTION

The life-cycle of a lytic bacteriophage involves, the phage binding to specific cell receptors on their host, injecting their genetic material and using their host's machinery to replicate themselves. Once the progeny phage are produced, generally a combination of holins and lysins are produced. The holins create holes in the membrane to allow lysins to reach their target to break open the cell wall.

Lysins are highly evolved enzymes produced by the phage to digest the bacterial cell wall for phage progeny release (Fischetti, 2005). They accumulate in the cytosol during late stage of infection and hydrolyse the bacterial hosts cell wall (Fenton et al., 2010). Lysins generally need the holin protein to allow them to get to their cell wall target. Bacteriophage lysins are highly specific for their host cells. The basic structure of phage lysins consist of two domains; a catalytic domain, which is involved in the breakdown of the host cell wall, and the highly specific binding domain, which brings the catalytic side to the specific site of action for their host (Schmelcher et al., 2010).

In Gram-positive organisms, bacteriophage lysins have been used externally to lyse cells. As the peptidoglycan layer of Gram-positive cell walls are found on the outside of the cell, expressed recombinant lysin proteins are able to reach their target without the need of the holin protein. This has been carried out on pathogenic Gram-positive organisms such as; *Listeria monocytogenes* (Loessner et al., 1996), *Staphylococcus aureus* (O'Flaherty et al., 2009) and *Streptococcus pneumoniae* (Loeffler and Fischetti, 2003). However the effects of phage lysins on Gram-negative bacteria have not been fully exploited, due to outer membrane, creating a barrier for the lysins to interact with the peptidoglycan cell wall (Fischetti, 2005).

There are two lysin genes in bacteriophage D29; Lysin A and Lysin B (Pohane et al., 2014). The unusual mycolic acid rich cell wall of mycobacteria means that the phage, not only have to get through the peptidoglycan layer, but also penetrate the mycolic acid outer membrane. It has been postulated that Lysin A has the ability to degrade the peptidoglycan layer, whereas Lysin B cleaves mycolarabinogalactan to release the mycolic acids (Payne et al., 2009). Where

Lysin A is involved directly with cell lysis, Lysin B is thought to aid in the efficiency of lysis by disrupting the outer membrane sufficiently to allow the progeny phage release (Payne et al. 2009).

Lysin B from mycobacteriophage Ms6 has been found to have activity on the outside of the cell. The function of Lysin B from Ms6 has similar functions to the D29's Lysin B, where they both have sites of action on mycolarabinogalactan - peptidoglycan complex (Gil et al., 2010).

The aim of these investigations was to clone and over express both Lysin A and Lysin B from phage D29 and to determine whether they had the ability to inhibit the growth of different mycobacteria.

RESULTS

Cloning and expressing phage D29 lysins

Primers were designed to amplify both Lysin A and B from DNA extracted from phage D29 and to allow directional cloning into the plasmid pET 23a (Invitrogen, UK). Both genes were initially processed through the NEB Cutter online software to determine what restriction sites might be present within the gene. The results show that none of the restriction sites present in the pET23a plasmid sequence were present in either of the lysin gene sequences. Thus each primer for each gene was designed to carry *Bam*HI on the 5' end and *Nhe*I on the 3' end. *Sma*I was also added to each end of the gene. The stop codon was removed from each sequence and added after 6 x His sequence to allow the protein to be His-Tag purified. The two lysin genes were amplified and cloned into the plasmid (pET 23a; Fig 1). The plasmid was then transformed into chemically competent *E. coli* (Top10) and grown overnight on ampicillin selective LB agar. Colonies that had grown on the plates were then picked and patch plated and in parallel screened by PCR for the correct inserts. The successful clones were mini-prepped and transformed into an expression strain (*E. coli* BL21 DE3).

A pilot expression experiment was then carried out. The plasmid was transformed into the expression strain of *E. coli* and was incubated overnight at 37 °C. The samples were then split and one induced with IPTG (0.5 mM) and one was not. The cells were incubated for 5 h and every hour, starting at time point zero, samples were taken and analysed using SDS-page. The results show that no extra bands were detected from the protein prep of Lysin A or Lysin B (data not shown). This may be due to the proteins being insoluble. Indeed if the lysins are meant to interact within the lipid rich, cell wall of the mycobacteria, being insoluble would be likely. Thus the insoluble protein fraction was extracted from

the cells. The results show, however that once again no significant bands were present, suggesting no expression of soluble or insoluble recombinant proteins.

Figure 1. Amplification of the lysin A and B

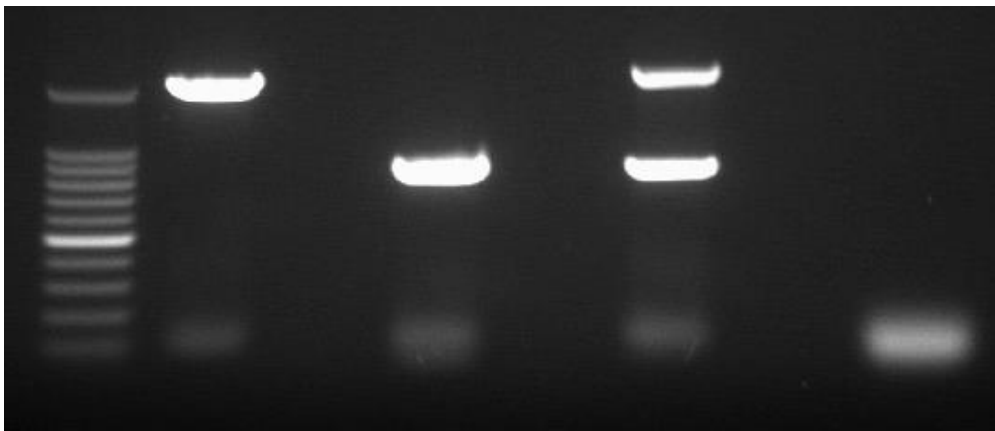


Image shows lane 1; 100 bp ladder. Lane 2 amplification of lysin A DNA from cloned plasmid, lane 3; amplification of lysin B DNA from cloned plasmid, lane 4, amplification of lysin A and B DNA from DNA extraction from phage D29 and lane 5, negative control (SDW).

The cells, left over from the pilot protein expression were used to determine whether the Lysin DNA was still present in the *E. coli*. Lysin specific PCR's were carried on DNA extracted from the *E. coli* using a crude boiling method. The template DNA was diluted 1 in 100 and the PCR carried out. The results show that there was no Lysin DNA present in either of the lysin preparations.

As mentioned in the introduction, lysin proteins generally have two domains, a highly specific binding domain and a catalytic domain, which is generally more broad ranging in activity. The lysin proteins are therefore likely to be toxic to the *E. coli* host, and 'leaky' expression of the protein, by the BL21 strain of *E. coli* may have resulted in the gene not being expressed. As well as this, expression into a high copy-number plasmid such as pET23a may result in over expression of this toxic gene. Therefore the cloning strategy was altered to adjust for toxic gene expression.

The primers of the lysin gene were altered for TOPO directional cloning into a commercial linearised expression plasmid, pET101-D (Invitrogen, UK). The lysin primers were designed to have a four nucleotide sequences on the 5' end of the gene to clone into the compatible ends of the linearised plasmid. The cloned plasmid was transformed into chemically competent *E. coli* (TOP10). The samples were then plated onto ampicillin selective LB agar and incubated overnight. Colonies that formed were in parallel; patch plated and screened by PCR for the Lysin genes. The successful clones' plasmids were screened again for the inserts, to ensure the lysin DNA was still present in the sample, the results show that the both were.

The plasmids were then transformed into an expression strain of *E. coli* - BL21 (DE3) pLysS - that is under the control of IPTG, and has a T7 lysozyme that lowers the background expression level of target genes under the control of the T7 promoter, but does not interfere with the level of expression following induction with IPTG. By having a tighter control on the expression of potentially toxic proteins, leaky expression causing the gene to be knocked out will be less likely to occur. The samples were expressed fractions were analysed every hour by SDS-page and results show that once again there was no expression of the recombinant protein.

Optimising lysin protein expression

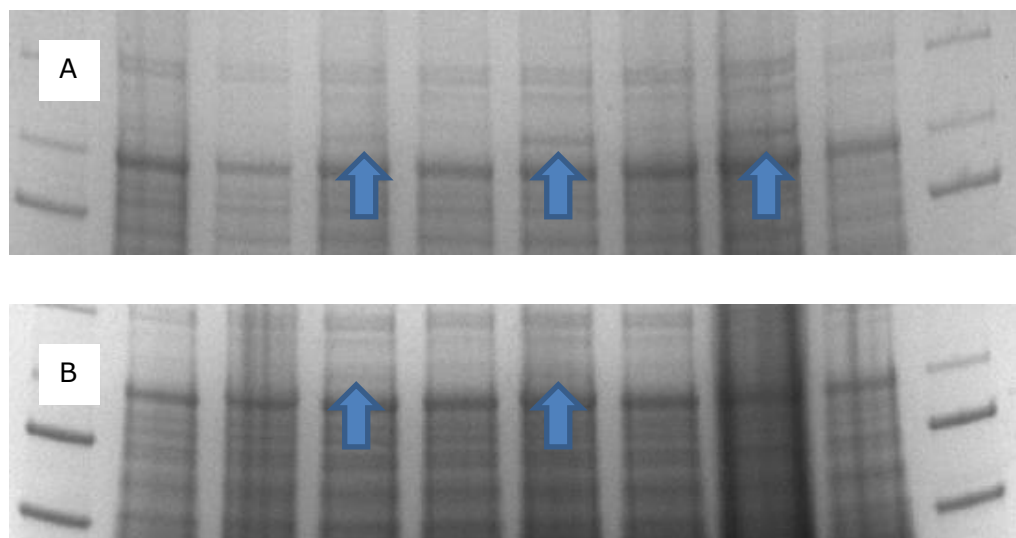
No recombinant protein was seen in both of the pilot protein expression experiments. Proteins can take some time after expression to correctly fold and express. The time for expression was therefore increased from a maximum of 5 h to 8 and 10 h. the temperature the *E. coli* was induced and grown at was also

reduced to 25 °C. The results show that both Lysin A and Lysin B produced a new band in the soluble and insoluble fraction (Fig. 2).

As the lysin looked to be expressed after IPTG induction, colonies harbouring the successful clone were plated onto plates containing IPTG and incubated overnight. The cells were then killed and lysed with chloroform to expose any lysin expressed by the cells. As a control, colonies were also plated on media without IPTG so that no lysin proteins would be expressed. A soft agar overlay was plated onto the lysed cells after overnight incubation containing 1×10^7 cfu ml^{-1} *M. smegmatis* and this was incubated at 37 °C for 24 h.

The results show that there were zones of clearing from where *E. coli* was expressing the lysin genes (Fig. 3). On the negative control, there was no inhibition of growth from the lysin genes.

Figure 2. SDS-page analysis of lysin gene expression



SDS-page analysis of protein expression of lysin A (Panel A) and lysin B (Panel B). Arrows mark areas of increase band intensity after protein induction with IPTG.

Figure 3. Crude cell lysis on lysin A and B test

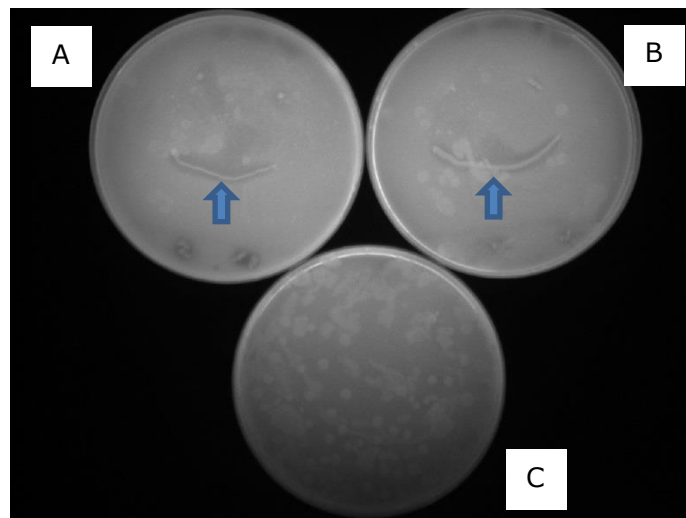


Figure showing the inhibition (arrows) of growth on *M. smegmatis* using a chloroform crude cell lysis method on cultures expressing lysin A (picture A), lysin b (picture B) and a mixture of unexpressed colonies containing genes that encode lysin A and lysin B (picture C).

Future Work

The initial results show that it was possible to clone in both phage lysins into strains of *E. coli*. Although the plasmids were not stable within the *E. coli* host, it was possible to have active protein expressed and in a crude method to inhibit the growth of *M. smegmatis*. Further work will be carried out on trying to purify the phage lysins, using the His-tags and to characterise their mode of action and their optimal conditions for lysis.

Appendix 4.1. Mead's resource equations

Obtained from: Mead R. 1988. The design of experiments. Cambridge, New York: Cambridge University Press. 620 p

The Resource equation method (Mead 1988) of determining sample size is appropriate for experiments which can be analysed using the analysis of variance such as:

The method depends on the law of diminishing returns. Adding one experimental unit to a small experiment gives good returns, while adding it to a large experiment does not do so. In the general experimental situation the total variation is divided into three components, each serving a different function." These three components consist of:

1. The treatment component, T, corresponding to the questions being asked
2. The blocking component B, representing environmental effects allowed for in the design
3. The error component E, being used to estimate the variance, S^2 which is used for calculating the standard errors for treatment comparisons.

The method equation is:

$$E=N-B-T,$$

Where E is the error degrees of freedom (df) and should be between 10 and 20, N is the total df, B is the blocks df, and T is the treatments df.

Example: suppose an experiment is planned with four treatments, with eight animals per group (32 rats total). In this case $N=31$, $B=0$, $T=3$, so $E=28$.

Conclusion: this experiment is a bit too large, and six animals per group might be more appropriate.

Appendix 7.1. CODON optimisation table for *E. coli* – Malloy et al. (1996)

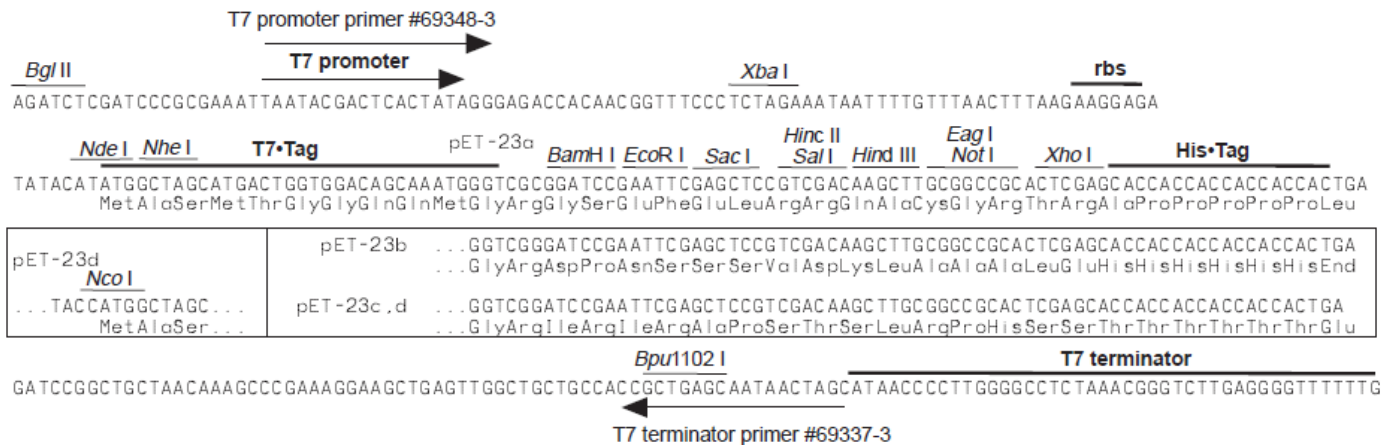
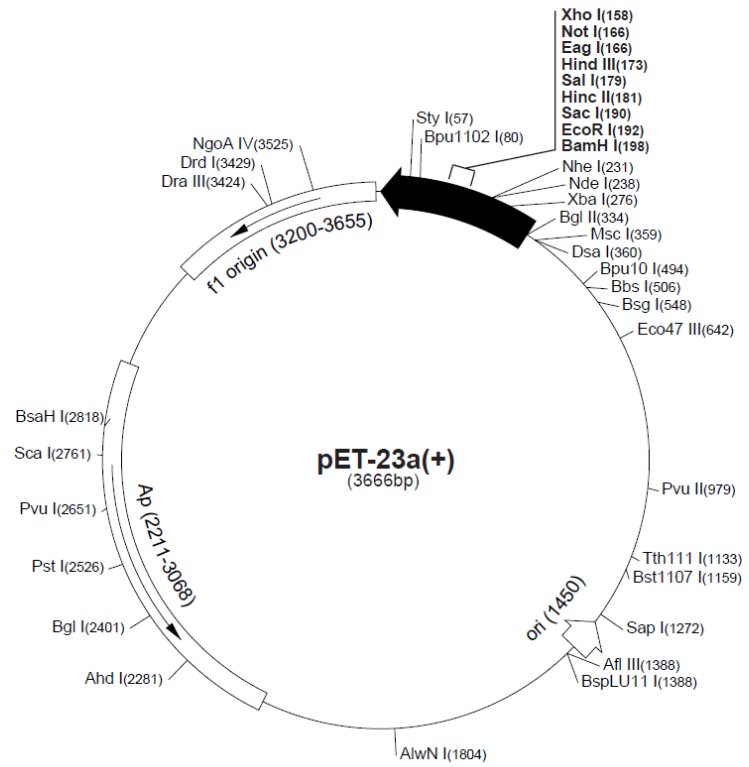
Amino Acid	Abbreviation	Codon	Total number	Fraction
Glycine	G	GGG	17628.00	0.15
Glycine	G	GGA	12696.00	0.11
Glycine	G	GGT	39862.00	0.34
Glycine	G	GGC	47212.00	0.40
Glutamate	E	GAG	28529.00	0.31
Glutamate	E	GAA	63484.00	0.69
Aspartate	D	GAT	51670.00	0.63
Aspartate	D	GAC	30559.00	0.37
Valine	V	GTG	42097.00	0.37
Valine	V	GTA	17443.00	0.15
Valine	V	GTT	29487.00	0.26
Valine	V	GTC	24406.00	0.22
Alanine	A	GCG	53984.00	0.36
Alanine	A	GCA	32529.00	0.21
Alanine	A	GCC	40914.00	0.27
Serine	S	AGT	13976.00	0.15
Serine	S	AGC	25716.00	0.28
Lysine	K	AAG	16370.00	0.23
Lysine	K	AAA	53920.00	0.77
Asparagine	N	AAT	28256.00	0.45
Asparagine	N	AAC	34752.00	0.55
Methionine	M	ATG	44539.00	1.00
Isoleucine	I	ATA	6866.00	0.07
Isoleucine	I	ATT	48766.00	0.51
Isoleucine	I	ATC	40097.00	0.42
Threonine	T	ACG	23056.00	0.27
Threonine	T	ACA	11267.00	0.13
Threonine	T	ACT	14303.00	0.17
Threonine	T	ACC	37495.00	0.44
Tryptophan	W	TGG	24553.00	1.00
Cysteine	C	TGT	8306.00	0.45
Cysteine	C	TGC	10330.00	0.55
Tyrosine	Y	TAT	26180.00	0.57
Tyrosine	Y	TAC	19675.00	0.43
Phenylalanine	F	TTT	35930.00	0.57
Phenylalanine	F	TTC	26609.00	0.43
Serine	S	TCG	14305.00	0.15
Serine	S	TCA	11438.00	0.12
Serine	S	TCT	13633.00	0.15
Serine	S	TCC	13783.00	0.15
Arginine	R	CGG	8631.00	0.10
Arginine	R	CGT	33711.00	0.38
Arginine	R	CGC	35311.00	0.40
Arginine	R	AGG	1949.00	0.02
Arginine	R	AGA	3291.00	0.04
Glutamine	Q	CAG	46256.00	0.65
Glutamine	Q	CAA	24787.00	0.35
Histadine	H	CAT	20686.00	0.57
Histadine	H	CAC	15595.00	0.43
Leucine	L	CTG	84714.00	0.50
Leucine	L	CTT	17707.00	0.10
Leucine	L	TTG	22000.00	0.13
Leucine	L	TTA	22279.00	0.13
Proline	P	CCG	37316.00	0.52
Proline	P	CCA	13664.00	0.19
Proline	P	CCT	11291.00	0.16
Proline	P	CCC	8861.00	0.12

Appendix 7.2. Plasmid maps

pET-23a(+) sequence landmarks

T7 promoter	303-319
T7 transcription start	302
T7•Tag coding sequence	207-239
Multiple cloning sites (<i>Bam</i> H I - <i>Xho</i> I)	158-203
His•Tag coding sequence	140-157
T7 terminator	26-72
pBR322 origin	1450
<i>bla</i> coding sequence	2211-3068
f1 origin	3200-3655

The maps for pET-23b(+), pET-23c(+) and pET-23d(+) are the same as pET-23a(+) (shown) with the following exceptions:
 pET-23b(+) is a 3665bp plasmid; subtract 1bp from each site beyond *Bam*H I at 198.
 pET-23c(+) is a 3664bp plasmid; subtract 2bp from each site beyond *Bam*H I at 198.
 pET-23d(+) is a 3663bp plasmid; the *Bam*H I site is in the same reading frame as in pET-23c(+). An *Nco* I site is substituted for the *Nde* I site with a net 1bp deletion at position 238 of pET-23c(+). As a result, *Nco* I cuts pET-23d(+) at 234, and *Nhe* I cuts at 229. For the rest of the sites, subtract 3bp from each site beyond position 239 in pET-23a(+). *Nde* I does not cut pET-23d(+). Note also that *Sty* I is not unique in pET-23d(+).



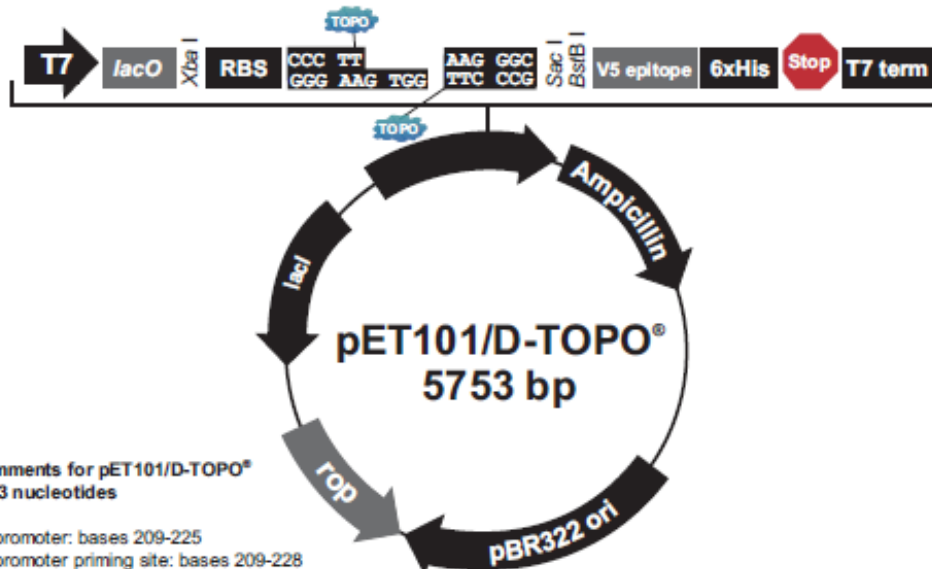
pET-23a-d(+) cloning/expression region

Sourced from pET expression manual.

Map and Features of pET101/D-TOPO[®]

pET101/D-TOPO[®] Map

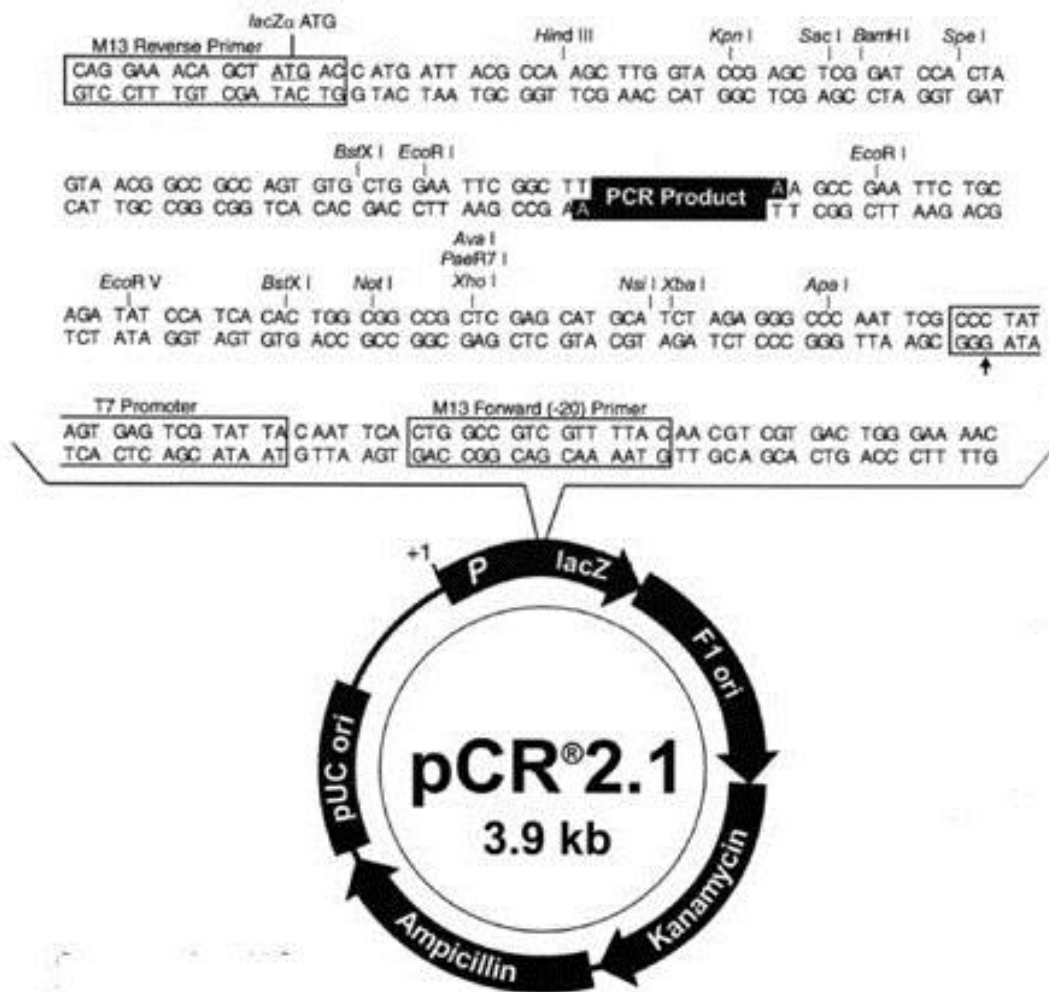
The figure below shows the features of the pET101/D-TOPO[®] (5753 bp) vector. The complete sequence of the vector is available for downloading from our Web site (www.invitrogen.com) or by contacting Technical Service (see page 56).



Comments for pET101/D-TOPO[®] 5753 nucleotides

T7 promoter: bases 209-225
 T7 promoter priming site: bases 209-228
 lac operator (lacO): bases 228-252
 Ribosome binding site (RBS): bases 282-288, 292-296
 TOPO[®] cloning site (directional): bases 297-310
 V5 epitope: bases 333-374
 Polyhistidine (6xHis) region: bases 384-401
 T7 reverse priming site: bases 455-474
 T7 transcription termination region: bases 416-544
 bla promoter: bases 845-943
 Ampicillin (bla) resistance gene (ORF): bases 944-1804
 pBR322 origin: bases 1949-2622
 ROP ORF: bases 2990-3181 (complementary strand)
 lacI ORF: bases 4493-5584 (complementary strand)

Sourced from Invitrogen TOPO cloning manual.



Sourced from Invitrogen TOPO cloning manual.

CHAPTER 11
PUBLICATIONS



Development of a rapid phage-based method for the detection of viable *Mycobacterium avium* subsp. *paratuberculosis* in blood within 48 h[☆]



Benjamin M.C. Swift^{a,*}, Emily J. Denton^b, Sophie A. Mahendran^b, Jonathan N. Huxley^b, Catherine E.D. Rees^a

^a School of Biosciences, University of Nottingham, Sutton Bonington Campus, Loughborough, Leics, LE12 5RD, UK

^b School of Veterinary and Medicine Science, University of Nottingham, Sutton Bonington Campus, Loughborough, Leics, LE12 5RD, UK

ARTICLE INFO

Article history:

Received 14 March 2013

Received in revised form 4 June 2013

Accepted 12 June 2013

Available online 25 June 2013

Keywords:

Bacteriophage
Johne's disease
Magnetic separation
Paratuberculosis
Rapid detection

ABSTRACT

The aim of this study was to develop a methodology to rapidly detect viable *Mycobacterium avium* subsp. *paratuberculosis* (MAP) in clinical blood samples. MAP cells spiked into commercially available blood were recovered using optimised peptide-mediated magnetic separation (PMMS) and detected using a phage-based method, and the identity of the cells detected confirmed using nested-PCR amplification of MAP signature sequences (IS900). The limit of detection was determined to be 10 MAP cells per ml of blood and was used to detect MAP present in clinical bovine blood samples. Using the PMMS-phage method there was no difference when detecting MAP from whole blood or from isolated buffy coat. MAP was detected in animals that were milk-ELISA positive (15 animals) by PMMS-phage and no MAP was detected in blood samples from an accredited Johne's disease free herd (5 animals). In a set of samples from one herd (10 animals) that came from animals with variable milk ELISA status, the PMMS-phage results agreed with the positive milk-ELISA results in all but one case. These results show that the PMMS-phage method can detect MAP present in naturally infected blood. Total assay time is 48 h and, unlike PCR-based detection tests, only viable cells are detected. A rapid method for detecting MAP in blood could further the understanding of disseminated infection in animals with Johne's disease.

© 2013 The Authors. Published by Elsevier B.V. All rights reserved.

1. Introduction

Mycobacterium avium subsp. *paratuberculosis* (MAP) is the causative agent of Johne's disease which is a wasting disease of cattle and other ruminants that results in lower meat and milk yields, and significant financial losses to both the dairy and beef industries (Raizman et al., 2009). Paratuberculosis occurs throughout the world and is considered endemic in many countries (Fridriksdottir et al., 1999). MAP is transmitted vertically through contaminated milk and colostrum or horizontally via contaminated feed (Whittington and Sergeant, 2001). The disease can be controlled but early detection and reliable diagnostics are paramount in stopping transmission between animals. In Europe herd prevalence ranges from 7% to 55% but the sub-clinical nature of the disease and the limitations of available diagnostic tests can result in underreporting (Manning and Collins, 2001).

The identification of MAP in the blood of animals susceptible to Johne's disease has been carried out using techniques such as PCR and culture (see Bower et al., 2010 for a review). The use of PCR,

although rapid does not distinguish between live and dead organisms. Culture is extremely slow and can take up to 16 weeks to form colonies and in some cases requires decontamination, which can reduce the number of viable cells in a sample (Grant et al., 2003; Gumber and Whittington, 2007). Although Bower et al. (2010) has indicated that some decontamination methods may affect certain MAP strains more than others. Most recently Bower et al. (2010) has described an optimised method for culture of MAP from decontaminated erythrocyte-lysed washed buffy coat, with a reported sensitivity of 10 MAP per ml of spiked whole blood, but this still required up to 12 weeks incubation. Hence this long time required for culture can hamper efforts to understand different phases of disease and determining when an animal develops disseminated infection.

The FASTplaqueTB™ assay (FPTB; Lab21, UK) is a phage-based detection method for human tuberculosis that has been adapted for the detection of viable MAP in milk and cheese (Altic et al., 2007; Botsaris et al., 2010; Stanley et al., 2007). To increase the specificity of the method the phage-based assay was combined with PCR amplification of the multi-copy IS900 element. During the development of the phage-based assay it was noted that substances present in the sample matrix can inhibit phage infection. Sample processing was required to ensure these are removed. Magnetic separation is a very simple method of capturing and concentrating cells from a matrix using magnet beads coated with a specific binding agent (either antibody

Abbreviations: PMMS, Peptide mediated magnetic separation; FPTB, FASTplaqueTB assay; MP, Media Plus.

[☆] This is an open-access article distributed under the terms of the Creative Commons Attribution License, which permits unrestricted use, distribution, and reproduction in any medium, provided the original author and source are credited.

* Corresponding author. Tel.: +44 1159516161.

E-mail address: stxbs@nottingham.ac.uk (B.M.C. Swift).

or peptide). MAP-specific binding peptides coupled to magnetic beads described by Stratmann et al. (2006), have been used to recover MAP cells from milk samples (Foddai et al., 2010).

The aim of this study was to combine existing technologies to develop a novel protocol that could be used to rapidly detect MAP cells in blood using a combined phage-PCR approach, and then to test whether this could be used to detect viable MAP in clinical blood samples.

2. Materials and methods

2.1. Bacterial strains, bacteriophage and growth media

MAP strains K10 and ATCC 19698 were used in the initial experiments to optimise the phage assay. The *Mycobacterium smegmatis* strain and the bacteriophage used (Actiphage) were those supplied in the FASTPlaqueTB™ kit. All cultures of MAP were prepared using FASTPlaqueTB™ Media Plus (modified 7H9/OADC media) supplemented with Mycobactin J ($2 \mu\text{g } \mu\text{l}^{-1}$; Synbiotics Corporation, France).

To culture from beads, 100 μl of each sample, after PMMS (Section 2.3) were inoculated on Herrold's egg yolk medium (HEYM) slopes supplemented with Mycobactin J (BD, France). After inoculation, tubes were incubated slanted with the caps lightly screwed at 37 °C. After one week of inoculation slopes were examined for growth of contaminating organisms. After two weeks the caps were sealed and the slopes incubated up right. The slopes were then examined every week for 16 weeks, and every month up to six months after for growth. After six months, if there was no visible growth, a slope wash detection method was carried out.

2.2. Slope wash detection of MAP growth

The slope wash was based on a method by Williams and Monif (2009). Briefly, 1 ml of sterile reverse osmosis (RO) water was added to a slope with no visible growth. Using a sterile loop, the surface of the agar was gently scraped to loosen any cells present. The slopes were vortexed for 30 s and the liquid transferred to 1.5 ml centrifuge tube and centrifuged (15 min, 17000 $\times g$). The supernatant was removed, frozen at -80 °C and then rapidly thawed before boiling for 10 min to induce cell lysis. The samples were then centrifuged for 3 min (17000 $\times g$) and the supernatant (10 μl) used as template DNA for PCR amplification of IS900 (Section 2.6).

2.3. Preparation of peptide-coated magnetic beads

Biotinylated peptides were supplied by Cambridge Peptides Ltd. Magnetic beads (Dynabeads - MyOne Tosylactivated, Invitrogen) were individually coated with peptides aMp3 and aMptD (Stratmann et al., 2006) according to the manufacturers' instructions.

2.4. Sample preparation and recovery of MAP cells from blood

For development of the assay, MAP cells were added to commercial horse or sheep's blood (Oxoid, UK). To recover MAP cells, 1 ml blood samples were diluted with 9 ml of Media Plus. Peptide mediated magnetic separation was performed using an adaptation of the method described (Foddai et al., 2010) by adding 10 μl of peptide coated beads (5 μl each of aMp3- and aMptD-coated beads) to each sample and mixing at 18 rpm for 30 min (Dynabeads-MX mixer, Invitrogen). Beads and bound MAP cells were recovered by centrifugation at 4500 $\times g$ for 15 min. The supernatant was removed and the beads washed using 9 ml of fresh Media Plus. The beads were again recovered by centrifugation (4500 $\times g$, 15 min) and finally resuspended in 1 ml of Media Plus before being transferred into a microcentrifuge tube for PMMS. Finally, the beads resuspended in 1 ml of Media Plus and Mycobacteria cells present detected using the FPTB assay reagents.

2.5. Detection and enumeration of MAP using the FASTPlaqueTB™ (FPTB) assay

The FPTB (Lab21, Cambridge, UK) assay was carried out according to the manufacturer's instructions. To perform the assay, samples containing MAP are mixed with a broad spectrum mycobacteriophage; D29. After the infection period any extracellular phage are inactivated using a virucide; only phage that have successfully infected a cell are protected from the virucide. The virucide is then neutralised by dilution and infected cells are then plated in a lawn of fast growing *M. smegmatis* using soft agar. Lysis of the infected cells releases new phage which then infect the *M. smegmatis* cells and leads to the formation of a plaque in the lawn. Hence each plaque formed represents one MAP cell in the original sample. Standard FPTB assay positive and negative controls were used each time the assay was performed. Enumeration of MAP cells in inocula was determined using the modification of the FPTB assay as described by Rees and Botsaris (2012) which involves diluting samples until countable numbers of plaques are obtained (data reported as pfu ml⁻¹).

2.6. PCR for the identification of MAP cells

When a MAP cell is present in the initial sample, its DNA is preserved in the centre of the plaque (Stanley et al., 2007). Identification of the cell detected within single plaques was achieved by PCR amplification of IS900 signature sequences from this DNA using a modification of the plaque-PCR method described by (Botsaris et al., 2010). In this study DNA was extracted from five plaques and concentrated from plaque agar using Zymo-Gel DNA Recovery Spin Columns™, (ZymoResearch, USA). IS900-specific nested PCR (Bull et al., 2003) was performed using a 5 μl sample of DNA as template. Purified MAP K10 DNA was used as a positive PCR control and DNA extracted from plaques only containing *M. smegmatis* cells (the FPTB positive control samples) as a negative control.

2.7. Detection of MAP in clinical blood samples

Blood samples were provided as superfluous material under the Veterinary Surgeons Act as part of an on-going herd health screening programme. The study protocol was approved by the University of Nottingham, School of Veterinary Medicine and Science ethical review panel prior to sample usage. Blood samples were collected from nine cows, which had produced positive Johne's milk ELISA test results on three separate occasions (Set A). Blood samples were collected from five cows that belong to an accredited Johne's disease-free herd (Set B). Before sampling, the site of venipuncture was cleaned twice with alcohol. Blood was drawn into either sterile sodium heparin Vacutainer tubes (for phage assay) or plain Vacutainer tubes for blood ELISA. The blood ELISA was performed by a commercial laboratory (Nationwide Laboratories, Leeds, UK).

2.8. Isolation of buffy coat and plasma

The isolation of the buffy coat from cows blood was carried out using Ficoll-Paque Plus (GE Healthcare Life Sciences, UK). The buffy coat layer from 2 ml of whole blood was isolated according to the manufacturer's instructions. The plasma layer was also taken and resuspended after the final centrifugation in MP. The samples were then processed as whole blood in Section 2.4.

3. Results

3.1. Optimisation of PMMS and sample preparation

To develop the method, MAP cells were spiked into commercially available blood. To determine the efficiency of the PMMS recovery, 3.5×10^1 pfu.ml⁻¹ was spiked into blood. Magnetic recovery of

beads directly from blood samples was found to be inefficient (over 90% loss of sample). Therefore magnetic recovery was replaced by centrifugation which improved bead capture. Using this method, when MAP was spiked into horse blood, still no cells were detectable. However when sheep blood was used, 33% of the cells were recovered (Fig. 1). Assuming that the blood was inhibiting either the peptide binding or phage assay, the blood was diluted using FPTB Media Plus. After dilution the number of MAP cells detected from samples was significantly higher ($P < 0.01$) than that recovered from the undiluted blood, resulting in 92% recovery of MAP for a 1 in 10 dilution and 73% when a 1 in 50 dilution of the sample was used (Fig. 1). Accordingly, a 1 in 10 dilution was adopted as the standard method as it resulted in the most efficient recovery of MAP cells.

3.2. Determining limit of detection of PMMS-phage method

The number of MAP cells in a liquid culture was first determined using the modified FPTB assay (Section 2.5). These cultures were then diluted and spiked into sheep blood at different levels, down to approximately 1 MAP cell per ml. Using these samples, it was found that the optimised PMMS-phage method was able to reproducibly detect 10 MAP cells per ml of blood (Table 1).

3.3. Optimisation of nested-IS900 plaque-PCR

To confirm the detection of MAP by the phage assay, Stanley et al. (2007) extracted DNA from individual plaques and carried out a MAP specific PCR. In this study DNA was extracted from 5 plaques using a gel extraction kit and a nested-PCR (Bull et al., 2003) was used to amplify IS900 signature sequences. Using this approach IS900 DNA was always amplified from DNA extracted from the five plaques. To confirm that it was still possible to detect the DNA from a single MAP plaque within this sample, agar extracted from one MAP-positive and four MAP-negative plaques were mixed together. Even at this low concentration of target DNA, IS900 DNA was routinely detectable (Fig. 2).

3.4. Detection of MAP in clinical blood samples

To determine whether the test developed in the laboratory was applicable to clinical blood samples, the optimised method was used to test bovine blood samples. Samples from a farm with a known Johne's disease problem were obtained from nine animals

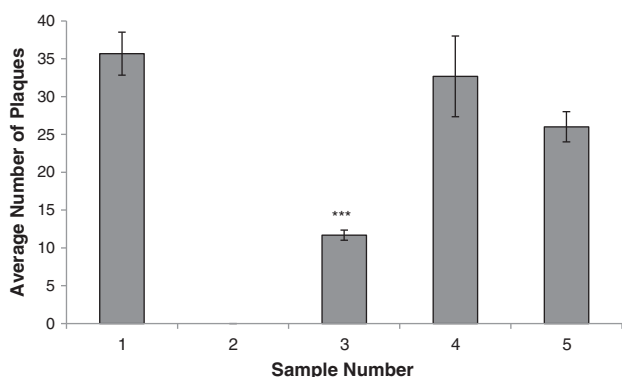


Fig. 1. Effect of blood on detection of MAP by PMMS-phage assay. Graph showing plaque numbers recovered after performing the PMMS and phage assay on: Sample 1; MAP in 1 ml Media Plus. Sample 2; MAP in 1 ml of horse blood. Sample 3; MAP in 1 ml of sheep blood. Sample 4; MAP in 1 ml of sheep blood diluted 1:10 Media Plus. Sample 5; MAP in 1 ml of sheep blood diluted 1:50 Media Plus. A One-way ANOVA, followed by the Dunnett's test was used to analyse significance ($*P < 0.001$) in the reduction of plaque number when compared to Sample 1. Error bars represent the standard deviations of the means of number of plaques recovered from the phage assay performed in triplicate.

Table 1
Limit of detection of phage assay in spiked sheep blood.

Approx. number of MAP cells in inoculum (pfu)	Number of MAP detected (pfu)
10^4	Confluent ^a
10^3	TNTC ^b
10^2	151
10^1	9
10^0	0

^a Confluent: lysis of 80% to 90% of the lawn of *M. smegmatis* cells.

^b TNTC: Too numerous to count; merging of plaques.

that had given three positive milk-ELISA test results (Set A). In addition five samples were obtained from an accredited Johne's disease-free herd (Set B). For comparative purposes, blood ELISA assays were performed in parallel with the PMMS-phage method. All of the animals in Set B gave negative blood ELISA results whereas all animals in Set A gave a positive blood ELISA result, except cow 8 (Table 2).

The results from the PMMS-phage method showed viable MAP cells were detected in all nine of the samples from Set A and no MAP was detected in any samples from Set B (Table 2). Two of the samples from Set B produced plaques (animal 11 and 13), but the IS900 PCR did not detect any MAP DNA in these plaques indicating that no MAP cells were detected.

3.5. Comparison of MAP detection from whole blood and the buffy coat

To determine whether the number of MAP cells detected could be improved by isolation of the buffy coat layer, blood samples were obtained from a second set of ten animals, which now included cows that have given strong, intermediate or negative milk ELISA test results at the last time of testing (Set C). Blood ELISA tests were again performed, and antigens against MAP were detected in 4 out of the 10 animals (Table 3).

Each blood sample was tested using the PMMS-phage method both using whole blood and after buffy coat preparation. PCR-positive MAP plaques were detected in eight of the ten blood samples irrespective of the method of sample preparation, and there was no significant difference ($P > 0.05$) between the number of plaques isolated from whole blood or from the buffy coat layer (Table 3). After buffy coat isolation, the plasma fraction was recovered, but MAP was not detected using the PMMS-phage method in these samples (data not shown).

3.6. Culture of MAP following PMMS of blood

For the blood samples from Set C, culture was performed after PMMS of both whole blood and buffy coat layers using 0.1 ml samples plated onto Mycobactin J HEYM slopes. No chemical decontamination was performed, and no loss of samples to contamination was seen. However no growth was seen in any of the samples and the absence of any detectable MAP growth was confirmed using slope-wash and direct IS900 PCR.

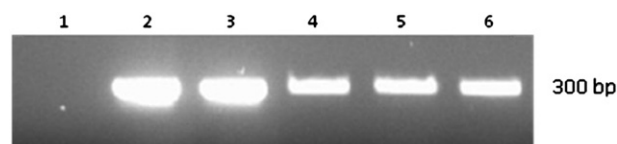


Fig. 2. Confirming detection of MAP DNA from mixed plaque samples. Nested-PCR amplification of the 300 bp IS900 DNA region specific for MAP (Bull et al., 2003). Lane 1; DNA extracted from 5 *M. smegmatis* plaques. Lanes 2; DNA extracted from 5 MAP plaques. Lane 3; 4 MAP plaques mixed with 1 *M. smegmatis* plaque. Lane 4; 3 MAP plaques mixed with 2 *M. smegmatis* plaques. Lane 5; 2 MAP plaques mixed with 3 *M. smegmatis* plaques. Lane 6; 1 MAP plaque mixed with 4 *M. smegmatis* plaques.

Table 2
Results of analysis of blood samples from animals in Sets A and B.

Cow Number	Milk ELISA Status (3 tests)	Blood ELISA Status (OD Readings)	Plaque Number ^a		IS900 Plaque PCR		
Set A	1	+	+	(190)	35	27	+
	2	+	+	(>227)	15	13	+
	3	+	+	(221)	19	25	+
	4	+	+	(111)	31	31	+
	5	+	+	(>227)	11	25	+
	6	+	+	(>227)	10	10	+
	7	+	+	(>227)	35	29	+
	8	+	–	(1.47)	10	18	+
	9	+	+	(193)	5	9	+
Set B	10	–	–	–	0	0	NR
	11	–	–	–	2	0	–
	12	–	–	–	0	0	NR
	13	–	–	–	1	0	–
	14	–	–	–	0	0	NR

Numbers 1–9 represent Set A, Numbers 10–19 represent Set B and Numbers 10–14 represent set B.

NR - 'not required' shows there were no plaques formed, therefore no PCR required.

^a - Values show the numbers of plaques obtained in two independently tested samples.

3.7. Reproducibility of the PMMS-phage method

To give an indication of the reproducibility, the phage assay was repeated for all blood samples twice, independently. There was a good agreement ($r^2 = 0.73$) between the two independent test results for each blood sample tested. The results gained for the MAP-positive samples (Sets A and C) ranged from 3 to 35 pfu ml⁻¹, indicating that only low numbers of cells were detected. For MAP-negative samples (defined as plaques that were IS900-PCR negative) the number of plaques was 5 or below (Tables 2 and 3).

4. Discussion

The use of PMMS to recover cells from the sample has two benefits; it allows concentration of cells and does not affect the viability of MAP. The main obstacle for development of the assay was to achieve efficient capture of MAP cells in blood samples. Diluting the blood sample 1 in 10 using modified Media Plus (modified 7H9 media) gave the best improvement in recovery of MAP cells from spiked blood samples. The viscosity of horse blood is much higher than that of sheep blood (Windberger et al., 2003) and therefore limitation of bead movement in the sample may have hindered capture of MAP cells. Interestingly, the addition of Media Plus to the blood

samples induced lysis of the blood cells. This may have contributed to the success of the assay when using clinical blood samples, since any intracellular MAP cells would be released into the medium and available for both PMMS and phage infection. This may also explain why no difference was seen in the efficiency of MAP detection in whole blood compared to isolated buffy coat layer. Thus negating the need to prepare the buffy coat layer before testing blood samples using this phage detection method.

The cows from Set A were selected using standard current diagnostic criteria for Johne's disease which requires repeat testing over a period of six months. The blood ELISA results for these animals agreed with this diagnosis in all but one case (cow #8) which gave an indeterminate test result. In contrast the PMMS-phage method detected viable organisms in blood samples from all animals in Set A, and this result agreed with the milk ELISA results. In Set B, two samples (animals 11 and 13) produced MAP DNA negative plaques, which may be because the virucide did not destroy all the phage before plating in the lawn of *M. smegmatis*. Break-through has been reported before when performing the FPTB assay but the introduction of the PCR identification step overcomes this problem. Hence in this study samples are not scored as MAP-positive unless the IS900 sequence can be amplified from the plaque.

In Set C, three of the animals gave negative milk and blood ELISA test results and two of these were also negative for MAP using the PMMS-phage method. However the PMMS-phage method detected viable MAP in the blood from one animal (cow #22), and the plaque numbers were equivalent to those of the majority of the other milk ELISA-positive animals. This indicates that results gained using a method that directly detects the viable organism can differ from test results based on the immune response of the animal to infection. Further work is now needed to understand the relationship between the immune response of the animal and the presence of viable organisms in the blood.

When PMMS-phage MAP-positive samples were cultured, no growth was detected. Since the plaque number indicates that there were fewer than 42 MAP cells per ml in all of these samples, the lack of growth is to be expected as this number is below the limit of detection for the culture method used. MAP has been detected in blood samples by PCR-based methods and culture (Bower et al., 2010, 2011; Gwozdz et al., 2000; Naser et al., 2004). Although viable cells can be cultured from these samples, the time required makes this of limited practical value and the need for decontamination before culture may reduce the number of viable cells present in a sample (Reddacliff et al., 2003). Interestingly here, following PMMS of blood samples, no contamination of cultures was seen suggesting that the selectivity of the PMMS followed by the extensive washing

Table 3
Results of analysis of blood samples from Set C animals.

Cow Number	Milk ELISA Status (most recent ^a)	Blood ELISA Status	Plaque Number		Plaque PCR	Culture		
			Whole Blood ^b	Buffy Coat ^b				
15	Red	–	20	25	38	42	+	–
16	Red	+	3	7	22	21	+	–
17	Red	+	22	15	28	32	+	–
18	Red	+	12	3	17	12	+	–
19	Red	–	13	23	15	5	+	–
20	Red	+	8	6	9	5	+	–
21	Amber	–	21	11	32	31	+	–
22	Green	–	22	26	22	22	+	–
23	Green	–	1	1	2	0	–	–
24	Green	–	3	5	2	5	–	–

Red – denotes a strong positive Milk ELISA reading.

Amber – denotes an inconclusive Milk ELISA reading.

Green – denotes a negative Milk ELISA reading.

^a Represents the most recent Milk-ELISA status.

^b Values show the numbers of plaques obtained in two independently tested samples.

used in this method is sufficient to remove contaminating microflora from the sample without the need to apply chemical decontamination.

In contrast to culture, PCR-based MAP detection methods are more rapid but they do not determine the viability of the cell detected. The results gained here show that the combined PMMS-phage-PCR assay can achieve rapid detection and identification of viable MAP in clinical samples within 48 h, and in addition provides an indication of the number of cells present in the sample. The limit of detection determined here is in agreement with an optimised MAP blood culture method reported by Bower et al (2010) but this method requires a 12 week incubation before results are available.

5. Conclusion

Here we have shown that we are able to detect viable MAP cells from spiked blood samples within 48 h, with a limit of detection of 10^1 cells per millilitre of blood which can be combined with a sensitive PCR assay that specifically identifies the organism detected. The method was also tested using clinical blood samples, by selecting animals that were presumptively identified as having Johne's disease on the basis of repeated milk ELISA test results. Although this study was limited to small sample set, this is the first demonstration of a new method that can directly detect viable organisms in blood. This assay will allow researchers to better understand the development of disseminated infection, and may therefore lead to a better understanding of the pathogenesis of the disease and the immune response of the animal (Bower et al., 2010). In addition we believe that the assay could also be applied to blood samples from all susceptible animal species.

Acknowledgments

B.M.C.S was funded by a Lab21 PhD studentship. E.J.D. and S.M. were supported a BBSRC and Wellcome Trust Summer Studentships, respectively. We would also like to acknowledge Dr Irene Grant, University of Belfast, for her help in developing the PMMS method.

References

- Altic, L.C., Rowe, M.T., Grant, I.R., 2007. UV light inactivation of *Mycobacterium avium* subsp. *paratuberculosis* in milk as assessed by FASTPlaqueTB phage assay and culture. *Appl. Environ. Microbiol.* 73, 3728–3733.
- Botsaris, G., Slana, I., Liapi, M., Dodd, C., Economides, C., Rees, C., Pavlik, I., 2010. Rapid detection methods for viable *Mycobacterium avium* subspecies *paratuberculosis* in milk and cheese. *Int. J. Food Microbiol.* 141, S87–S90.

- Bower, K., Begg, D.J., Whittington, R.J., 2010. Optimisation of culture of *Mycobacterium avium* subspecies *paratuberculosis* from blood samples. *J. Microbiol. Methods* 80, 93–99.
- Bower, K.L., Begg, D.J., Whittington, R.J., 2011. Culture of *Mycobacterium avium* subspecies *paratuberculosis* (MAP) from blood and extra-intestinal tissues in experimentally infected sheep. *Vet. Microbiol.* 147, 127–132.
- Bull, T.J., McMinin, E.J., Sidi-Boumedine, K., Skull, A., Durkin, D., Neild, P., Rhodes, G., Pickup, R., Hermon-Taylor, J., 2003. Detection and verification of *Mycobacterium avium* subsp. *paratuberculosis* in fresh ileocolonic mucosal biopsy specimens from individuals with and without Crohn's disease. *J. Clin. Microbiol.* 41, 2915–2923.
- Foddai, A., Elliott, C.T., Grant, I.R., 2010. Maximizing Capture Efficiency and Specificity of Magnetic Separation for *Mycobacterium avium* subsp. *paratuberculosis* Cells. *Appl. Environ. Microbiol.* 76, 7550–7558.
- Fridriksdottir, V., Gunnarsson, E., Sigurdarson, S., Gudmundsdottir, K.B., 1999. Paratuberculosis in Iceland: Epidemiology and control measures, past and present. *Proceedings of the Sixth International Colloquium on Paratuberculosis*, pp. 105–108.
- Grant, I.R., Kirk, R.B., Hitchings, E., Rowe, M.T., 2003. Comparative evaluation of the MGIT (TM) and BACTEC culture systems for the recovery of *Mycobacterium avium* subsp. *paratuberculosis* from milk. *J. Appl. Microbiol.* 95, 196–201.
- Gumber, S., Whittington, R.J., 2007. Comparison of BACTEC 460 and MGIT 960 systems for the culture of *Mycobacterium avium* subsp. *paratuberculosis* S strain and observations on the effect of inclusion of ampicillin in culture media to reduce contamination. *Vet. Microbiol.* 119, 42–52.
- Gwozdz, J.M., Thompson, K.G., Murray, A., West, D.M., Manktelow, B.W., 2000. Use of the polymerase chain reaction assay for the detection of *Mycobacterium avium* subspecies *paratuberculosis* in blood and liver biopsies from experimentally infected sheep. *Aust. Vet. J.* 78, 622–624.
- Manning, E.J.B., Collins, M.T., 2001. *Mycobacterium avium* subsp. *paratuberculosis*: pathogen, pathogenesis and diagnosis. *Rev. Sci. Tech. Off. Int. Epiz.* 20, 133–150.
- Naser, S.A., Ghobrial, G., Romero, C., Valentine, J.F., 2004. Culture of *Mycobacterium avium* subspecies *paratuberculosis* from the blood of patients with Crohn's disease. *Lancet* 364, 1039–1044.
- Raizman, E.A., Fetrow, J.P., Wells, S.J., 2009. Loss of income from cows shedding *Mycobacterium avium* subspecies *paratuberculosis* prior to calving compared with cows not shedding the organism on two Minnesota dairy farms. *J. Dairy Sci.* 92, 4929–4936.
- Reddacliff, L.A., Vadali, A., Whittington, R.J., 2003. The effect of decontamination protocols on the numbers of sheep strain *Mycobacterium avium* subsp. *paratuberculosis* isolated from tissues and faeces. *Vet. Microbiol.* 95, 271–282.
- Rees, C.R., Botsaris, G., 2012. The Use of Phage for Detection, Antibiotic Sensitivity Testing and Enumeration. In: Cardona, P.-J. (Ed.), *Understanding Tuberculosis - Global Experiences and Innovative Approaches to the Diagnosis*, InTech, Rijeka, pp. 293–306.
- Stanley, E.C., Mole, R.J., Smith, R.J., Glenn, S.M., Barer, M.R., McGowan, M., Rees, C.E.D., 2007. Development of a new, combined rapid method using phage and PCR for detection and identification of viable *Mycobacterium paratuberculosis* bacteria within 48 hours. *Appl. Environ. Microbiol.* 73, 1851–1857.
- Stratmann, J., Dohmann, K., Heinzmann, J., Gerlach, G.F., 2006. Peptide aMptD-mediated capture PCR for detection of *Mycobacterium avium* subsp. *paratuberculosis* in bulk milk samples. *Appl. Environ. Microbiol.* 72, 5150–5158.
- Whittington, R.J., Sergeant, E.S.G., 2001. Progress towards understanding the spread, detection and control of *Mycobacterium avium* subsp. *paratuberculosis* in animal populations. *Aust. Vet. J.* 79, 267–278.
- Williams, J.E., Monif, G.R., 2009. A procedure to assist in the identification of slow growing *Mycobacterium* from slant cultures. *The Paratuberculosis Newsletter*. IAP 5.
- Windberger, U., Bartholovitsch, A., Plasenzotti, R., Korak, K.J., Heinze, G., 2003. Whole blood viscosity, plasma viscosity and erythrocyte aggregation in nine mammalian species: reference values and comparison of data. *Exp. Physiol.* 88, 431–440.

EDITORIAL

Detecting mycobacteria in cattle blood

Benjamin M. C. Swift, Catherine E. D. Rees

THE standard tests used to identify bovine TB in cattle rely on monitoring the immune response as an indicator of infection. While the skin test provides a simple and cost-effective assay, it cannot differentiate between infected animals and those that have been vaccinated against infection. In countries where the disease is endemic, vaccination – of both cattle and potential wildlife reservoirs – is considered to be the best long-term strategy to reduce the threat of bovine TB. However, introducing routine vaccination negates the value of the current standard diagnostic tests. There is therefore a real need for new tests that can differentiate between naturally infected and vaccinated animals (termed DIVA). One approach would be to directly detect *Mycobacterium bovis*, the main causative agent of bovine TB, in samples from infected animals. While this approach can be used for many bacterial infections, it is problematic when working with mycobacteria.

The slow growth of some pathogenic mycobacteria makes detection by traditional culture extremely difficult. For instance, culture results for *M bovis* can take up to eight weeks. Similarly, *Mycobacterium avium* subspecies *paratuberculosis* (MAP), which causes Johne's disease, can take up to 16 weeks to culture. Even rapid, automated culture methods for bovine TB take up to 15 days. The lengthy incubation times and poor levels of sensitivity achieved when culturing mycobacteria from blood limits the diagnostic power of this method and it has not been used for many years.

Benjamin M. C. Swift, BSc (Hons), MRes,
Catherine E. D. Rees, BA (Oxon), PhD
University of Nottingham, Sutton Bonington Campus,
Loughborough LE12 5RD, UK
e-mail: stxbs@nottingham.ac.uk

Molecular methods are often used to detect bacterial DNA as an alternative to culture. Blood assays based on PCR amplification of genomic signature sequences from *Mycobacterium* have been described, but these do not differentiate between living and dead cells. When trying to confirm infection, it is important that only viable cells are detected rather than residual DNA from cells that have been inactivated, either by the host immune system or by treatment. Unfortunately, PCR-based bovine TB detection methods have been found to be limited both by specificity and sensitivity (Parra and others 2008).

These difficulties have led to the use of the intradermal skin test as the standard method of identifying bovine TB-infected cattle. The sensitivity of the skin test is known to be highly variable and results are affected by factors such as the stage and severity of disease and cross-reactions to other mycobacterial infections. Hence a positive skin test always requires further tests to confirm the diagnosis; this may be visible lesions in the carcase or culture of lymph node material. Interferon- γ tests can also be used to confirm infection; however, false-positives can occur when animals are infected with other pathogenic mycobacteria and, again, this test does not differentiate between infected and vaccinated animals.

The licensed vaccine for both human and bovine TB is Bacillus Calmette-Guérin (BCG), an attenuated strain of *M bovis*, but the level of protection achieved is variable (Hope and Vordermeier 2005). More importantly, use of the BCG vaccine in cattle is incompatible with the current diagnostic tests for bovine TB. Research is being undertaken to identify recombinant vaccines based on specific antigens that

prevent cross-reaction with the skin test, but this is in its early stages (Whelan and others 2010). PCR-based methods have been described that can differentiate between *M. bovis* and BCG cells (Huard and others 2003), but their usefulness in the clinical setting is also limited by issues of sensitivity and an inability to differentiate between living and dead cells.

Bacteriophage-based detection

Bacteriophages are viruses that infect bacterial cells. They have a specific host range and will only replicate within a viable cell. These features have been exploited for the development of many bacteriophage-based detection methods (Monk and others 2010). A commercial phage-based detection platform has been developed for the detection of *M. tuberculosis* in sputum samples as a diagnostic test in people (Albert and others 2002). For the past six years we have been working on new applications of this assay, specifically focusing on methods to detect and enumerate viable MAP in milk and bovine blood samples (the RapidMAP assay). This has led to a range of assay formats that can report on the presence of viable mycobacterial cells in a sample within two days (Stanley and others 2007, Botsaris and others 2010, Swift and others 2013). Rather than waiting for the growth of the mycobacterial cells, the assay monitors the replication of the bacteriophage in a viable host cell. The identity of the cell detected is then confirmed by PCR (Fig 1). This can be done as a species-specific test (Swift and others 2013) or multiplex PCR assays have been developed that will simultaneously report on the presence of a range of different pathogenic mycobacteria (bovine TB and MAP) (Stanley and others 2007). These phage-based assays are low cost and do not need investment in specialist equipment or expensive reagents, and results are available within 48 hours.

RapidMAP uses mycobacteriophage D29 that has a broad host range within the *Mycobacterium* genus, including the faster growing non-pathogens. The assay has been successfully used to detect viable MAP in the blood of cattle with Johne's disease (Swift and others 2013). Results show that it is able to reproducibly detect low numbers of viable cells with better sensitivity than direct PCR and it even detected bacteria in the early stages of infection in blood ELISA-negative animals. Having developed a method to identify viable mycobacteria in blood, this opens up the possibility of creating a bovine TB DIVA test using the PCR step to distinguish between wildtype bovine TB and BCG, or other vaccine strains. There is a good prospect that the assay can be applied to sensitively detect low levels of bovine TB in blood samples and hence the development of a rapid bacteriophage-based DIVA test that differentiates between viable and non-viable

cells is a real possibility.

In its current format, the RapidMAP test is labour intensive; the need to incubate plates determines the test time and is not readily automatable so the existing technology would be challenging if applied on a national herd level. Recently we have patented a tube format that is able to detect viable mycobacteria within eight hours which removes the need for agar plates and could be automated. The method retains the advantages of the RapidMAP technology in that it still detects only viable cells and incorporates a species-specific PCR to identify the cell detected.

We are now starting to further develop this technology, not only as a potential DIVA test but as a method to rapidly detect and enumerate viable mycobacteria in a range of samples, from blood to milk (Rees and Botsaris 2012). This technology therefore has potential to be applied in a number of ways to facilitate future bovine TB research, including significantly shortening the period required for confirmatory culture of samples from positive skin test animals.

References

- ALBERT, H., HEYDENRYCH, A., BROOKES, R., MOLE, R. J., HARLEY, B., SUBOTSKY, E., HENRY, R. & AZEVEDO, V. (2002) Performance of a rapid phage-based test, FASTPlaqueTB, to diagnose pulmonary tuberculosis from sputum specimens in South Africa. *International Journal of Tuberculosis and Lung Disease* **6**, 529-37
- BOTSARIS, G., SLANA, I., LIAPI, M., DODD, C., ECONOMIDES, C., REES, C. & PAVLIK, I. (2010) Rapid detection methods for viable *Mycobacterium avium* subspecies *paratuberculosis* in milk and cheese. *International Journal of Food Microbiology* **141**, S87-S90
- HOPE, J. C. & VORDERMEIER, H. M. (2005) Vaccines for bovine tuberculosis: current views and future prospects. *Expert Review of Vaccines* **4**, 891-902
- HUARD, R. C., LAZZARINI, L. C. D., BUTLER, W. R., VAN SOOLINGEN, D. & HO, J. L. (2003) PCR-based method to differentiate the subspecies of the *Mycobacterium tuberculosis* complex on the basis of genomic deletions. *Journal of Clinical Microbiology* **41**, 1637-1650
- MONK, A. B., REES, C. D., BARROW, P., HAGENS, S. & HARPER, D. R. (2010) Bacteriophage applications: where are we now? *Letters in Applied Microbiology* **51**, 363-9
- PARRA, A., GARCIA, N., GARCIA, A., LACOMBE, A., MORENO, F., FREIRE, F., MORAN, J. & DE MENDOZA, J. H. (2008) Development of a molecular diagnostic test applied to experimental abattoir surveillance on bovine tuberculosis. *Veterinary Microbiology* **127**, 315-324
- REES, C. R. & BOTSARIS, G. (2012) The Use of phage for detection, antibiotic sensitivity testing and enumeration. In *Understanding Tuberculosis - Global Experiences and Innovative Approaches to the Diagnosis*. Ed P. J. Cardona. Rijeka: InTech
- STANLEY, E. C., MOLE, R. J., SMITH, R. J., GLENN, S. M., BARER, M. R., MCGOWAN, M. & REES, C. E. D. (2007) Development of a new, combined rapid method using phage and PCR for detection and identification of viable *Mycobacterium paratuberculosis* bacteria within 48 hours. *Applied and Environmental Microbiology* **73**, 1851-1857
- SWIFT, B. M., DENTON, E. J., MAHENDRAN, S. A., HUXLEY, J. N. & REES, C. E. (2013) Development of a rapid phage-based method for the detection of viable *Mycobacterium avium* subsp. *paratuberculosis* in blood within 48 h. *Journal of Microbiological Methods* **94**, 175-179
- WHELAN, A. O., CLIFFORD, D., UPADHYAY, B., BREADON, E. L., MCNAIR, J., HEWINSON, G. R. & VORDERMEIER, M. H. (2010) Development of a skin test for bovine tuberculosis for differentiating infected from vaccinated animals. *Journal of Clinical Microbiology* **48**, 3176-81

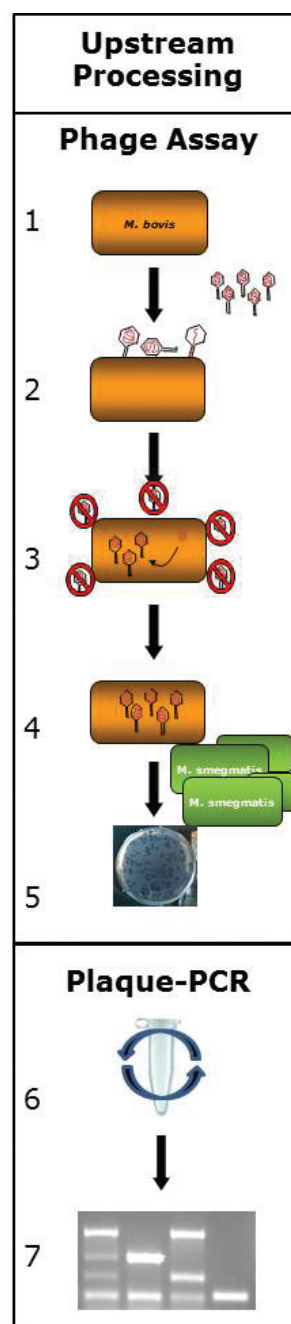


FIG 1: Assay for detecting viable MAP in milk and bovine blood. Specimens that may contain mycobacteria (1) are mixed with phage D29 for one hour (2) to allow the virus to infect its target cells. Any extracellular phage that have not infected a host cell are chemically inactivated using a virucide (3) that does not affect the viability of mycobacterial cells in the sample. Only phage that have infected their host are protected from the virucide and continue to replicate (4). The new phage released from these infected target cells are then detected using a plaque assay. This uses a fast growing non-pathogenic mycobacteria (*M. smegmatis*) that phage D29 also infects. Zones of lysis in the bacterial lawn (or plaques) (5, 6) indicate the position of one original phage-infected *Mycobacterium* in the test sample. The number of mycobacteria in the specimen is represented by the number of plaques formed. The time it takes from blood collection to plaques on a plate is 24 hours. To determine the identity of these cells, DNA is extracted from the centre of the plaque (6) and PCR is used to amplify diagnostic signature sequences present in the mycobacterial genome (7)

doi: 10.1136/vr.f7067

Detecting mycobacteria in cattle blood

Benjamin M. C. Swift and Catherine E. D. Rees

Veterinary Record 2013 173: 522-523

doi: 10.1136/vr.f7067

Updated information and services can be found at:

<http://veterinaryrecord.bmj.com/content/173/21/522.full.html>

These include:

References

This article cites 9 articles, 3 of which can be accessed free at:

<http://veterinaryrecord.bmj.com/content/173/21/522.full.html#ref-list-1>

Email alerting service

Receive free email alerts when new articles cite this article. Sign up in the box at the top right corner of the online article.

Notes

To request permissions go to:

<http://group.bmj.com/group/rights-licensing/permissions>

To order reprints go to:

<http://journals.bmj.com/cgi/reprintform>

To subscribe to BMJ go to:

<http://group.bmj.com/subscribe/>



ELSEVIER

ENCYCLOPEDIA OF FOOD MICROBIOLOGY, SECOND EDITION - CONTRIBUTORS' INSTRUCTIONS

PROOFREADING

The text content for your contribution is in final form when you receive proofs. Please read proofs for accuracy and clarity, as well as for typographical errors, but please **DO NOT REWRITE**.

At the beginning of your article there is a page containing any author queries, keywords, and the authors' full address details.

Please address author queries as necessary. While it is appreciated that some articles will require updating/revising, please try to keep any alterations to a minimum. Excessive alterations may be charged to the contributors.

The shorter version of the address at the beginning of the article will appear under your author/co-author name(s) in the published work and also in a List of Contributors. The longer version shows full contact details and will be used to keep our internal records up-to-date (they will not appear in the published work). For the lead author, this is the address that the honorarium and any offprints will be sent to. Please check that these addresses are correct.

Titles and headings should be checked carefully for spelling and capitalization. Please be sure that the correct typeface and size have been used to indicate the proper level of heading. Review numbered items for proper order – e.g., tables, figures, footnotes, and lists. Proofread the captions and credit lines of illustrations and tables. Ensure that any material requiring permissions has the required credit line, and that the corresponding documentation has been sent to Elsevier.

Note that these proofs may not resemble the image quality of the final printed version of the work, and are for content checking only. Artwork will have been redrawn/relabelled as necessary, and is represented at the final size. **PLEASE KEEP A COPY OF ANY CORRECTIONS YOU MAKE.**

DESPATCH OF CORRECTIONS


Proof corrections should be returned in one communication to **Justin Taylor, at the Elsevier MRW Dept.** within 7 days from receiving the proofs sent out by the typesetter using one of the following methods:

1. **PREFERRED:** If corrections are minor they should either be **annotated on the PDF of your proof**, or can be listed in an e-mail to Justin Taylor, at fmb2_proofs@elsevier.com. The e-mail should state the article code number in the subject line. Listed corrections should be consecutively numbered and should state the paragraph number, line number within that paragraph, and the correction.

2. If corrections are substantial, send the amended hardcopy by courier to the Elsevier MRW Department (The Boulevard, Langford Lane, Kidlington, Oxford, OX5 1GB, UK). If it is not possible to courier your corrections, fax the relevant marked pages to the Elsevier MRW Department with a covering note clearly stating the article code number and title. (Fax number: +44 (0)1865 843974).

Note that a delay in the return of proofs could mean a delay in publication. Should we not receive your corrected proofs within 7 days, Elsevier may have to proceed without your corrections.

CHECKLIST

- Author queries addressed/answered?
- Affiliations, names and addresses checked and verified?
- 'Further Reading' section checked and completed?
- Permissions details checked and completed?
- Outstanding permissions letters attached/enclosed?
- Figures and tables checked? 

If you have any questions regarding these proofs please contact the Elsevier MRW Department at: fmb2_proofs@elsevier.com.

Non Print Items**Author and Co-author Contact Information**

Catherine E.D. Rees,
Division of Food Sciences,
University of Nottingham,
Sutton Bonington Campus,
Loughborough LE12 5RD,
United Kingdom.
Tel.: +44 115 951 6167;
fax: +44 115 951 6162.
E-mail: cath.rees@nottingham.ac.uk

Benjamin M.C. Swift,
Division of Food Sciences,
University of Nottingham,
Sutton Bonington Campus,
Loughborough LE12 5RD,
United Kingdom.
Tel.: +44 115 951 6161;
fax: +44 115 951 6162.
E-mail: stxbs@nottingham.ac.uk

George Botsaris,
Department of Agricultural Sciences,
Biotechnology and Food Science,
Cyprus University of Technology,
Cyprus.
Tel.: +357 25 002582;
fax: +357 25 002840.
E-mail: george.botsaris@cut.ac.cy

Abstract

Bacteriophage have been used for many years as an established typing scheme for bacterial isolates recovered from food. More recently, there has also been a resurgence in interest in the use of bacteriophage as biocontrol agents in food. Although these two applications are well developed, this review focuses on the use of bacteriophage – or bacteriophage products – for the rapid detection of bacterial pathogens. Rapid detection methods that use both engineered (termed reporter phage) and nonengineered bacteriophage are described, along with the application of purified bacteriophage lysins in detection assays.

Keywords

Bacteriophage, Cell lysis, Detection, Lysine, Phage amplification, Rapid methods, Reporter phage

Author Query Form



ELSEVIER

Title: FMB2**Article Title/Article ID:** Bacteriophage-Based Techniques for Detection of FoodBorne Pathogens/00032

Dear Author,

During the preparation of your manuscript for typesetting some questions have arisen. These are listed below. Please check your typeset proof carefully and mark any corrections in the margin of the proof or compile them as a separate list. Your responses should then be returned with your marked proof/list of corrections to Justin Taylor at Elsevier via fmb2_proofs@elsevier.com

Queries and/or remarks

[AU1]	Please specify from what the phage lysin was isolated, in the sentence 'For instance, purified...'
[AU2]	Reference Anon, 2002 is cited in the text but not listed in the reference list. Please check.
[AU3]	Please give full form of MRSA and MSSA in the sentence 'These tests combine ...'.
[AU4]	Please provide biography and photo for the authors 'Catherine E.D. Rees, Benjamin M.C. Swift, George Botsaris'.
[AU5]	Do all these figures 1–5 require permission? If so, please supply relevant correspondence granting permission and ensure that any publisher-required credit line is added to the caption.
[AU6]	Please provide caption for Figure 5.
[AU7]	Please give full form of BTM in the sentence 'Reproducibility of phage ...'.
[AU8]	Please provide the full reference for the source of Figure 6 as it is not provided in 'Further Reading' list.
[AU9]	There are no cross references to other articles. Please check and provide.

a0005 **Bacteriophage-Based Techniques for Detection of FoodBorne Pathogens**

CED Rees and BMC Swift, University of Nottingham, United Kingdom
G Botsaris, Cyprus University of Technology, Cyprus

© 2014 Elsevier Ltd. All rights reserved.

This article is a revision of the previous edition article by Richard J. Mole, Vinod K. Dhir, Stephen P. Denyer, Gordon S.A.B. Stewart (dec), volume 1, pp 203–210, © 1999, Elsevier Ltd.

AU4

s0005 **Introduction**

p0015 When testing food products, the limitation of traditional culture-based methods is the requirement for results to be rapidly available. These are needed to either confirm successful application of critical control point treatments during production or to confirm the microbiological quality of food products before release. Hence, methods that rely on extended periods of culture are either (1) too slow to be of benefit during production or (2) reduce the shelf life of products that require test results before release (positive-release). When tests take days, or even weeks, to complete (e.g., confirming the absence of *Listeria monocytogenes* in samples of ready-to-eat products that will support growth of the organism takes a minimum of 5 days; ISO 11290-1-1998), products often have to be released before the test results are available. This can lead to product recalls that may have a negative impact on customer confidence and ultimately may affect the long-term viability of food producers. Hence, there is a drive to find methods that will allow for the rapid detection of bacterial pathogens that has focused on novel technologies that circumvent the need for culture-based methods.

p0020 The challenge for applications in food microbiology is not developing a robust method that can identify the organism; it is developing methods that can sensitively detect a single cell present in a complex matrix. Many researchers have described polymerase chain reaction (PCR)-based methods for the direct detection of bacteria in food samples, but often these cannot routinely achieve the detection of a single cell in a 25 g sample of the food. An additional concern is that the cost of the test should not be prohibitive. Unlike in the field of medical diagnostics, the cost per test must be kept to a level that is economically sustainable when large numbers of tests need to be performed on a low-unit-value product. Given these constraints, bacteriophage seem to be a good candidate to form a basis of rapid methods for the detection of bacterial pathogens in food.

p0025 Bacteriophage are viruses that infect bacterial cells. They were first discovered in the early part of the nineteenth century by Twort and d'Herelle and quickly were applied as antimicrobial agents. Their use in the treatment of infections, however, fell out of favor following the discovery of antibiotics; however, in the postantibiotic era, interest has revived in the use of phage as specific antimicrobial agents. Like all viruses, phage will only infect their specific host cells, and after infection, they replicate rapidly inside the bacterial cells. The host cell specificity has evolved over millions of years of coexistence and either can be relatively broad within a group or can be quite specific. This has to be exploited to develop phage-based tests that either detect all members of a group or subtypes of an organism. The rapid growth of the virus inside the host cell can be exploited to replace the slower replication of the host cell,

so rather than requiring long periods of time for a single cell to reach detectable levels, growth of the phage can be monitored (Figure 1).

The bacteriophage-based methods reported to date fall into p0030 two main types; first is the use of unmodified phage as specific lysing agents and the detection of bacteria by release of specific cellular components. This may be achieved by using intact phage or by applying phage-encoded enzymes that induce cell lysis. The second approach detects only the growth of the bacteriophage on a specific host cell. This can be achieved either by engineering the phage to express reporter genes to indicate that a specific target cell has been infected or by directly detecting bacteriophage growth (termed 'phage amplification').

Bacteriophage Characteristics

s0010 Bacteriophage are viral parasites that infect bacteria. Like all p0035 viruses, when outside the host, they are metabolically inactive and therefore are described as obligate parasites. The virus structure consists of the nucleic acid surrounded by a protein coat (called a capsid), and in some instances, the capsids may contain lipid layers or even be surrounded by a lipid envelope. The nucleic acid most commonly consists of double-stranded DNA, but some phage have single-stranded DNA genomes. Others have RNA genomes, and phage with both ssRNA and dsRNA have been identified. Unique among viruses is the presence on some bacteriophage of a complex tail structure that is involved in recognition of the host cell surface and delivery of the nucleic acid into the host cell during the first stage of infection. The length and complexity of the tail structure is variable, however, and some phage do not possess tail structures at all. These three characteristics (capsid structure, tail structure/presence, and nucleic acid type) are used as a basis for morphological characterization of phage. The majority of phage described to date and used to develop diagnostic methods fall into two morphological groups – the Myoviridae and the Siphoviridae – both of which have double-stranded DNA genomes packaged into an icosahedral capsid. The Siphoviridae have simple, long, noncontractile tails, and the Myoviridae possess rigid, contractile tails and additional tail fibers and complex base plate structures are seen (Figure 2).

Bacteriophage particles have evolved to be relatively robust p0040 and are capable of existing for long periods of time between release from the parent cell and contact with new host cells. In the presence of an appropriate host cell, the phage becomes attached to the cellular surface and the viral nucleic acid enters the cell (Figure 3). When this happens, the phage enters what is known as the eclipse phase – this is the time during which the phage DNA is not packaged into a capsid but rather is replicating inside the host cell and new phage particles have not yet been formed. During this period, the bacteriophage takes over

2 Bacteriophage-Based Techniques for Detection of FoodBorne Pathogens

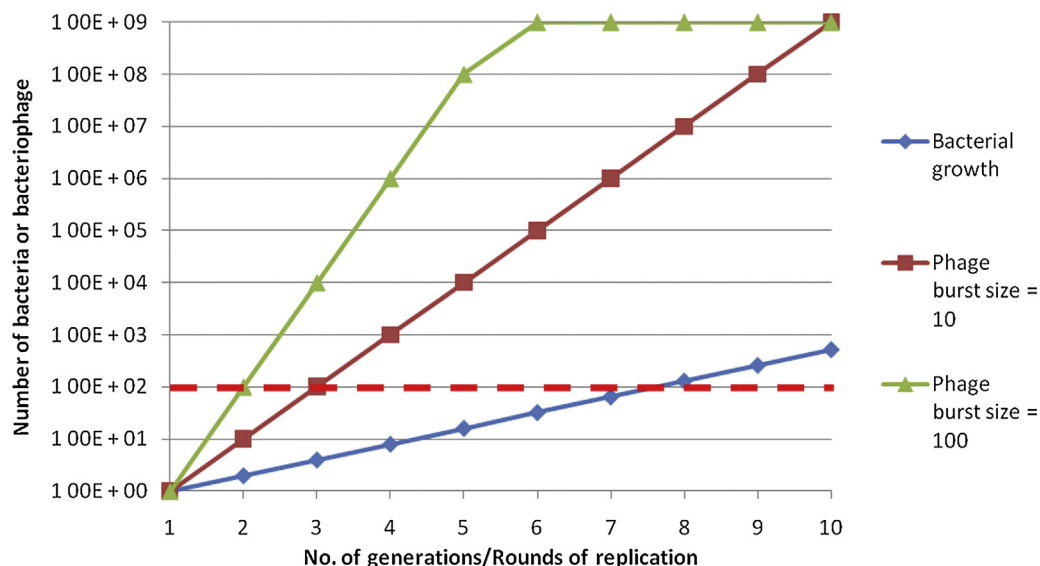


Figure 1 Graph showing difference in theoretical rate of change of bacterial cell number per generation or bacteriophage particles produced per round of replication. Two lines are shown for the bacteriophage, representing phage with different burst sizes: either low (10 phage particles per infection) or high (100 phage particles per infection). The dashed line represents the limit of detection achieved by many rapid methods (10^2 cells). For one cell to reach this threshold, eight generations of growth is required, whereas phage numbers increase far more rapidly. The time taken to complete one round of infection is similar to the generation time of the bacterium, although it can be longer as normal host cell growth normally is inhibited when a cell is infected by a bacteriophage.

CAU5

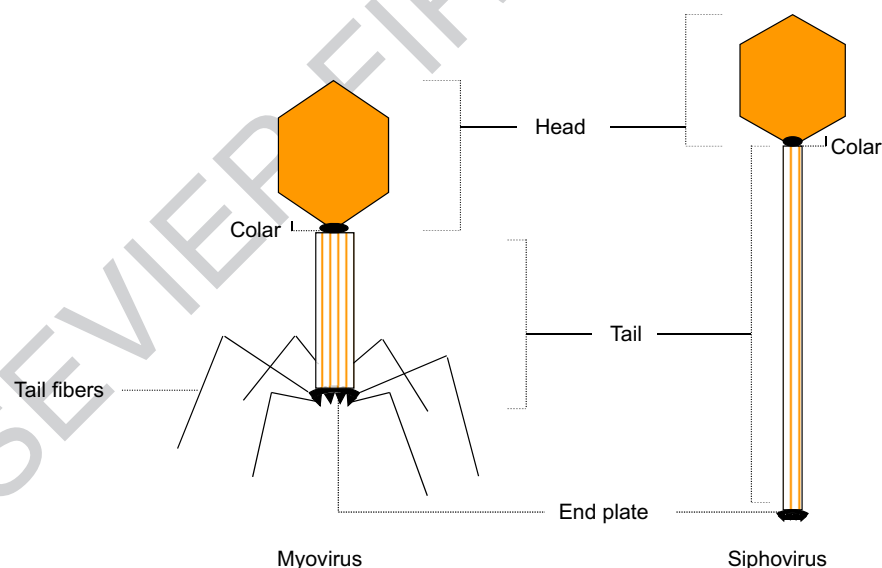
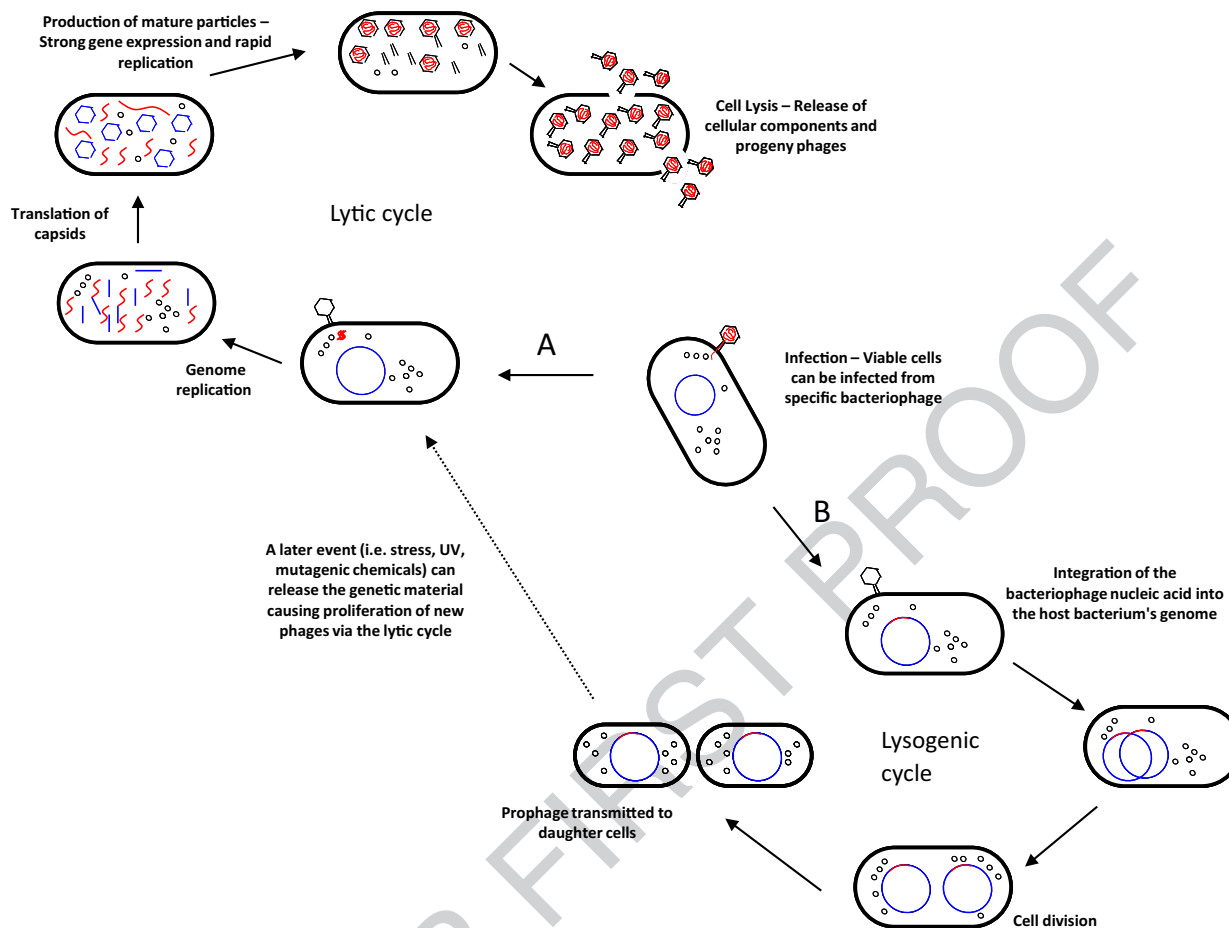


Figure 2 Bacteriophage structure.

the host's metabolic machinery to replicate the viral genome and synthesize new capsids and tails. The phage also encodes a number of proteins required for the assembly of these components into new mature phage particles, which then need to be released from the infected host cell. This normally is achieved by phage-induced breakdown of the bacterial peptidoglycan layer, resulting in loss of the structural integrity of the cell wall, causing the cell to rupture and release progeny bacteriophage. This process often is mediated by a two-component system, composed of a peptidoglycan digesting

enzyme (lysin) and a transport protein (holin). This system is required to allow the lysin protein to cross the inner membrane of the cell and access the peptidoglycan present in the periplasm of Gram-negative bacteria or in the outer layer of the cell wall of Gram-positive bacteria. Not all phage require specific genes to achieve phage lysis, however. Some, such as ϕ X174, weaken the cell wall and induce lysis by interfering with host cell wall synthesis pathways. Others, such as the filamentous phage M13 or Fd, create a persistent infection and extrude phage particles from the host cell in an adenosine triphosphate



f0020 **Figure 3** Bacteriophage replication.

(ATP)-dependent manner, and in this case, the host cells do not lyse. These examples are the exceptions, however, and the majority of phage encode lytic enzymes that can be exploited as biocontrol agents or to develop detection methods (see the following section).

s0015 **Applications of Bacteriophages for the Identification of Bacterial Pathogens**

s0020 **Phage Typing**

p0045 One of the most established uses of bacteriophage is for the differentiation of subtypes of a bacterial species. Robust and widely adopted phage-typing schemes exist for both Gram-negative bacteria and Gram-positive bacteria, and in this case, bacteriophage are chosen that have a relatively limited host range. Thus, the phage chosen for inclusion in phage-typing sets will not be those that can infect all members of the group, but rather those that only infect a subset of the species are selected. A number of such phage with different host ranges are used to form a phage-typing panel, and then a bacterial isolate is infected separately with each of the phage. The results are recorded as either phage sensitivity (lysis of the bacterial cell) or resistance (no infection occurs) and the pattern of results is used to determine the phage type. Many host cell

factors affect the ability of a bacteriophage to infect host cells and the methodology has been developed carefully to create a simple test that accommodates any biological variation in results obtained. The typical reaction patterns for a variety of phage are published and both public health agencies and commercial companies routinely use these methods for the subtyping of a range of foodborne pathogens, such as *Salmonella enterica*, *Escherichia coli* O157, and *Vibrio cholera*. Phage typing is both rapid and low cost, which explains why the method still is used routinely for subtyping bacterial isolates, despite the fact that much finer discrimination between strains can be achieved using DNA-based subtyping methods.

Phage-Based Detection Methods

When selecting phage for detection tests, phage with the widest host range are selected, preferably those that can infect all members of the genus, species, subspecies to be detected. There are many examples of such broad host range phage, including *Salmonella* phage Felix O1, which infects more than 95% of *Salmonella* isolates, phage A511 and P100 that can infect a broad range of *Listeria* isolates, and phage D29, which can infect a wide range of species within the *Mycobacterium* genus. All of these have been used to develop rapid phage-based methods for the identification of bacterial pathogens in food

s0025

p0050

4 Bacteriophage-Based Techniques for Detection of FoodBorne Pathogens

samples (see the following section). In addition, broad host range phage such as these have been used as biocontrol agents to control levels of pathogens in food products. Using these broad host range phage, many different phage-based assay formats have been developed, but generally they can be divided into phage lysis-based methods and phage replication-based methods.

s0030 Phage Lysis-Based Methods

p0055 Many rapid detection methods rely on detection of cellular components and a limitation of these methods often is achieving efficient cell lysis. The advantage of using bacteriophage to lyse cells as part of a detection assay is that they have evolved over millions of years to be both host specific as well as efficient at lysing open cells to allow phage release. ATP has been adopted widely in the food industry as a molecule that can be used to indirectly detect the presence of microbes. This is the basis of several commercially produced, rapid, hygiene tests. As the level of ATP produced by all bacterial cells is approximately the same, measuring ATP provides an indication of the numbers of bacterial cells present in a sample. The reagents used to measure the ATP will not freely permeate cell membranes. Therefore, to detect the ATP, they must be first lysed open. In general hygiene tests, this is achieved using a chemical lysing agent, but this does not specifically lyse one cell type. To add specificity to these hygiene tests, phage – or phage components – have been used to allow specific cell types to be detected.

p0060 Such pathogen-specific ATP assays have been described for rapid and sensitive detection of bacterial pathogens, such as *Salmonella*, *E. coli* O157, and *Listeria* in food samples, and a commercial assay, marketed as FastrAK, was made available. All of these assays require some time for pre-enrichment, however, so that cells can reach a detectable level and also include other rapid method technologies to increase both specificity and sensitivity. For instance, the FastrAK assay included four stages; (1) an 8 h pre-enrichment, (2) immunomagnetic separation and concentration of cells from the pre-enrichment broth, (3) specific phage-mediated lysis, and (4) an ATP assay to detect the presence of target cells. Using this combination of methods, the assay was able detect less than 10 bacterial cells in under 11 h, even in the presence of a highly competitive microflora. Therefore, this method achieved a level of sensitivity as good as conventional culture methods. When using intact phage to achieve phage lysis, however, time is required to complete the phage replication cycle, including synthesis and assembly of new phage particles, before the cells will lyse open. This extends the time required for a detection assay to be performed.

p0065 Hence, purified bacteriophage lysins have been used to replace phage as lysing agents, as these retain both host specificity and can efficiently lyse cells rapidly. For instance, purified phage lysin isolated from a was found to be specific for the type of peptidoglycan found in *Listeria* cell walls and was incapable of digesting the peptidoglycan from other bacterial genera (except two strains of its close genetic relative, *Bacillus*). Extensive studies of the structure and function of the phage lysins have revealed that this specificity comes from their structure, whereby the module with enzyme activity is linked to

a specific substrate-recognition module (termed CBD for carbohydrate-binding domain). Extensive research has been undertaken to produce recombinant forms of these enzymes with both enhanced activity and extended substrate specificity, although this research has focused mostly on generating biocontrol agents rather than agents that can be used to detect bacterial pathogens.

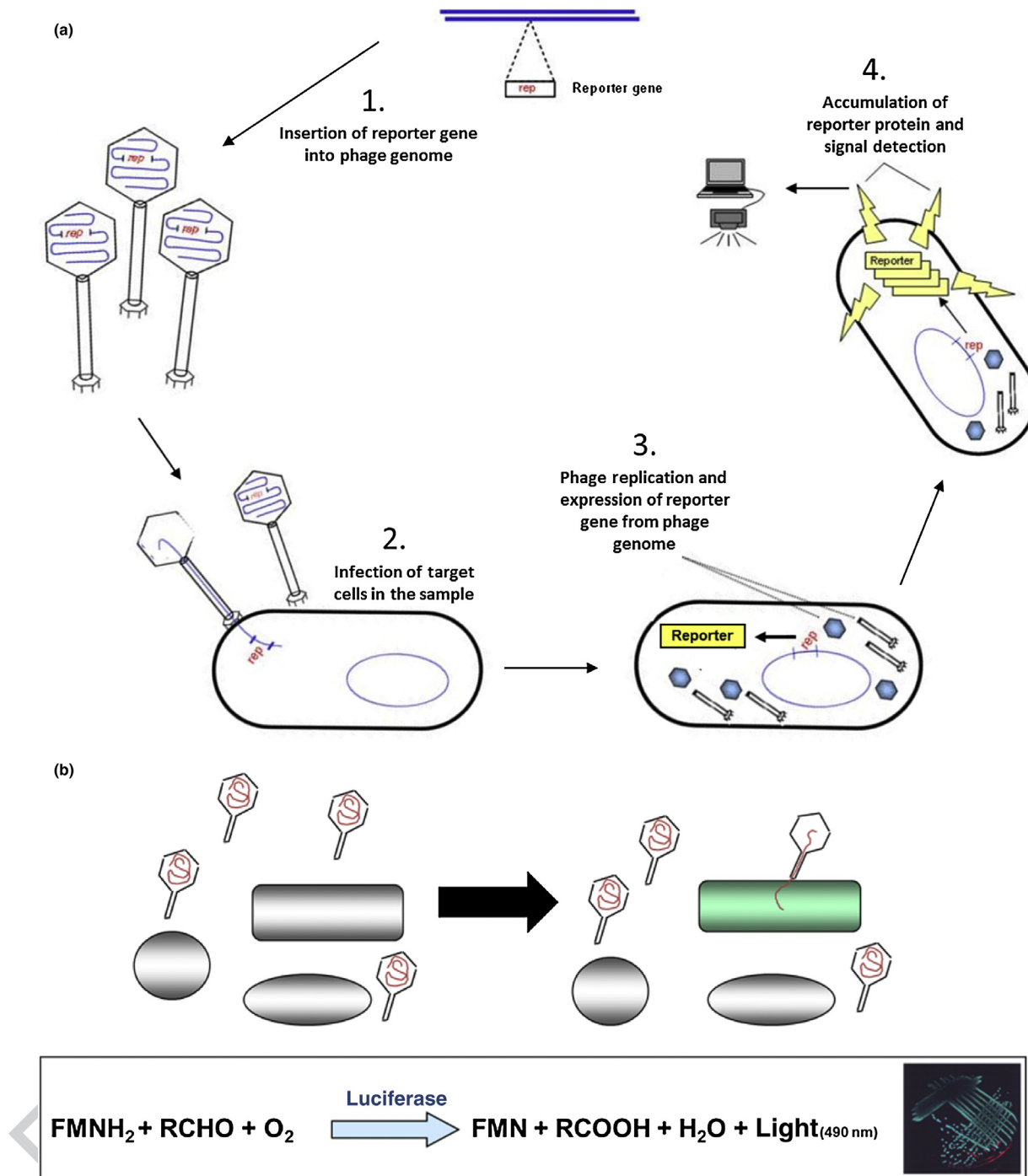
The limitation of phage lysins is that they are most effective against Gram-positive bacteria since their substrates (cell wall carbohydrates and peptidoglycan) are exposed on the outer surface of the cells. In Gram-negative bacteria, the presence of the outer membrane prevents the enzyme reaching its target site. Although modifications of lysozyme have been used to improve the activity of a lytic enzyme against Gram-negative bacteria, this has not been attempted using other phage lysins and no commercial detection assay have been developed to date that take advantage of the specificity of these phage lysins.

Phage Replication-Based Methods

Phage replication-based methods also can be split into two different types; those that use genetically engineered phage that carry a reporter gene that is expressed when the host cell is infected and those that simply detect the replication of the bacteriophage. When using engineered phage – generically termed ‘reporter phage’, the assays utilize the fact that bacteriophage are metabolically inert until they infect their host cell. Hence, the gene for a protein with a detectable characteristic (the reporter gene) is not expressed until the phage infects a suitable host, and therefore induction of measurable protein production signals the fact that a host cell is present in a sample (Figure 4). In contrast, assays that monitor phage growth can take a variety of formats. Traditional culture techniques rely on the exponential doubling of bacterial cells, whereas replication of bacteriophage particles results in the release of many phage particles per cell, and so they can reach detectable levels within a much shorter time frame. For example, bacterial growth over 30 min will result in a doubling of cell numbers (assuming a doubling time of 30 min), whereas the replication of bacteriophages would generate a twenty- to a hundred-fold increase in phage particles (see Figure 1). The liberation of progeny phage can be detected in a variety of ways, either by plaque formation on lawns of susceptible bacteria (visualization is possible after 4 h on lawns of *Salmonella*) or by lysis of liquid cultures, but one of the best developed is the phage amplification assay, which has been produced as a commercial assay (see the following section).

Reporter Phage

The key characteristic of a reporter phage is that the bacteriophage has been engineered to carry a reporter gene that produces a signal that can be measured. A variety of different reporter genes have been used, including both bacterial and firefly luciferases (*lux* and *luc*, respectively), ice nucleation (*ina*), fluorescent proteins, such as green fluorescent protein (*gfp*), and more common enzymatic reporter genes, such as β -galactosidase (*lacZ*). This list, however, is not exhaustive and more examples of reporter phage that have been engineered to carry different reporter genes continually are appearing in the



f0025 **Figure 4** Panel a. Schematic showing general principles of reporter phage technology. Panel b. Application of the *lux* reporter phage. The phage is added to a sample that can contain a mixture of different bacterial cell types (represented by the different gray shaded shapes). Within this complex mixture, the reporter phage can infect only the cell type for which it is specific, removing the need for selective enrichment or capture before the detection event. After phage infection, the target cell synthesizes the *lux* genes (represented by the green shaded cell) and the signal is detected without the need for culture. The accompanying equation shows the bacterial luciferase reaction used in many of the reporter phage developed for food applications. The image of phage shows light produced from bacterial cells expressing the bacterial *lux* genes. Light produced is blue green (peak emission at 490 nm).

literature. For instance, recently, a reporter phage incorporated a hyperthermostable glycosidase from *Pyrococcus furiosus* (*celB*), which can be detected using either chromogenic, fluorescent, or chemiluminescent substrates.

When developing a reporter phage, there are two main considerations. The first is the issue of packaging constraint (defined as the maximum amount of genetic material that can be packaged into a bacteriophage capsid). All development of

6 Bacteriophage-Based Techniques for Detection of FoodBorne Pathogens

engineered bacteriophage is limited by the amount of additional information that can be introduced into the phage genome before the size of the genome exceeds the packaging constraint. For this reason, the smaller reporter genes such as *gfp* (750 bp) and *luc* (Renilla (*Rluc*) = 936 bp, Firefly (*Fluc*) = 1650 bp) have been favored over the longer reporter genes such as *lux* (two genes – *luxA* and *luxB* – are required, which together are approximately 2 kbp). If a reporter gene does exceed the packaging constraints of the phage, then compensatory deletions of nonessential bacteriophage genes are required. Although this is possible with well-studied bacteriophage (such as bacteriophage Lambda), it is in practice difficult to achieve for a phage that has not been extensively genetically characterized and would make the cost of developing the reagent for a food application prohibitive.

p0090 The next factor that must be considered is the promoter chosen to control expression of the reporter gene. To achieve sensitive detection, high-level expression of the reporter gene is required, preferably during the early stages of phage infection to reduce the time to detection (if the genes are expressed only late during the phage infection, a longer incubation time will be required). Hence, the promoter chosen (1) needs to allow high-level expression of the gene, (2) is functional during phage infection (some phage specifically repress expression of host genes during infection), and (3) is ideally expressed early during phage infection.

p0095 One specific advantage of using reporter phage that should be remembered is that the cells detected must be viable for a signal to be generated, because the infected cell must still allow transcription and translation of the reporter gene before the signal is detected. This is also true for phage replication-based assays (see the following section), and this is a major difference between these phage-based methods, and those that either sensitively detected DNA sequences (e.g., PCR) or proteins found on cells (e.g., ELISA assays). Most reporter phage described to date have been developed with a clinical application in mind – for example, bacteriophage specific for *Mycobacteria* carrying the *Fluc* gene have been extensively evaluated for the rapid diagnosis of human tuberculosis. The examples described here, however, focus on those developed specifically for food analysis.

s0045 Reporter Phage Carrying the *lux* Genes

p0100 The *luxAB* genes encode a dimeric enzyme (luciferase), which is responsible for the bioluminescence produced by a number of marine bacteria. In the production of light in this reaction, aldehyde (R.CHO) is converted to carboxylic acid (R.COOH). The reaction also requires both the reducing agent flavin mononucleotide (FMNH₂) and oxygen (Figure 4). The aldehyde substrate is produced by a complex of three genes encoded by *luxC*, *luxD*, and *luxE*. Although all five genes are found in the native *lux* operons found in naturally bioluminescent bacteria, the size of the complete operon approaches 7 kbp, and hence to meet the requirements of the packaging constraint, bacteriophage normally are engineered to contain just the *luxAB* genes and light is produced following the addition of exogenous aldehyde substrate to the sample, because many of these aldehydes will freely permeate bacterial cells. The light produced can be detected by using either sensitive cameras or luminometers, and many such instruments have been

developed for use in routine testing and diagnostics. Modern light detection equipment is capable of detecting the light produced from single cells within an hour.

Listeria lux Phage

One well-studied example of a *lux* reporter phage is the *Listeria* A511::*luxAB* phage. In this case, the *luxAB* genes from *Vibrio harveyi* were introduced into the A511 genome downstream of the major capsid protein gene, *cps*, without exceeding the packaging constraints for this phage. The promoter of the *cps* gene is highly induced during the later stages of the bacteriophage replicative cycle, such that luciferase expression and light production is detected 20 min postinfection. The ability of this reporter phage to detect *L. monocytogenes* in food samples was evaluated, but it was found that the maximum sensitivity approximately 100 cells ml⁻¹, which is insufficient to allow direct testing of food samples. The incorporation of standard broth enrichment procedures before infection with the reporter phage improved the sensitivity of the test. For example, *L. monocytogenes* was detected in food samples seeded at 0.1 cfu g⁻¹ (cabbage), 1 cfu (milk), and 10 cfu (Camembert cheese). The variability in the cell detection limits observed in different foods is thought to a reflection of the complexity of the food matrices and the level of competitive microflora found within the food. Applying these reporter phage after enrichment stages allows the presence of *Listeria* to be confirmed after just 24 h in contrast to conventional culture-based techniques, which take up to 4 days for presumptive detection of *Listeria*.

Other Reporter Phage for Detection of Foodborne Bacteria

In addition to the two examples described previously, reporter phage have been developed for the identification of the whole *E. coli* species (bacteriophage Lambda), *Salmonella* species 3 (bacteriophage Felix-01), and specific serovars of *S. enterica* (Typhimurium and Enteritidis). In most cases, these have used *lux* genes as the reporter because the background levels of natural bioluminescent produced by food substances is very low. Unfortunately, many foods – especially those that contain either large amounts of plant material or are vitamin rich – do contain components that are naturally fluorescent, and this limits the sensitivity with which a fluorescent signal can be detected. Recently, a *Listeria* reporter phage containing the *celB* reporter gene (A511::*celB*) was described, which was able to detect low numbers of *Listeria* (10 cfu g⁻¹ or fewer) in spiked samples of chocolate milk and salmon within 6 h. In this case, the heat-resistant properties of the enzyme are used to reduce levels of background noise in the sample and increase the sensitivity of the test. Similar modifications of protocol, or combinations with immunomagnetic capture, have been described to produce reporter phage that are sensitive enough to be of value to the food industry, but despite this large body of work, no commercial application of the reporter phage for food applications has yet been developed.

Phage Amplification

The phage amplification technique for detecting bacteria relies on two key characteristics; the specificity of bacteriophages to target cells, and the ability of a potent virucidal agent to rapidly inactivate free (extracellular) phage, while remaining

s0050
p0105

s0055
p0110

s0060
p0115

nondestructive to bacterial cells. These attributes permit the detection of specific groups of bacteria on the basis of their ability to protect the phage from the destruction by the virucide once they have infected a host cell and then allow for the production of new (progeny) phage particles. A variety of compounds can be used as the virucide, including chemicals, such as ferrous ammonium sulfate, and plant extracts, such as tea and pomegranate rind.

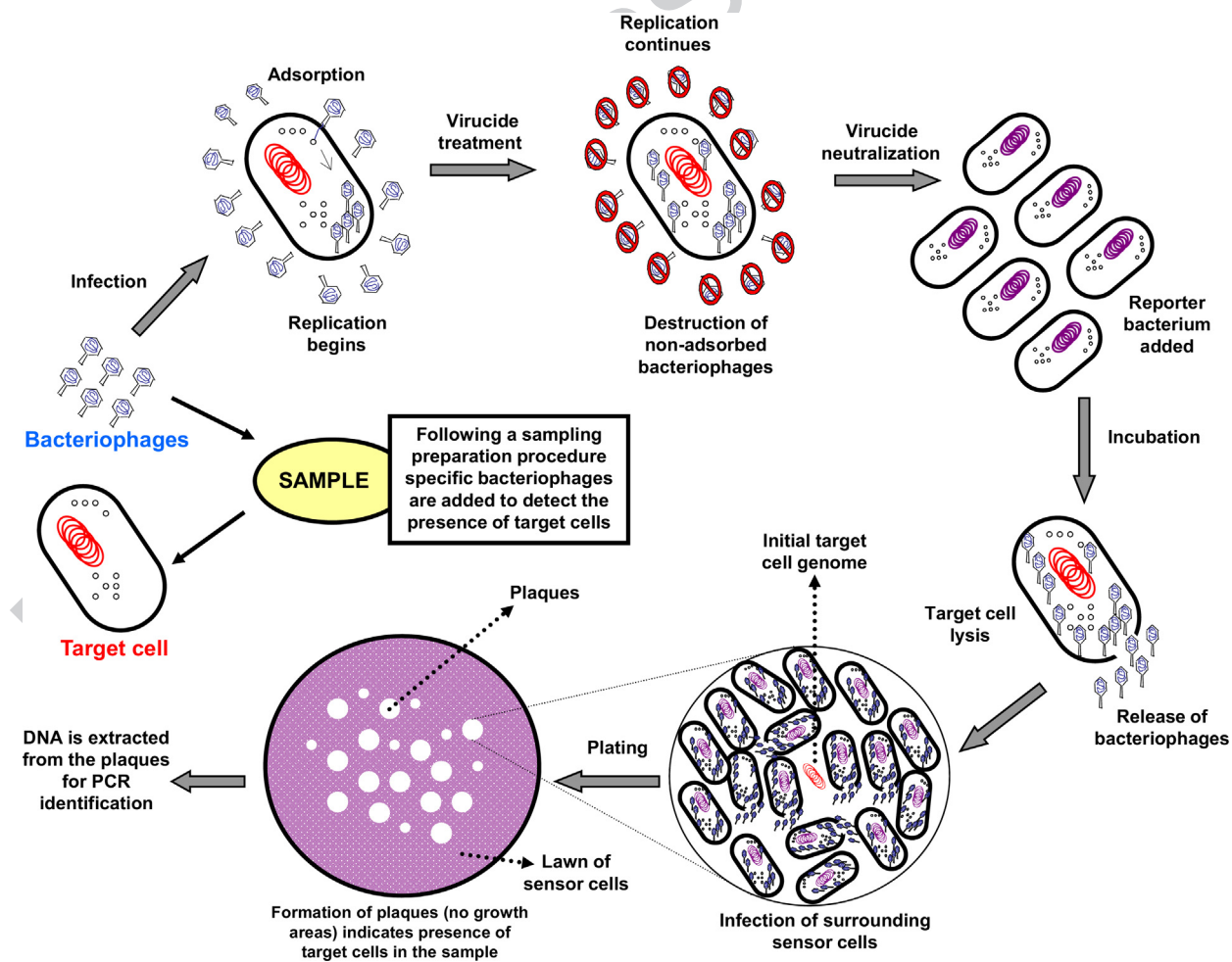
p0120 In the phage amplification assay, a positive indication of the presence of bacteria is the formation of plaques at the end of the assay (Figure 5). The sample containing the target cell is first infected with the bacteriophage. An incubation period then follows to allow time for cell infection and for the phage to enter the eclipse phase. At this point, any exogenous phage are destroyed by the addition of a virucide, which does not affect the viability of the host strain but that will inactivate any phage that have not infected a target bacterium. Hence the assay is in essence a phage-protection assay; only those that have infected an appropriate host cell will avoid inactivation and can replicate inside the host cell. To detect the phage released from this primary infection, a phage-susceptible, nonpathogenic variant is used as a host strain (termed the 'sensor strain'); a nonpathogenic variant is used to increase the safety of those working in the laboratory performing the assays. The sensor

strain is added to the sample after the virucide treatment, and the whole sample is mixed with soft agar and poured into Petri dish. The sensor cells will grow on the agar and form a lawn of phage-sensitive cells that will support phage replication. So, if any target cells are present in the original sample, these will lyse at the end of the lytic cycle, new phage will be released, and these then will infect the surrounding cells. This will result in the formation of plaques (areas of cell lysis) in the bacterial lawn.

The phage amplification assay can be tailored to the detection of specific bacterial genera by the choice of bacteriophage used in the assay. Visualization of plaques in lawns of *Salmonella* and *Pseudomonas* is possible within 4 h, permitting detection of these pathogens within a working day. Phage amplification has been applied successfully to the specific detection of *Campylobacter*, *Listeria*, *Pseudomonas*, *Salmonella*, *Staphylococcus*, and *Mycobacterium* cells, the latter has been developed as a commercial diagnostic test for human tuberculosis.

Detection of Mycobacteria by Phage Amplification

s0065
p0130
FASTplaqueTB™ (FPTB) is a commercially available test produced for the detection of *Mycobacterium tuberculosis* in human sputum samples. The commercial test uses the lytic mycobacteriophage D29 to infect the target mycobacteria cells



f0030 Figure 5

8 Bacteriophage-Based Techniques for Detection of FoodBorne Pathogens

in human sputum samples. It also has been shown that the components of the FPTB assay can be used for detection of *Mycobacterium avium* subspecies *paratuberculosis* (MAP) in raw milk and cheese samples. Unlike human sputum, raw milk is a sample that is more likely to contain other environmental mycobacteria in addition to the pathogens that are being targeted. Hence, infection by a broad host range phage alone is not sufficiently discriminating to allow for identification of the bacterium detected. This has led to the development of a PCR identification test that is used following the phage assay. The PCR assay can be species specific, or it can have a multiplex PCR format for the simultaneous identification of different species. The combination of phage amplification with PCR has been shown to deliver a high specificity and is very sensitive, with less than 10 cells per sample being detected routinely detected.

s0070 **Detection of *Mycobacterium avium* subspecies *paratuberculosis* in milk**

p0135 MAP is the infective agent responsible for paratuberculosis (John's disease), a chronic enteritis that can cause production losses and mortal diarrhea in cattle and other ruminants. Detection of MAP in milk has become a food microbiological issue because of the fact that MAP has long been suspected as a contributing agent to the development of Crohn's disease, and its presence in milk is a potential source of human exposure. Detection of MAP in milk currently relies on culture, immunoassays, and molecular techniques. The culture-based techniques require a long incubation period of about 3 months and therefore immunoassays also have been developed. These have a low sensitivity in milk, however, and no other reliable molecular-based detection method exists that can detect viable cells without requiring extensive culture.

p0140 With the application of a combined phage-PCR assay, detection of viable MAP cells is possible after only 18 h, with a higher sensitivity compared with the conventional culture

method. The test only identifies viable organisms, and therefore it is of use if trying to confirm the inactivation of the organism by pasteurization, which cannot be determined by enzyme-linked immunosorbent assay (ELISA), and only by the use of qPCR methods. An important feature of this assay is that despite the fact that the method requires several sample preparation steps, it still retains good reproducibility (Figure 6). An assay also has been described for the detection of MAP in milk that uses a lateral flow device to detect the growth of the bacteriophage. This is similar to the Microphage commercial technology (see the following section), although the cost of a lateral flow device may be more acceptable within a clinical environment.

An advantage of phage amplification technology is its adaptability. It can be adapted for use in detection of many bacteria, taking advantage of the specificity of the bacteriophage that will be applied. Very important is the selection of the propagating strain ('sensor cells'), which is better to be from a fast-growing nonpathogenic organism within the infection spectrum of the phage. Of critical importance is the cost, which is low compared with other rapid phage-based methods used.

Conclusion

Currently, no commercial tests for food applications are available; although some commercial tests have been launched, they have not proved to be long-term commercial successes, often failing due to issues surrounding either cost or sensitivity (e.g., Alaska Foods Diagnostics' fastrAK™ system; Anon, 2002). Recently, however, a commercial bacteriophage-based test for the detection of *Staphylococcus aureus* in clinical samples has been developed successfully by the U.S. company Microphage (KeyPath™ Pathogen Tests). These tests combine a bacteriophage amplification assay with a lateral flow detection device

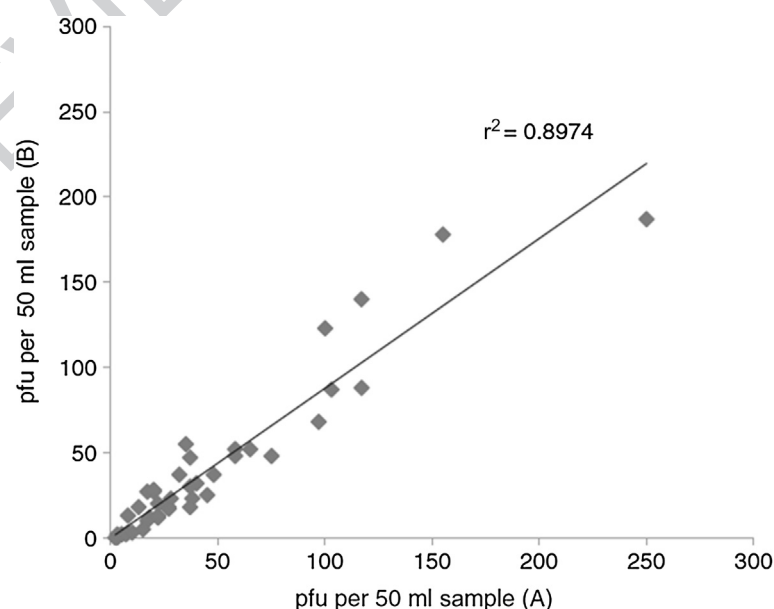


Figure 6 Reproducibility of phage assay results. Comparison of plaque results (pfu per 50 ml sample) for the 44 duplicate BTM samples that were tested independently using the phage amplification assay. Values were arbitrarily assigned to either group A or B ($r^2 = 0.897$). Taken from Botsaris et al. (2013).

and were approved by the U.S. Food and Drug Administration in 2011 for the rapid detection and discrimination between MRSA and MSSA in clinical settings. Microphage also reports evaluating the same technology for food applications, and developments in biosensor technology mean that it is likely that bacteriophage-based tests will become more practical and cost effective.

[AU3]

Further Reading

[AU9]

Ackermann, H.W., 2011. Phage or phages. *Bacteriophage* 1, 52–53.
Botsaris, G., Slana, I., Liapi, M., et al., 2010. Rapid detection methods for viable *Mycobacterium avium* subspecies *paratuberculosis* in milk and cheese. *International Journal of Food Microbiology* 141, S87–S90.
Carlton, R.M., Noordman, W.H., Biswas, B., et al., 2005. Bacteriophage P100 for control of *Listeria monocytogenes* in foods: genome sequence, bioinformatic

analyses, oral toxicity study, and application. *Regulatory Toxicology and Pharmacology* 43, 301–312.
García, P., Martínez, B., Obeso, J.M., et al., 2008. Bacteriophages and their application in food safety. Letter in *Applied Microbiology* 47, 479–485.
Graham, J., 1996. Timely test spots TB in hours. *New Scientist* 151 (2043), 21.
Loessner, M.J., Rudolf, M., Scherer, S., 1997. Evaluation of luciferase reporter bacteriophage A511::luxAB for detection of *Listeria monocytogenes* in contaminated foods. *Applied and Environmental Microbiology* 63, 2961–2965.
Monk, A.B., Rees, C.E.D., Barrow, P., et al., 2010. Bacteriophage applications: where are we now? Letters in *Applied Microbiology* 51, 363–369.
Rees, C.E.D., Dodd, C.E.R., 2006. Phage for rapid detection and control of bacterial pathogens in food. *Advances in Applied Microbiology* 59, 159–186.
Rees, C.E.D., Loessner, M.J., 2009. Phage identification of bacteria. In: Goldman, E., Green, L.H. (Eds.), *Practical Handbook of Microbiology*. CRC press, pp. 85–99.
Smith, D., 2010. Bacteriophage amplification for bacterial identification. *In Vitro Diagnostics Technology* 16, 28–35.
Stewart, G.S.A.B., 1997. Challenging food microbiology from a molecular perspective. *Microbiology* 143, 2099–2108.
Young, R.Y., 1992. Bacteriophage lysis: mechanism and regulation. *Microbiological Reviews* 56, 430–481.

ELSEVIER FIRST PROOF